

DISSERTATION

PROGRESS TOWARD THE TOTAL SYNTHESIS OF STEMOCURTISINE
AND ASYMMETRIC SYNTHESIS OF ENDOPEROXIDE ANTICANCER AGENTS VIA
BRØNSTED ACID CASCADE CATALYSIS

Submitted by

David Michael Rubush

Department of Chemistry

In partial fulfillment of the requirements

For the Degree of Doctor of Philosophy

Colorado State University

Fort Collins, Colorado

Fall 2012

Doctoral Committee:

Advisor: Tomislav Rovis

Alan Kennan

Debbie Crans

Eugene Chen

Shane Kanatous

ABSTRACT

PROGRESS TOWARD THE TOTAL SYNTHESIS OF STEMOCURTISINE AND ASYMMETRIC SYNTHESIS OF ENDOPEROXIDE ANTICANCER AGENTS VIA BRØNSTED ACID CASCADE CATALYSIS

A viable route toward the pyrido-azepine core of stemocurtisine involving an *N*-heterocyclic carbene catalyzed Stetter reaction has been realized. The key steps involve a formal [3+2] cycloaddition of enones with isocyanoacetates and a catalytic asymmetric intramolecular Stetter reaction. Additionally, a diastereoselective intramolecular Stetter reaction was achieved to access highly substituted pyrrolidines.

Asymmetric Brønsted acid catalyzed cascade reactions were also investigated. A diastereoselective acetalization/oxa-Michael cascade has been developed to provide dioxolanes and oxazolidines using diphenylphosphinic acid as a catalyst. The enantioselective variant of this reaction was explored with minor success.

The desymmetrization of *p*-peroxyquinols using a Brønsted acid catalyzed acetalization/oxa-Michael cascade was achieved in high yields and selectivities for a variety of aliphatic and aryl aldehydes. Mechanistic studies suggest that the reaction proceeds through a dynamic kinetic resolution of the peroxy-hemiacetal intermediate. The resulting 1,2,4-trioxane products were derivatized and show potent cytotoxicity toward specific cancer cells.

ACKNOWLEDGMENTS

The work contained in this dissertation would not have been possible without the time and efforts of my colleagues, friends and family. First I would like to thank Professor Tom Rovis for being an outstanding advisor and mentor. His commitment to developing excellent scientists allowed me to become the chemist I am today. There were many times when I was frustrated with chemistry but Tom spurred me on and challenged me to solve important problems. I will always be grateful for the opportunities he gave me.

I want to thank my committee members Professors Alan Kennan, Debbie Crans, Eugene Chen and Shane Kanatous for insightful discussions throughout my graduate career.

I thank the entire Rovis group for their intellectual contributions and most importantly their timeless friendships. Many thanks to all of the Rovis group postdocs who offered invaluable wisdom: Jeff, Oleg, Art, Matt, Ernest, Stéphane, Brandon, Cat, Jef, Ya, Xiaodon, Brian, Ben, Tim and Tyler. I want to especially thank my B311 labmates for creating an awesome work environment: Jamie, Derek, Stephen, Brian, Matt, Brandon, Steve, Becky, Johannah, Darrin, and Dan. I thank the rest of the Rovis group for helpful discussions, trips to Road and breaks to go running: Kerr, Naz, Qin, Robert, Jen, Harit, Mark, Becca, Kate, Phil, Dan, Kevin, Claire, Oz, Todd, Nick, Tim, Garrett, Natthawat, Kyle and John.

I thank Calvin College professors Ronald Blankespoor, Arie Leegwater and Kenneth Piers for their dedication to train undergraduate researchers and for introducing me to the exciting world of organic synthesis.

I acknowledge my collaborator Dr. Christine Olver at the Colorado State University Veterinary Teaching Hospital for screening the trioxane molecules for antimalarial activities. I

also want to thank Dr. Douglas Thamm, Michelle Morges and Barb Rose at the Colorado State University Animal Cancer Center for testing the trioxanes for cancer cell cytotoxicity.

I am blessed to have an amazing family and I thank them for always being a positive influence in my life. In particular, my parents have continually encouraged me to pursue my dreams and I will always be grateful for the sacrifices they made to support my education.

Most importantly I would like to thank my loving and patient wife Katie, who has always been alongside of me through the ups and downs. Her unconditional love and encouragement are what helped me get through graduate school and what will allow me to continue to achieve my goals.

TABLE OF CONTENTS

ABSTRACT.....	ii
ACKNOWLEDGEMENTS.....	iii
Chapter 1. <i>N</i> -Heterocyclic Carbene Catalysis and Stemocurtisine.....	1
1.1 <i>N</i> -Heterocyclic Carbene Catalysis	1
1.1.1 Introduction	1
1.1.2 Benzoin Reaction.....	2
1.1.3 Stetter Reaction.....	4
1.1.4 Stetter Reactions in Total Synthesis	10
1.1.5 Conclusion.....	13
1.2 Stemocurtisine.....	14
1.2.1 Introduction	14
1.2.2 <i>Stemona</i> Alkaloids.....	14
1.2.3 Total Synthesis of <i>Stemona</i> Alkaloids.....	15
1.2.4 Previous Work Toward Asparagamine A in the Rovis Group.....	17
1.2.5 Conclusion.....	18
References.....	19
Chapter 2. Synthetic Efforts Toward Stemocurtisine via an Intramolecular Stetter Reaction	23
2.1 First Generation Approach.....	23

2.1.1 Retrosynthesis.....	23
2.1.2 Photoisomerization Stetter Results.....	26
2.1.3 Summary.....	30
2.2 Oxazine Strategy.....	31
2.3 Pyrrole Dearomatization Strategy.....	32
2.4. Pyrroline Strategy.....	34
2.4.1 Retrosynthesis.....	34
2.4.2 Vinylogous Amide Stetter.....	34
2.4.3 Vinylogous Imide Stetter.....	36
2.4.4 Enantioselective Stetter.....	38
2.4.5 Pyrrolidine Ring Opening.....	39
2.5 Route Optimization.....	41
2.6 Diastereoselective Stetter.....	44
2.7 Western Fragment.....	46
2.8 End Game.....	46
2.9 Conclusion.....	47
References.....	48
Chapter 3. Brønsted-Acid Cascade Catalysis and the Development of a Diastereoselective Acetalization/Oxa-Michael Cascade.....	51
3.1 Introduction.....	51

3.1.1 Asymmetric Brønsted Acid Catalysis.....	51
3.1.2 Importance of Chiral Acetals and Aminals	52
3.1.3 Asymmetric Formation of Acetals and Aminals	53
3.1.4 Cascade Catalysis	54
3.1.5 Asymmetric Brønsted Acid Cascades	56
3.1.6 Cyclohexenone Desymmetrizations	56
3.2 Results	59
3.2.1 Acetalization/Oxa-Michael Cascade	59
3.2.2 Quinol Substrate Synthesis	61
3.2.3 Dioxolane Reaction Optimization	62
3.2.4 Dioxolane Substrate Scope	63
3.2.5 Oxazolidine Substrate Scope	67
3.3 Asymmetric Formal [3 + 2].....	71
3.4 Conclusion.....	74
References.....	75
Chapter 4. Development of an Enantioselective Synthesis of Trioxanes via a Formal [4+2]	
Cycloaddition.....	78
4.1 Introduction.....	78
4.1.1 Trioxanes	78
4.1.2 Catalytic Asymmetric Synthesis of Peroxides.....	78

4.2 Enantioselective Trioxane Synthesis.....	80
4.2.1 Synthetic Approach	80
4.2.2 Reaction Development	81
4.2.3 Catalyst Development.....	83
4.2.4 Co-Catalyst Effects.....	85
4.2.5 Substrate Scope.....	88
4.3 Mechanistic Studies.....	93
4.4 Trioxane Derivatization.....	95
4.5 Conclusion.....	97
References.....	98
Chapter 5. Investigation of the Antimalarial and Cytotoxic Activities of Synthetic Trioxanes.	101
5.1 Biological Activity of Artemisinin.....	101
5.1.1 Introduction	101
5.1.2 Trioxane Mode of Action	101
5.1.3 Synthetic Trioxanes	103
5.2 Biological Testing of Synthetic Endoperoxides.....	104
5.2.1 Synthetic Endoperoxides	104
5.2.2 Antimalarial Activities of Synthetic Trioxanes and Dioxazinanes	105
5.2.3 D17 Canine Carcinoma Cell Cytotoxicity Studies of Synthetic Trioxanes.....	106
5.2.4 Human and Canine Cell Line Cytotoxicity Studies of Synthetic Trioxanes	109

5.2.4 Further Canine Cell Line Cytotoxicity Studies of Synthetic Trioxane (18).....	111
5.3 Conclusion.....	113
References.....	115
Appendix 1. Chapter 2 Supporting Information	118
Appendix 2. Chapter 3 Supporting Information	151
Appendix 3. Chapter 4 Supporting Information	167
Appendix 4. Chapter 5 Supporting Information	212

Chapter 1

N-Heterocyclic Carbene Catalysis and Stemocurtisine

1.1 *N*-Heterocyclic Carbene Catalysis

1.1.1 Introduction

N-heterocyclic carbenes (NHCs) are versatile catalysts that have played an important role in the construction of complex molecules.¹ Wanzlick identified nucleophilic carbenes as reactive intermediates² and first examples of isolable NHCs were reported by Arduengo and Bertrand.³ Since their discovery, NHCs have been used as ligands for metal catalyzed reactions and as organocatalysts for C-C bond formation.⁴ The predominant role of NHCs as organocatalysts is to transform naturally electrophilic aldehydes into nucleophiles at the carbonyl carbon. The term “umpolung reactivity” has been coined for this polarity reversal. The two major C-C bond forming reactions in which the nucleophilic aldehyde is employed are the Stetter and benzoin reactions. In the benzoin reaction, the nucleophilic aldehyde, also called the acyl anion equivalent (**2**), adds into another aldehyde (**1**) to form α -hydroxy ketones (**3**) (Figure 1.1). In the Stetter reaction, the same acyl anion equivalent adds to a Michael acceptor (**4**) to form 1,4-difunctionalized products (**5**).

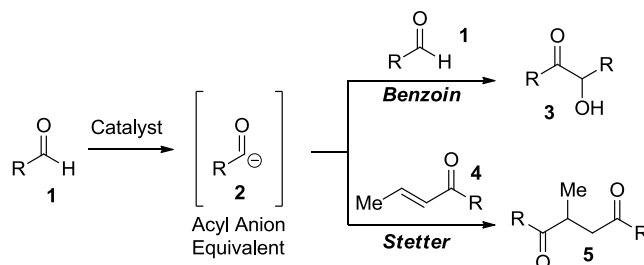


Figure 1.1

1.1.2 Benzoin Reaction

The benzoin reaction was discovered in 1832 when Wöhler and Liebig demonstrated that cyanide could catalyze the formation of benzoin from benzaldehyde.⁵ Lapworth first proposed the currently accepted mechanism for the cyanide-catalyzed benzoin reaction in 1903,⁶ and Breslow eventually elucidated this mechanism using thiamin as a catalyst.⁷ This catalysis process begins by deprotonation of the thiazolium with a base to reveal the NHC catalyst (Figure 1.2). This carbene adds nucleophilically into an aldehyde to form tetrahedral intermediate **8**. After intermolecular proton transfer, the acyl anion (**9**) is generated and the resonance structure of this species has been aptly named the Breslow intermediate (**9** \leftrightarrow **10**). Once the aldehyde has been rendered nucleophilic, it adds to another equivalent of aldehyde forming a C-C bond. Intermediate **11** subsequently undergoes a proton transfer to form **12** which collapses to yield the α -hydroxy ketone product (**13**), regenerating the carbene catalyst (**7**).

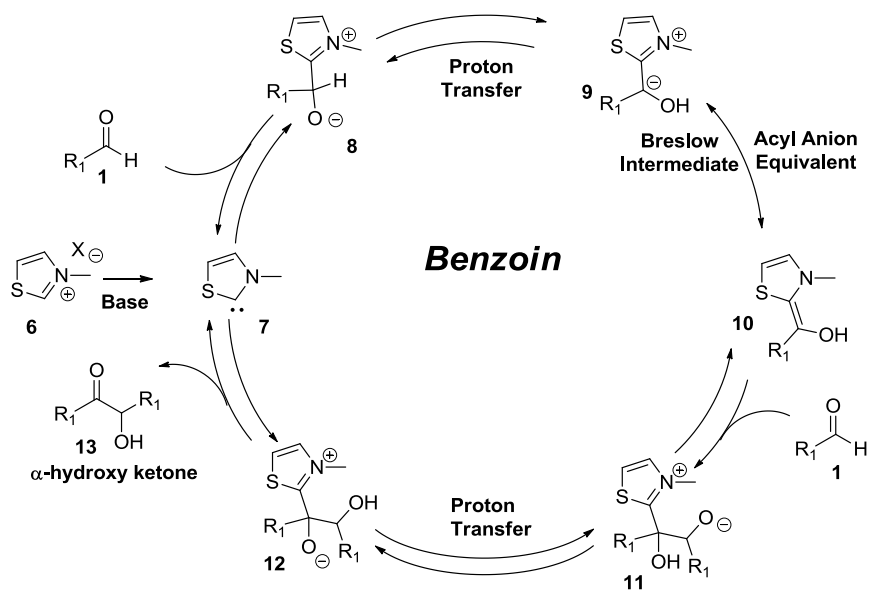


Figure 1.2

Unlike cyanide, thiazolylidene carbenes have the potential to be chiral. A chiral acyl anion (**14**) would create the potential for enantioselective Benzoin and Stetter reactions (Figure 1.3). As shown in the previously described mechanism, the benzoin reaction is reversible, and thus creates a challenge for developing an asymmetric variant.

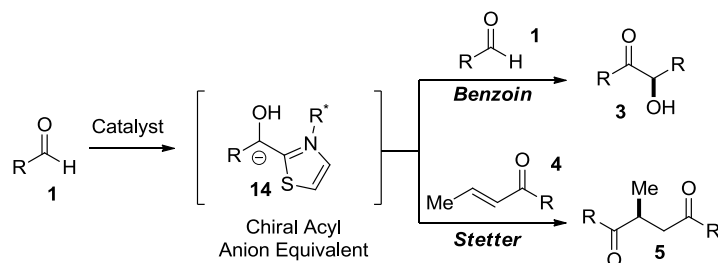


Figure 1.3

Almost a century after the initial report, Ukai showed that thiazolium salts could affect the same homobenzoin reaction.⁸ This was a major breakthrough because it allowed for the construction of chiral carbene catalysts. In 1974, Sheehan took advantage of this discovery and developed a chiral thiazolium that produced benzoin (**16**) in 22% ee, albeit in a very low yield (Table 1.1).⁹ Enders demonstrated that a new triazolium scaffold could improve selectivity to 75% ee with modest yields. A few years later, Leeper illustrated that a more rigid triazolium further enhanced the ee of the benzoin reaction.¹⁰ Many other groups tried to attain high enantioselectivities but they were unsuccessful.¹¹ In 2002, Enders employed a hindered triazolium to produce benzoin in synthetically useful yields and 90% ee.¹²

Table 1.1

Entry	Catalyst	Author/Year	Yield	ee
1		Sheehan/1974	9%	22%
2		Enders/1996	66%	75%
3		Leeper/1998	45%	80%
4		Enders/2002	83%	90%

1.1.3 Stetter Reaction

In 1973, Stetter expanded the utility of acyl anions, using Michael acceptors as electrophilic partners.¹³ With cyanide or a thiazolylidene carbene as the catalyst, he demonstrated that aliphatic and aromatic aldehydes added to α,β -unsaturated ketones, esters and nitriles to produce an array of 1,4-difunctionalized products (Figure 1.4).¹⁴ This reaction provided products in good yields but was not very tolerant of substituents at the β -position of the Michael acceptor.

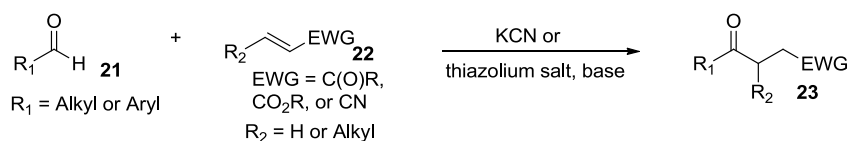


Figure 1.4

The mechanism of the Stetter reaction was initially proposed to be similar to Breslow's benzoin mechanism, and Yates has recently provided supported for this hypothesis.¹⁵ The Stetter begins in the same fashion as the benzoin with formation of Breslow intermediate (**9**↔**10**) (Figure 1.5). Instead of adding to an aldehyde, the nucleophilic species adds to a Michael acceptor forming tetrahedral intermediate **25**. After a proton transfer, resultant intermediate **26** collapses to form the 1,4-dicarbonyl product (**27**) and regenerate the carbene catalyst (**7**).

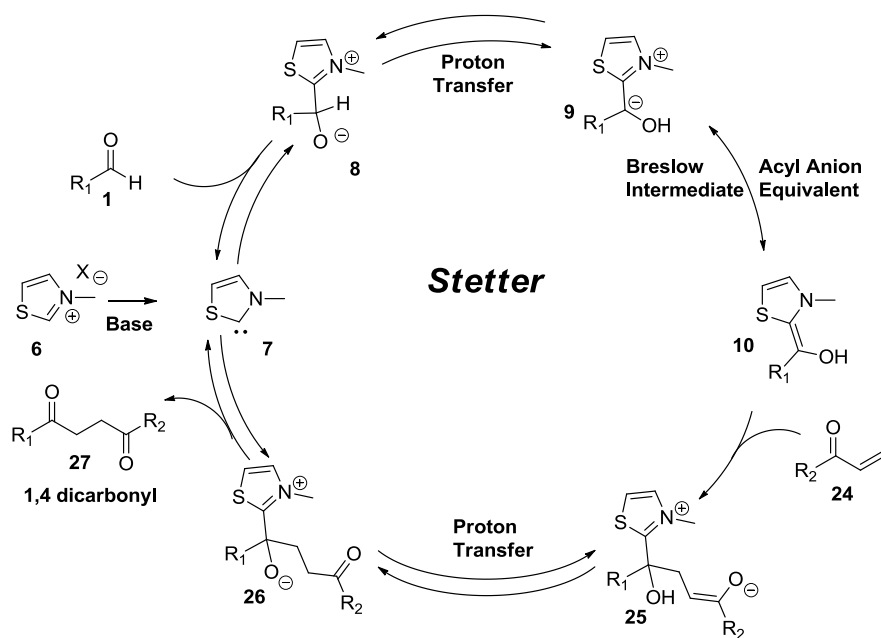


Figure 1.5

Almost 20 years after Stetter's original account, Ciganek reported an intramolecular variant of the Stetter reaction using salicylaldehyde derivatives to produce chromanone products.¹⁶ This substrate (**28**) has been used as a benchmark for testing new catalyst scaffolds. Enders reported the first asymmetric intramolecular Stetter in 60% ee using triazolium salt **18** as a precatalyst (Figure 1.6).¹⁷ Subsequent to our work, Miller demonstrated that peptide-based chiral thiazolium derived catalysts can reach modest enantioselectivities.¹⁸ The Rovis group has investigated the

mechanism of this particular intramolecular Stetter reaction. Evidence from kinetic isotope effect and competition studies suggest that proton transfer from the first tetrahedral intermediate (**4**) to Breslow intermediate (**8**↔**9**) is the turnover-limiting step.¹⁹

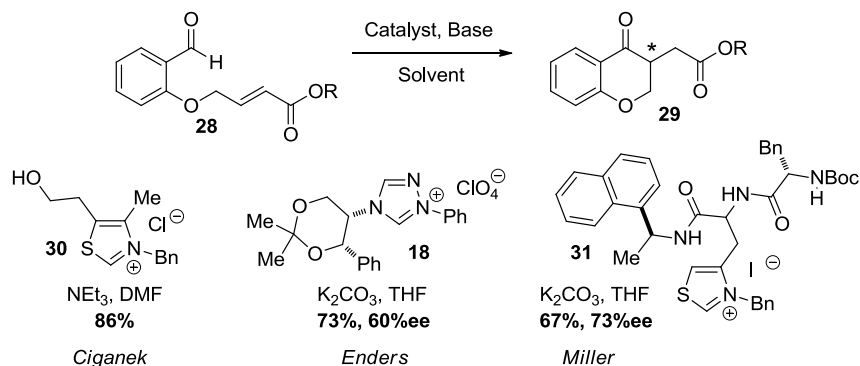


Figure 1.6

In 2002 the Rovis group developed a series of triazolium catalysts which increased the enantioselectivity of the intramolecular Stetter reaction to the high 90's. These catalysts are significantly better than their thiazolium counterparts, because they are more rigid and could block three of four quadrants (Figure 1.7).²⁰

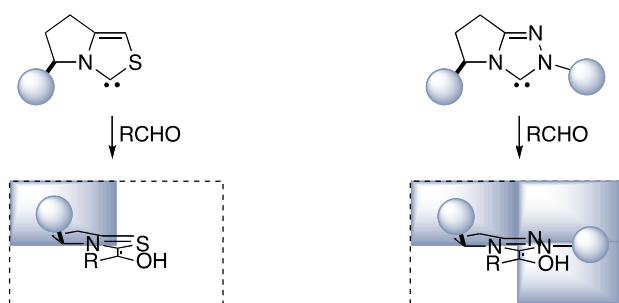


Figure 1.7

A variety of Stetter reactions have been conducted with these catalysts. The benchmark substrate **32** is converted to product **33** in excellent yield and 94% ee (Figure 1.8).²¹ Quaternary

stereocenters can be formed in up to 98% ee from tethered aliphatic aldehydes.²² The Stetter reaction can be used in a desymmetrization of cyclohexadienones to afford benzofuranones in superb enantioselectivity and diastereoselectivity (Figure 1.8).²³

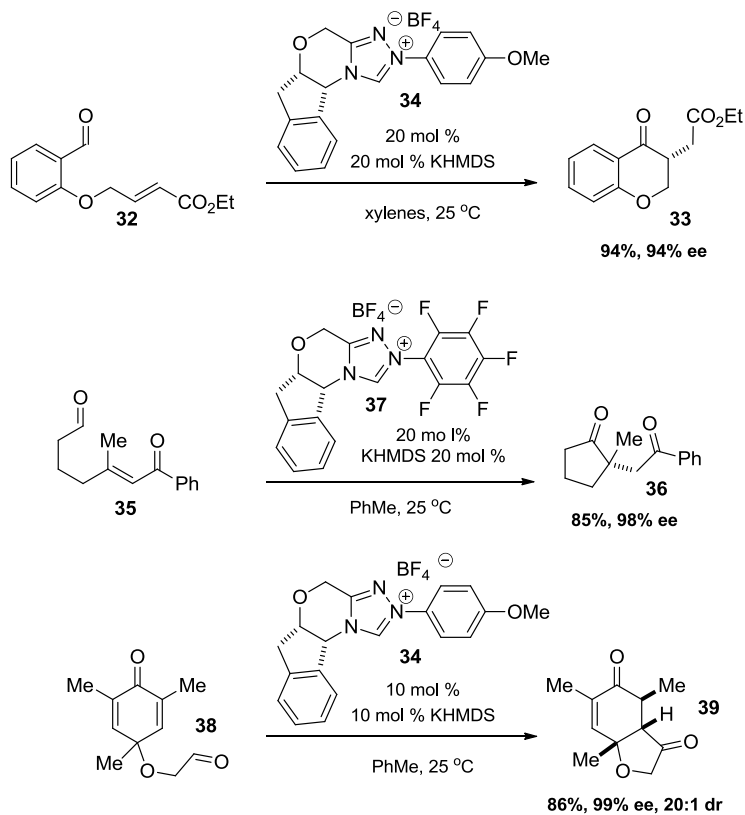


Figure 1.8

When preexisting stereocenters are present in a Stetter substrate, enantioselectivities are not compromised unless they are adjacent to the aldehyde (Figure 1.9).²⁴ However, these chiral centers do not provide any diastereoselectivity unless they are adjacent to the aldehyde.

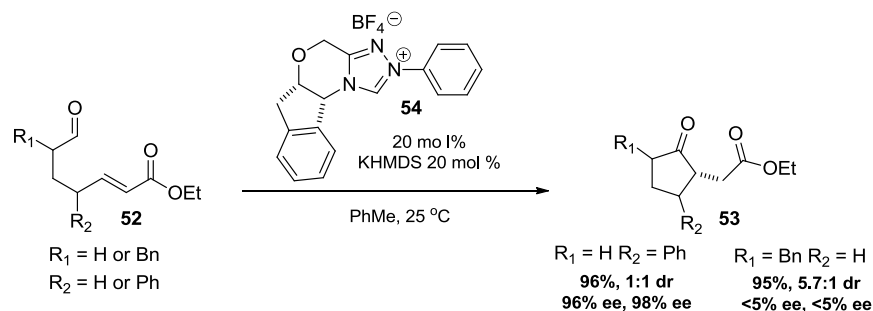


Figure 1.9

The asymmetric Stetter reaction was found to be highly diastereoselective in the chromanone system (Figure 1.10). It was initially proposed that an intramolecular protonation of the enolate intermediate (**46**) was fast and occurred before C-C bond rotation. This gives rise to an overall syn-addition of aldehyde and proton on the Stetter product. This hypothesis was supported when opposite olefin isomers yielded different diastereomers; although, the E-enoate gives much higher selectivities (Figure 1.10).²⁵

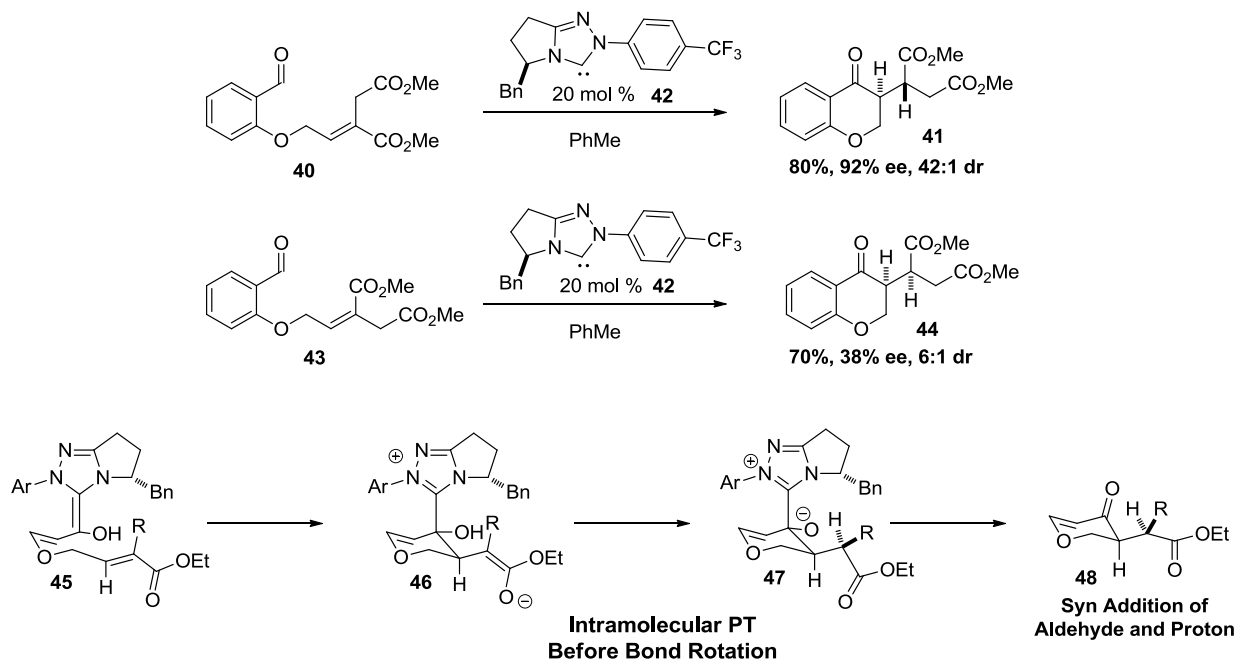


Figure 1.10

Recent publications showed that a Stetter reaction could occur on substrates lacking a true Michael acceptor (Figure 1.11).²⁶ This suggests that the C-C bond formation and protonation may follow a concerted hydroacylation mechanism that is reminiscent of the reverse-Cope elimination.²⁷

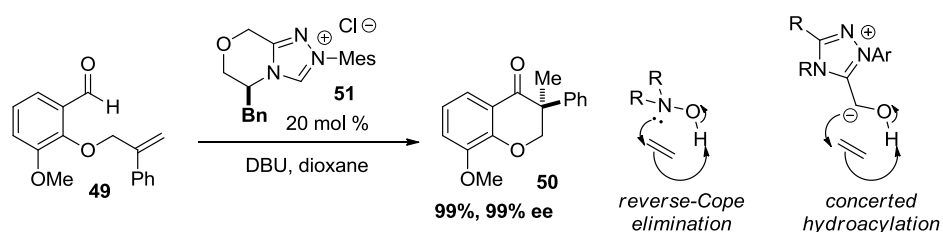


Figure 1.11

Although there are numerous examples of asymmetric intramolecular Stetter reactions, the intermolecular Stetter has been a bit more elusive. Enders reported that benzaldehyde and chalcone could undergo a Stetter reaction to form the 1,4-dicarbonyl compound (**57**) in good yield and modest enantioselectivity (Figure 1.12).²⁸ In 2008, the Rovis group showed the first highly enantioselective intermolecular Stetter using glyoxamides and alkylidenemalonates.²⁹ The scope of reaction has been further expanded to nitro alkene Michael acceptors using fluorinated chiral triazoliums.³⁰

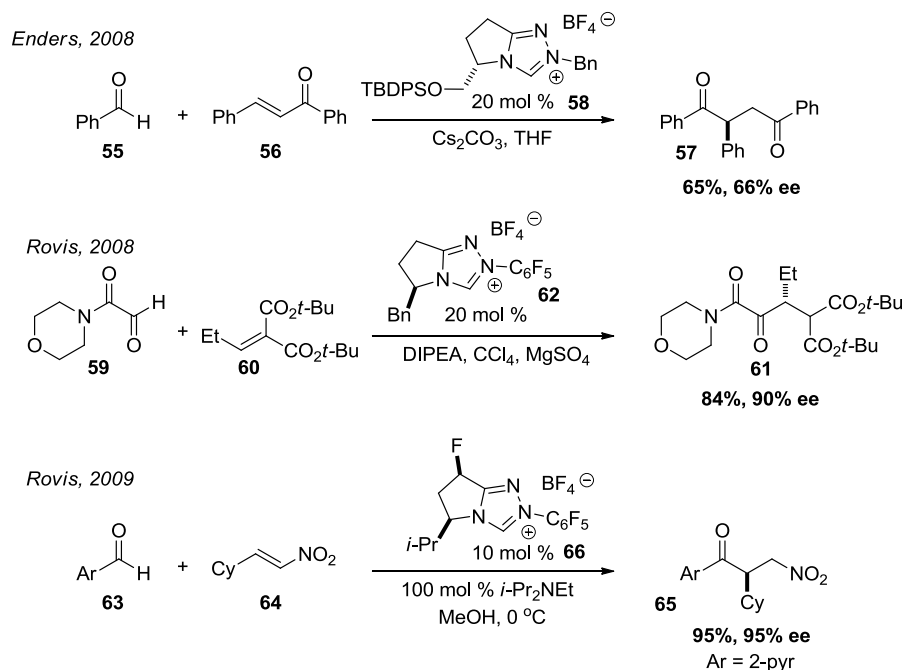


Figure 1.12

1.1.4 Stetter Reactions in Total Synthesis

The Stetter reaction is a powerful method to form 1,4-difunctionalized products but its use in the total synthesis of natural products has been limited. Shortly after his discovery of the reaction, Stetter used his method to synthesize the fragrance compound *cis*-jasmon (**72**) (Figure 1.13).³¹ A thiazolidene catalyzed addition of aliphatic aldehyde **67** to methyl vinyl ketone (**68**) forms a diketone (**71**) which undergoes an aldol condensation to produce the natural product. A similar Stetter-aldol sequence was used by Galopin in the synthesis of *trans*-sabinene hydrate (**77**).³²

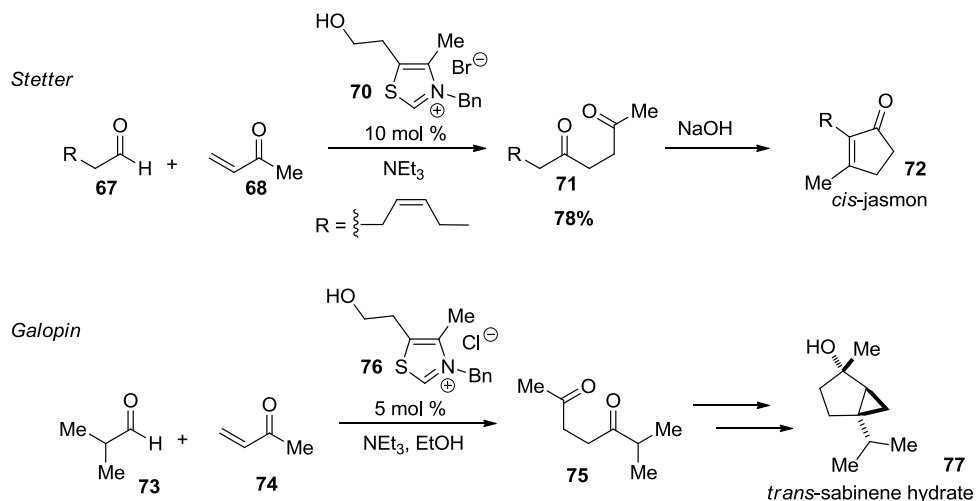


Figure 1.13

Trost and coworkers reported the first asymmetric synthesis of (+/-) hirsutic acid C using a Stetter reaction as one of the key steps (Figure 1.14).³³ Aldehyde **78** undergoes an intramolecular Stetter to form tricyclic ketone **79**. Unfortunately 230 mol % of thiazolium salt **80** was necessary to attain a reasonable yield. Nicolaou and co-workers have illustrated a triazolidene-mediated Stetter as an important C-C bond formation in their formal synthesis of platensimycin.³⁴ When aliphatic aldehyde **82** is treated with a stoichiometric amount of carbene generated from **84**, the Stetter adduct is produced in 64% yield and 20:1 dr. Another natural product, roseophilin, was completed by Tius and coworkers using a catalytic, intermolecular Stetter reaction and a ring-closing metathesis as the key steps.³⁵

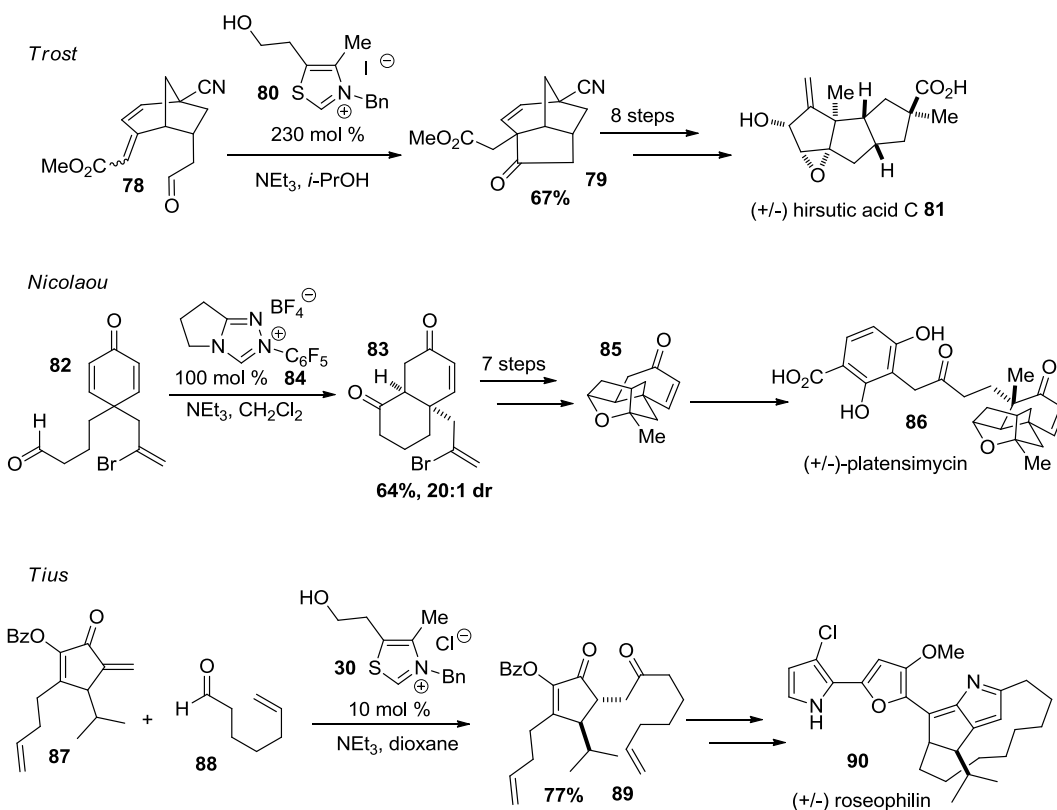


Figure 1.14

Diastereoselective Stetter reactions have been implemented in the synthesis of a few complex molecules. Although the enantioselective Stetter reaction shows great potential for the construction of complex molecules, it has only been explored in a couple of systems. In 2008, the Rovis group synthesized the core of FD-838 employing a highly enantioselective Stetter reaction.³⁶ An aliphatic aldehyde tethered to a maleimide was treated with chiral triazolium **37** and KHMDS to afford spirocyclic **92** in 99% ee (Figure 1.15). The Rovis group also developed a photoisomerization/Stetter sequence to access 8-epi-cephalimysin.³⁷ E-enal **95** was isomerized to the reactive Z-enal with ultraviolet light and the resulting aldehyde underwent an enantioselective Stetter reaction to yield spirocycle **96** in 95% ee.

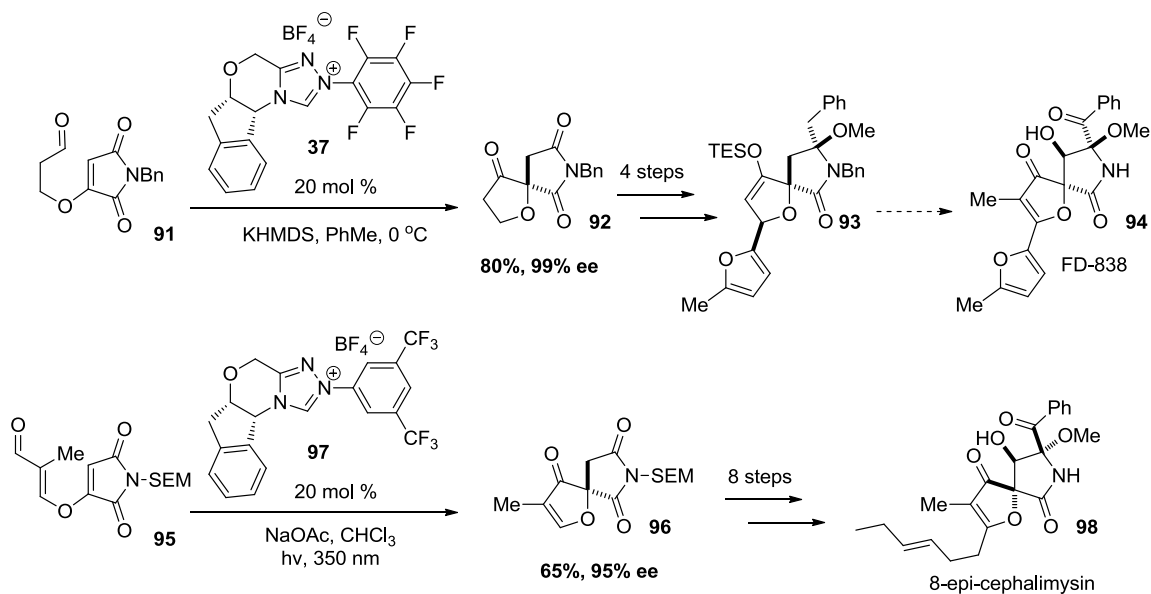


Figure 1.15

1.1.5 Conclusion

NHCs are versatile catalysts that have been used in the benzoin and Stetter reactions. After Ukai first reported thiamin to be an effective catalyst for the benzoin reaction, Enders introduced a new triazolium-based catalyst that paved the way for the development of asymmetric benzoin and Stetter reactions. The Rovis group built on this discovery by constructing new triazolium precatalyst scaffolds that achieved excellent enantioselectivities in both the intra- and intermolecular Stetter reactions. These synthetic methods have been applied to a number of natural products, but the potential of the enantioselective Stetter reaction has yet to be fully realized.

1.2 Stemocurtisine

1.2.1 Introduction

The Rovis group has shown the power of the Stetter reaction through the publication of particular methodologies, but we were also interested in applying these tools to the asymmetric synthesis of natural products. In doing so, this would both highlight the strengths of the Stetter reaction and identify shortcomings that need to be addressed. Currently, there are no completed natural product syntheses that utilize an asymmetric Stetter reaction; however, the synthesis of 8-epi-cephalimysin (**98**) is very close.³⁷

1.2.2 *Stemona* Alkaloids

The *Stemona* alkaloids are a unique class of complex natural products, which are exclusively isolated from the Stemonaceae family in Southeast Asia.³⁸ Initial investigations of these plants were driven by their use in traditional Chinese and Japanese medicine as anti-cough remedies and anthelmintics.³⁹ Even today, the roots and extracts are offered for sale in Asian markets and online. Currently, almost 100 *Stemona* alkaloids have been isolated and most of the alkaloids share a common pyrrolo[1,2- α]-azepine core (**99**). Starting in 2003, a handful of natural products were isolated containing a pyrido[1,2- α]-azepine motif (**100**) (Figure 1.16).⁴⁰ The first of these new alkaloids to be identified was stemocurtisine (**101**) (Figure 1.16).⁴¹ It was isolated in Thailand from the root extract of *Stemona curtisii* by Pyne and coworkers. The structure was elucidated using X-ray crystallography with the absolute stereochemistry assumed on the basis of the known configurations of similar *Stemona* alkaloids.⁴² It should be noted that none of the pyrido[1,2- α]-azepine containing compounds have had their absolute stereochemistry confirmed.

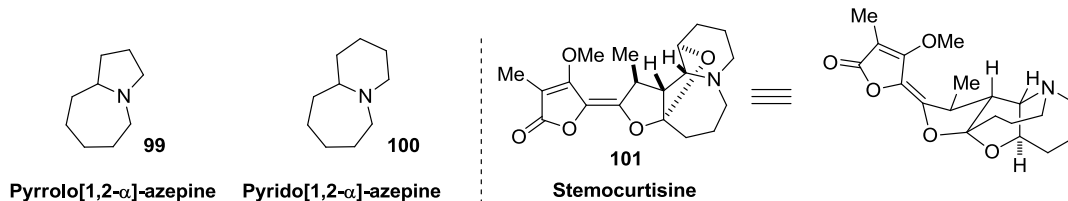


Figure 1.16

Although its biological properties are largely unexplored, stemocurtisine (**101**) exhibits larvicidal activity on malaria carrying mosquito larva with an LC_{50} of 18 ppm.⁴³ It also has mild insecticidal properties towards neonate larvae of *Spodoptera littoralis*, more commonly known as the cotton leaf worm, with an LC_{50} value of 149 ppm (Figure 1.17).⁴⁴ While this is not a very effective concentration, the closely related oxystemokerrine (**102**) has an LC_{50} of 5.9 ppm. The most potent of the *Stemona* alkaloids is hexacyclic didehydrostemofoline, also known as asparagamine A (**103**), and it has an LC_{50} value of 0.8 ppm (Figure 1.17). To put this in perspective, one of the more promising insecticides azadirachtin has an LC_{50} of 8.2 ppm. This demonstrates that the *Stemona* alkaloids and their derivatives have the potential to be developed into a potent and practical insecticide.

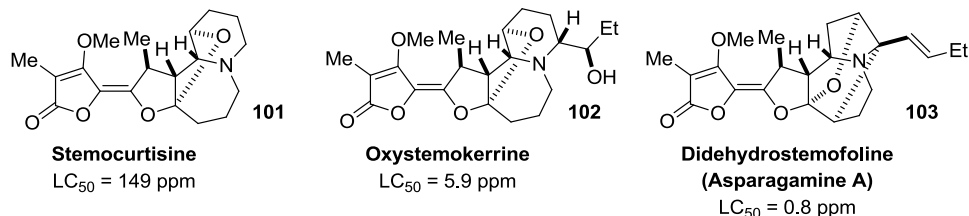


Figure 1.17

1.2.3 Total Synthesis of *Stemona* Alkaloids

The complex architecture and the promising biological activities of the *Stemona* alkaloids make them attractive targets for total synthesis. Less than 20% of the molecules containing the

pyrrolo[1,2- α]-azepine core have been synthesized and only 6 were achieved enantioselectively. Currently, there are no reported syntheses of stemocurtisine or any of the other pyrido[1,2- α]-azepines. Two of the most significant *Stemona* alkaloid total syntheses are Kende's approach to isostemofoline (**110**) and Overman's synthesis of asparagine A (**103**). Kende's work produced one of the first syntheses of the *Stemona* alkaloids employing a formal [4+3] cycloaddition as the key step (Figure 1.18).⁴⁵ Readily available pyrrole **104** underwent a [4+3] cycloaddition with diazo compound **105** in the presence of a rhodium catalyst to form [3.2.1] azabicycle **106**. After a 16-step sequence of transformations, the bicyclic core was converted to aldehyde **107**. Lithium enolate **108** was added into the aldehyde followed by a Dess-Martin oxidation to afford ketone **109**. Upon treatment with TFA, the MOM and Boc groups were removed and a cascade cyclization formed the pentacyclic core. The resulting alcohol was dehydrated with TFAA to form (\pm) isostemofoline (**110**) in 0.008% yield over 27 linear steps. It should be noted that the final step was low yielding because of a competing retroaldol reaction.

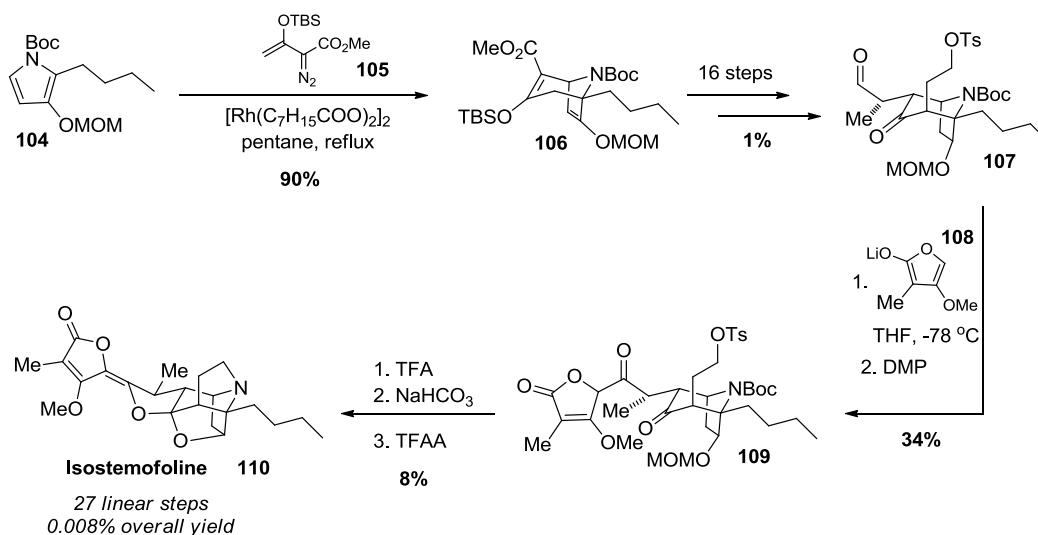


Figure 1.18

Overman's synthesis of asparagine A (**103**) commenced with a Diels-Alder cycloaddition of pyrrole **111** and the regioinverted ketene equivalent **112** (Figure 1.19).⁴⁶ After hydrogenation, the resulting [2.2.1] azabicyclo system **113** was subjected to nine standard transformations to afford amine hydroiodide salt **114**. Treatment of compound **114** with formaldehyde commenced an aza-Cope/Mannich cascade, which generated the desired tricyclo **115** in good yield. After eleven standard transformations, aldehyde **116** was obtained and subjected to an enolate addition of **108**. This was followed by alcohol deprotection and IBX oxidation to produce dihemiacetal **117**. The thiocarbamate of **117** was formed and treated with trimethyl phosphite in a Corey-Winter reaction to produce (±)-asparagine A (**103**) in 0.06% yield over 28 steps. Overman's synthesis was better yielding and the end-game strategy alleviated the retro-aldol problems that Kende's synthesis suffered.

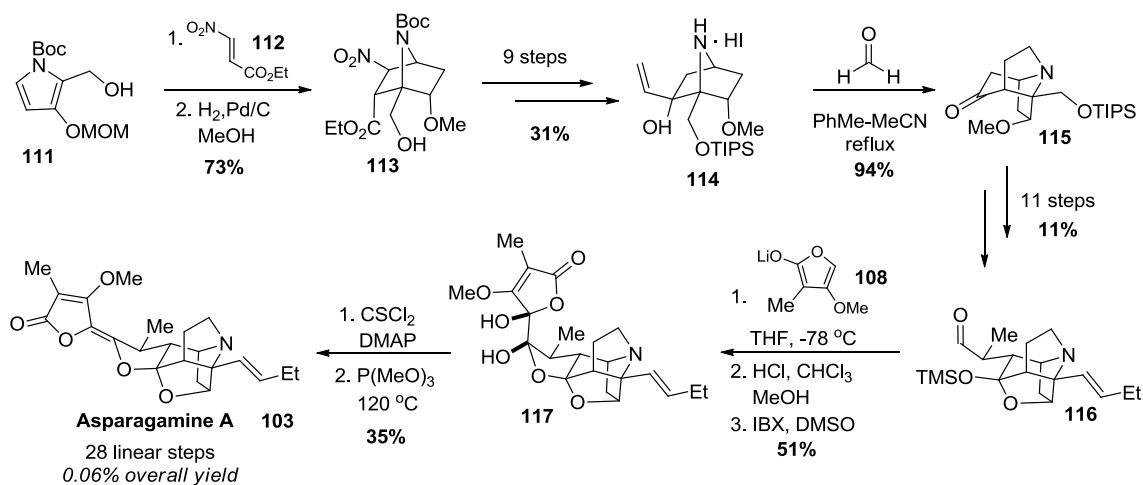


Figure 1.19

1.2.4 Previous Work Toward Asparagine A in the Rovis Group

Within the Rovis group, graduate student Mark Kerr used the Stetter reaction to set the key all carbon quaternary stereocenter in asparagine A.⁴⁷ Stetter precursor **119** was synthesized in

five steps from diethyl malonate (**118**) (Figure 1.20). Using chiral triazolium precatalyst **54** and KHMDS, the Stetter reaction was executed in good yield and 91% ee. Following Boc deprotection the HCl salt **120** was isolated. Although intermediate **120** was never further elaborated, this example shows the Stetter reaction's potential for application toward the *Stemona* alkaloids.

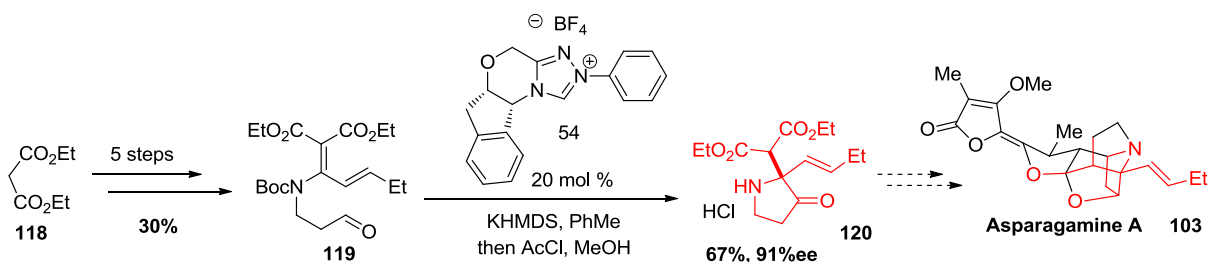


Figure 1.20

1.2.5 Conclusion

The *Stemona* alkaloids are a family of compounds that are structurally complex, biologically interesting and relatively unexplored through synthesis. In particular, stemocurtisine and related pyrido[1,2- α]-azepines have never been synthesized and their absolute stereochemistry has yet to be definitively assigned. We believe that the Stetter reaction provides a great way to access these molecules in a stereoselective manner.

References

- ¹ Bourissou, D.; Guerret, O.; Gabbai, F. P.; Bertrand, G. *Chem. Rev.* **2000**, *100*, 39-91.
- ² H.-W. Wanzlick and E. Schikora. *Angew. Chem.* **1960**, *72*, 494.
- ³ Igau, A.; Grutzmacher, H.; Baceiredo, A.; Bertrand, G. *J. Am. Chem. Soc.* **1988**, *110*, 6463–6466.
- ⁴ (a) Enders, D.; Breuer, K.; Raabe, G.; Runsink, J.; Teles, J. H.; Melder, J. P.; Ebel, K.; Brode, S. *Angew. Chem. Int. Ed.* **1995**, *34*, 1021-1023. (b) Enders, D.; Niemeier, O.; Henseler, A. *Chem. Rev.* **2007**, *107*, 5606-5655.
- ⁵ Wohler, F.; Liebig, J.; *Annalen der Pharmacie* **1832**, 249-282.
- ⁶ Lapworth, A. *J. Chem. Soc.* **1903**, *83*, 995-1005.
- ⁷ Breslow, R. *J. Chem. Soc.* **1958**, *80*, 995-1005.
- ⁸ Ukai, T.; Tanaka, R.; Dokawa, T. *J. Pharm. Soc. Jpn.* **1943**, *63*, 296-300.
- ⁹ Sheehan, J. C.; Hunneman, D. H. *J. Am. Chem. Soc.* **1966**, *88*, 3666-3667.
- ¹⁰ Knight, R. L.; Leeper, F. J. *J. Chem. Soc., Perkin Trans. 1*, **1998**, 1891-1893.
- ¹¹ (a) Sheehan J. C.; Hara, T. *J. Org. Chem.* **1974**, *39*, 1196-1199. (b) Tagaki, W.; Tamura, Y.; Yano, Y. *Bull. Chem. Soc. Jpn.* **1980**, *53*, 874-880. (c) Castells, J.; Lopez-Calahorra, F. *Tetrahedron Lett.* **1993**, *34*, 521-524. (d) Yamashita, K.; Sasaki, S.; Osaki, T.; Nango, M.; Tsuda, K. *Tetrahedron Lett.* **1995**, *36*, 4817-4820.
- ¹² Enders, D.; Kallfass, U. *Angew. Chem. Int. Ed.* **2002**, *41*, 1743-1745.
- ¹³ (a) Stetter, H.; Schreckenber, M. *Angew. Chem. Int. Ed. Engl.* **1973**, *12*, 81. (b) Stetter, H.; Kuhlmann, H. *Chem. Ber.* **1976**, *109*, 2890-2896.
- ¹⁴ Stetter, H.; Kuhlmann, H. *Organic Reactions*, Vol. 40; Paquette, L. A.; Ed.; Wiley: New York, **1991**, 407-496.

- ¹⁵ Hawkes, K. J.; Yates, B. F. *Eur. J. Org. Chem.* **2008**, *33*, 5563-5570.
- ¹⁶ Ciganek, E. *Synthesis*, **1995**, 1311-1314.
- ¹⁷ Enders, D.; Breuer, K.; Runsink, J.; Teles, J. H. *Helv. Chim Acta* **1996**, *79*, 1899-1902.
- ¹⁸ Mennen, S. M.; Blank, J. T.; Tran-Dube, M. B.; Imbriglio, J. E.; Miller, S. J. *Chem. Commun.* **2005**, 195-197.
- ¹⁹ (a) Moore, J. L.; Silvestri, A. P.; Read de Alaniz, J.; DiRocco, D. A.; Rovis, T. *Org. Lett.* **2011**, *13*, 1742-1745. (b) Singleton, D. A.; Rovis, T. *Unpublished Results*.
- ²⁰ Rovis, T. *Chem. Lett.* **2008**, *37*, 2-7.
- ²¹ (a) Kerr, M.; Read de Alaniz, J.; Rovis, T. *J. Am. Chem. Soc.* **2002**, *124*, 10298-10299. (b) Kerr, M.; Read de Alaniz, J.; Moore, J.; Rovis, T. *J. Org. Chem.* **2008**, *73*, 2033-2040.
- ²² Kerr, M. S.; Rovis, T. *J. Am. Chem. Soc.* **2004**, *126*, 8876-8877.
- ²³ (a) Liu, Q.; Rovis, T. *J. Am. Chem. Soc.* **2006**, *128*, 2552-2553. (b) Liu, Q.; Rovis, T. *Org. Process Res. Dev.* **2007**, *11*, 598-604.
- ²⁴ Reynolds, N. T.; Rovis, T. *Tetrahedron* **2005**, *61*, 6368-6378.
- ²⁵ Read de Alaniz, J.; Rovis, T. *J. Am. Chem. Soc.* **2005**, *127*, 6284-6289.
- ²⁶ Piel, I.; Steinmetz, M.; Hirano, K.; Fröhlich, R.; Grimme, S.; Glorius, F. *Angew. Chem. Int. Ed.* **2011**, *50*, 4983-4987. (b) Bugaut, X.; Liu, F.; Glorius, F. *J. Am. Chem. Soc.* **2011**, *133*, 8130-8133. (c) Liu, F.; Bugaut, X.; Schedler, M.; Fröhlich, R.; Glorius, F. *Angew. Chem. Int. Ed.* **2011**, *50*, 12626-12630.
- ²⁷ DiRocco, D. A.; Rovis, T. *Angew. Chem. Int. Ed.* **2011**, *50*, 7982-7983.
- ²⁸ Enders, D. *Chem. Commun.* **2008**, 3989-3991.
- ²⁹ (a) Liu, Q.; Perreault, S.; Rovis, T. *J. Am. Chem. Soc.* **2008**, *130*, 14066-14067. (b) Liu, Q.; Rovis, T. *Org. Lett.* **2009**, *11*, 2856-2859.

- ³⁰ (a) DiRocco, D. A.; Oberg, K. M.; Dalton, D. M.; Rovis, T. *Journal of the American Chemical Society* **2009**, *131*, 10872-10874. (b) DiRocco, D. A.; Rovis, T. *J. Am. Chem. Soc.* **2011**, *133*, 10402-10405. (c) Um, J. M.; DiRocco, D. A.; Noey, E. L.; Rovis, T.; Houk, K. N *J. Am. Chem. Soc.* **2011**, *133*, 11249-11254 .
- ³¹ Stetter, H.; Kuhlmann, H.; *Synthesis* **1975**, 379.
- ³² Galopin, C. C. *Tetrahedron Lett.* **2001**, *42*, 5589.
- ³³ Trost, B. H.; Shuey, C. D.; DiNinno, F.; McElvain, S. S. *J. Am. Chem. Soc.* **1979**, *101*, 1284.
- ³⁴ Nicolaou, K. C.; Tang, Y.; Wang, J. *Chem. Commun.* **2007**, 1922.
- ³⁵ Harrington, P. E.; Tius, M. A. *Org. Lett.* **1999**, *1*, 649.
- ³⁶ Orellana, A.; Rovis, T. *Chem. Commun.* **2008**, 730.
- ³⁷ Stephen P. Lathrop, Ph.D. Thesis Colorado State University **2011**.
- ³⁸ (a) Pilli, R. A.; Ferreira de Oliveira, M. C. *Nat. Prod. Rep.* **2000**, *17*, 117. (b) Greger, H. *Planta Med.* **2006**, *72*, 99. (c) Pilli, R. A.; Rosso, B. G.; Ferreira de Oliveira, M. C. *Nat. Prod. Rep.* **2010**, *27*, 1908-1937.
- ³⁹ Hou, J. P.; Jin, Y. *The Healing Power of Chinese Herbs and Medicinal Recipes*, The Haworth Press Inc.: Binghamton, New York, **2005**.
- ⁴⁰ (a) Pyne, S. G.; Ung, A. T.; Jatisatiener, A.; Mungkornasawakul, P. *Mj. Int. J. Sci. and Tech.* **2007**, *1*, 157. (b) Schinnerl, J.; Brem, B.; But, P. P. H.; Vajraodaya, S.; Hofer, O.; Greger, H. *Phytochemistry* **2007**, *68*, 1417.
- ⁴¹ Mungkornasawakul, P.; Pyne, S. G.; Jatisatiener, A.; Supyen, D.; Lie, W.; Ung, A. T.; Skelton, B. W.; White, A. H. *J. Nat. Prod.* **2003**, *66*, 980.

- ⁴² Mungkornasawakul, P.; Matthews, H.; Ung, A. T.; Pyne, S. G.; Jatisatiener, A.; Lie, W.; Skelton, B. W.; White, A. H. *ACGC Chem. Res. Comm.* **2005**, *19*, 30.
- ⁴³ Mungkornasawakul, P.; Pyne, S. G.; Jatisatiener, A.; Supyen, D.; Jatisatiener, C.; Lie, W.; Ung, A. T.; Skelton, B. W.; White, A. H. *J. Nat. Prod.* **2004**, *67*, 675.
- ⁴⁴ (a) Kaltenecker, E.; Brem, B.; Mereiter, K.; Kalchhauser, H.; Kalhlig, H.; Hofer, O.; Vajraodaya, S.; Greger, H. *Phytochemistry* **2003**, *63*, 803.
- ⁴⁵ Kende, A. S.; Smalley, T. L. Jr.; Huang, H. *J. Am. Chem. Soc.* **1999**, *121*, 7431.
- ⁴⁶ Brüggemann, M.; McDonald, A. I.; Overman, L. E.; Rosen, M. D.; Schwink, L.; Scott, J. P. *J. Am. Chem. Soc.* **2003**, *125*, 15284.
- ⁴⁷ Mark S. Kerr, Ph.D. Thesis Colorado State University **2006**.

Chapter 2

Synthetic Efforts Toward Stemocurtisine via an Intramolecular Stetter Reaction

2.1 First Generation Approach

2.1.1 Retrosynthesis

The asymmetric Stetter reaction is a powerful yet underutilized method. We are particularly interested in applying our synthetic technology to the assembly of the structurally complex and synthetically unexplored *Stemona* alkaloid stemocurtisine (**1**). An initial look at stemocurtisine reveals a 1,4-carbonyl moiety (C1-C4) embedded in its core (Figure 2.1). We proposed that an intramolecular Stetter reaction of aldehyde **3** could be used to form the C-C bond between C-3 and C-4. Additionally, if a chiral catalyst was used, then the stereochemistry at C-2 and C-3 could be controlled.

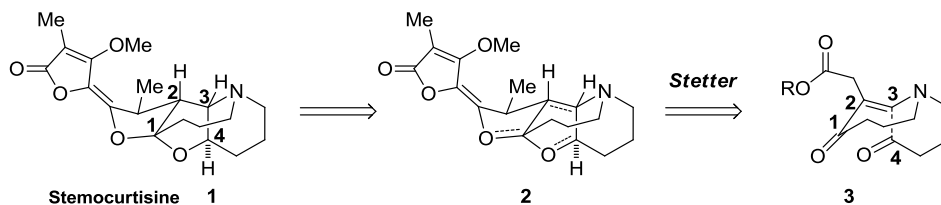


Figure 2.1

Working backwards from the natural product (**1**), we hypothesized that the “western” γ -ylidene tetronate fragment could be installed from lithium methyl tetronate addition into lactone **4** (Figure 2.2). If this is unsuccessful we could utilize the end-game sequence developed by Overman for asparagamine A (*vide supra*, Ch. 1, Sect.1.2.3). Lactone **4** could be derived from a reduction of diketone **5** followed by an acetalization cascade. The pyrido-azepine could be

formed from a Stetter reaction of an aliphatic aldehyde tethered to a vinylogous amide Michael acceptor (**6**).

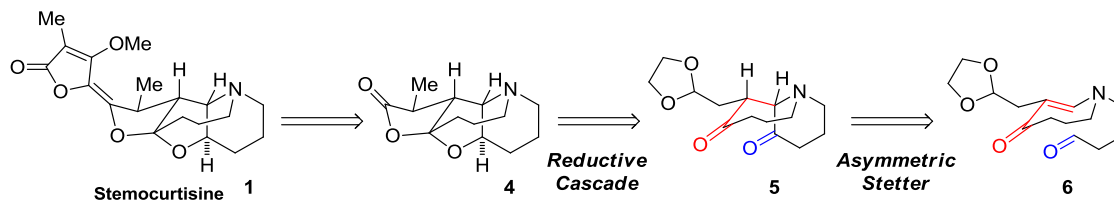


Figure 2.2

The Stetter reaction is proposed to proceed through a concerted hydroacylation affecting an overall *syn*-addition of the aldehyde and proton (*vide supra*, Ch. 1, Sect.1.1.3). If this mechanism holds true in the proposed Stetter of substrate (**6**), it will form product **7** which contains the wrong relative stereochemistry (Figure 2.1.2). To solve this problem, we propose that the *cis*-vinylogous amide **6** be photoisomerized to *trans*-olefin **8** which will undergo a subsequent Stetter reaction to afford azabicyclic **5** containing the correct stereochemistry (Figure 2.3). Additionally, *trans*-olefin **8** should be much more reactive than *cis*-olefin **6** because its ground-state energy is higher. This will prevent formation of the undesired diastereomer and potentially increase the reactivity of our substrate.

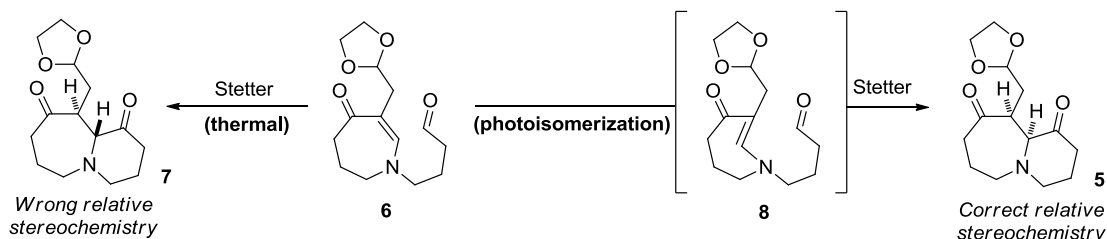


Figure 2.3

This type of photoisomerization reactivity was first demonstrated by Eaton and Corey.⁴⁸ They observed *trans*-fused Diels-Alder products when ultraviolet light was implemented. Specifically, enone **9** was pretreated with UV light and then reacted with cyclopentadiene **11** in the dark at low temperatures. To their delight, the *trans*-fused product **12** was formed exclusively (Figure 2.4). It was hypothesized that a *trans*-enone intermediate **10** was operative and this was supported using infrared and ultraviolet spectroscopy. There have been a number of groups who have applied this reactivity,⁴⁹ but one of the more important developments was by Rawal. His group expanded on this methodology by demonstrating that triene **13** undergoes a Diels-Alder in the presence of UV light forming a product with *trans*-geometry at the top ring juncture.⁵⁰ When the same substrate was reacted without UV light, very forcing conditions were necessary to provide the *cis*-fused product. The increase in reactivity found with the UV light conditions can be explained by the higher ground state energy of the *trans*-cycloheptenone intermediate (**15**). Davies also illustrated the power of this methodology by applying it toward the synthesis of Vibsanin E.⁵¹ An intermolecular Diels-Alder of 2-methyl butadiene **18** and *trans*-cycloheptenone intermediate **19** produced products **20** and **21** which both contained *trans*-ring junctions. More relevant to our proposal is Beauchemin's work, which demonstrates that benzimidazole **24** will add 1,4 to cycloheptenone **22** at room temperature using UV light (Figure 2.4).⁵² Under thermal conditions the conjugate addition product is never isolated. They also propose a *trans*-cycloheptenone intermediate which they observed by NMR at low temperatures. These results gave us confidence that a photoisomerization of Stetter substrate **6** was plausible.

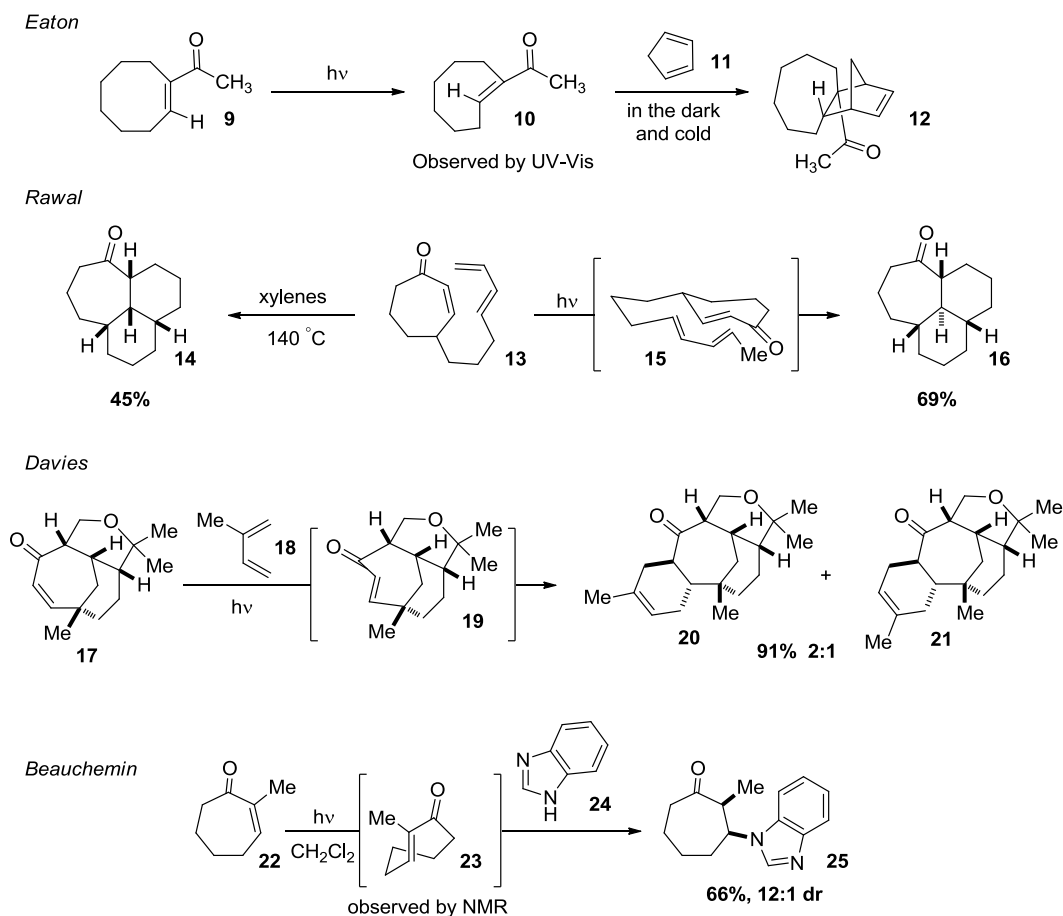


Figure 2.4

2.1.2 Photoisomerization Stetter Results

We proposed that the aldehyde required for the photoisomerization/Stetter could be synthesized in four steps. First, pyrrolidinone (**26**) would be condensed with aldehyde **27**. Then the *N*-vinyl amide (**28**) would be transformed to the seven membered vinylogous amide (**29**) via a relatively unknown photochemical 1,3-shift.⁵³ This interesting Norrish Type I reaction proceeds through homolytic cleavage of the amide bond. Radical recombination with the other site of the allylic radical forms seven-membered imine **32** and subsequent tautomerization affords the product. This type of reactivity is common with esters as seen in the photo-Fries reaction, but there are

only a handful of examples involving amides. The tethered aldehyde required for the Stetter would be installed through alkylation and dimethyl acetal deprotection.

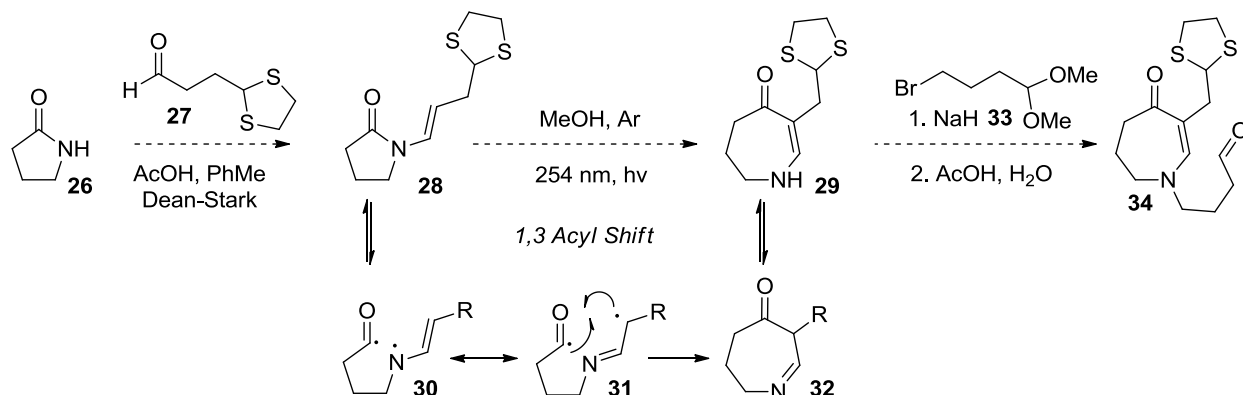


Figure 2.5

We began our synthetic investigation of the photoisomerization/Stetter reaction using a model system. Pyrrolidinone (**35**) was condensed with propionaldehyde, phenylacetaldehyde and hydrocinnamyl aldehyde to form the *N*-vinyl amides (**37-39**) in good yields. These products and commercially available *N*-vinyl pyrrolidinone were treated with 254 nm UV light in degassed methanol to yield the vinylogous amides (**40-43**).

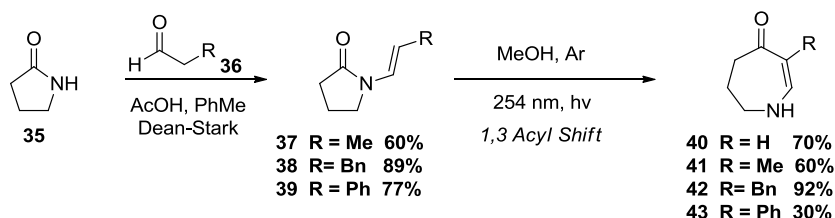


Figure 2.6

Amine **42** was coupled with alkyl bromide **33** in the presence of sodium hydride. The dimethyl acetal was deprotected with wet TFA to arrive at Stetter precursor **44**. A variety of Stetter

reactions were explored that included both photochemical and thermal conditions, but none of the desired pyrido-azepine **46** was observed.

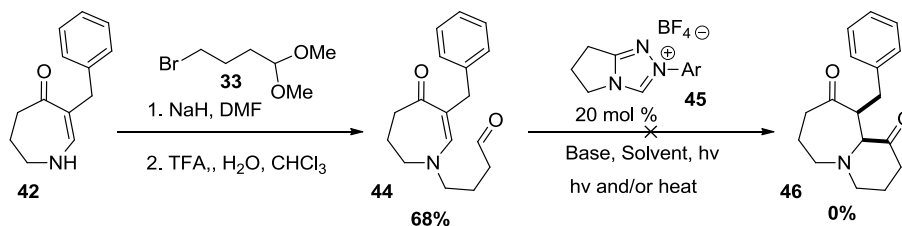


Figure 2.7

At this point we thought that the Michael acceptor might be too electron rich. One potential solution was to place a carbonyl on either side of the nitrogen to withdraw the electron density from the olefin. This was implemented by amidation of amines **40-43** with acid chloride **47**⁵⁴ followed by dithiane deprotection. All four aldehydes were screened with a variety of triazolium precatalysts, bases and solvents. Unfortunately none of the desired product was ever isolated. Most of the reactions resulted in starting material decomposition or benzoin aldehyde homodimerization.

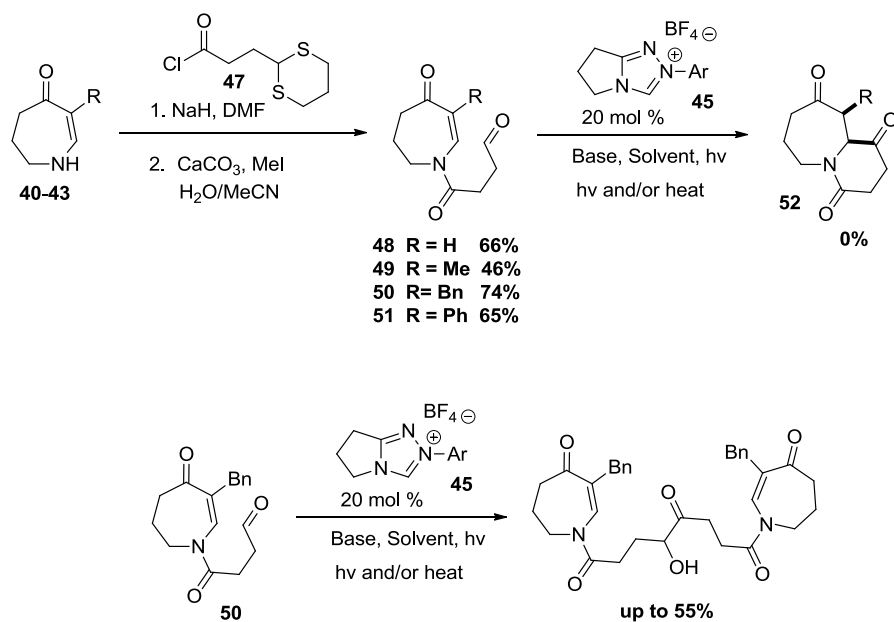


Figure 2.8

We next tried to install a carbonyl adjacent to the nitrogen within the seven-membered ring. We started by alkylating succinimide (**53**) with allyl bromide and isomerizing the terminal-olefin using [Ir(COD)Cl]₂ (Figure 2.9).⁵⁵ This imide was then exposed to 254 nm light in degassed methanol, but the desired vinylogous amide was not formed. Instead, the imine and methanol aminal adduct were observed by crude NMR, but they decomposed upon chromatography. To circumvent the methanol addition problem, the imide photo-rearrangement was run using non-nucleophilic solvents like hexanes, ether and acetonitrile, but again, the vinylogous amide synthesis was unsuccessful. Although this route was not fully realized, the discovery of an unprecedented imide 1,3 acyl shift to form intermediate **55** is significant and may lead to new useful methodologies.

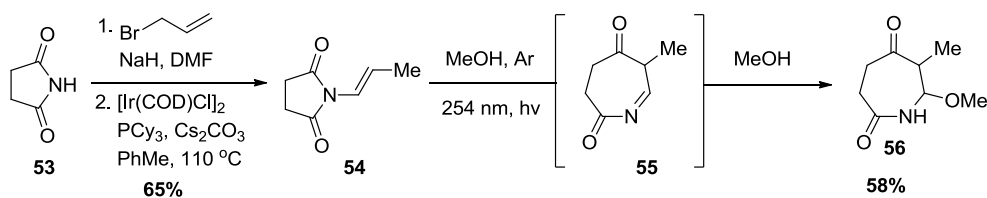


Figure 2.9

Another potential solution to the unreactive Michael acceptor was to add another electron withdrawing group on the alkene. Ester **57** was isolated in good yield after a Heck reaction of pyrrolidinone and methyl acrylate (Figure 2.10).⁵⁶ When treated with UV light in methanol, ester **57** isomerized to a mixture of *cis* and *trans*-olefins, but no photo-rearranged product was detected.

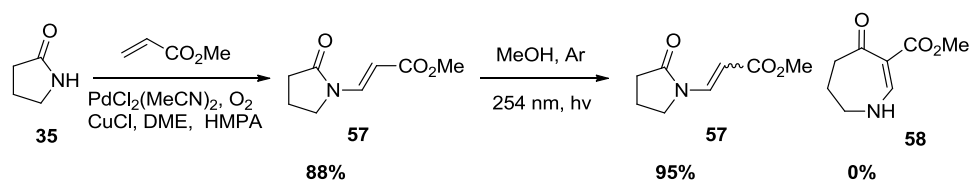


Figure 2.10

2.1.3 Summary

We proposed that the correct relative stereochemistry needed for the synthesis of stemocurtisine could be accessed via a novel photoisomerization Stetter reaction. A number of model system substrates were synthesized using a relatively unexplored photochemical 1,3 acyl shift. We tested our aldehydes in a variety of thermal and photochemical Stetter conditions, but we could not arrive at the desired pyrido-azepine.

2.2 Oxazine Strategy

Since our photoisomerization/Stetter reaction was unachievable, we revised our approach. Starting from diketone **5**, we envisioned that the seven-membered ring could be attained from an intramolecular *N*-alkylation or macrolactamization of amine **59** (Figure 2.11). After C-C bond rotation the hydrogen atoms on the two key stereocenters have a *trans*-relationship. The desired stereochemistry on **59** can be achieved from a diastereoselective Stetter reaction of an *E*-alkene. The configuration of the *E*-alkene can be easily controlled by locking it in a ring. We envisioned the ring could be formed through an N-O bond from the amine and the aldehyde. Using this strategy, intermediate **59** could be derived from cleavage of oxazinane **60**. An asymmetric Stetter reaction on the *E*-alkene of **61** would lead to the desired *trans*-diastereomer.

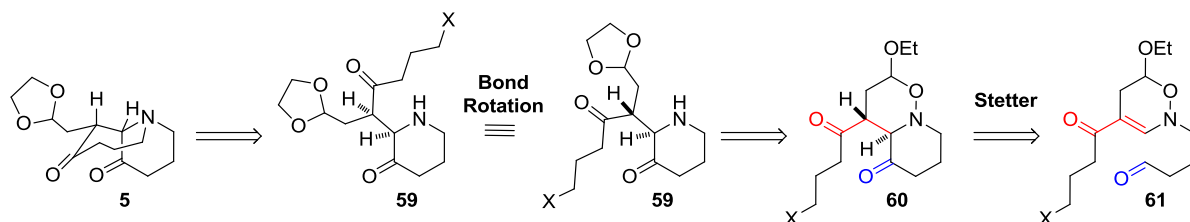


Figure 2.11

Synthesis of oxazine **61** began with a copper catalyzed cyclopropanation of diene **62** and methyl diazoacetate (**63**) to form cyclopropanol **64** (Figure 2.12).⁵⁷ Ring opening of the cyclopropanol with sodium nitrite delivered ketone **65**. Under silylating conditions, nitro ketone **65** forms a nitroso enone which subsequently undergoes a [4+2] cycloaddition with ethyl vinyl ether to deliver oxazine **67** after workup.⁵⁸ Subsequent coupling with acid chloride **47** and dithiane deprotection produces desired acyl oxazine **68**.⁵⁹ Aldehyde **68** was subjected to Stetter reaction conditions, but it resisted cyclization. Simple DFT calculations suggest the requisite amide geometry for the cyclization is disfavored, which can explain the observation of no product.

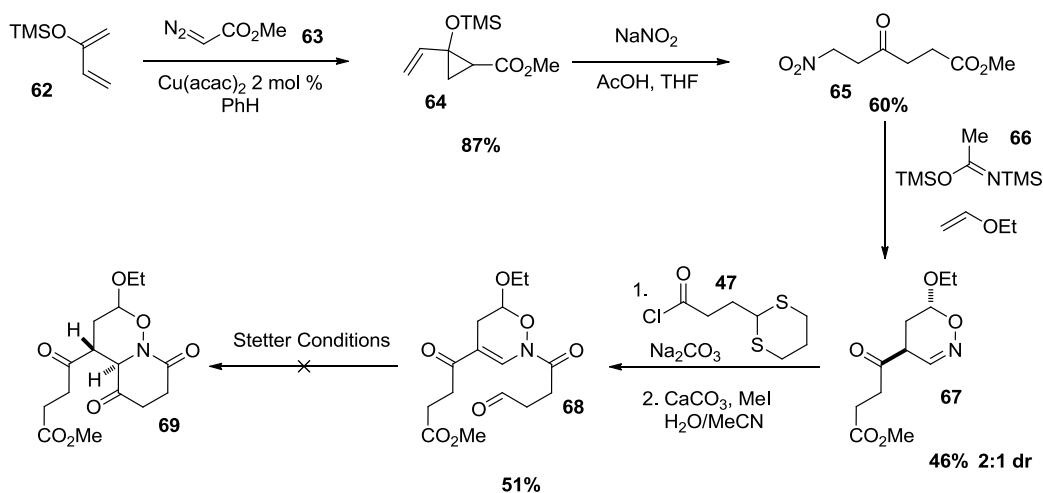


Figure 2.12

2.3 Pyrrole Dearomatization Strategy

Although the oxazine Stetter did not work, we thought a similar strategy could be used with a different ring tether. The previous retrosynthetic intermediate **59** could arise from hydrolysis of enamine **70**. This could be accessed from an unprecedented dearomatizing Stetter reaction of aldehyde **71** (Figure 2.13).

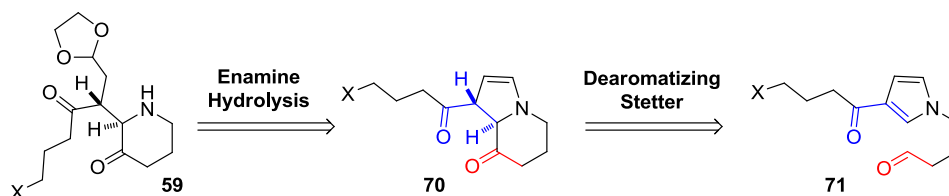


Figure 2.13

Asymmetric dearomatizations are uncommon and most utilize oxidative chemistry,⁶⁰ with more limited studies reporting alkylative methods.⁶¹ The reason these process are unfavorable is because they must overcome the aromatic stabilization energy. Pyrrole's aromatic stabilization energy of 22 kcal/mol is significantly less than that of benzene (36 kcal/mol), but it is still a

formidable barrier. In spite of this challenge there has been recent progress in the asymmetric dearomatization of pyrroles.⁶² Miyashita has shown that aldehydes can undergo nucleophilic aromatic substitution with 4-fluoronitrobenzene, demonstrating that acyl anion equivalents can be used to access dearomatized intermediates.⁶³

If successful, this methodology would be an extremely powerful way to construct chiral molecules from simple starting materials. Investigation into the viability of this strategy began with assembly of 3-acyl pyrrole **77** (Figure 2.14). TIPS protection of pyrrole (**72**) and subsequent Friedel-Crafts acylation with succinic anhydride delivers 3-acyl pyrrole **73**.⁶⁴ Esterification of **71** followed by amine deprotection and alkylation with homoallyl bromide (**75**) produces *N*-alkyl pyrrole **76**. Lemieux-Johnson oxidation then affords the Stetter precursor **75** in seven total steps. To our disappointment, treatment of aldehyde **77** with a number of different carbenes failed to produce desired Stetter product **78**. Instead, the benzoin-derived self-dimer was isolated. We hypothesize that the reaction is unproductive due to the high barrier to dearomatize the pyrrole.

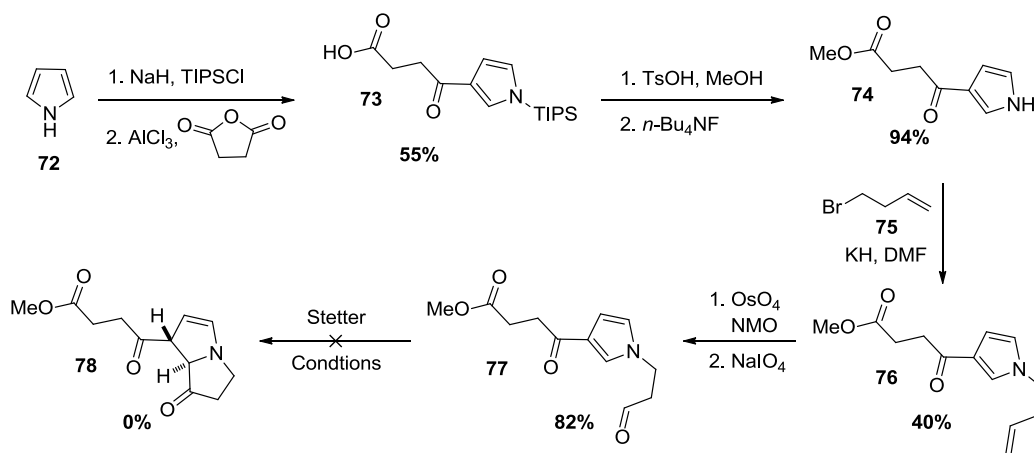


Figure 2.14

2.4. Pyrroline Strategy

2.4.1 Retrosynthesis

While the barrier for pyrrole dearomatization is too high to be broken by a moderate nucleophile like an acyl anion equivalent, we envisioned that this route could be salvaged by using a non-aromatic pyrroline substrate for the Stetter reaction (Figure 2.15). Piperidine **59** could result from oxidative cleavage of pyrrolidine **79**. This azabicyclic could arise from an asymmetric Stetter reaction of **80**, following pyrroline formation through a formal [3+2] cycloaddition of an enone and an isocyanoacetate.

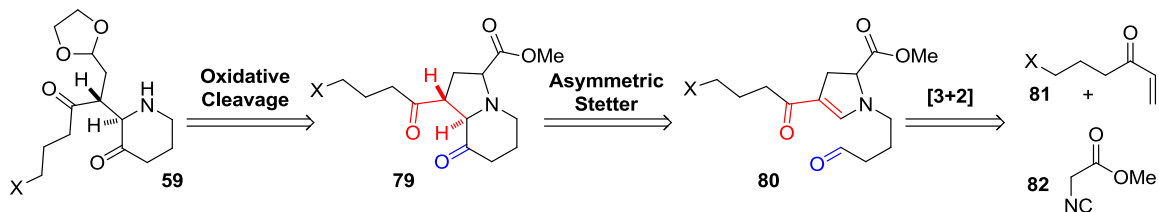


Figure 2.15

2.4.2 Vinylogous Amide Stetter

The new approach to stemocurtisine relied on 2-pyrroline **88** as the Stetter precursor (Figure 2.16). Not only would this substrate be more activated toward nucleophilic attack than the corresponding pyrrole, but its ester moiety would serve as a functional handle for later C-N bond cleavage. To begin the synthesis, dihydropyrrole **87** was accessed in excellent yield via a silver acetate-catalyzed [3+2] cycloaddition of enone **82**⁶⁵ and isocyanoacetate **84** (Figure 2.15).⁶⁶ The previous pyrrole route installed the aliphatic aldehyde using an alkylation followed by an

oxidative olefin cleavage. Unfortunately, these conditions readily oxidized the pyrroline to the unreactive pyrrole.

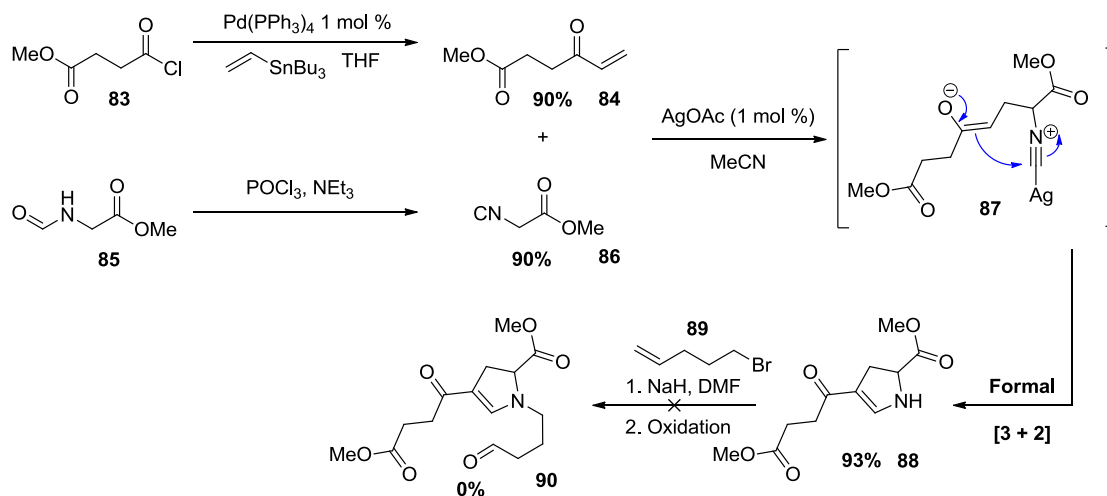
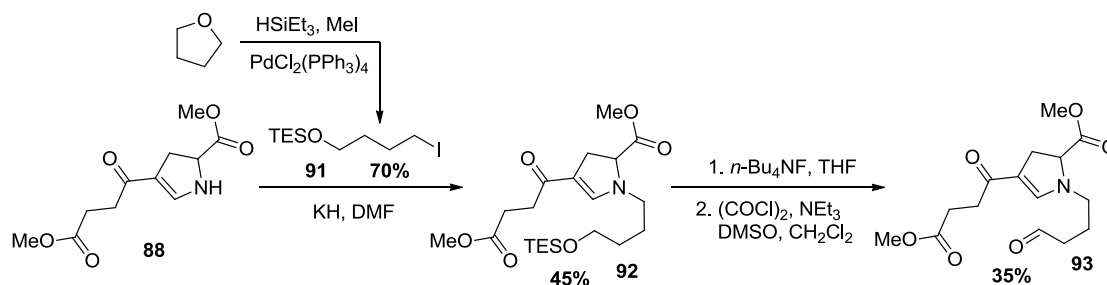


Figure 2.16

Alkyl iodide **91**, prepared from ring opening/iodosilation of THF, was coupled with pyrroline **88**. TBAF deprotection of the TES group and Swern oxidation delivered aldehyde **93** in five linear steps. At this point, **93** was subjected to Stetter reaction conditions, but no desired product was isolated (Figure 2.17). Instead, the benzoin aldehyde homodimerization product **95** was observed.



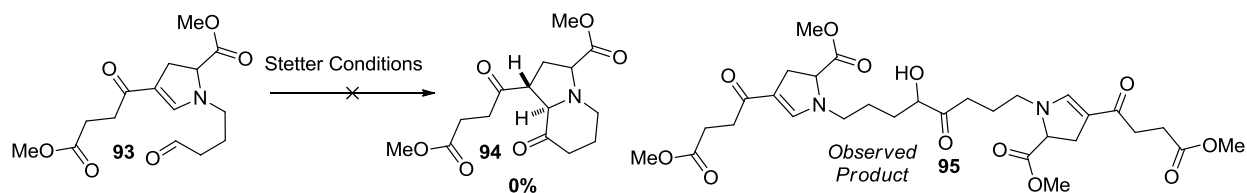


Figure 2.17

2.4.3 Vinylogous Imide Stetter

We believed that the Michael acceptor of the vinylogous amide was still too electron rich so we decided to test a vinylogous imide substrate. Our initial attempt began with a coupling of **88** with acid **96**⁶⁷ to afford amide **97** in 50% yield (Figure 2.18). To our dismay, attempts to deprotect the silyl alcohol resulted in decomposition to pyrroline **88**. This is presumed to proceed via acidic or basic formation of γ -butyrolactone (**99**). The decomposition could be avoided by performing a Swern oxidation directly on TES protected alcohol **100**, but the yields were low. A better approach employs dimethylacetal **104**⁶⁸ and pyrroline **103** which is made from the [3+2] of **84** and benzyloxyacetate.⁶⁹ The dimethyl acetal of this does not have the same lactonization problems as **97** and the benzyl ester allows for differentiation from the methyl ester. As we had hoped, the amidation of **103** and subsequent acidic deprotection delivered desired aldehyde **106**.

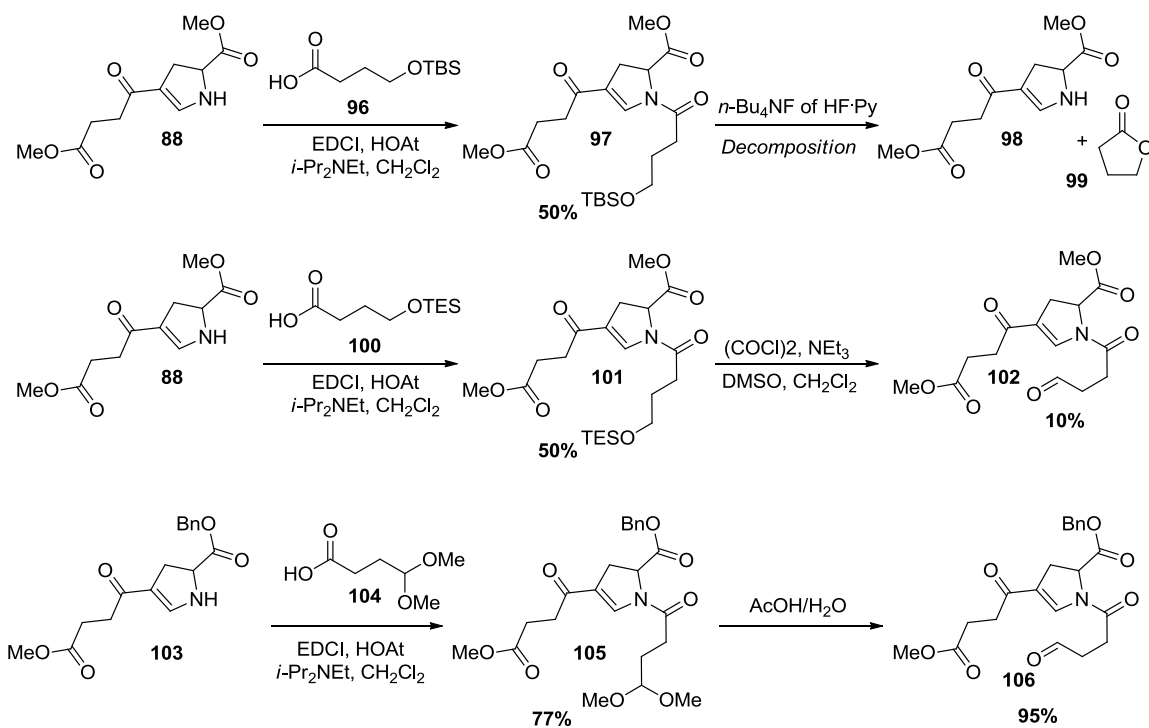


Figure 2.18

Vinylogous imide Stetter substrate **106** was subjected to triazolium precatalyst **107** and KHMDS. To our delight, the Stetter product was isolated in 65% yield and 2:1 dr (Figure 2.19).

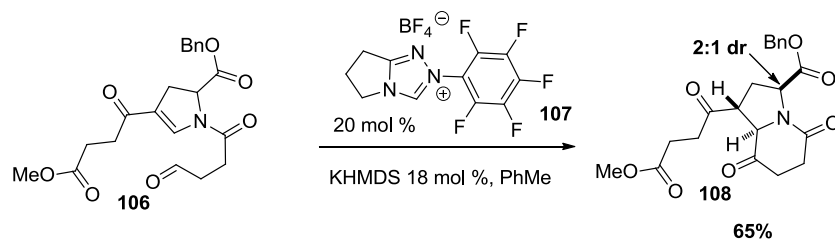


Figure 2.19

The 2:1 diastereoselectivity of Stetter product **108** was at the carbon containing the benzyl ester. This selectivity is irrelevant because the stereocenter will be destroyed when the ring is opened. The relative stereochemistry of **108** was confirmed by x-ray crystallography with the help of Derek Dalton (Figure 2.20).

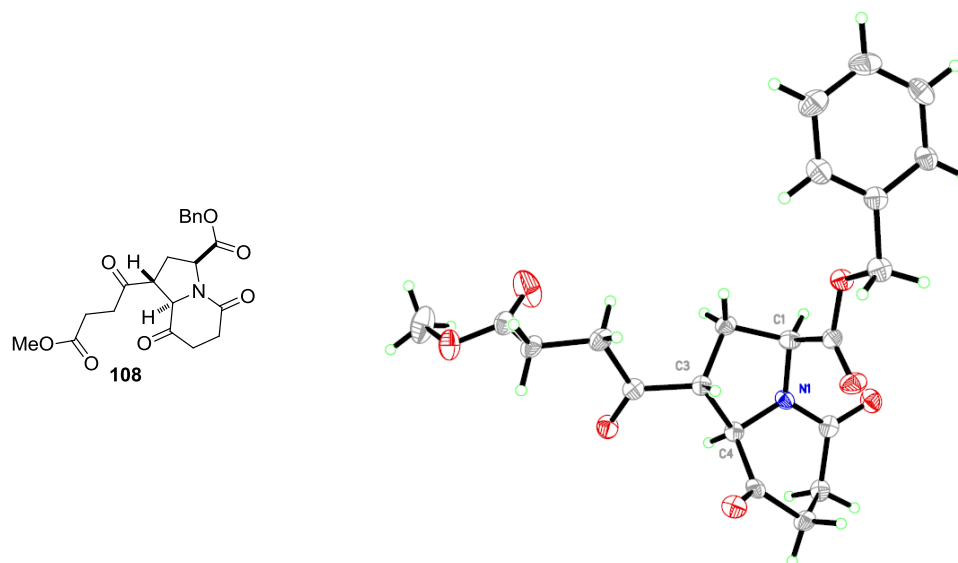


Figure 2.20

2.4.4 Enantioselective Stetter

After our success with the racemic Stetter reaction, we explored the asymmetric variant using our arsenal of chiral catalysts. In general, catalysts with electron rich or large aryl groups on the nitrogen give high enantioselectivity (up to 99% ee) but low yields (Figure 2.21). The electron deficient aryl catalysts give good yields but moderate to poor enantioselectivities. At this point, we were optimistic that this reaction could be further improved. However, we were uncertain if this would be the final substrate used in our synthesis, so instead of fully optimizing this reaction, we continued our synthesis to test its viability.

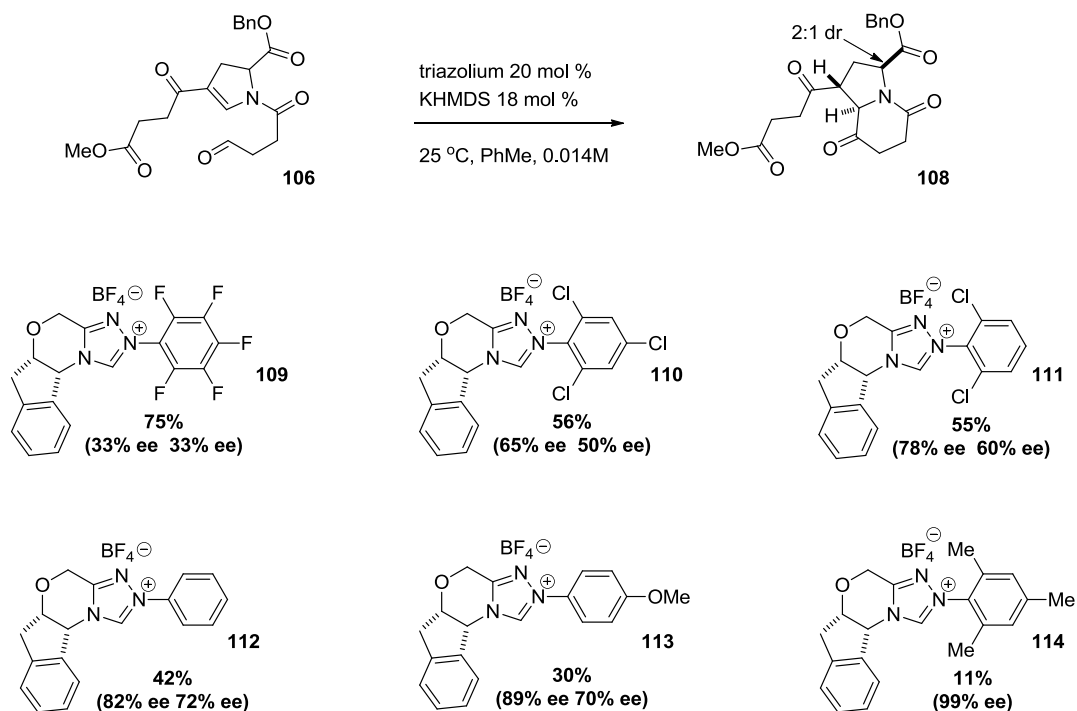


Figure 2.21

2.4.5 Pyrrolidine Ring Opening

The next step in the synthesis was cleavage the pyrrolidine ring in Stetter product **108**. The C-N bond adjacent to the benzyl ester of **108** would be oxidized to afford a ring opened product. We thought this could be accomplished through hydrolysis of the ester and ring opening via acyl azide formation followed by Curtius rearrangement and acid hydrolysis. This was first demonstrated by Sheehan using protected penicillin derivative **115** (Figure 2.20).⁷⁰

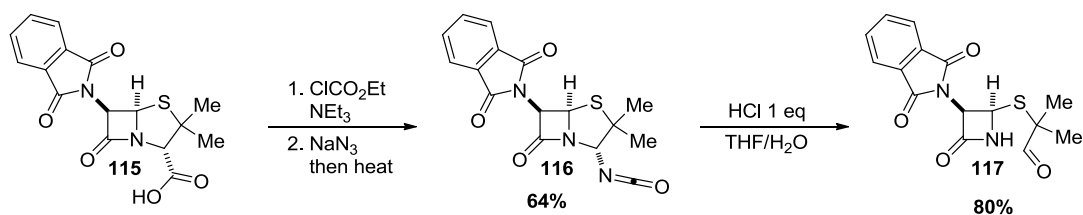


Figure 2.22

Using this tactic, we first reduced the benzyl ester to acid **118** using H₂ and Pd/C (Figure 2.23). This was followed by acyl azide formation and Curtius rearrangement to isocyanate **120**. This isocyanate was hydrolyzed in the presence of ethylene glycol to afford ring opened product **121**, albeit in low yield. Ester **121** was saponified with LiOH to deliver acid **122**, but the α -amino ketone stereocenter was epimerized. This issue was resolved with Nicolaou's mild procedure using trimethyl tin hydroxide and the resulting acid was cyclized to form the pyrido-azepine ring system (Figure 2.23).⁷¹

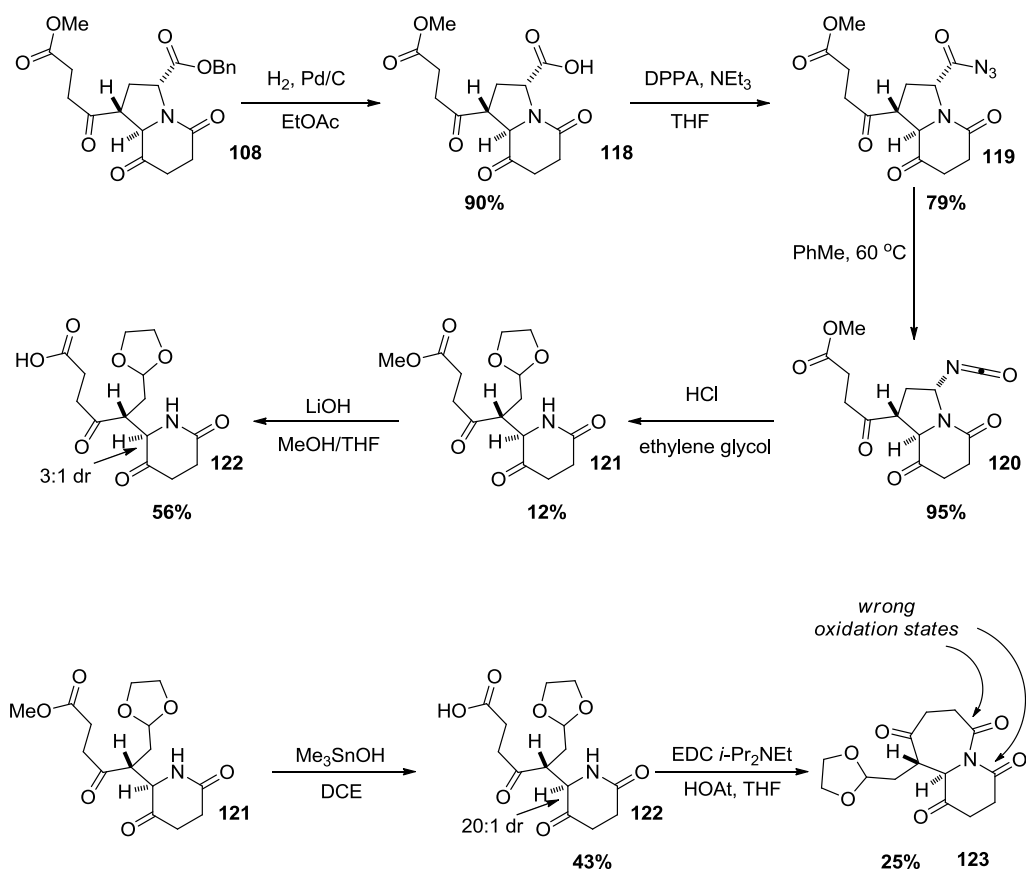


Figure 2.23

2.5 Route Optimization

This route seemed to be promising but some low yielding steps and the projected length of the synthesis were not ideal. We believed that it could be optimized by minimizing future redox transformations. Our substrate was not ideal because it has two ester carbons in the wrong oxidation state (Figure 2.23). By starting with the proper oxidation states we could reduce the step count and potentially increase the overall yield of our approach. We believed that an alkyl halide could be used in the place of the methyl ester in **106**. This would allow for the 7-membered ring to be formed via *N*-alkylation and there would not be any necessary reductions. Synthesis of this substrate began with a Kulinkovich reaction of ester **123** to form the cyclopropanol **124** (Figure 2.24).⁷² Using NBS, the cyclopropanol was opened and the resulting alkyl bromide elimination to form the desired enone. When enones **125** were reacted under our standard [3+2] conditions, none of the desired pyrrolines were isolated. Conditions using other silver or copper catalysts were also unsuccessful. Control experiments found that enone **123** was not being decomposed by the catalyst but the alkyl halide was inhibiting the [3+2] reaction.

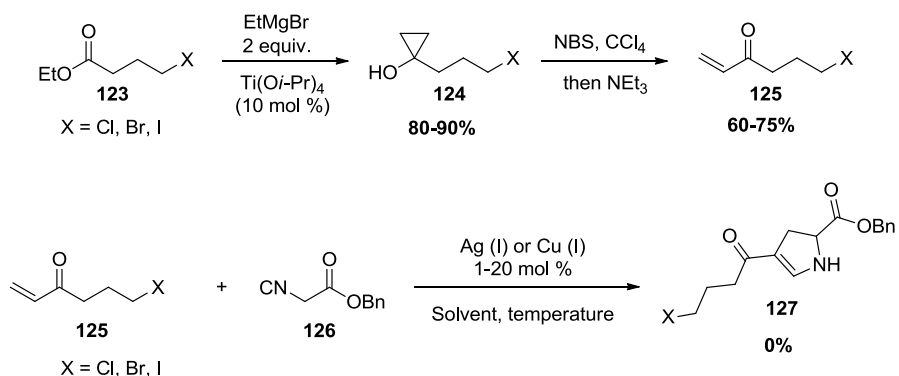


Figure 2.24

We thought a mesylated alcohol could avoid the problems presented by the halides. We synthesized mesyl alcohol **129** from γ -butyrolactone (**99**) using a sequence similar to the one used for the alkyl halides (Figure 2.25). When subjected to the [3+2] conditions, a cycloadduct was isolated but the mesyl alcohol had eliminated.

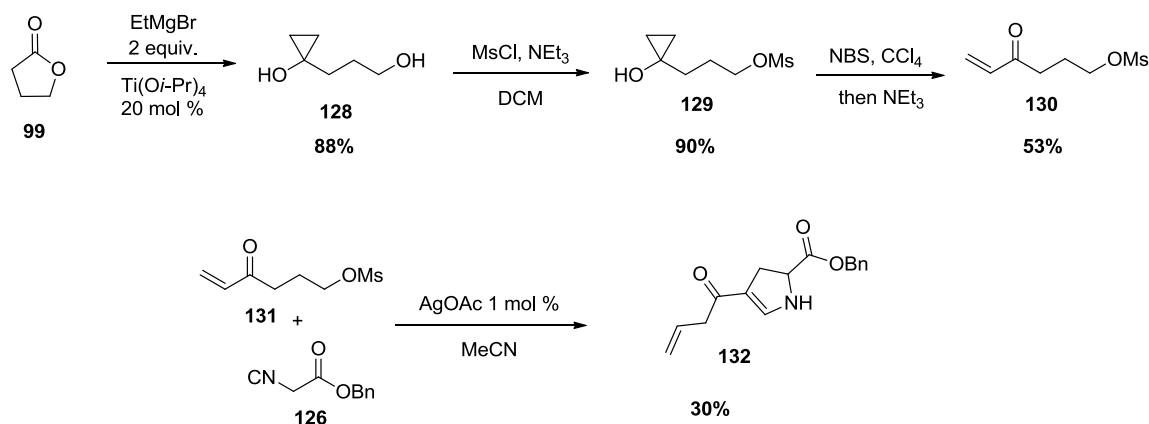


Figure 2.25

Determined to test this approach, we synthesized enone **135** (Figure 2.26). When **135** was reacted with isocyanoacetate **126** and a silver acetate catalyst, the pyrroline was isolated in 88% yield. Vinylogous amide **136** was coupled with acid **137** and the dimethyl acetal was deprotected to reveal aldehyde **138**.

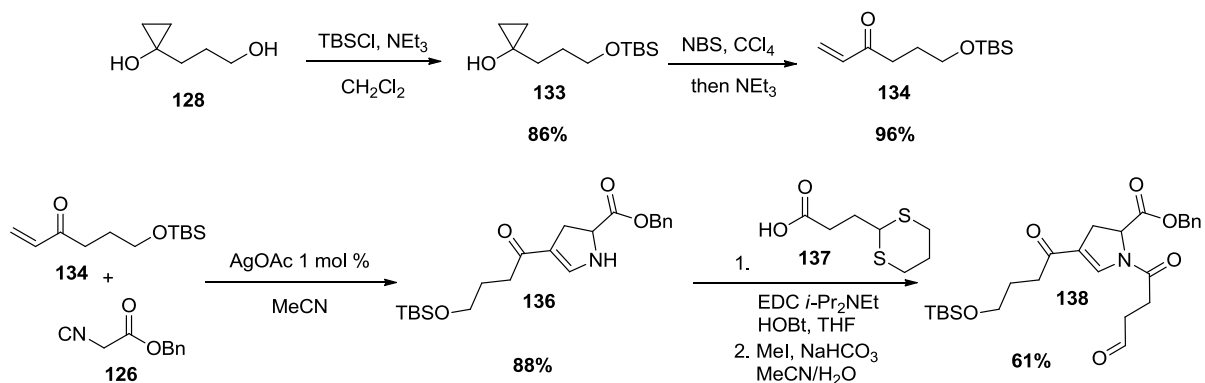


Figure 2.26

In addition to substrate **138**, other aldehydes were synthesized through a similar route or by derivatizing **138**. These were all reacted under our semi-optimized Stetter reaction conditions and good enantioselectivities were obtained with modest yields (Figure 2.27).

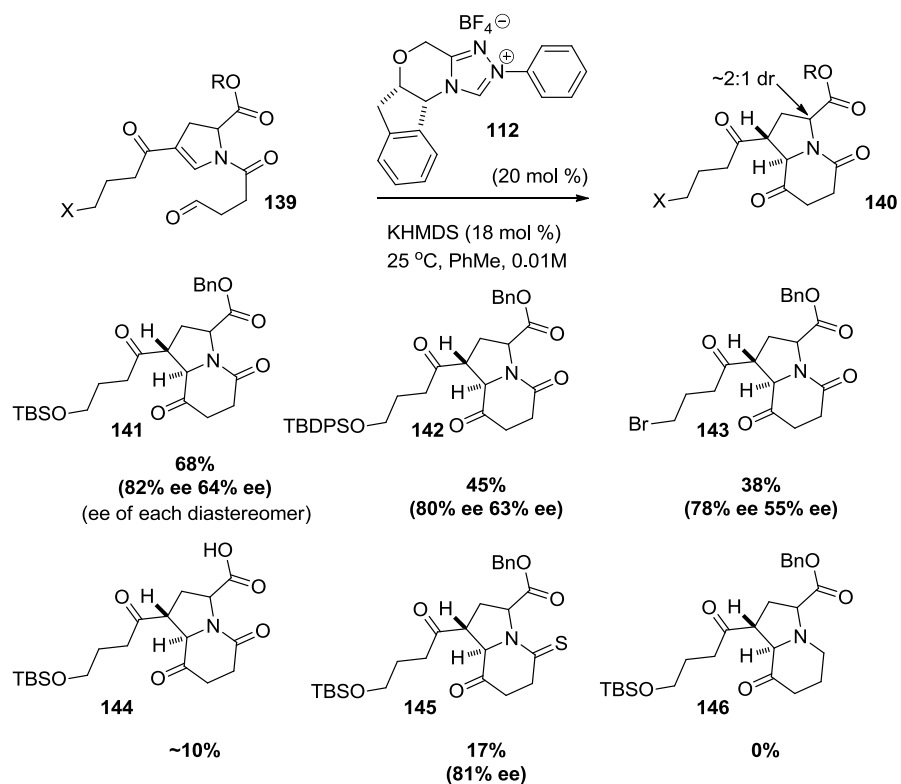


Figure 2.27

We also thought that a thio-vinylogous imide could be a good substrate for the Stetter reaction. A thioamide would allow for simultaneous benzyl ester deprotection and thioamide reduction using Raney nickel. Grignard addition into carbon disulfide afforded dithioester **147**,⁷³ which was reacted with pyrroline **103** yielding the thioamide (Figure 2.28).⁷⁴ Unfortunately deprotection of the dimethyl acetal led to mostly decomposition. Under aqueous conditions the aldehyde was deprotected but unfortunately the thioamide was converted to the oxoamide presumably via hemithioaminal intermediate (**150**).⁷⁵ A dithiane protecting group was also implemented but it

could not be removed without thioamide decomposition. Because the deprotection of the aldehyde was low yielding we abandoned this approach.

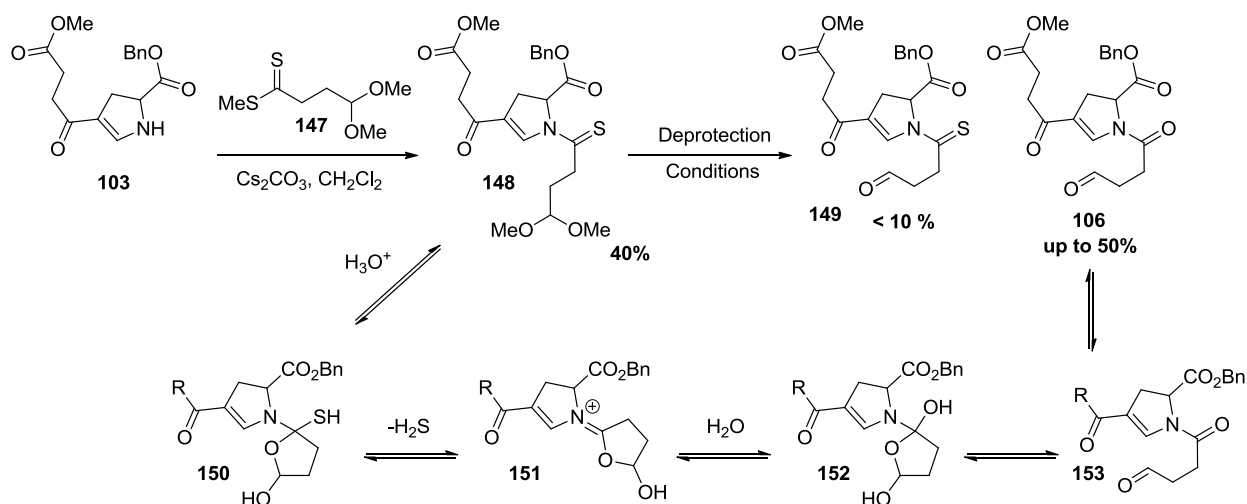


Figure 2.28

2.6 Diastereoselective Stetter

In our retrosynthesis, we proposed a late stage diastereoselective alkylation to install the methyl group. This strategy is not ideal and we believed that an earlier introduction could be possible. We envisioned intermediate **154** could come from a diastereoselective Stetter reaction (Figure 2.29). The substituted pyrroline could be accessed from an enantioselective [3+2] cycloaddition of β -methyl enone **156** and isocyanoacetate **126**. The recent thesis of Joshua Bishop in Scott Schaus' group reports an enantioselective formal [3+2] cycloaddition of isocyanoacetate and enones using Trost's DACH-Ph ligand and Indabox ligands on silver (I).⁷⁶ This methodology can potentially be applied to our synthesis in conjunction with a diastereoselective Stetter to access the key stereocenters in stemocurtisine.

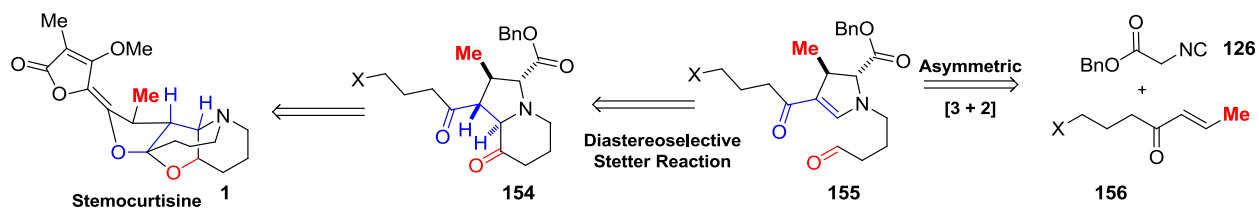


Figure 2.29

We tested our idea by synthesizing α,β -unsaturated ketone **159** from an addition of vinyl lithium **158** into aldehyde **157** followed by alcohol oxidation (Figure 2.30). Next a diastereoselective [3+2] was performed at low temperatures providing pyrroline **160** in high diastereoselectivity. After amidation and dithiane deprotection, the resulting aldehyde was treated with triazolium **107** and sodium acetate as a base. We were happy to discover that Stetter reaction of aldehyde **161** only affords a single diastereomer. This process demonstrates the power of the diastereoselective Stetter reaction and future work may continue this route to stemocurtisine.

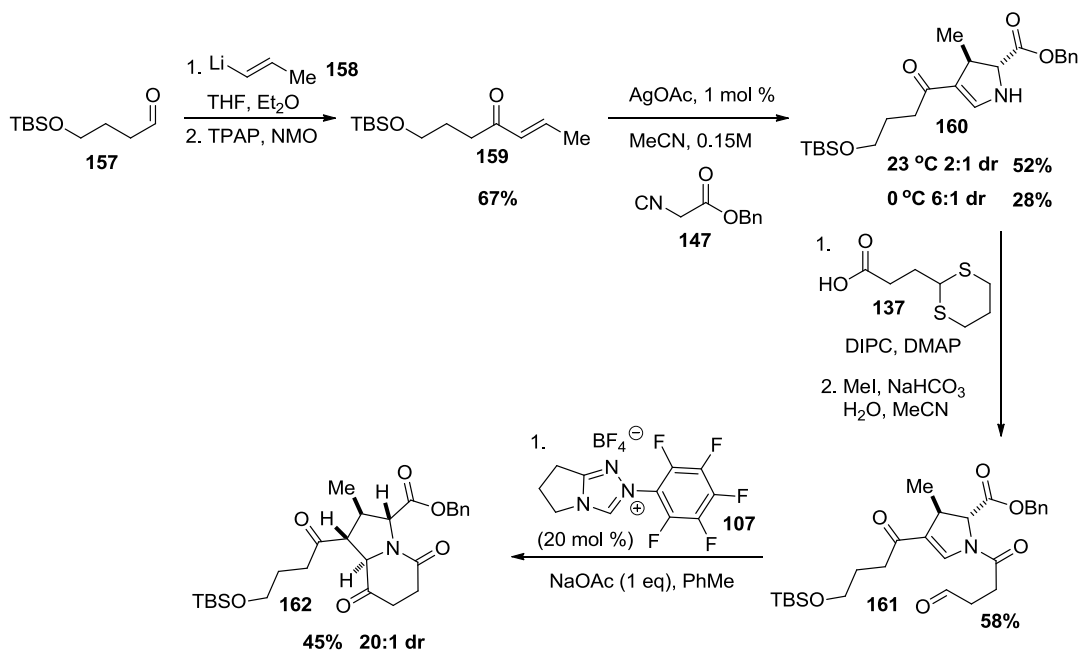


Figure 2.30

2.7 Western Fragment

Instead of applying Overman's lengthy end-game of asparagamine A to stemocurtisine, we think we could use Olivo's methodology.⁷⁷ This method adds lithium enolate **166** into a lactone using alkylative conditions and then the alkoxy group is eliminated with TiCl_4 (Figure 2.31). Unfortunately when a methyl group is present alpha to the lactone the wrong olefin isomer predominates. Additionally, the alkylative conditions would probably not tolerate the tertiary amine present in our substrate. This procedure was reproduced and is a possible approach to the addition of the butenolide moiety but other approaches should be considered.

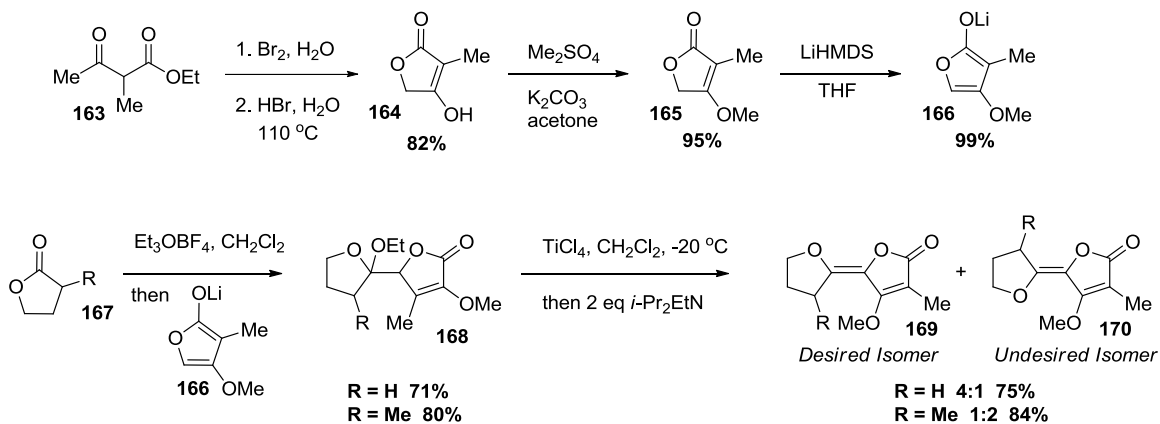


Figure 2.31

2.8 End Game

The completion of stemocurtisine **1** is envisioned to proceed via reduction of the amide and chemoselective reduction of the diketone **172** (Figure 2.32). The chemoselectivity can be rationalized by the ketone's proximity to the amine sigma-withdrawing group. This reduction will be followed by an acid catalyzed cyclization of alcohol **173**, lactol oxidation and

diastereoselective methylation (Figure 2.29). Lastly, butenolide addition into lactone **175** followed by dehydration or Corey-Winter olefination should afford stemocurtisine **1**.

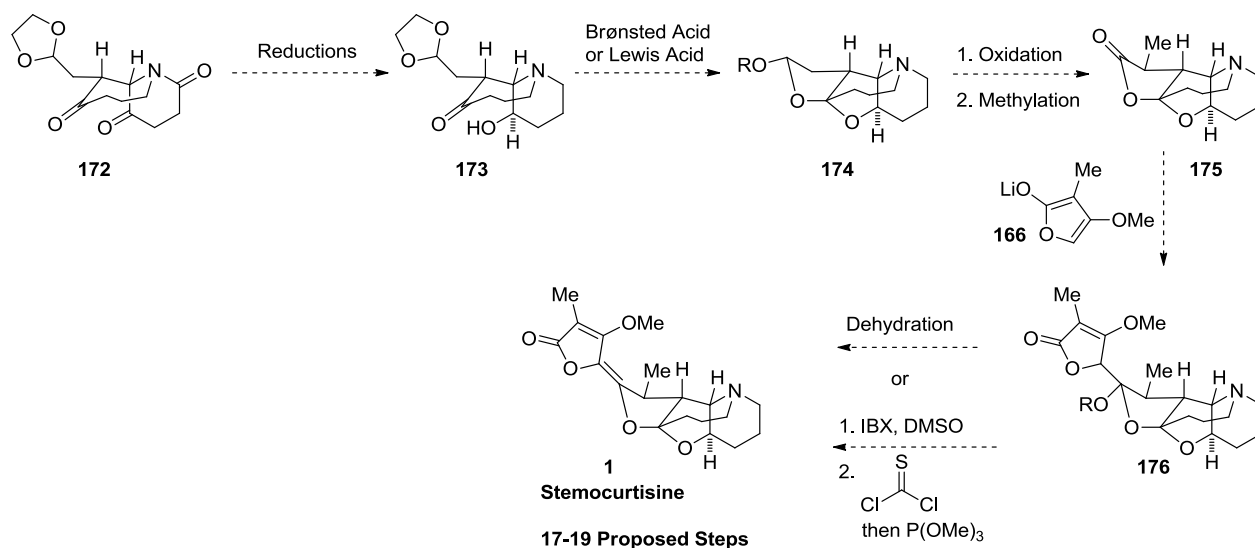


Figure 2.32

2.9 Conclusion

In summary, we have explored a few different routes toward stemocurtisine **1**. The first three were aggressive yet unsuccessful because the proposed Stetter reactions were unattainable. The current approach showcases the asymmetric Stetter reaction on a vinylogous imide to afford hexahydro-indolizinone **108** in good yields and up to 99% enantiomeric excess. This intermediate was further elaborated to the pyrido-azepine core in five steps. Other modifications to this route were investigated but did not lead to significant improvement. A diastereoselective Stetter reaction was also developed to for the synthesis of highly functionalized pyrrolidines. As planned, the total synthesis of stemocurtisine **1** should be achieved in 17 linear steps and provide a method to explore the syntheses of similar *Stemona* alkaloids.

References

- ⁴⁸ (a) Eaton, P. E.; Lin, K. *J. Am. Chem. Soc.* **1964**, *86*, 2087-2088. (b) Corey, E. J.; LaMahieu, R. *J. Am. Chem. Soc.* **1965**, *87*, 2051-2052. (c) Eaton, P. E.; Lin, K. *J. Am. Chem. Soc.* **1965**, *87*, 2052-2054. (d) For an excellent summary of the early work, see Eaton, P. E. *Acc. Chem. Res.* **1968**, *1*, 50-57.
- ⁴⁹ (a) Crandall, J. K.; Haseltine, R. P. *J. Am. Chem. Soc.* **1968**, *90*, 6251-6253. (b) Noyori, R.; Inoue, H.; Kato, M. *J. Chem. Soc., Chem. Commun.* **1970**, 1695-1696. (c) Shinozaki, H.; Arai, S.; Tada, M. *Bull. Chem. Soc. Jpn.* **1976**, *49*, 821-822. (d) Dunkelblum, E.; Hart, H.; Suzuki, M. *J. Am. Chem. Soc.* **1977**, *99*, 5074-5082. (e) Mintas, M.; Schuster, D. I.; Williard, P. G. *Tetrahedron* **1988**, *44*, 6001-6012. (f) Ghosh, S.; Roy, S. S.; Saha, G. *Tetrahedron* **1988**, *44*, 6235-6240.
- ⁵⁰ Dorr, H.; Rawal, V. H. *J. Am. Chem. Soc.* **1999**, *121*, 10229-10230.
- ⁵¹ Davies, H. M. L.; Loe, Ø.; Stafford, D. G. *Org. Lett.* **2005**, *7*, 5561.
- ⁵² Moran, J.; Dornan, P.; Beauchemin, A. M. *Org. Lett.* **2007**, *8*, 3893.
- ⁵³ (a) Yang, N. C.; Lenz, G. R. *Tetrahedron Lett.* **1967**, *48*, 4897-4900. (b) Hoffmann, R. W.; Eicken, K. R. *Tetrahedron Lett.* **1968**, *14*, 1759-1762. 4-Aza-cycloalk-2-enones and the Processes for their Preparation, German DE Patent 2013761, March, 20, **1970**. (c) Couture, A.; Dubiesz, R.; Lablache-Combier, A. *Tetrahedron*, **1984**, *40*, 1835-1844. (d) Couture, A.; Deniau, E.; Grandclaoudon, P.; Lebrun, S. *Tetrahedron Lett.* **1996**, *37*, 7749-7752. (e) Song, F.; Snook, J. H.; Foxman, B. F.; Snider, B. B. *Tetrahedron* **1998**, *54*, 13035-13044.
- ⁵⁴ Ghiringhelli, D. *Tetrahedron, Lett.* **1983**, *24*, 287-290.
- ⁵⁵ Neugnot, B.; Cintrat, J.-C.; Rousseau, B. *Tetrahedron*, **2004**, *60*, 3575-3579.

- ⁵⁶ Hosokawa, T.; Takano, M.; Kuroki, Y.; Murahashi, S.-I.; *Tetrahedron Lett.* **1992**, *33*, 6643-6646.
- ⁵⁷ Grimm, E. L.; Zschiesche, R.; Reissig, H.-U. *J. Org. Chem.* **1985**, *50*, 5543-5545.
- ⁵⁸ Ioffe, S. L.; Lyapkalo, I. M.; Tishkov, A. A.; Danilenko, V. M.; Strelenko, Y. A.; Tartakovsky, V. A. *Tetrahedron* **1997**, *53*, 13085-13098.
- ⁵⁹ Reissig, H.-U.; Ioffe, S. L. *Synlett* **2002**, 863-866.
- ⁶⁰ (a) Ding, F.; Valahovic, M. T.; Keane, J. M.; Anstey, M. R.; Sabat, M.; Trindle, C. O.; Harman, W. D. *J. Org. Chem.* **2004**, *69*, 2257–2267. (b) Zhu, J.; Grigoriadis, N. P.; Lee, J. P.; Porco, J. A. Jr. *J. Am. Chem. Soc.* **2005**, *127*, 9342–9343. (c) Dong, S.; Zhu, J.; Porco, J. A. Jr. *J. Am. Chem. Soc.* **2008**, *130*, 2738–2739. (d) Mejorado, L. H.; Pettus, T. R. R. *J. Am. Chem. Soc.* **2006**, *128*, 15625–15631. (e) Vo, N. T.; Pace, R. D. M.; O'Hara, F.; Gaunt, M. J. *J. Am. Chem. Soc.* **2008**, *130*, 404–405. (f) Dohi, T.; Maruyama, A.; Takenage, N.; Senami, K.; Minamitsuji, Y.; Fujioka, H.; Caemmerer, S.; Kita, Y. *Angew. Chem. Int. Ed.* **2008**, *47*, 3787–3790.
- ⁶¹ (a) Lovchik, M. A.; Goekeb, A.; Frater, G. *Tetrahedron: Asymmetry* **2006**, *17*, 1693–1699. (b) Garcia-Fortanet, J.; Kessler, F.; Buchwald, S. L. *J. Am. Chem. Soc.* **2009**, *131*, 6676–6677. (c) Qi, J.; Beeler, A. B.; Zhang, Q.; Porco, J. A. Jr. *J. Am. Chem. Soc.* **2010**, *132*, 13643-13644.
- ⁶² Zhuo, C.-X.; Liu, W.-B.; Wu, Q.-F.; You, S.-L. *Chem. Sci.* **2012**, *3*, 205-208.
- ⁶³ (a) Miyashito, A.; Obae, K.; Suzuki, Y.; Oishi, E.; Iwamoto, K.; Higashimo, T. *Heterocycles* **1997**, *45*, 2159. (b) Miyashito, A.; Suzuki, Y.; Oishi, E.; Iwamoto, K.; Higashimo, T. *Heterocycles* **1998**, *49*, 405. (c) Miyashito, A.; Suzuki, Y.; Iwamoto, K.; Higashimo, T. *Chem. Pharm. Bull.* **1998**, *46*, 390. (d) Suzuki, Y.; Toyota, T.; Imada, F.; Sato, M.; Miyashito, A. *Chem. Commun.* **2003**, 1314.
- ⁶⁴ Schmuck, C.; Rupprecht, D. *Synthesis*, **2007**, 3095-3110.

- ⁶⁵ Tang, G.; Tian, H.; Ma, D. *Tetrahedron* **2004**, *60*, 10547-10552.
- ⁶⁶ Grigg, R.; Lansdell, M. I.; Thornton-Pett, M. *Tetrahedron* **1999**, *55*, 2025.
- ⁶⁷ Renton, P.; Shen, L.; Eckert, J.; Lee, G. M.; Gala, D.; Chen, G.; Pramanik, B.; Schumacher, D. *Org. Process Rev. Dev.* **2002**, *6*, 36-41.
- ⁶⁸ Vader, J.; Sengers, H.; De Groot, D. *Tetrahedron*, **1989**, *45*, 2131-2142.
- ⁶⁹ Ono, Noboro, Katayama, H.; Nisuiyama, S.; Ogawa, T. *J. Heterocyclic Chem.*, **1994**, *31*, 707-710.
- ⁷⁰ Sheehan, J. C.; Brandt, K. G. *J. Am. Chem. Soc.* **1965**, *87*, 5468-5469.
- ⁷¹ Nicolaou, K. C.; Estrada, A. A.; Zak, M.; Lee, S. H.; Safina, B. S. *Angew. Chem., Int. Ed.* **2005**, *44*, 1378-1382.
- ⁷² Kulinkovich, O.; Masalov, N.; Tyvorskii, V. *Tetrahedron Lett.* **1996**, *37*, 1095-1096.
- ⁷³ Based on procedure from Seebach, D.; Pohmakotr, M. *Tetrahedron*, **1981**, *37*, 4047-4058.
- ⁷⁴ Schaumann, E. *In Comprehensive Organic Synthesis*; "Synthesis of Thioamides and Thiolactams", Vol 6; Trost, B. M.; Fleming, I.; Eds.; Pergamon, Oxford, 1991; p419 and cited references.
- ⁷⁵ Kaloustian, M. K.; Aguilar-Laurents de Gutierrez, M. I.; Nader, R. B. *J. Org. Chem.* **1979**, *44*, 666-668.
- ⁷⁶ Joshua Aaron Bishop, PhD. Dissertation, Boston University, 2011.
- ⁷⁷ Valázquez, F.; Olivo, H. F. *Org. Lett.* **2002**, *4*, 3175-3178.

Chapter 3

Brønsted-Acid Cascade Catalysis and the Development of a Diastereoselective Acetalization/Oxa-Michael Cascade

3.1 Introduction

3.1.1 Asymmetric Brønsted Acid Catalysis

There are a multitude of reactions that are catalyzed by Brønsted acids: Mannich, Strecker, Biginelli, Diels-Alder, Nazarov, aza-Henry, aza-Petasis–Ferrier, Semi-Pinacol, Aldol, Friedel-Crafts and many more. The development of asymmetric Brønsted acid catalysis was a difficult task because the transformation requires a chiral proton source. In spite of this, it is now a rich field that began with Jacobsen's serendipitous discovery that peptide-based chiral thiourea **3**, without any metals, could catalyze the Strecker reaction in up to 91% ee (Figure 3.1).⁷⁸

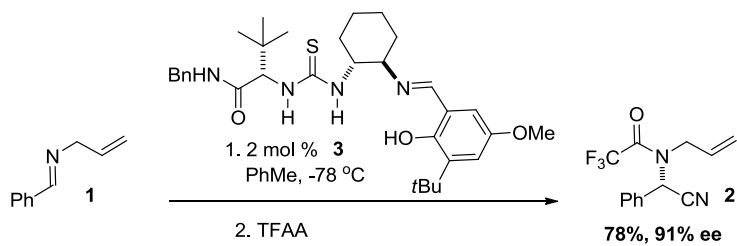


Figure 3.1

The next major advancement occurred in 2004 when Terada⁷⁹ and Akiyama⁸⁰, concurrently and independently, developed axially chiral BINOL derived phosphoric acid catalysts. They used these catalysts to perform asymmetric Mannich reactions (Figure 3.2). Since their landmark contributions, numerous acid-catalyzed transformations have been rendered asymmetric using BINOL derived phosphoric acids.⁸¹

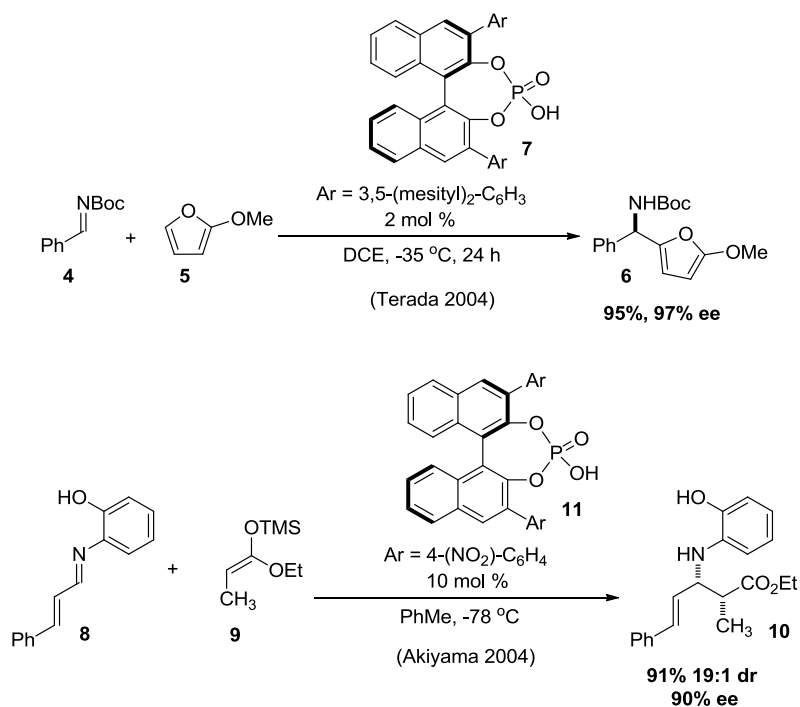


Figure 3.2

3.1.2 Importance of Chiral Acetals and Aminals

Acetals and amins are important structural motifs that are found in a variety of pharmaceuticals and biologically important natural products. One interesting impact of acetal stereochemistry is on insect signaling molecules. The simple sex pheromone, olean, contains only a single stereocenter which is an acetal. One enantiomer of the pheromone attracts male olive fruit flies while the other attracts females.⁸² The stereochemistry of amins is also important to biological properties as exhibited by De Brabander's cytotoxicity studies of psymberin.⁸³ The enantioselective formation of acetals and amins has been a long standing problem in organic synthesis because of the inherent reversibility and the product's ease of racemization.

3.1.3 Asymmetric Formation of Acetals and Aminals

Terada and Akiyama's concept of C_2 symmetric Brønsted acids has been successfully applied to the catalytic asymmetric synthesis of acetals and aminals. Antilla's group has provided practical solutions for enantioselective N,O -aminal and N,N -aminal formations.⁸⁴ In his seminal publication, chiral phosphoric acid **14** catalyzed the enantioselective addition of alcohols into N -acyl imines to provide N,O -aminal products (**13**) in up to 95% ee (Figure 3.3).^{84a}

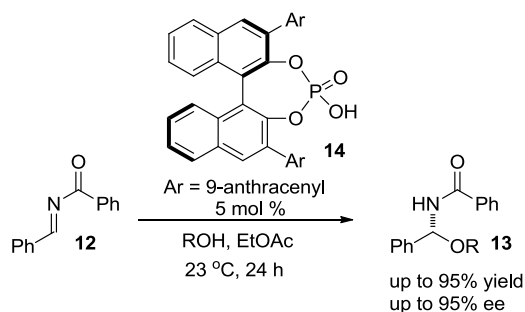


Figure 3.3

List has played a large role in developing new chiral phosphoric acids and applying them to synthetic challenges such as acetals and aminals.⁸⁵ In particular, he reported a new spiro-bisindane based Brønsted acid **18** which catalyzes an asymmetric transacetalization.^{85b} This procedure was then applied to the kinetic resolution of racemic alcohols (Figure 3.4).^{85c} Using an extremely sterically hindered catalyst, his group showed that simple spirocyclic acetals, such as olefin, could be synthesized in high enantioselectivity (Figure 3.5).^{85d} Toste synthesized spirocyclic acetals in high selectivities via a chiral phosphoric acid catalyzed fluorocyclization (Figure 3.6).⁸⁶

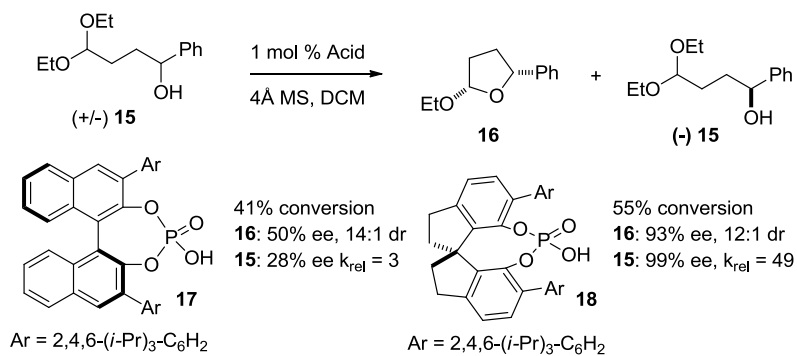


Figure 3.4

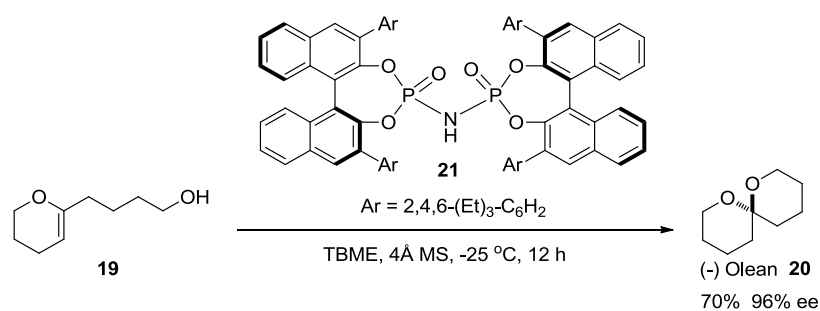


Figure 3.5

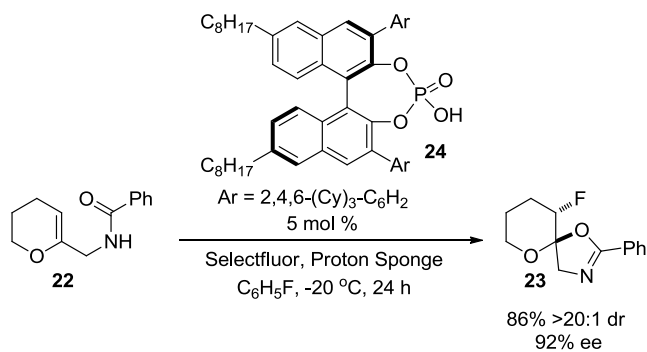


Figure 3.6

3.1.4 Cascade Catalysis

Nature has been constructing complex molecules as single stereoisomers with apparent ease for a long time. The key to its efficiency is the use of a sequence of enzyme catalyzed transformations

which quickly convert simple raw materials into ones that are architecturally advanced. The disadvantage to biological processes is their narrow substrate scope. In contrast, synthetic methods have a broad scope, and using current technology, almost any organic compound can be accessed. Unfortunately, these processes can be expensive, inefficient and time consuming. The major drawbacks arise from linear approaches, stoichiometric reagents and purifications. One recent advance in the field that is helping to alleviate these problems is asymmetric cascade catalysis.⁸⁷ It has been nicely defined by Tietze as, “the transformation of two or more bond-forming reactions under identical reaction conditions, in which the latter transformations take place at the functionalities obtained in the former bond-forming reactions” (Figure 3.7).⁸⁸

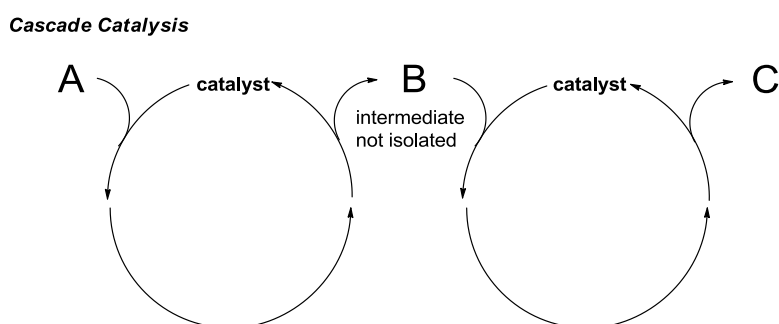


Figure 3.7

Asymmetric cascade catalysis can achieve multiple stereoselective transformations in a single synthetic sequence which reduces synthetic operations and bypasses the purification of sensitive intermediates. This powerful method has been utilized by many research groups,⁸⁹ including our own,⁹⁰ to construct complex molecules containing multiple stereocenters in a rapid and efficient manner.

3.1.5 Asymmetric Brønsted Acid Cascades

Brønsted acid catalysts have been utilized in cascade reactions and have shown compatibility with other organocatalysts.⁹¹ Rueping pioneered this area with the asymmetric reduction of 2-substituted quinolines (**25**) through transfer hydrogenation using Hantzsch esters (Figure 3.8).^{89a} The cascade begins with a 1,4-reduction of the protonated quinoline to form an enamine. After tautomerization and protonation, the resulting iminium with a chiral phosphate counterion undergoes an enantioselective 1,2-reduction to form the tetrahydroquinoline (**27**).

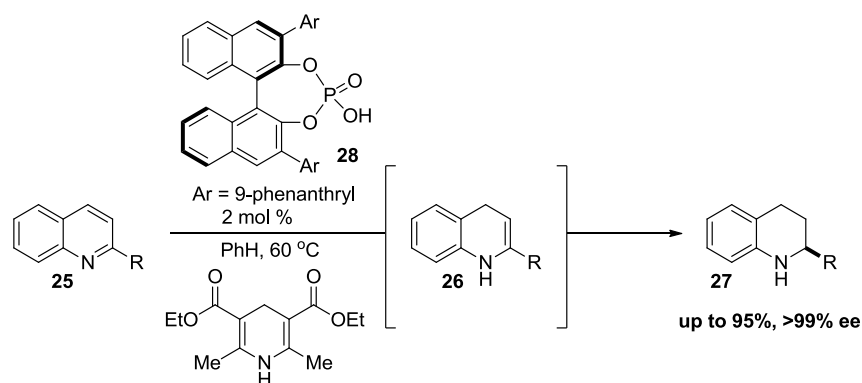


Figure 3.8

3.1.6 Cyclohexenone Desymmetrizations

Another significant advance in asymmetric catalysis is the desymmetrization⁹² reaction which converts a symmetric prochiral molecule into a chiral one. One example of this process is the desymmetrization of a cyclohexadienone which usually sets more than two stereocenters and the product contains synthetic handles for further functionalization. Feringa reported the first asymmetric cyclohexadienone desymmetrization using a copper phosphoramidite-catalyzed conjugate addition of dialkyl zinc reagents.^{92a} His group also demonstrated an asymmetric intramolecular Heck reaction using a chiral phosphoramidite ligand (Figure 3.9).^{92b} Hayashi

reported a highly enantioselective intramolecular Michael reaction using a secondary amine catalyst.^{92c} This was further developed by Gaunt's group in a one pot oxidation/Michael reaction to synthesize [4.4.0]-bicycloalkanones from phenols.^{92e} The Rovis group has also contributed to this field with an intramolecular Stetter desymmetrization to form hydrobenzafuranones in excellent yields and selectivities.^{92d} More recently, the You group has been active in the field of cyclohexanone desymmetrization. They have developed desymmetrizations involving Michael, oxa-Michael, aza-Michael and Stetter reactions to afford products in high enantioselectivities (Figure 3.9).^{92f,h,i,k}

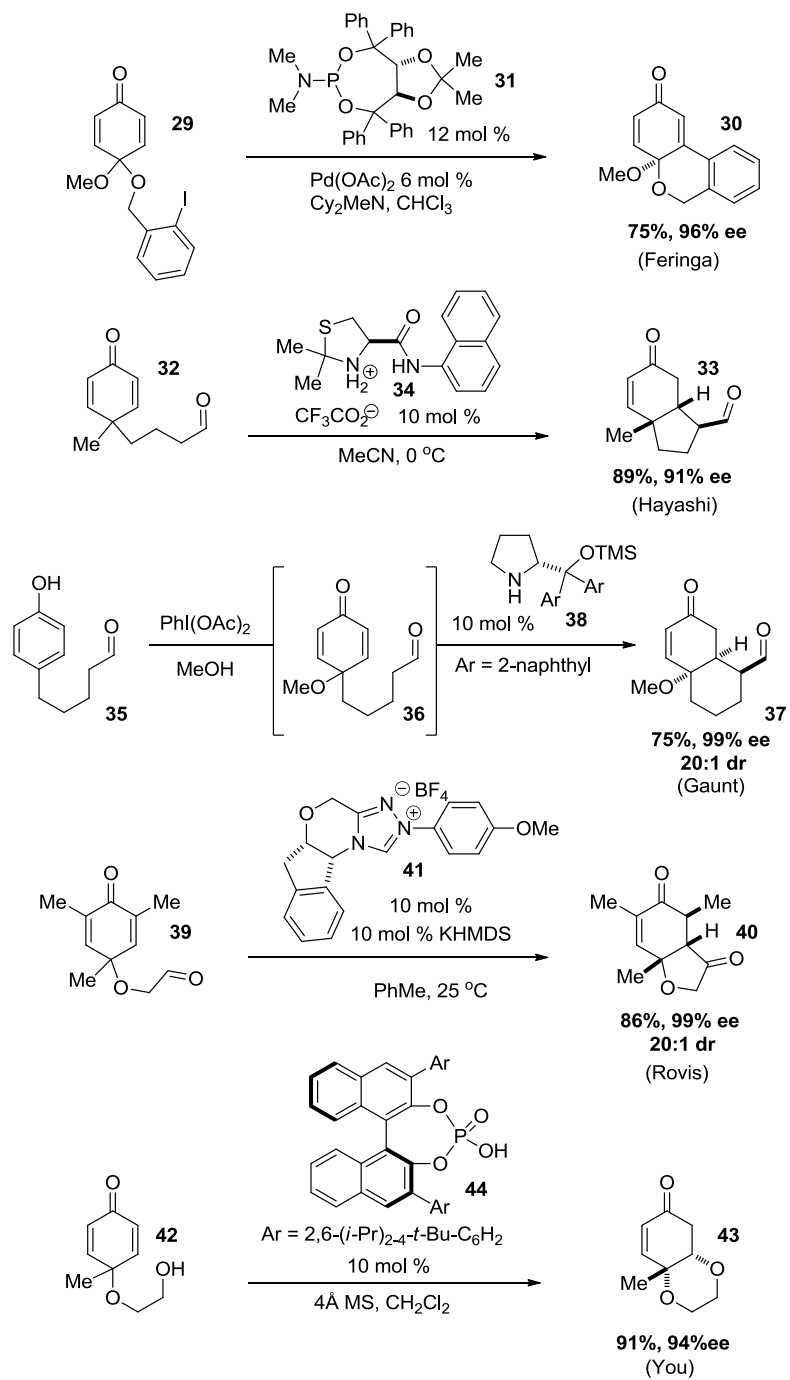


Figure 3.9

3.2 Results

3.2.1 Acetalization/Oxa-Michael Cascade

We initially proposed that substituted *p*-quinols could be desymmetrized with aldehydes, ketones or imines using a chiral Brønsted acid catalyst (Figure 3.10).

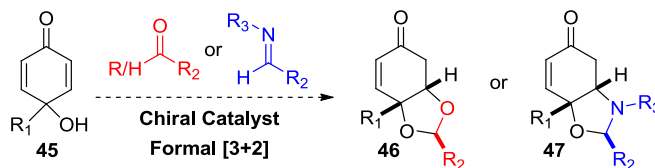


Figure 3.10

This process begins with an acetalization of a *p*-quinol to form a hemiacetal (shown) or a hemiaminal (Figure 3.11). Intermediate **48** then undergoes a 5-*exo-trig* oxa-Michael reaction to form bicyclic product **46**.

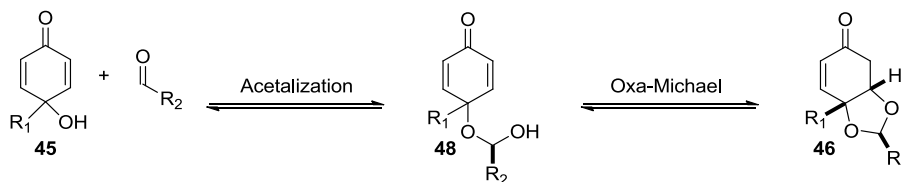


Figure 3.11

This type of cascade was initially discovered by Jefford who showed that 4-methyl-4-hydroxybenzoquinone could be reacted with acetaldehyde and polymer-bound sulfonic acid catalyst, Amberlyst-15, to produce the 1,3-dioxolane product in good yield but with no diastereoselectivity at the acetal carbon (Figure 3.12)⁹³.

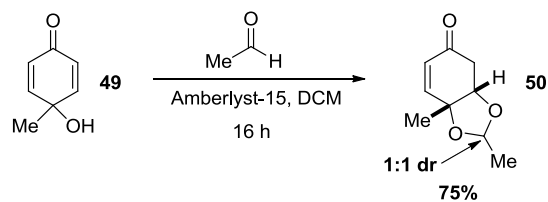


Figure 3.12

Carreño and coworkers recently improved this reaction by using DMAP and electron deficient aryl aldehydes.⁹⁴ Their basic conditions allowed the aryl dioxolanes to be isolated in 4:1 to 9:1 dr with reaction times of three days (Figure 3.13).

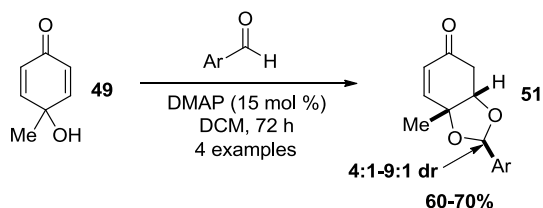


Figure 3.13

Another challenge in our approach is the oxa-Michael. Like acetal formation it can be reversible and difficult to control. In the past decade, some progress has been made in this field.⁹⁵ Concurrently with our work, Matsubara showed that aldehydes react with γ -hydroxy- α,β -unsaturated ketones and aryl thioesters to provide dioxolane products in high enantioselectivity but moderate to low diastereoselectivity (Figure 3.14).⁹⁶

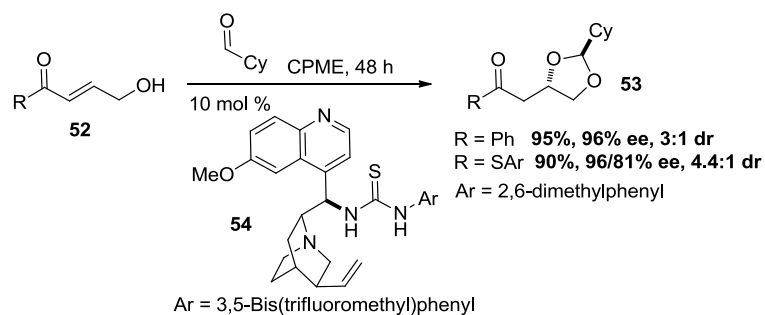


Figure 3.14

3.2.2 Quinol Substrate Synthesis.

The *p*-quinol substrates for our planned desymmetrization were synthesized using a protocol developed by Carreño in which singlet oxygen generated from oxone and NaHCO_3 undergoes a hetero-Diels-Alder with a phenol (**55**).⁹⁷ The resulting endoperoxide **56** is opened in water and the hydroperoxide is reduced with sodium thiosulfate. The scope of this oxidation was explored and it tolerates most alkyl groups and substitution around the quinol, but electron withdrawing substituents shutdown the Diels-Alder (Figure 3.15).

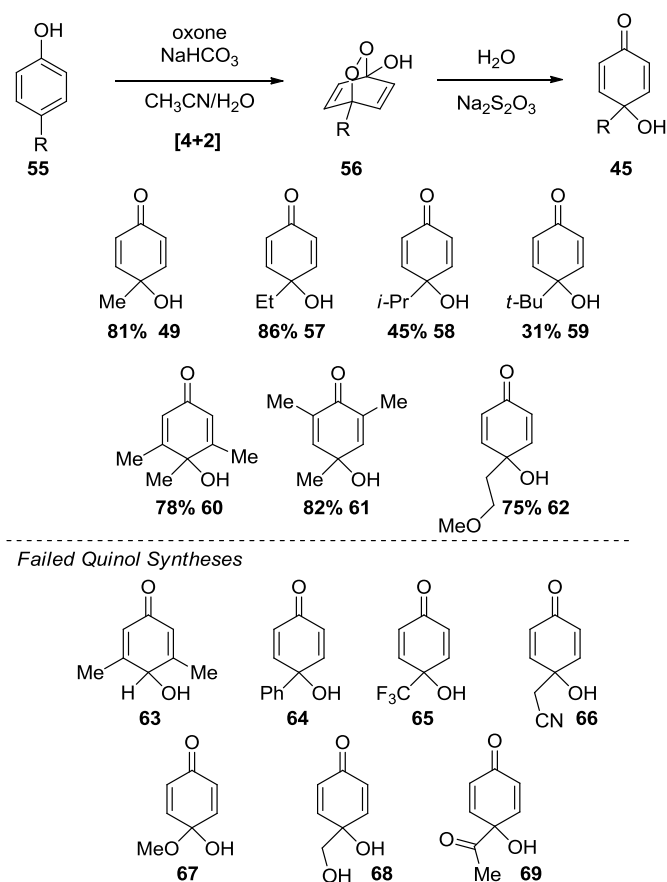


Figure 3.15

3.2.3 Dioxolane Reaction Optimization

We initiated our investigation by exploring the racemic desymmetrization of *p*-quinol **57** with isobutyraldehyde. A screen of Brønsted acid catalysts demonstrated that Amberlyst-15 (polymer bound sulfonic acid), (+/-) camphorsulfonic acid, TsOH and H₃PO₄ all afford the desired dioxolane **70** in good yield but poor diastereoselectivity ranging from 1:1 to 2.2:1 (Table 3.1). Switching to TFA improved the selectivity to 14:1. We hypothesized that a bifunctional and sterically hindered catalyst might create a more rigid conformation in the transition state and select for the kinetic product. This was achieved using diphenylphosphinic acid which improved the selectivity to >20:1 and maintained good yields (Table 3.1, Entry 6). By increasing the

temperature to 50 °C, we were able to decrease the reaction times and reduce the catalyst loading while still maintaining excellent diastereoselectivity (Entry 7).

Table 3.1

Entry	Catalyst	Yield (%) ^a	dr ^b
1	Amberlyst-15	93	1:1
2	TsOH	78	1.6:1
3	H ₃ PO ₄	85	1.9:1
4	CSA	85	2.2:1
5	TFA	91	14:1
6	Ph ₂ PO ₂ H	92	>20:1
7 ^c	Ph ₂ PO ₂ H	91	>20:1

^a Isolated yields after column chromatography. ^b dr reported based on crude NMR ^c Temperature of 50 °C and 5 mol % catalyst

3.2.4 Dioxolane Substrate Scope

Our optimized reaction conditions were applied to a variety of aldehydes (Table 3.2). Paraformaldehyde as well as sterically hindered aliphatic aldehydes all provided the 1,3-dioxolane products in good yields and high diastereoselectivity. Alkenes, alkynes, thioethers and protected alcohols are tolerated under the reaction conditions.

Table 3.2

Entry	Aldehyde	Product	Yield (%)	dr
1	(paraformaldehyde)		89	> 20:1
2			84	> 20:1
4			75	> 20:1
5			95	> 20:1
6			83	> 20:1
7			74	> 20:1
8			71	13:1
9			84	> 20:1

We also expanded the reaction scope to a variety of substituted quinols and the diastereoselectivity remained high (Table 3.3). Unfortunately, quinol substrates with *iso*-propyl and *t*-butyl substituents in the 4-position decomposed under the acidic reaction conditions. 2,4,6-trimethyl quinol **61** led to a complex mixture because of non-diastereoselective enol protonation.

Table 3.3

Entry	<i>p</i> -quinol	Product	Yield (%)	dr
1			84	20:1
2			trace (quinol decomposition)	na
3			trace (quinol decomposition)	na
4			74	20:1
5			68	20:1
6			complex mixture	na

Aryl aldehydes were also explored but their reactivity was low. Electron deficient aryl aldehydes give a moderate amount of product but electron rich substrates such as *p*-methoxybenzaldehyde afforded no product (Table 3.4). Additionally, α,β -unsaturated aldehydes were screened and only trace amounts of product were observed.

Table 3.4

Entry	Aldehyde	Product	Yield (%)	dr
1			63	20:1
2			26	20:1
3			trace	na
4			trace	na
5			5%	3.3:1

Ketones including acetone and benzophenone were tested and they show low reactivity even at higher temperatures with prolonged reaction times (Table 3.5). The lower yields for the electron rich aromatic aldehydes, enals and ketones can be attributed to their hemiacetal/hemiketal formation being less thermodynamically favorable. Calculations show that the hydration equilibrium constants for ketones and electron rich aryl aldehydes are much lower than those of aliphatic aldehydes.⁹⁸

Table 3.5

Reaction scheme: 49 + R-C(=O)-R $\xrightarrow[\text{DCE, 65 } ^\circ\text{C, 72 h}]{\text{Ph}_2\text{PO}_2\text{H (5 mol \%)}}$ 74a-b

Entry	Ketone	Product	Yield (%)	dr
1			16	20:1
2			0	na

3.2.5 Oxazolidine Substrate Scope

In addition to aldehydes and ketones, imines were found to be competent partners for the formal [3+2] cycloaddition. *N*-alkyl and *N*-aryl imines afforded the desired oxazolidine products in good yields and high diastereoselectivity (Table 3.6). These products allow for the synthesis of *vicinal*-amino alcohols after cleavage of the aminal. The reaction was somewhat limited in the substituents on nitrogen. *N*-sulfonyl imines, *O*-methyl oximes or tosyl-hydrazones did not participate in the reaction.

Table 3.6

Entry	Imine	Product	Yield (%)	dr
1			65	20:1
2			73	20:1
3			76	20:1
4			23	6:1
5			0	na
6			0	na

The diastereoselectivity of the desymmetrization reaction can be explained through transition states **76** and **77**. In the preferred conformation for the oxa-Michael, the aldehyde substituent R is in the pseudo-equatorial position whereas in the minor diastereomer it is pseudo-axial (Figure 3.16).

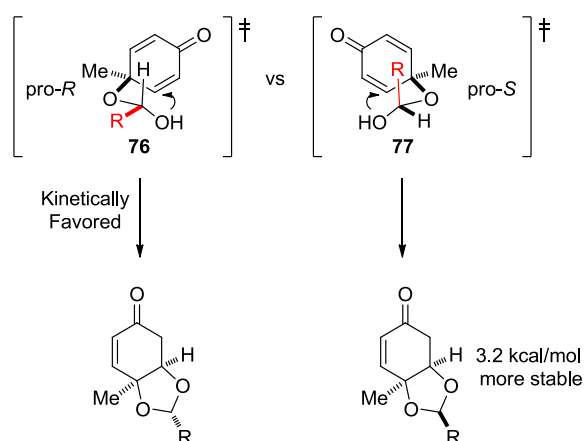
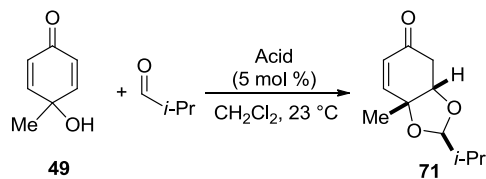


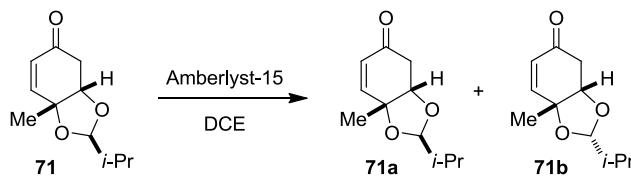
Figure 3.16

DFT calculations found that the *trans*-product is more stable than the *cis*-product by 3.2 kcal/mol. However, this energy difference is probably artificially high. Monitoring the diastereoselectivity throughout the course of the reaction under thermodynamic conditions with Amberlyst-15 found that the ratio is always 1:1 (Table 3.7). Diphenyl phosphoric acid produced the kinetic product in >20:1 diastereoselectivity during the entire reaction.

Table 3.7

Entry	Acid	Time	Conversion	dr
1	Ph ₂ PO ₂ H	5 min	< 5	20:1 dr
2	Ph ₂ PO ₂ H	1 h	23	20:1 dr
3	Ph ₂ PO ₂ H	24 h	95	20:1 dr
4	Amberlyst-15	5 min	5	1:1 dr
5	Amberlyst-15	1 h	35	1:1 dr
6	Amberlyst-15	24 h	99	1:1 dr

The enriched kinetic *cis*-product was subjected to the Amberlyst-15 conditions and over the course of two days, the ratio was slowly eroded to 4:1 (Table 3.8). This supports the hypothesis that the diphenyl phosphinic acid is forming the kinetic product and suggests that Amberlyst-15 is initially forming the thermodynamic mixture. When the 1:1 product mixture was treated with diphenyl phosphinic acid no enrichment was observed. Therefore, the formation of the dioxolane from the hemiacetal is under kinetic control when diphenylphosphinic acid is used.

Table 3.8

Entry	Time	dr
1	0 h	20:1
2	1 h	20:1
3	24 h	8:1
4	48 h	4:1

3.3 Asymmetric Formal [3 + 2]

After improving the diastereoselectivity, expanding the scope and exploring the reaction mechanism, we hoped to render the reaction asymmetric with the use of a chiral Brønsted acid (Table 3.9). Isobutyraldehyde and quinol **49** were screened with a variety of chiral catalysts. Using 2,4,6-*(i*-Pr)₃-C₆H₂ substituted BINOL phosphoric acid **17**, the product was isolated in a meager 10% ee. Chiral squaramide catalyst **78** gives the same result as **17**. A cinchonidine based thiourea increases selectivity to 38% ee but the best result came with spiro-bisindane scaffold **18** which improved the reaction to 45% ee.

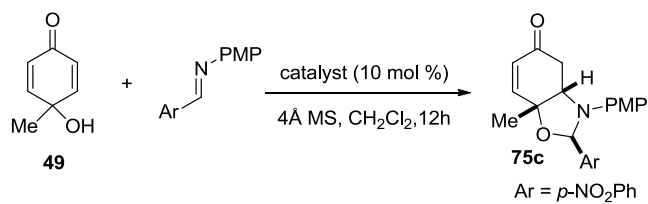
Table 3.9

Reaction scheme: 49 $\xrightarrow[\text{CH}_2\text{Cl}_2, 12\text{h}]{\text{catalyst (10 mol \%), } i\text{-PrCHO, 4Å MS}}$ 71

Entry	Catalyst	yield (%) ^a	ee (%) ^b
1	<p>17 Ar = 2,4,6-(<i>i</i>-Pr)₃-C₆H₂</p>	89	10
2	<p>78 Ar = 4-CF₃-C₆H₄</p>	32	10
3	<p>54 Ar = 3,5-(CF₃)₂-C₆H₃</p>	75	38
4	<p>18 Ar = 2,4,6-(<i>i</i>-Pr)₃-C₆H₂</p>	76	45

The enantioselective synthesis of an oxazolidine was also investigated using quinol **49** (Table 3.10). The best result came with catalyst **17** which gave the product 32% yield and 53% ee. The more hindered catalyst **18** only produced a trace amount of desired oxazolidine **75c**. Johnston's BAM⁹⁹ **79** and PBAM¹⁰⁰ **80** catalysts that are used for aza-Henry reactions did not afford any product.

Table 3.10



Entry	Catalyst	yield (%)	ee (%)
1	<p>17 Ar = 2,4,6-<i>i</i>-Pr₃-C₆H₂</p>	32	53
2	<p>54 Ar = 3,5-(CF₃)₂-C₆H₃</p>	19	40
3	<p>18 Ar = 2,4,6-<i>i</i>-Pr₃-C₆H₂</p>	< 5%	NA
4	<p>79^{⊕⊖} OTf</p>	0	NA
5	<p>80^{⊕⊖} OTf</p>	0	NA

3.4 Conclusion

In summary we have developed a diastereoselective synthesis of dioxolanes and oxazolidines via a diphenyl phosphinic acid catalyzed acetalization/oxa-Michael cascade. The scope tolerates a variety of aliphatic and aryl aldehydes as well as ketones and imines. Mechanistic studies showed that the kinetic product was being formed with diphenyl phosphinic acid, and the single diastereomer could be slowly epimerized using Amberlyst-15. Our attempt to develop the asymmetric variant with the highest enantioselectivity resulted in a maximum of 53% ee and this paved the way for our success in the highly enantioselective synthesis of trioxanes.

References

- ⁷⁸ M. S. Sigman, E. N. Jacobsen, *J. Am. Chem. Soc.* **1998**, *120*, 4901-4902.
- ⁷⁹ Uraguchi, D.; Sorimachi, K.; Terada, M. *J. Am. Chem. Soc.* **2004**, *126*, 11804-11805.
- ⁸⁰ Akiyama, T.; Itoh, J.; Yokota, K.; Fuchibe, K. *Angew. Chem., Int. Ed.* **2004**, *43*, 1566-1568.
- ⁸¹ Reuping, M.; Kuenkel, A.; Atodiressei, I. *Chem. Soc. Rev.* **2011**, *40*, 4539-4549.
- ⁸² Haniotakis, G.; Francke, W.; Mori, K.; Redlich, H.; Schurig, V.; *J. Chem. Ecol.* **1986**, *12*, 1559-1568.
- ⁸³ Jiang, X.; Williams, N.; De Brabander, J. K. *Org. Lett.* **2007**, *9*, 227.
- ⁸⁴ (a) Rowland, G. B.; Zhang, H.; Rowland, E. B.; Chennamadhavuni, S.; Wang, Y.; Antilla, J. *C. J. Am. Chem. Soc.* **2005**, *127*, 15696. (b) Liang, Y.; Rowland, E. B.; Rowland, G. B.; Perman, J. A.; Antilla, J. C. *Chem. Commun.* **2007**, 4477. (c) Li, G.-L.; Fronczek, F. R.; Antilla, J. C. *J. Am. Chem. Soc.* **2008**, *130*, 12216.
- ⁸⁵ (a) Cheng, X.; Vellalath, S.; Goddard, R.; List, B. *J. Am. Chem. Soc.* **2008**, *130*, 15787. (b) Čorić, I.; Vellalath, S.; List, B. *J. Am. Chem. Soc.* **2010**, *132*, 8536. (c) Čorić, I.; Müller, S.; List, B. *J. Am. Chem. Soc.* **2010**, *132*, 17370. (d) Čorić, I.; List, B. *Nature* **2012**, *483*, 315.
- ⁸⁶ Rauniyar, V.; Lackner, A. D.; Hamilton, G. L.; Toste, F. D. *Science* **2011**, *334*, 1681.
- ⁸⁷ (a) Enders, D.; Grondal, C.; Hüttl, M. R. M. *Angew. Chem., Int. Ed.* **2007**, *46*, 1570. (b) Grondal, C.; Jeanty, M.; Enders, D. *Nat. Chem.* **2010**, *2*, 167. (c) Zhou, J. *Chem. Asian J.* **2010**, *5*, 422. (d) Albrecht, L.; Jiang, H.; Jørgensen, K.-A. *Angew. Chem., Int. Ed.* **2011**, *50*, 8492. (e) Pellissier, H. *Adv. Synth. Catal.* **2012**, *354*, 237.
- ⁸⁸ Tietze, L. F.; Brasche, G.; Gericke, K. M.; *Domino Reactions in Organic Synthesis* Wiley-VCH: Verlag GmbH and Co. KGaA: Weinheim, Germany **2006**.

- ⁸⁹ Chiral Brønsted acid cascade examples: (a) Rueping, M.; Antonchik, A. P.; Theissmann, T. *Angew. Chem., Int. Ed.* **2006**, *44*, 3683. (b) Zhou, J.; List, B. *J. Am. Chem. Soc.* **2007**, *129*, 7498. (c) Terada, M.; Machioka, K.; Sorimachi, K. *J. Am. Chem. Soc.* **2007**, *129*, 10336. (d) Mukherjee, S.; List, B. *J. Am. Chem. Soc.* **2007**, *129*, 11336. (e) Enders, D.; Narine, A. A.; Toulgoat, F.; Bisschops, T. *Angew. Chem., Int. Ed.* **2008**, *47*, 5662. (f) Rueping, M.; Antonchik, A. P. *Angew. Chem., Int. Ed.* **2008**, *47*, 5836. (g) Cai, Q.; Zaho, Z.-A.; You, S.-L. *Angew. Chem., Int. Ed.* **2009**, *48*, 7428. (h) Liu, H.; Dagousset, G.; Masson, G.; Retailleau, P.; Zhu, J.; *J. Am. Chem. Soc.* **2009**, *131*, 4598. (i) Han, Z.-Y.; Xiao, H.; Chen, X.-H.; Gong, L.-Z. *J. Am. Chem. Soc.* **2009**, *131*, 9182. (j) Muratore, M. E.; Holloway, C. A.; Pilling, A. W.; Storer, R. I.; Trevitt, G.; Dixon, D. J. *J. Am. Chem. Soc.* **2009**, *131*, 10796. (k) Liu, X.-Y.; Che, C.-M. *Org. Lett.* **2009**, *11*, 4204. (l) Holloway, C. A.; Muratore, M. E.; Storer, R. I.; Dixon, D. J. *Org. Lett.* **2010**, *12*, 4720. (m) He, Y.; Lin, M.; Li, Z.; Liang, X.; Li, G.; Antilla, J. C. *Org. Lett.* **2011**, *13*, 4490. (n) Dagousset, G.; Zhu, J.; Masson, G.; *J. Am. Chem. Soc.* **2011**, *133*, 14804.
- ⁹⁰ (a) Lathrop, S. P.; Rovis, T. *J. Am. Chem. Soc.* **2009**, *131*, 13628. (b) Filloux, C. M.; Lathrop, S. P.; Rovis, T. *Proc. Natl. Acad. Sci. U.S.A.* **2010**, *107*, 20666. (c) Ozboya, K. E.; Rovis, T. *Chem. Sci.* **2011**, *2*, 1835.
- ⁹¹ Peng, F.-Z.; Shao, Z.-H. *Curr. Org. Chem.* **2011**, *15*, 4144.
- ⁹² (a) Imbos, R.; Brilman, M. H. G.; Pineschi, M.; Feringa, B. L. *Org. Lett.* **1999**, *1*, 623. (b) Imbos, R.; Minnaard, A. J.; Feringa, B. L. *J. Am. Chem. Soc.* **2002**, *124*, 184. (c) Hayashi, Y.; Gotoh, H.; Tamura, T.; Yamaguchi, H.; Masui, R.; Shoji, M. *J. Am. Chem. Soc.* **2005**, *127*, 16028. (d) Liu, Q.; Rovis, T. *J. Am. Chem. Soc.* **2006**, *128*, 2552. (e) Vo, N. T.; Pace, R. D. M.; O'Hara, F.; Gaunt, M. J. *J. Am. Chem. Soc.* **2008**, *130*, 404. (f) Gu, Q.; Rong, Z.-Q.; You, S.-L. *J. Am. Chem. Soc.* **2010**, *132*, 4056. (g) Leon, R.; Jawalekar, A.; Redert, T.; Gaunt, M. J. *Chem.*

Sci. **2011** *3*, 1487-1490. (h) Gu, Q.; You, S.-L. *Chem. Sci.* **2011**, *2*, 1519. (i) Gu, Q.; You, S.-L. *Org. Lett.* **2011**, *13*, 5192-5195. (j) Tello-Aburto, R.; Kalstabakken, K. A.; Volp, K. A.; Harned, A. M. *Org. Biomol. Chem.* **2011**, *9*, 7849. (k) Jia, M.-Q.; You, S.-L. *Chem. Commun.* **2012**, *48*, 6363-6365.

⁹³ Jefford, C. W.; Rossier, J. C.; Kohmoto, S.; Boukouvalas, J. *Synthesis* **1985**, 29.

⁹⁴ Redondo, M. C.; Ribagorda, M.; Carreño, M. C. *Org. Lett.* **2010**, *12*, 568.

⁹⁵ (a) Christoffers, J.; Koripelly, G.; Rosiak, A.; Rössle, M. *Synthesis* **2007**, 1279. (b) Yang, J. W.; Hoffmann, S.; List, B. *Chem. Rev.* **2007**, *107*, 5471. (c) Nising, C. F.; Bräse, S. *Chem. Soc. Rev.* **2008**, *37*, 1218-1228. (d) Nising, C. F.; Bräse, S. *Chem. Soc. Rev.* **2012**, *41*, 988-999.

⁹⁶ (a) Asano, K.; Matsubara, S. *Org. Lett.* **2012**, *14*, 1620. (b) Okamura, T.; Asano, K.; Matsubara, S. *Chem. Commun.* **2012**, *48*, 5076-5078.

⁹⁷ Carreño, M. C.; González-López, M.; Urbano, A.; *Angew. Chem., Int. Ed.* **2006**, *45*, 2737.

⁹⁸ Gómez-Bombarelli, R.; González-Pérez, M.; Pérez-Prior, M. T.; Calle, E.; Casado, J. *J. Phys. Chem. A* **2009**, *113*, 11423-11428.

⁹⁹ Nugent, B. M.; Yoder, R. A.; Johnston, J. N. *J. Am. Chem. Soc.* **2004**, *126*, 3418.

¹⁰⁰ Davis, T.; Wilt, J. C.; Johnston, J. N. *J. Am. Chem. Soc.* **2010**, *132*, 2880.

Chapter 4

Development of an Enantioselective Synthesis of Trioxanes via a Formal [4+2]

Cycloaddition

4.1 Introduction

4.1.1 Trioxanes

The 1,2,4-trioxane moiety is found in a number of molecules with antimalarial, anticancer and antibacterial activities.¹⁰¹ In particular, artemisinin is administered as part of a combination therapy for the frontline treatment of malaria and contains a 1,2,4-trioxane as the key pharmacophore. The recent emergence of an artemisinin-resistant malaria strain,¹⁰² combined with the fact that artemisinin's mode of action remains under debate,¹⁰³ increases the difficulty of treating malaria and makes the pursuit of novel therapeutic agents more urgent.¹⁰⁴ One potential solution is the development of new, synthetic endoperoxides.¹⁰⁵ Although enantiomers of a few synthetic trioxanes have similar anti-malarial activities,¹⁰⁶ stereochemistry has a demonstrated impact on anti-cancer activity,¹⁰⁷ making the development of enantioselective methods relevant and important.

4.1.2 Catalytic Asymmetric Synthesis of Peroxides

There are no enantioselective methods to synthesize 1,2,4-trioxanes. Current methods for the synthesis of enantioenriched trioxanes use chiral pool starting materials, stoichiometric chiral reagents or chiral separations.^{6,108} However, there are a few enantioselective peroxidations that have been recently developed. Deng's group reported the peroxidation of α,β -unsaturated ketones using cumene hydroperoxide, TFA, and a cinchona alkaloid derived primary amine catalyst (Figure 4.1).¹⁰⁹ The resulting peroxides were isolated in excellent yields and

enantioselectivities. At the same time as Deng, List independently reported an enantioselective synthesis of peroxyhemiketals using the same catalyst **3**.¹¹⁰ In 2010, Antilla published the chiral phosphoric acid catalyzed conjugate addition of *tert*-alkyl hydroperoxides into *N*-Acyl aryl imines.¹¹¹ The α -amino peroxides were generated in good yields and high enantioselectivities but the scope of this reaction is limited to specialized aryl imines.

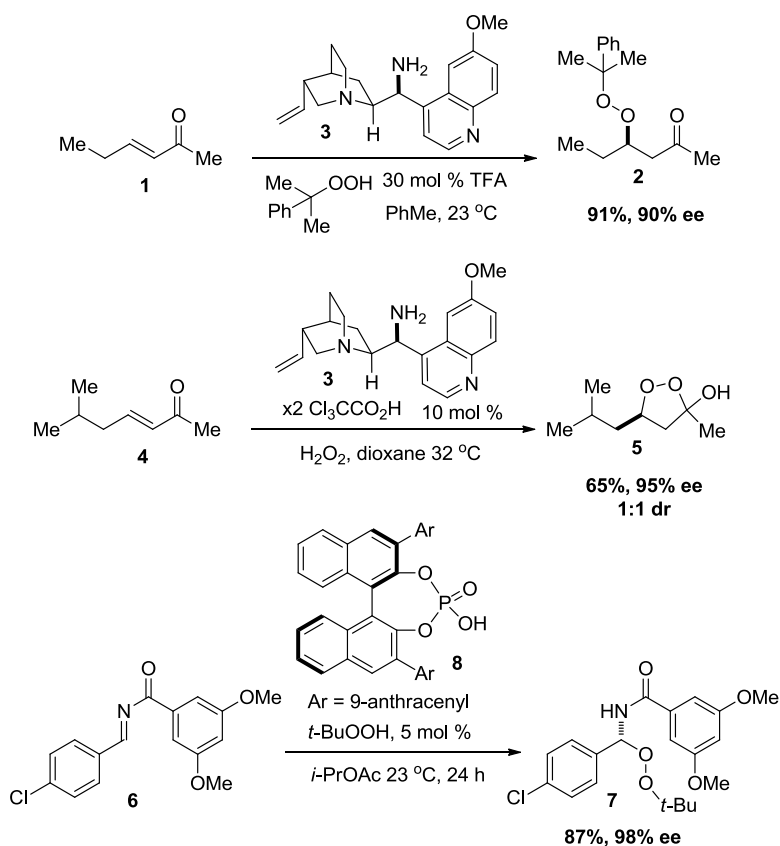


Figure 4.1

4.2 Enantioselective Trioxane Synthesis

4.2.1 Synthetic Approach

We envisioned that trioxanes could be accessed quickly and enantioselectively through a desymmetrization of *p*-peroxyquinols via an acetalization/oxa-Michael cascade, first reported by Jefford.¹¹² His group published four examples of hydroxy enones reacting with aldehydes and Amberlyst-15 to form trioxanes in excellent yields and high diastereoselectivities (Figure 4.2).

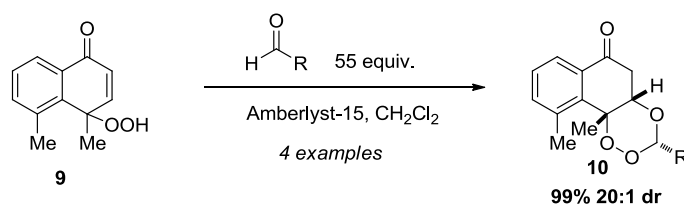


Figure 4.2

Our proposed cascade begins with the formation of a peroxy-hemiacetal intermediate (**12**) (Figure 4.3). **12** will subsequently undergo an oxa-Michael to form the trioxane product **13**. Our goal was to develop conditions for the enantioselective addition of peroxyquinols into aldehydes. The resulting chiral peroxy-hemiacetal intermediate might be too sensitive to isolated. However, since it is part of a cascade, it should exist long enough to undergo a diastereoselective oxa-Michael to provide enantioenriched trioxanes.

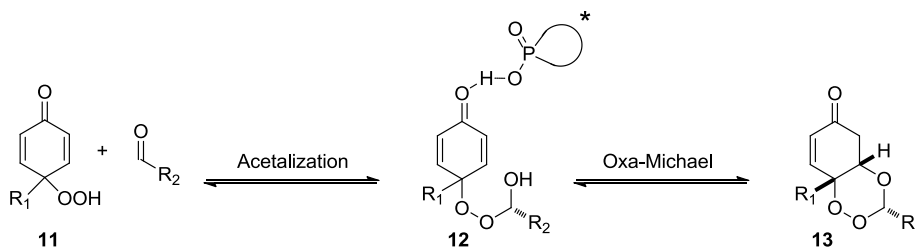
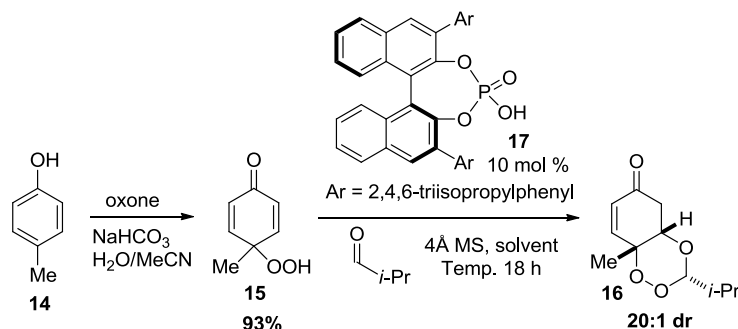


Figure 4.3

4.2.2 Reaction Development

The previous chapter discussed the inherent difficulties of asymmetric Brønsted acid catalyzed acetalizations. Additionally, the enantioselective oxa-Michael reaction has proved difficult. Undaunted, we were emboldened by the precedent set by other groups and began our investigation by studying the desymmetrization of *p*-peroxyquinol **15**. Starting material **15** is easily accessed from a hetero-Diels-Alder of cresol **14** and $^1\text{O}_2$.¹¹³ Using isobutyraldehyde and chiral Brønsted acid catalyst **17**, various solvents were screened (Table 4.1). Dichloromethane and dichloroethane both afforded trioxane **16** in modest yields, 20:1 dr and 85% ee. Dichloroethane was selected as it was better suited for higher temperatures, which led to an improvement in yield while maintaining high selectivities (Table 4.1).

Table 4.1



Entry	Solvent	Temperature	Yield (%)	ee%
1	THF	25 °C	< 5%	NA
2	Dioxane	25 °C	< 5%	NA
3	Toluene	25 °C	29%	49%
4	CH ₂ Cl ₂	25 °C	38%	85%
5	DCE	25 °C	40%	85%
6	DCE	0 °C	10%	85%
7	DCE	50 °C	88%	85%
8	DCE	65 °C	85%	85%

The high diastereoselectivity of the desymmetrization reaction can be explained by reduced 1,3-diaxial interactions in the transition state leading to the favored product (Figure 4.4).

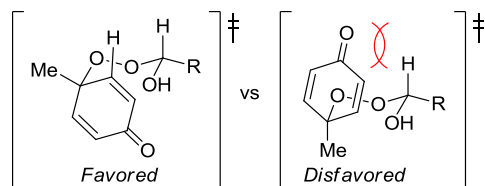


Figure 4.4

Next we investigated the effects of catalyst loading on reactivity. At less than 5 mol % of catalyst **17**, the yield dropped off drastically, and at even lower loadings, the enantioselectivity suffered. Additionally, 4Å MS were necessary for high enantioselectivities (Table 4.2). Initial reaction optimization gave a high watermark of 86% ee. To improve this, we pursued catalyst development.

Table 4.2

Entry	Catalyst Loading	Yield (%)	ee%
1	1 mol %	13%	69%
2	2.5 mol %	20%	73%
3	5 mol %	33%	76%
4	10 mol %	92%	86%
5 ^a	10 mol %	90%	74%
6	25 mol %	40%	86%

^a No 4Å MS

4.2.3 Catalyst Development

We began by replacing BINOL scaffold with a spiro-bisindane. This diol was first reported by Birman¹¹⁴ and in 2010 List developed the phosphoric acid.¹¹⁵ Catalyst **19** and its derivatives (**18**, **20-22**) were synthesized from *m*-anisaldehyde in 13-15 steps (Figures 4.5 and 4.6). The first step is a double aldol condensation of **23** and acetone. The enone product was reduced with Raney Ni and brominated to afford **24**. Using polyphosphoric acid, **24** undergoes a dehydrative spirocyclization to form the spiro-bisindane core. Subsequent bromine removal and deprotection leads to desired diol (+/-) **25**. The racemate is then resolved using chromatographic separation of the menthol derivatized diastereomers. The diol is protected with MOM groups, and after iodination, a Kumada cross coupling with Grignard **27** affords **28** in modest yields. After the protecting groups were removed, diol **29** was condensed with POCl₃ and subsequently hydrolyzed with water to provide phosphoric acid **19**.

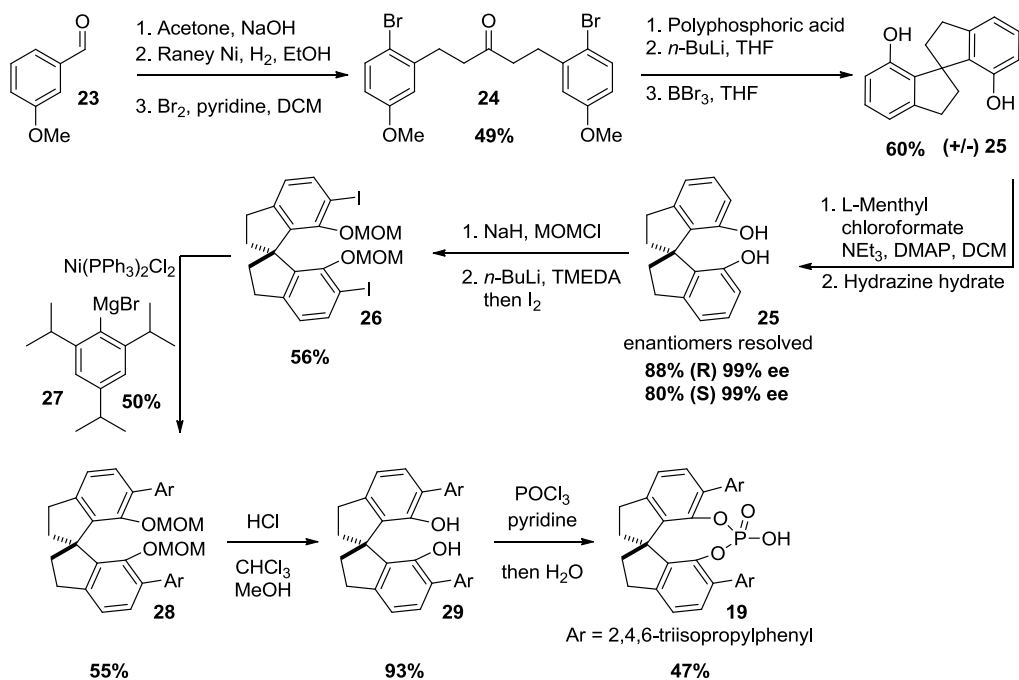


Figure 4.5

The synthesis of the more acidic thio-phosphoric acids and thio-phosphoramides was attempted using a similar route as **19** (Figure 4.6). PSOCl_3 was used in place of POCl_3 to form the thiophosphoryl chlorides, but any attempts to add nucleophiles into these species were met with failure. To circumvent this issue, the less hindered phosphorobromidite was prepared and then reacted with the desired nucleophile. Following successful addition to phosphorous, the resulting phosphoramidites were oxidized using elemental sulfur to deliver the desired Brønsted acid catalysts.

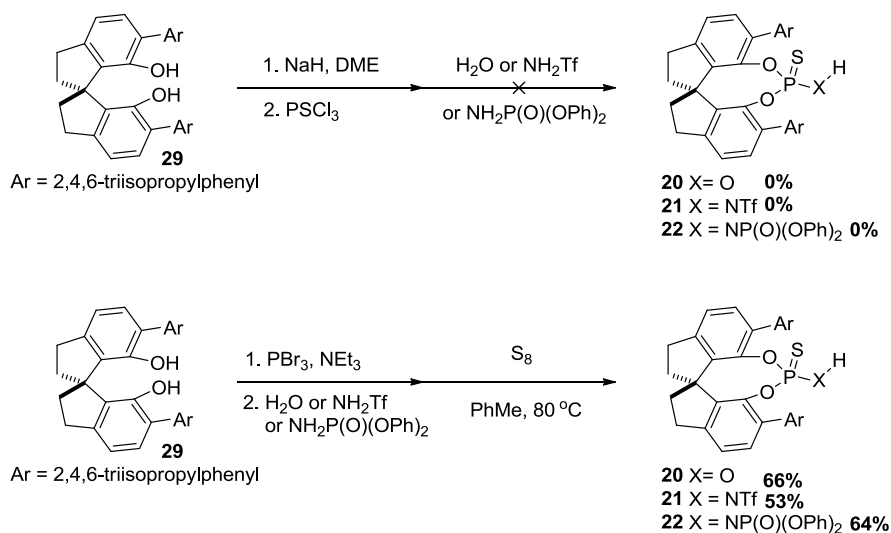


Figure 4.6

After preparing our new catalysts, we screened them using our optimized conditions. To our delight, catalyst **19** improved enantioselectivity to a respectable 96% (Figure 4.7). Switching the 3,3'-substituents from 2,4,6- $(i\text{-Pr})_3\text{-C}_6\text{H}_2$ to 9-anthracenyl led to a decrease in ee.¹¹⁶ We rationalized that a more acidic catalyst might give better reactivity so we synthesized spiro-bisindane based catalysts **20-22**. These new Brønsted acid catalysts containing this scaffold were tested to decrease the 10 mol % catalyst loading. Unfortunately, they only exhibited similar or worse reactivities.

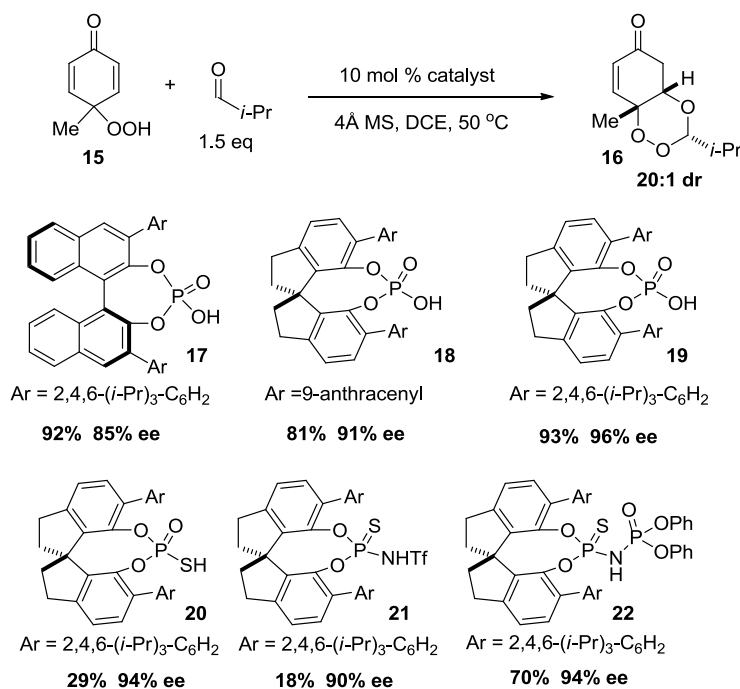


Figure 4.7

4.2.4 Co-Catalyst Effects

Since catalyst **19** is expensive and time consuming to make, we hoped to decrease the catalyst loading and maintain activity by adding a readily available co-catalyst. Catechol additives decomposed the *p*-peroxyquinol starting material presumably through an oxa-Michael. Weak Brønsted acids like acetic acid, hexafluoroisopropanol and ureas were tolerated but had little impact. To our surprise, when 5 mol % of electron-deficient thiourea **34** was used in combination with 5 mol % of acid **19**, the desired trioxane was isolated in the same yield as the conditions using 10 mol % **19** (Table 4.3). Even catalyst loadings as low as 2 mol % of **19** could be used with the aid of the thiourea co-catalyst (Table 4.3). This is significant because many Brønsted acid catalyzed reactions require 10-20 mol %. Thioureas are known to catalyze acetalizations¹¹⁷ but the restored activity might arise from the thiourea acting as a Brønsted acid to decrease the pK_a of acid **19** (Figure 4.8).

Table 4.3

5 mol % **19**
5 mol % co-catalyst
4Å MS, DCE, 50 °C

15 + 1.5 eq $\xrightarrow{\hspace{10em}}$ **16**
20:1 dr

Entry	Co-catalyst	Yield (%)	ee (%)
1	 30 R = H, <i>t</i> -Bu, CN, CO ₂ Et	< 5%	NA
2	 31	25%	96%
3	 32	31%	95%
4	 33	24%	96%
5	 34	92%	96%
6 ^a	 34	88%	95%

^a 2 mol % of **19** with 5 mol % **34**, 72 h

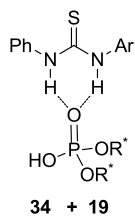


Figure 4.8

When catalyst loading of **19** was decreased to 1 mol % and combined with 10 mol % of thiourea **34**, a 2.3:1 ratio of the desired trioxane and the reduced dioxolane was isolated (Figure 4.9). If thiourea was used as the sole catalyst, then a similar result was obtained. A control experiment

showed that the *p*-peroxyquinol was being reduced by thiourea **34** to alcohol **36**. This data suggests that the thiourea can decompose the starting material but when it is in an equimolar ratio with the phosphoric acid, the decomposition pathway is minimized due to a thiourea phosphoric acid complex (**35 + 19**).

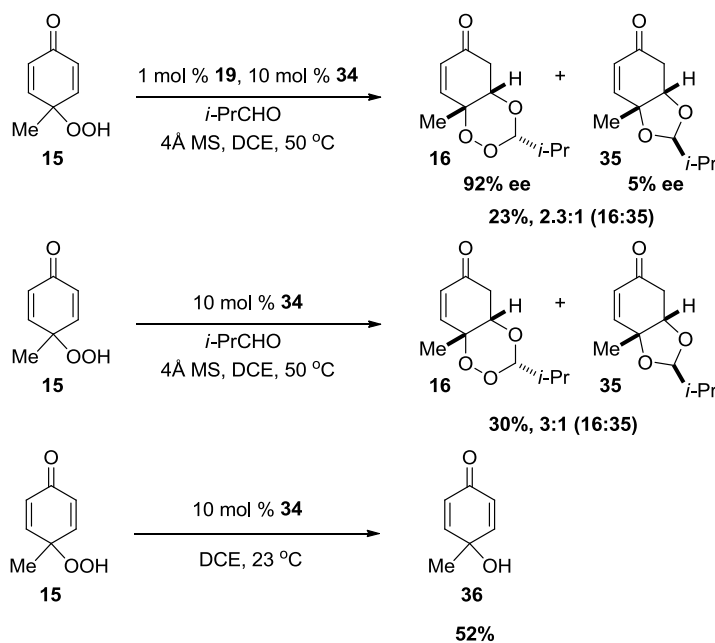
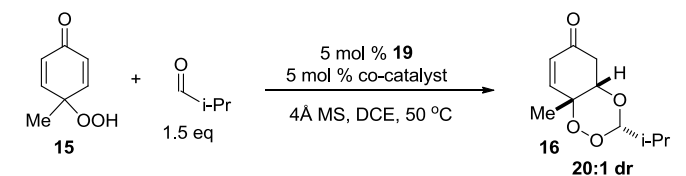


Figure 4.9

We also screened chiral thioureas and related squaramides as co-catalysts but they did not improve the reaction (Table 4.4). These catalysts may be ineffective because the tertiary amines may form ammonium salts with phosphoric acid. It is also possible that the peroxides oxidize the tertiary amines to the *N*-oxides.

Table 4.4



Entry	Co-catalyst	Yield (%)	ee (%)
1		12%	96%
2		15%	96%
3		21%	96%
4		< 5 %	NA

^aReactions were performed on 0.1 mmol scale (0.25 M solution) ^bIsolated yields of analytically pure material. ^cEnantiomeric excess determined by HPLC using a chiral stationary phase.

4.2.5 Substrate Scope

With our optimized reaction conditions, we explored the aldehyde scope of the reaction (Figure 4.4). Paraformaldehyde and a variety of sterically hindered aliphatic aldehydes work well. Aldehydes containing alkyl halides, protected alcohols and protected amines are tolerated, affording trioxanes with excellent selectivities (Table 4.5). Aromatic aldehydes also participate in the reaction with high enantioselectivity but slightly decreased yields. The decrease in yield

for electron rich aryl aldehydes is a result of a thermodynamically less favorable peroxy-hemiacetal formation.¹¹⁸

Table 4.5

Reaction scheme: 15 + R-CHO $\xrightarrow[4\text{\AA MS, DCE, } 50\text{ }^\circ\text{C}]{5\text{ mol \% } 19, 5\text{ mol \% } 34}$ 41a-h

Entry	Aldehyde	Product	Yield (%)	ee (%)	dr
1	(paraformaldehyde)		89	94	> 20:1
2			90	94	> 20:1
3			84	96	> 20:1
4			75	96	> 20:1
5			95	97	> 20:1
6			83	97	> 20:1
7			89	94	> 20:1
8			83	90	> 20:1

^a Reactions were performed on 0.1 mmol scale (0.25 M solution) ^b Isolated yields of analytically pure material after chromatography. ^c Diastereomeric ratio determined from crude NMR ^d Enantiomeric excess determined by HPLC using a chiral stationary phase.

Table 4.6

Reaction scheme showing the conversion of **15** (2-methyl-4-oxocyclohex-2-en-1-yl hydroperoxide) and an aldehyde (R-CHO) to product **41i-o** (2-methyl-4-oxocyclohex-2-en-1-yl acetal) using 5 mol % **19**, 5 mol % **34**, 4Å MS, DCE, 50 °C.

Entry ^a	Aldehyde	Product	Yield (%) ^b	ee (%) ^d	dr ^c
1			84	97	> 20:1
2			71	94	> 20:1
3			81	98	> 20:1
4			79	96	> 20:1
5 ^e			66	91	> 20:1
6			53	91	> 20:1
7			45	91	> 20:1

^a Reactions were performed on 0.1 mmol scale (0.25 M solution) ^b Isolated yields of analytically pure material after chromatography. ^c Diastereomeric ratio determined from crude NMR ^d Enantiomeric excess determined by HPLC using a chiral stationary phase. ^e The opposite enantiomer of **19** was used for **41m**. Absolute configuration was established by X-ray analysis of **41m** and the rest were assigned by analogy.

The absolute configuration of the products was established by X-ray analysis of **41m** and the rest were assigned by analogy (Figure 4.10).

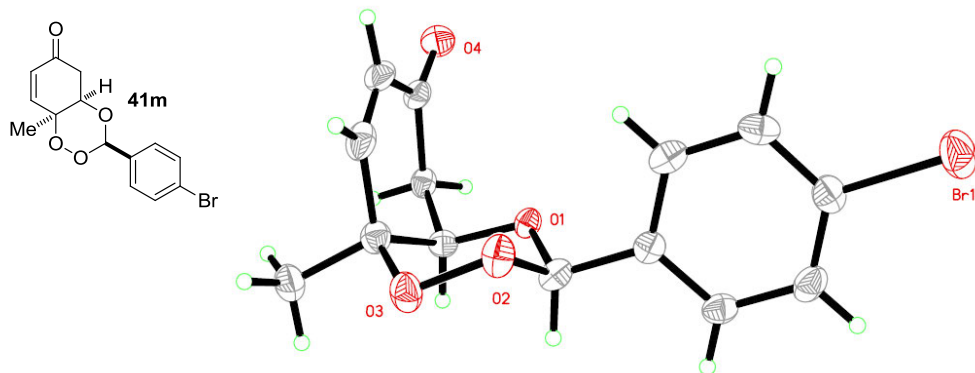


Figure 4.10

The reaction also proved tolerant of substitution on the *p*-peroxyquinol. Products with esters, ethers and multiple tetrasubstituted stereocenters were isolated in good yields and selectivities (Table 4.7).

Table 4.7

Entry	Quinol	Product	Yield (%)	ee (%)	dr
1			79	95	> 20:1
2			63	90	> 20:1
3			66	96	> 20:1
4			67	95	> 20:1

4.3 Mechanistic Studies

We propose that the reaction proceeds via a dynamic kinetic resolution of peroxyhemiacetal (+/-) **44** (Figure 4.11). Once the peroxyhemiacetal is formed, each enantiomer can form two diastereomers from the oxa-Michael reaction. The diastereoselectivity is dictated by 1,3-diaxial interactions in the transition state causing **16a** and **16c** to be favored. Stereoisomer **16a** predominates because it is selected through a matched interaction of catalyst **19** and intermediate **44a**. Peroxy-hemiacetal **44b** has a mismatched interaction with **19** and cyclizes more slowly. The unproductive enantiomer **44b** can be racemized because the first step is highly reversible. This

racemization paired with the kinetic resolution of the intermediates theoretically allows for 100% of the racemic mixture to be converted to single enantiomer.

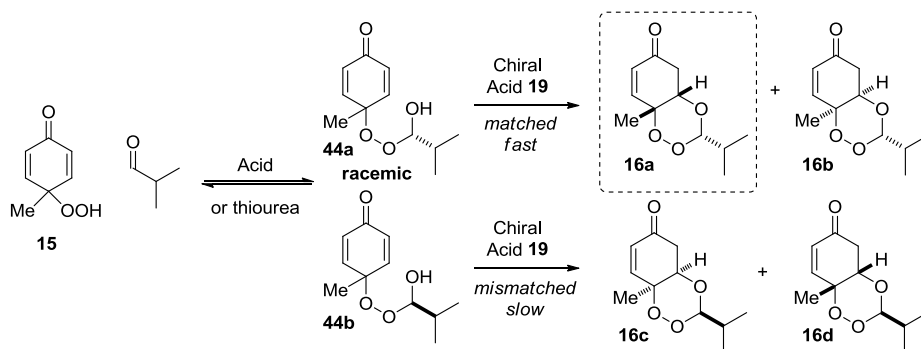


Figure 4.11

The high enantioselectivity achieved when paraformaldehyde is used in the desymmetrization suggests that the enantiodetermining step is the oxa-Michael event (Table 4.5). Additionally, the enantioselectivity was excellent even at higher temperatures, which could cause racemization of the sensitive peroxy-hemiacetal intermediate.

To further investigate this reaction, racemic peroxy-hemiacetal **44** was formed by heating *p*-peroxyquinol **2a** with isobutyraldehyde. After excess aldehyde was removed, unpurified (+/-) **44** was subjected to chiral acid **19**. To our delight, trioxane **16** was formed in good yield as a single diastereomer in 94% ee (Figure 4.12). This suggests that peroxyhemiacetal **44** is resolved through a dynamic kinetic resolution. A crossover experiment subjecting trioxane **16** to *n*-butyraldehyde showed that the oxa-Michael is not reversible under the reaction conditions (Figure 4.12).

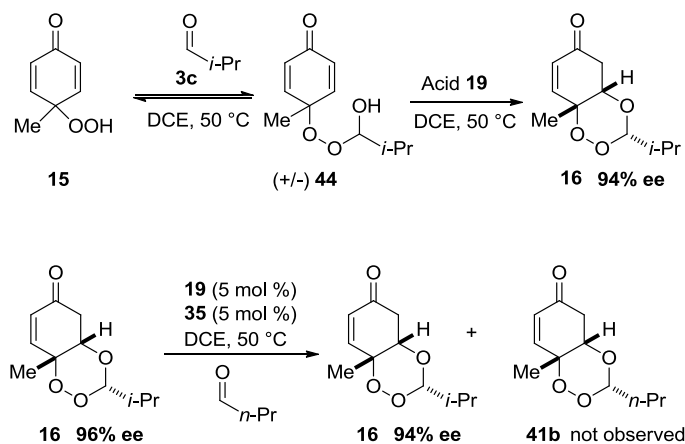
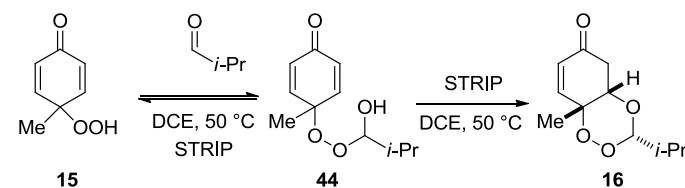


Figure 4.12

To further investigate the reaction under standard conditions with catalyst **19**, the reaction was monitored by chiral HPLC. We found that the peroxyhemiacetal **44** remains as a racemate throughout the course of the reaction and the product is always above 92% ee (Table 4.7).

Table 4.7



Entry	Time	ee 44	ee 16
1	5 min	0%	> 92% trace
2	1 h	0%	96%
3	4 h	0%	96%
4	8 h	0%	96%
5	12 h	trace	96%

4.4 Trioxane Derivatization

The 1,2,4 trioxane products of the desymmetrization have a variety of synthetic handles for subsequent derivatization. We first attempted to chemoselectively reduce the olefin of **16** in the

presence of a trioxane, but standard conditions led to a complex mixture of products (Figure 4.13). Eventually, suitable conditions were achieved using Rh/Al₂O₃ and Adams' catalyst.¹¹⁹

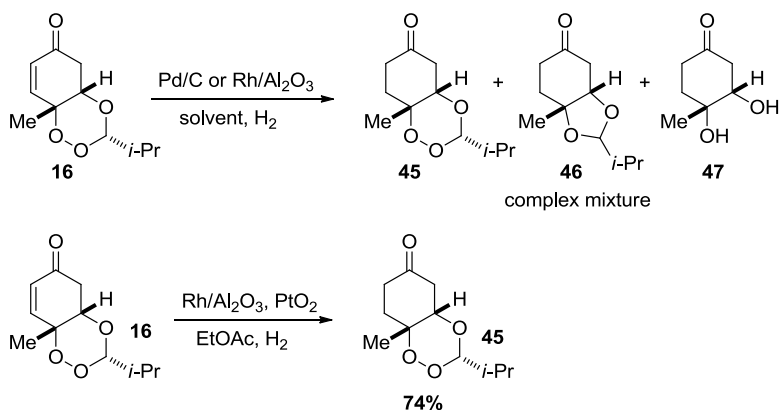


Figure 4.13

We next attempted to reduce the trioxane and unmask a vicinal diol. However, when **16** was treated with zinc and acetic acid, it was converted to cresol. This problem can be circumvented by using trioxane **45** which afforded unreported diol **47** in good yield (4.14).

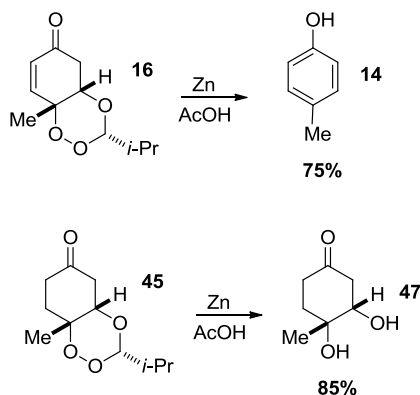


Figure 4.14

A Luche reduction of **16** forms the allylic alcohol **48** in 4:1 dr and a subsequent directed epoxidation delivers highly oxygenated cyclohexane **49** (Figure 4.15). Vinyl bromide **51** was

prepared via bromination of **16** followed by elimination. This synthetic handle allows for the incorporation of a variety of functional groups through cross coupling.

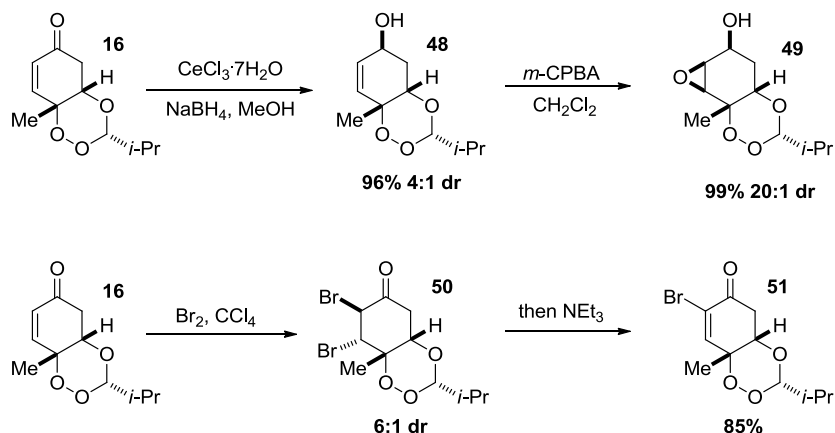


Figure 4.15

4.5 Conclusion

In conclusion, we report the first catalytic enantioselective synthesis of trioxanes using a desymmetrization of *p*-peroxyquinols via an acetalization/oxa-Michael cascade. The reaction tolerates a broad scope of aldehydes and *p*-peroxyquinols while maintaining high diastereoselectivity and enantioselectivities greater than 90%. Mechanistic studies suggest that the reaction proceeds through a dynamic kinetic resolution of a peroxyhemiacetal intermediate. The 1,2,4-trioxane products can be derivatized and allows for structure activity relationship studies.

References

- ¹⁰¹ (a) Efferth, T. *Curr. Drug Targets* **2006**, *7*, 407. (b) Posner, G. H.; D'Angelo, J.; O'Neill, P. M.; Mercer, A. *Expert Opin. Ther. Patents* **2006**, *16*, 1665-1672. (c) Hencken, C. P.; Kalinda, A. S.; D'Angelo, J. G. *Annu. Rep. Med. Chem.* **2009**, *44*, 359-378. (d) Chaturvedi, D.; Goswami, A.; Saikia, P. P.; Barua, N. C. *Chem. Soc. Rev.* **2010**, *39*, 435.
- ¹⁰² (a) Dondorp, A. M.; Nosten, F.; Yi, P.; Das, D.; Phyto, A. P.; Tarning, J.; Lwin, K. M.; Arie, F.; Hanpithakpong, W.; Lee, S. J.; Ringwald, P.; Silamut, K.; Imwong, M.; Chotivanich, K.; Lim, P.; Herdman, T.; An, S. S.; Yeung, S.; Singhasivanon, P.; Day, N. P. J.; Lindegardh, N.; Socheat, D.; White, N. J. *New Engl. J. Med.* **2009**, *361*, 455-467. (b) Hastings, I. *Trends Parasitol.* **2011**, *27*, 67-72. (c) Ding, X. C.; Beck, H.-P.; Raso, G. **2011**, *27*, 73-81. (d) O'Brien, C.; Henrich, P. P.; Passi, N.; Fidock, D. A. *Curr. Opin. Infect. Dis.* **2011**, *24*, 570.
- ¹⁰³ (a) Jefford, C. W. *Curr. Med. Chem.* **2001**, *8*, 1803. (b) Golenser, J.; Waknine, J. H.; Krugliak, M.; Hunt, N. H.; Grau, G. E. *Int. J. Parasitol.* **2006**, *36*, 1427. (c) O'Neill, P. M.; Barton, V. E.; Ward, S. A. *Molecules* **2010**, *15*, 1705.
- ¹⁰⁴ Grobusch, M. P.; van Vugt, M. *Future Microbiol.* **2010**, *5*, 1447-1449.
- ¹⁰⁵ (a) Tang, Y.; Dong, Y.; Vennerstorm, J. L. *Med. Res. Rev.* **2004**, *24*, 425-448. (b) Kumar, N.; Sharma, M.; Rawat, D. S. *Curr. Med. Chem.* **2011**, *18*, 3889. (c) Jefford, C. W. *Drug Discovery Today* **2012**, *12*, 487. (d) Jefford, C. W. *Curr. Top. Med. Chem.* **2012**, *12*, 373. (e) Slack R. D.; Jacobine A. M.; Posner G. H. *Med. Chem. Commun.* **2012**, *3*, 281.
- ¹⁰⁶ (a) Jefford, C. W.; Kohmoto, S.; Jaggi, D.; Timári, G.; Rossier, J.-C.; Rudaz, M.; Barbuzzi, O.; Gérard, D.; Burger, U.; Kamalaprija, P.; Mareda, J.; Bernardinelli, G. *Helv. Chem. Act.* **1995**,

- 78, 647-662. (b) 647-662. O’Niell, P. M.; Rawe, S. L.; Borstnik, K.; Miller, A.; Ward, S. A.; Bray, P. G.; Davies, J.; Oh, C. H.; Posner, G. H. *ChemBioChem*. **2005**, *6*, 2048.
- ¹⁰⁷ Beekman, A. C.; Barentsen, A. R. W.; Woerdenbag, H. J.; Van Uden, W. Pras, N.; Konings, A. W. T.; El-Feraly, F. S.; Galal, A. M.; Wikström, H. V. *J. Nat. Prod.* **1997**, *60*, 325.
- ¹⁰⁸ (a) Avery, M. A.; Chong, W. K. M.; Jennings-White, C. *J. Am. Chem. Soc.* **1992**, *114*, 974-979. (b) Hamzaoui, M.; Provot, O.; Grégoire, F.; Riche, C.; Chiaroni, A.; Gay, F.; Moskowicz, H.; Mayrargue, J. *Tetrahedron-Asymmetr.* **1997**, *8*, 2085-2088. (c) Zouhiri, F.; Desmaële, D. d’Angelo, J.; Riche, C.; Gay, F.; Cicéron, L. *Tetrahedron Lett.* **1998**, *39*, 2969-2972. (d) O’Neill, P. M.; Miller, A.; Bickley, J. F.; Scheinmann, F.; Oh, C. H.; Posner, G. H. *Tetrahedron Lett.* **1999**, *40*, 9133-9136. (e) Lévesque, F.; Seeberger, P. H. *Angew. Chem., Int. Ed.* **2012**, *51*, 1706-1709.
- ¹⁰⁹ Lu, X.; Liu, Y.; Cindric, B.; Deng, L. *J. Am. Chem. Soc.* **2008**, *130*, 8134-8135.
- ¹¹⁰ (a) Reisinger, C. M.; Wang, X.; List, B. *Angew. Chem., Int. Ed.* **2008**, *47*, 8112-8115. (b) Lifchits, O.; Reisinger, C. M.; List, B. *J. Am. Chem. Soc.* **2010**, *132*, 10227-10229.
- ¹¹¹ Zheng, W.; Wojtas, L.; Antilla, J. C. *Angew. Chem., Int. Ed.* **2010**, *49*, 6589-6591.
- ¹¹² (a) Jefford, C. W.; Jaggi, D.; Boukouvalas, J.; Kohmoto, S. *J. Am. Chem. Soc.* **1983**, *105*, 6497. (b) Jefford, C. W.; Kohmoto, S.; Boukouvalas, J.; Burger, U. *J. Am. Chem. Soc.* **1983**, *105*, 6498. (c) Jefford, C. W.; Jaggi, D.; Kohmoto, S.; Boukouvalas, J.; Bernardinelli, G. *Helv. Chim. Acta* **1984**, *67*, 2254.
- ¹¹³ Carreño, M. C.; González-López, M.; Urbano, A.; *Angew. Chem., Int. Ed.* **2006**, *45*, 2737.
- ¹¹⁴ Diol Synthesis: Birman, V. B.; Rheingold A. L.; Lam, K.-C. *Tetrahedron: Asymmetry* **1999**, *10*, 125.
- ¹¹⁵ Phosphoric acid synthesis: Čorić, I.; Müller, S.; List, B. *J. Am. Chem. Soc.* **2010**, *132*, 17370.

¹¹⁶ Xing, C.-H.; Liao, Y.-X.; Ng, J.; Hu, Q.-S. *J. Org. Chem.* **2011**, *76*, 4125-4131.

¹¹⁷ Kotke, M.; Schreiner, P. R. *Tetrahedron*, **2006**, *62*, 434-439.

¹¹⁸ Tsai, C.-Y.; Chen, L.-A.; Sung, K. *Can. J. Chem.* **2012**, *90*, 321-325.

¹¹⁹ Riviera, M. J.; La-Venia, A.; Mischne, M., P. *Tetrahedron Lett.* **2010**, *51*, 804-807.

Chapter 5

Investigation of the Antimalarial and Cytotoxic Activities of Synthetic Trioxanes

5.1 Biological Activity of Artemisinin

5.1.1 Introduction

Trioxanes are important scaffolds, which appear in molecules that exhibit antimalarial, anticancer and antibacterial activities.¹²⁰ One 1,2,4-trioxane containing natural product is artemisinin (**1**) (Figure 5.1). Chinese scientists discovered that extracts from sweet worm wood (*Artemisia annua*) could be used to cure malaria that was resistant to current drugs.¹²¹ The active compound was later identified as artemisinin and it is currently administered as a part of a combination therapy for the frontline treatment of malaria.

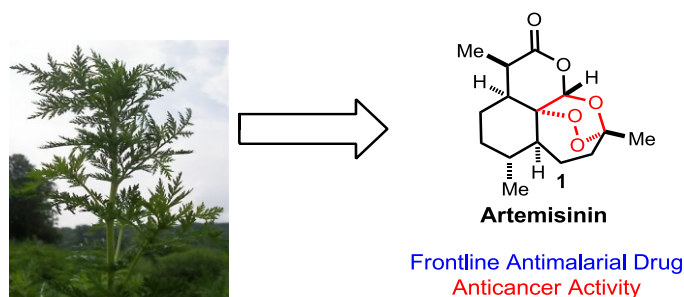


Figure 5.1

5.1.2 Trioxane Mode of Action

The 1,2,4-trioxane/endoperoxide is the key pharmacophore in artemisinin, but the exact mode of action still remains under debate. The two mechanisms proposed for its activity are both based on the iron-dependent bioactivation of the endoperoxide.¹²² It is hypothesized that artemisinin first accumulates in the malaria parasite's food vacuole and then reacts with iron from either

hematin or non-heme sources to create oxygen and carbon centered radicals. Artemisinin is relatively stable to intact healthy oxyhemoglobin, which is the most abundant form of iron in humans; however, it reacts with the free heme that is produced when malaria parasites are present.¹²³ This supports a heme based activation and explains the selective toxicity toward parasite infected erythrocytes.

There are two supported mechanisms for the bioactivation of artemisinin.¹²⁴ One model involves Fe (II) induced reductive homolysis of the endoperoxide. The resulting oxygen centered radicals (**2** and **4**) can either undergo a 1,5-H atom abstraction or β -scission to form destructive carbon centered radicals (**3** and **5**) (Figure 5.2). A different mechanism proposes that iron acts as a Lewis acid to cause heterolytic cleavage.¹²⁵ The addition of water creates a hydroperoxide **6** which can undergo Fenton reactions and create cytotoxic radicals.

In addition to its antiparasitic properties, artemisinin has been reported to be cytotoxic toward cancer cells.¹²⁶ The mechanism for artemisinin's cytotoxicity is also unclear, but it is hypothesized to proceed through a similar iron mediated release of radicals to induce DNA damage, mitochondrial depolarization and apoptosis.¹²⁷

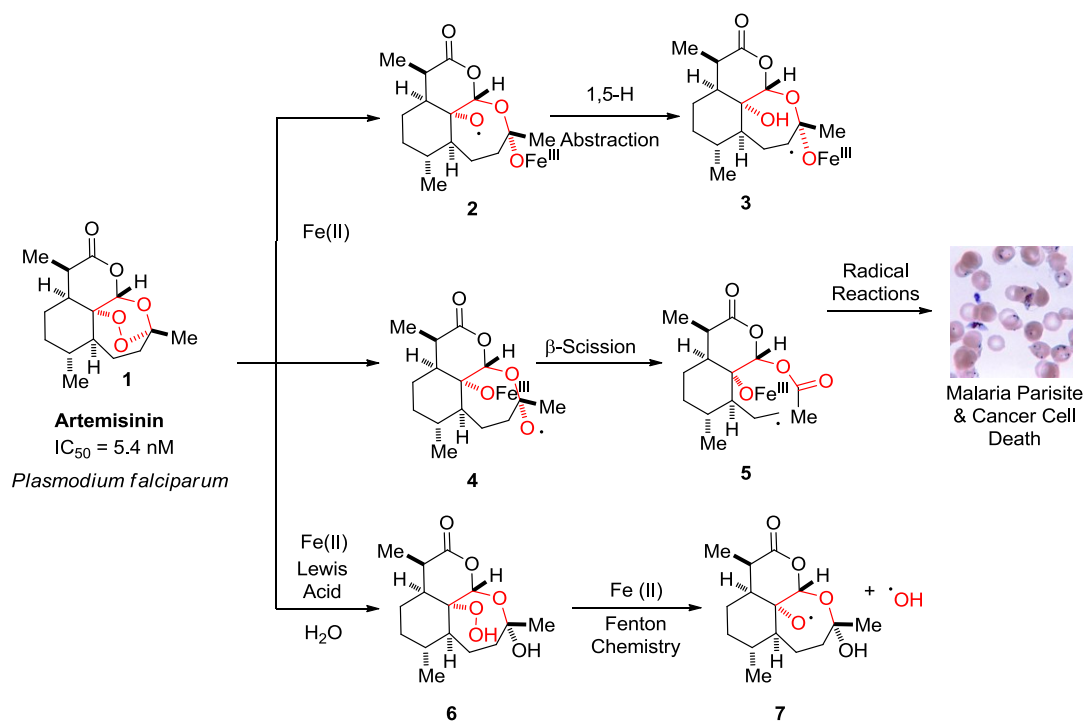


Figure 5.2

5.1.3 Synthetic Trioxanes

Once the 1,2,4-trioxane was linked to artemisinin's antimalarial activity and cancer cell cytotoxicity, researchers synthesized hundreds of artemisinin derivatives and synthetic endoperoxide containing molecules.¹²⁸ Many of the reported compounds involve lengthy syntheses and cannot be easily modified. Current methods for the synthesis of enantioenriched trioxanes use chiral pool starting materials, stoichiometric chiral reagents or chiral separations.¹²⁹ Although stereochemistry is not very important to trioxanes' anti-malarial activities,^{129b,g} it has a demonstrated impact on anti-cancer activity.^{129d} A concise and enantioselective synthesis of trioxanes is necessary for the development of practical drug candidates.

5.2 Biological Testing of Synthetic Endoperoxides

5.2.1 Synthetic Endoperoxides

Recently we developed a rapid two-step synthesis of 1,2,4-trioxanes and 1,2,4-dioxazinanes from cresol, oxone and either aldehydes, ketones or imines (Figure 5.3). Cresol and oxone are produced on commodity scales and are thus abundant and inexpensive. The reaction also proceeds asymmetrically to afford the products in high diastereoselectivity and enantioselectivity, a necessity should these analogs enter clinical trials. Importantly, the synthesis affords wide structural diversity at various positions around the trioxane core leading to the potential for rational probing of the active site and access to a full structure activity relationship profile. In addition to trioxanes, our process can tolerate imines which allows us to access synthetically unexplored 1,2,4-dioxazinanes **11**. These nitrogen containing heterocycles have never been synthesized or tested for antiparasitic activity and cancer cell cytotoxicity. The nitrogen atom may allow pharmacokinetic and pharmacodynamic properties to be improved while maintaining good activities.

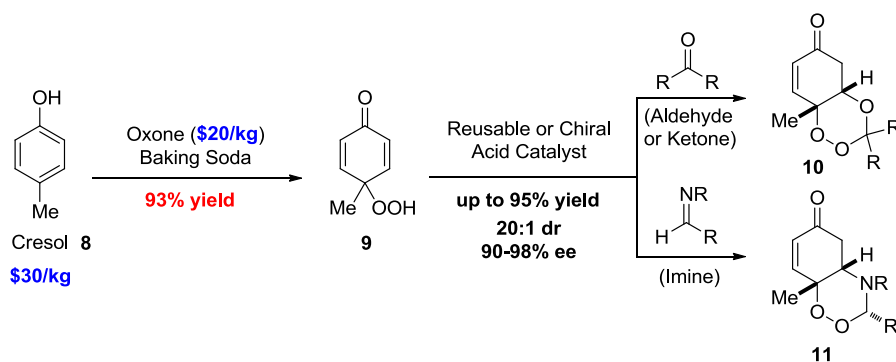


Figure 5.3

5.2.2 Antimalarial Activities of Synthetic Trioxanes and Dioxazinanes

In collaboration with Christine Olver at Colorado State University, a few of the endoperoxide containing molecules were tested for antimalarial activity towards the most deadly malaria parasite, *Plasmodium falciparum*. Our compounds show modest to poor activity in comparison to artemisinin (Figure 5.4). The trioxane derived from pivaldehyde demonstrates the best activity with an IC_{50} of 35.3 nM. Although this is much less potent than artemisinin, additional synthetic trioxanes will be tested to find a more active molecule and develop a structure to activity relationship profile.

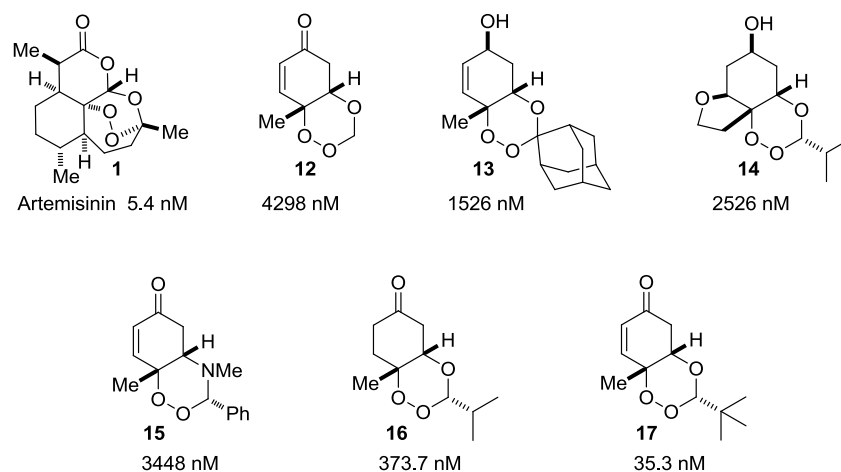


Figure 5.4

5.2.3 D17 Canine Carcinoma Cell Cytotoxicity Studies of Synthetic Trioxanes

In addition to serving as the frontline antimalarial agent, artemisinin derivatives are cytotoxic toward certain cancer cell lines and the 1,2,4-trioxane is proposed to play an important role.¹³⁰ In particular, dihydroartemisinin has shown promising cytotoxicity in canine osteosarcoma cells with IC_{50} values ranging from 8.7 to 43.6 μ M.¹³¹ Although a number of groups have reported the cytotoxicity data for artemisinin derivatives, completely synthetic trioxanes remain to be investigated. Indeed, in a recent review it was stated, “It would be interesting to ascertain if these structurally simpler fully synthetic endoperoxides were as effective in tumor cells as they are in *Plasmodia*.”^{122c}

We explored this question, in collaboration with Douglas Thamm, Michelle Morges and Barb Rose at the Colorado State University Animal Cancer Center, by screening our trioxanes and dioxazinanes for cytotoxicity against a variety of cancer cell lines. The initial study was conducted using D17 canine osteosarcoma cells and the compounds have *in vitro* IC_{50} values from 3.4 to 950 μ M (Figure 5.5). The most active compounds are derived from formaldehyde,

isobutyraldehyde and aryl aldehydes. Trioxanes with longer aliphatic groups give very low activities. The most potent trioxane **18** was modified at the 6-position and we discovered that substituents larger than a methyl group significantly reduce cytotoxicity.

IC₅₀ Values for D-17 Canine Osteosarcoma cells (μM)

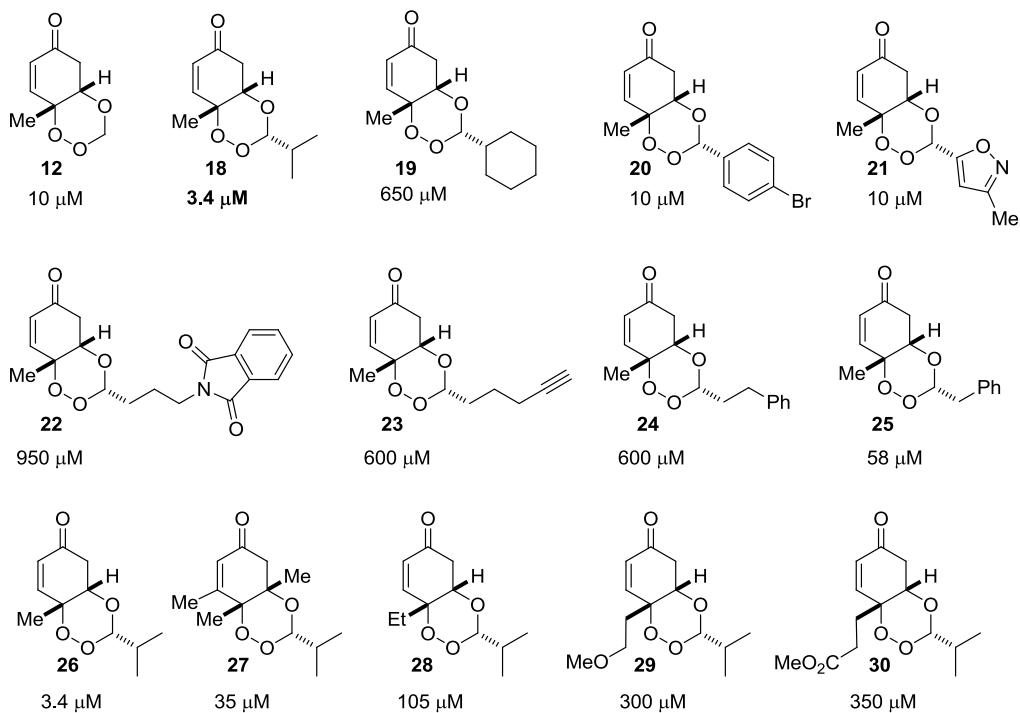


Figure 5.5

We thought that modification of the cyclohexenone ring could lead to improved activity. Unfortunately, reduction of the ketone on **18** leads to a drastic decrease (Figure 5.6). Semi-reduced compound **16** has moderate cytotoxicity but it is much worse than that of the parent compound. The only derivative that has similar activity is α -bromo enone **33**. While monomeric trioxanes have the best antimalarial properties, artemisinin dimers have shown an increase in cancer cytotoxicity so we produced a bis-trioxane from adipaldehyde. Its activity is very low in comparison to the monomer and this may be due to its solubility issues. This dimer contains a four carbon aliphatic linker and but our previously tested compounds with aliphatic chains show

almost no activity. More dimeric compounds should be synthesized with amine or ether linkers to increase the solubility of the compounds.

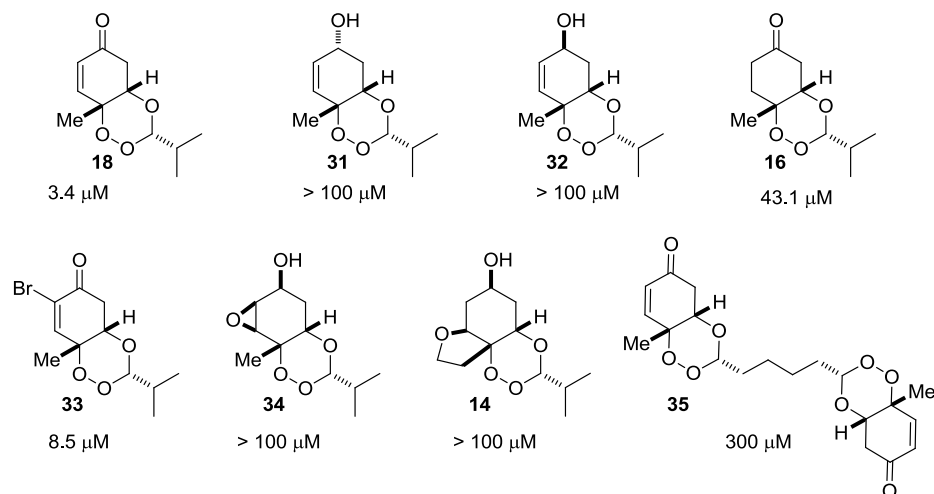


Figure 5.6

Adamantyl groups can play a key role in synthetic trioxanes' antimalarial activities¹³² so a few ketone derived trioxanes were synthesized. Their IC_{50} values were found to be moderate, but none were as good as **18** (Figure 5.7). As we previously observed, ketone reduction of **37** causes a dramatic decrease in cytotoxicity.

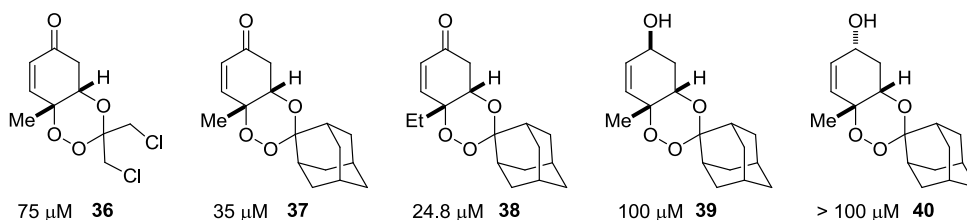


Figure 5.7

All of our compounds lost their activities when the enone was removed so we thought that the Michael acceptor, which is known to be toxic, might be responsible for our compound's cytotoxicity. To test this, we reduced the enone to the ketone (**16**) and found that the activity

decreased, but it was not lost completely (Figure 5.8). The dioxolane derivative **42** was synthesized to test a Michael acceptor containing molecule that lacked a trioxane. Even though it maintained a Michael acceptor, its activity was diminished in comparison to the parent trioxane. Cyclohexenone (**43**) was also tested and its IC₅₀ value is worse than **18**. Since both compounds lacking the trioxane showed an order of magnitude decrease in activity, this suggests that the endoperoxide is playing a key role in the cytotoxicity.

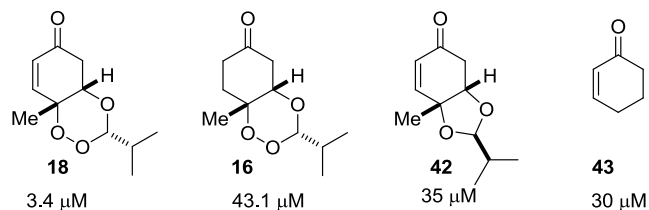


Figure 5.8

In addition, previously unexplored dioxazinanes were screened against the D17 canine osteosarcoma cell line (Figure 5.9). The 1,2,4-dioxazinane **15** exhibited excellent activity but reduction to the allylic alcohols **44** and **45** gave poor cytotoxicities.

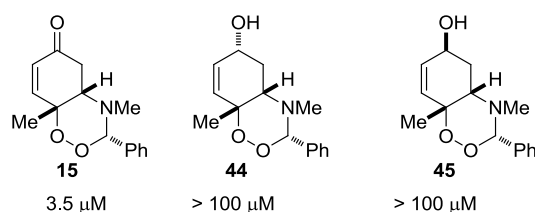


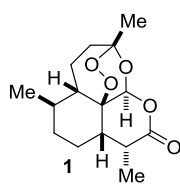
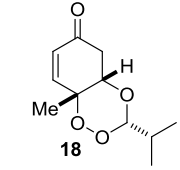
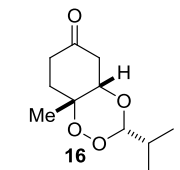
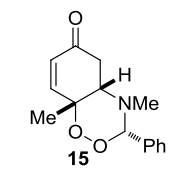
Figure 5.9

5.2.4 Human and Canine Cell Line Cytotoxicity Studies of Synthetic Trioxanes

Our studies show that trioxane **18** and dioxazinane **15** have the best activities toward D17 canine osteosarcoma. They were tested against a variety of human cancer cell lines to investigate their

efficacy and selectivity. Interestingly, artemisinin shows no cytotoxicity toward any of the cell lines.¹³³ Compounds **18** and **15** demonstrate good activities toward all of the cell lines except MDA human breast carcinoma (Table 5.1). This suggests that when the trioxane and Michael acceptor are both present the compounds are potent but not selective. The semi-reduced trioxane **16** has modest activity and it demonstrates some selectivity toward A549 human lung carcinoma with an IC₅₀ of 25 μM. **16** contains the trioxane and lacks the Michael acceptor demonstrating that our molecules' toxicity may be partially attributed to the trioxane.

Table 5.1

	D17 Canine Osteosarcoma	M21 Human Melanoma	MDA Human Breast Carcinoma	A549 Human Lung Carcinoma	PC3 Human Prostate Carcinoma
 1	> 100 μ M	> 100 μ M	> 100 μ M	> 100 μ M	> 100 μ M
 18	3.4 μ M	26.3 μ M	> 100 μ M	5.7 μ M	11.1 μ M
 16	43.1 μ M	100 μ M	> 100 μ M	25 μ M	100 μ M
 15	3.5 μ M	30.1 μ M	> 100 μ M	6.4 μ M	14.8 μ M

5.2.4 Further Canine Cell Line Cytotoxicity Studies of Synthetic Trioxane (18)

Compound **18** exhibits the best activity so it was tested against twenty four canine cancer cell lines to get a better idea of its mode of action. To our delight, it was not toxic to all of the cell lines and shows some interesting activity trends (Figure 5.10).

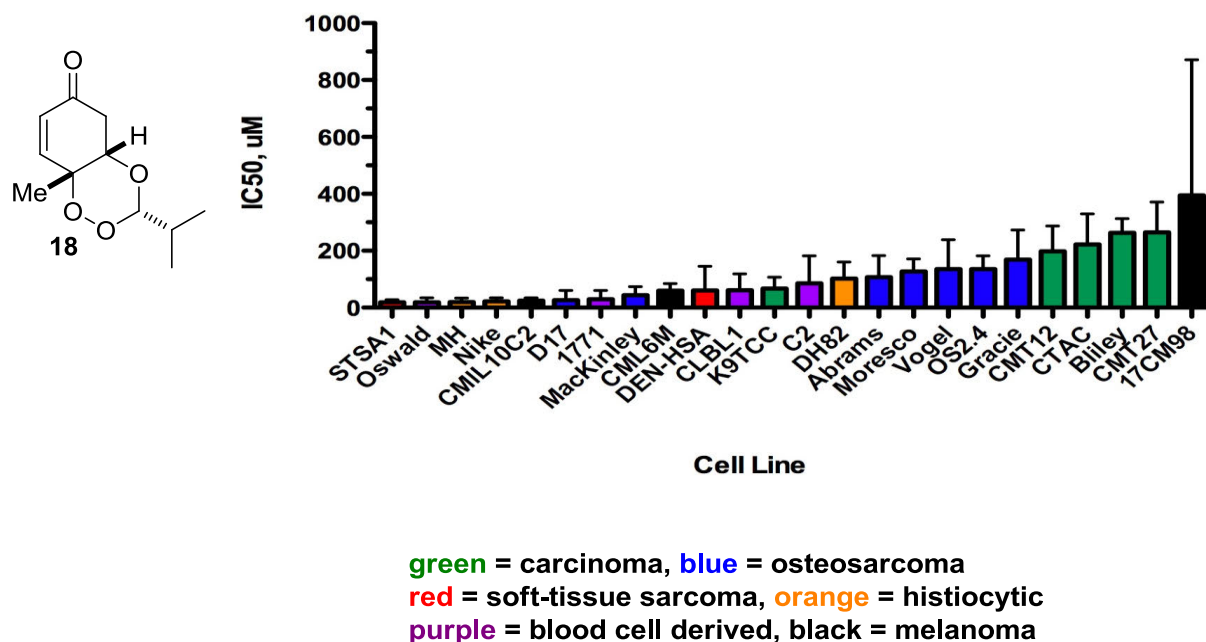


Figure 5.10

A log normalized graph gives a better picture of the relative activities. In general, trioxane **18** has more activity against tumors of blood cell origin (purple and orange) and less against tumors of epithelial origin (green) (Figure 5.11). This data will be integrated with gene expression information to get a better relationship. Additionally, the detection of iron-dependent generation of reactive oxygen species is ongoing and will give more insight to our synthetic trioxanes mode of action.

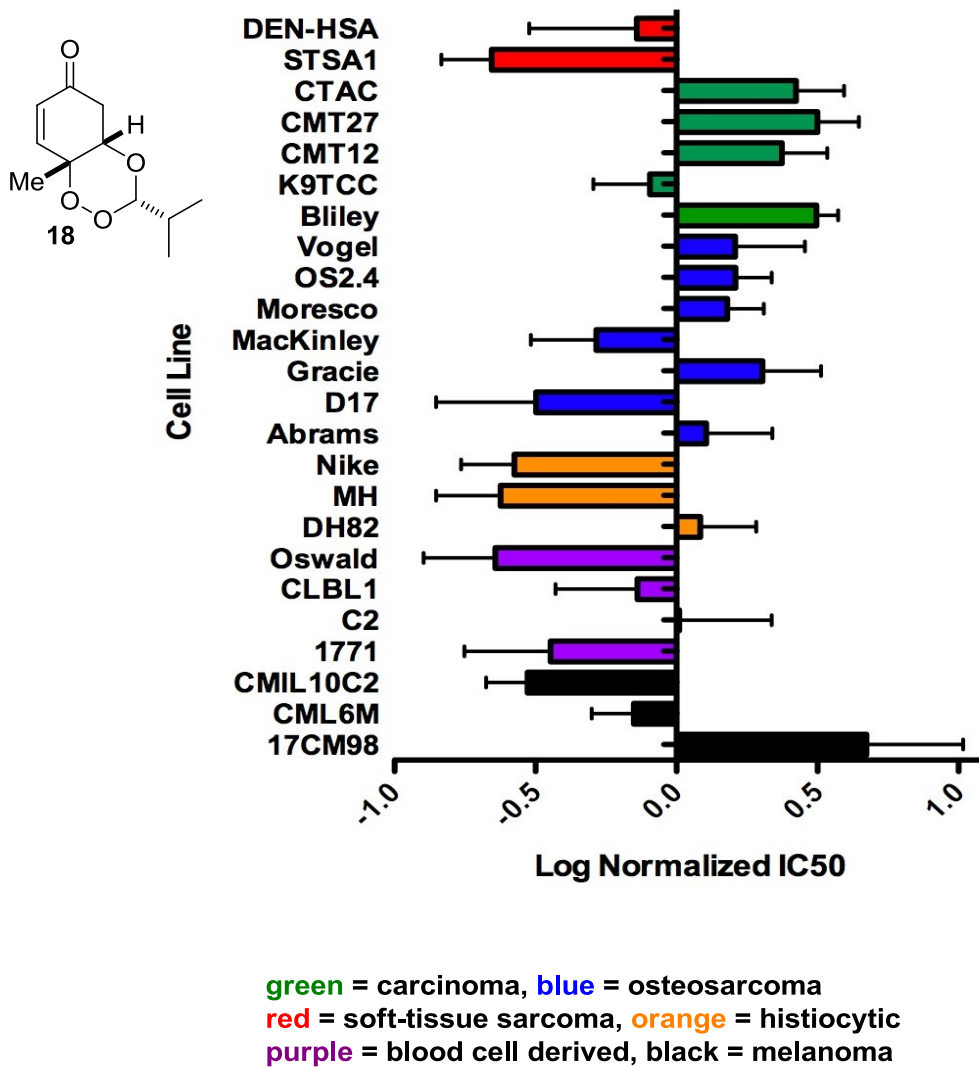


Figure 5.11

5.3 Conclusion

Trioxanes and dioxazinanes were synthesized using our process and tested for antimalarial and cytotoxicity. The pivaldehyde derived trioxane **17** shows modest activity towards *Plasmodium falciparum* with an *in vitro* IC₅₀ value of 35.3 nM. An extensive screen of synthetic endoperoxides found that the isobutyraldehyde derived trioxane **18** and dioxazinane **15** have the best cytotoxicity toward D17 canine osteosarcoma cells with *in vitro* IC₅₀ values of 3.4 and 3.5

μM respectively. These compounds were also found to be cytotoxic toward human cancer cell lines. Some of trioxane **18**'s toxicity may be attributed to its Michael acceptor, but semi-reduced ketone **16** demonstrated modest cytotoxicity and had better selectivity. Additionally, the activity for the dioxolane analog of **18** (**42**) diminished by an order of magnitude, thus demonstrating the importance of the endoperoxide in cancer cell cytotoxicity. These promising results will be further investigated in hopes to find a compound with nM activity and determine the trioxanes' mode of action.

References

- ¹²⁰ (a) Efferth, T. *Current Drug Targets* **2006**, *7*, 407. (b) Posner, G. H.; D'Angelo, J.; O'Neill, P. M.; Mercer, A. *Expert Opin. Ther. Patents* **2006**, *16*, 1665-1672. (c) Hencken, C. P.; Kalinda, A. S.; D'Angelo, J. G. *Annu. Rep. Med. Chem.* **2009**, *44*, 359-378. (d) Chaturvedi, D.; Goswami, A.; Saikia, P. P.; Barua, N. C. *Chem. Soc. Rev.* **2010**, *39*, 435.
- ¹²¹ Zhang, J.-F. A Detailed Chronological Record of Project 523 and the Discovery and Development of Qinghaosu (Artemisinin).), Yang Cheng Evening News Publishing Company, **2005**.
- ¹²² (a) Jefford, C. W. *Curr. Med. Chem.* **2001**, *8*, 1803. (b) Golenser, J.; Waknine, J. H.; Krugliak, M.; Hunt, N. H.; Grau, G. E. *Int. J. Parasitol.* **2006**, *36*, 1427. (c) O'Niell, P. M.; Barton, V. E.; Ward, S. A. *Molecules* **2010**, *15*, 1705.
- ¹²³ Creek, D. J.; Ryan, E.; Charman, W. N.; Chiu, F. C. K.; Prankerd, R. J.; Vennerstrom, J. L.; Charman, S. A. *Antimicrob. Agents Chemother.* **2009**, *53*, 3496-3500.
- ¹²⁴ (a) Posner, G. H.; Wang, D.; Cumming, J. N.; Oh, C. H.; French, A. N.; Bodley, A. L.; Shapiro, T. A. *J. Med. Chem.* **1995**, *38*, 2273-2275. (b) Posner, G. H.; Oh, C. H. *J. Am. Chem. Soc.* **1992**, *114*, 8328-8329. (c) Posner, G. H.; Oh, C. W.; Wang, D. S.; Gerena, L.; Milhous, W. K.; Meshnick, S. R.; Asawamahasadka, W. *J. Med. Chem.* **1994**, *37*, 1256-1258. (d) Jefford, C. W.; Favarger, F.; Vicente, M.; Jacquier, Y. *Helv. Chim. Acta* **1995**, *78*, 452-458. (e) Jefford, C. W.; Vicente, M. G. H.; Jacquier, Y.; Favarger, F.; Mareda, J.; Millasson-Schmidt, P.; Brunner, G.; Burger, U. *Helv. Chim. Acta* **1996**, *79*, 1475-1487.
- ¹²⁵ Haynes, R. K.; Chan, W. C.; Lung, C. M.; Uhlemann, A. C.; Eckstein, U.; Taramelli, D.; Parapini, S.; Monti, D.; Krishna, S. *ChemMedChem* **2007**, *2*, 1480-1497.

- ¹²⁶ Woerdenbag, H. J.; Moskal, T. A.; Pras, N.; Malingre, T. M.; Elferaly, F. S.; Kampinga, H. H.; Konings, A. W. T. *J. Nat. Prod.* **1993**, *56*, 849–856.
- ¹²⁷ (a) Efferth, T.; Benakis, A.; Romero, M. R.; Tomicic, M.; Rauh, R.; Steinbach, D.; Häfer, R.; Stamminger, T.; Oesch, F.; Kaina, B.; Marschall, M. *Free Radical Biol. Med.* **2004**, *37*, 998–1009. (b) Mercer, A.; Maggs, J.; Sun, X.; Cohen, G.; Chadwick, J.; O'Neill, P.; Park, B. *J. Biol. Chem.* **2007**, *282*, 9372–9382.
- ¹²⁸ (a) Tang, Y.; Dong, Y.; Vennerstorm, J. L. *Med. Res. Rev.* **2004**, *24*, 425–448. (b) Kumar, N.; Sharma, M.; Rawat, D. S. *Curr. Med. Chem.* **2011**, *18*, 3889. (c) Jefford, C. W. *Drug Discov. Today* **2012**, *12*, 487. (d) Jefford, C. W. *Curr. Top. Med. Chem.* **2012**, *12*, 373. (e) Slack R. D.; Jacobine A. M.; Posner G. H. *Med. Chem. Commun.* **2012**, *3*, 281.
- ¹²⁹ (a) Avery, M. A.; Chong, W. K. M.; Jennings-White, C. *J. Am. Chem. Soc.* **1992**, *114*, 974–979. (b) Jefford, C. W.; Kohmoto, S.; Jaggi, D.; Timári, G.; Rossier, J.-C.; Rudaz, M.; Barbuzzi, O.; Gérard, D.; Burger, U.; Kamalaprija, P.; Mareda, J.; Bernardinelli, G. *Helv. Chem. Act.* **1995**, *78*, 647–662. (c) Hamzaoui, M.; Provot, O.; Grégoire, F.; Riche, C.; Chiaroni, A.; Gay, F.; Moskowitz, H.; Mayrargue, J. *Tetrahedron-Asymmetr.* **1997**, *8*, 2085–2088. (d) Beekman, A. C.; Barentsen, A. R. W.; Woerdenbag, H. J.; Van Uden, W. Pras, N.; Konings, A. W. T.; El-Feraly, F. S.; Galal, A. M.; Wikström, H. V. *J. Nat. Prod.* **1997**, *60*, 325. (e) Zouhiri, F.; Desmaële, D. d'Angelo, J.; Riche, C.; Gay, F.; Cicéron, L. *Tetrahedron Lett.* **1998**, *39*, 2969–2972. (f) O'Neill, P. M.; Miller, A.; Bickley, J. F.; Scheinmann, F.; Oh, C. H.; Posner, G. H. *Tetrahedron Lett.* **1999**, *40*, 9133–9136. (g) 647–662. O'Neill, P. M.; Rawe, S. L.; Borstnik, K.; Miller, A.; Ward, S. A.; Bray, P. G.; Davies, J.; Oh, C. H.; Posner, G. H. *Chem. Bio. Chem.* **2005**, *6*, 2048. (h) Lévesque, F.; Seeberger, P. H. *Angew. Chem. Int. Ed.* **2012**, *51*, 1706–1709.

- ¹³⁰ Morrissey, C.; Gallis, B.; Solazzi, J. W.; Kim, B. J.; Gulati, R.; Vakar-Lopez, F.; Goodlett, D. R.; Vessella, R. L.; Sasaki, T. *Anticancer Drugs* **2010**, *21*, 423.
- ¹³¹ Hosoya, K.; Murahari, S.; Laio, A.; London, C. A.; Couto, C. G.; Kisseberth, W. C. *Am. J. Vet. Res.* **2008**, *69*, 519-526.
- ¹³² Griesbeck, A. G.; Schlundt, V. *Synlett* **2011**, *16*, 2430-2432.
- ¹³³ Ji, Y.; Zhang, Y.-C.; Pei, L.-B.; Shi, L.-L.; Yan, J.-L.; Ma, X.-H. *Mol. Cell. Biochem.* **2011**, *351*, 99-108.

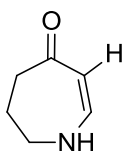
Appendix 1

Chapter 2 Supporting Information

General Methods:

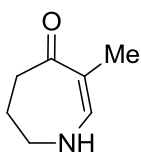
All reactions were carried out in oven-dried glassware with magnetic stirring. Dichloroethane (DCE) was degassed with argon and distilled from CaH₂. Dichloromethane was degassed with argon and passed through two columns of neutral alumina. Toluene was degassed with argon and passed through one column of neutral alumina and one column of Q5 reactant. Column chromatography was performed on Silicycle Inc. silica gel 60 (230-400 mesh). Thin layer chromatography was performed on Silicycle Inc. 0.25 mm silica gel 60-F plates. Visualization was accomplished with UV light (254 nm) and KMnO₄ followed by heating.

¹H NMR and ¹³C NMR spectra were obtained on Varian 300 or 400 MHz spectrometers in CDCl₃ at ambient temperature and chemical shifts are expressed in parts per million (δ, ppm). Proton chemical shifts are referenced to 7.26 ppm (CHCl₃) and carbon chemical shifts are referenced to 77.0 ppm (CDCl₃). NMR data reporting uses the following abbreviations: s, singlet; bs, broad singlet; d, doublet; t, triplet; q, quartet; m, multiplet; and *J*, coupling constant in Hz.

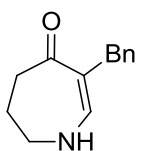


6,7-dihydro-1H-azepin-4(5H)-one (40). A solution of **40s** (25 mmol 1 eq) in 250 mL of degassed MeOH (0.16M) was added to a degassed quartz reaction tube. This mixture was irradiated with 254 nm UV light until the reaction was determined to be complete by TLC (~48h). The reaction mixture was concentrated *in vacuo* and purified using column chromatography on SiO₂ with 1:4 (hexanes:ethyl acetate) to afford analytically pure **40** as an off white solid (17.5 mmol). 70% yield; *R_f* = 0.50 (15:85 Hexanes:EtOAc); ¹H NMR (300

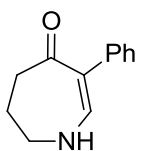
MHz, CDCl₃): δ 6.95 (bs, 1H), 6.56 (dd, J = 8.0, 9.7 Hz, 1H), 4.69 (dd, J = 1.0, 9.7 Hz, 1H), 3.45-3.38 (m, 2H), 2.59-2.53 (m, 2H), 1.95-1.86 (m, 2H); ¹³C NMR (75 MHz, CDCl₃): δ 200.6, 146.4, 98.4, 47.1, 43.1, 21.7.



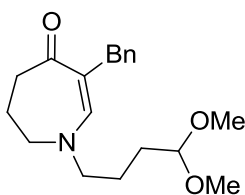
3-methyl-6,7-dihydro-1H-azepin-4(5H)-one (41). Prepared according to the procedure for **40**. 60% yield; R_f = 0.16 (15:85 Hexanes:EtOAc); ¹H NMR (300 MHz, CDCl₃): δ 6.78 (d, J = 8.0 Hz, 1H), 6.66 (bs, 1H), 3.32-3.24 (m, 2H), 2.59-2.53 (m, 2H), 1.90-1.80 (m, 2H), 1.61 (s, 3H); ¹³C NMR (75 MHz, CDCl₃): δ 198.7, 146.8, 102.9, 26.3, 43.1, 22.7, 18.1.



3-benzyl-6,7-dihydro-1H-azepin-4(5H)-one (42). Prepared according to the procedure for **40**. 92% yield; R_f = 0.28 (15:85 Hexanes:EtOAc); ¹H NMR (300 MHz, CDCl₃): δ 7.40-7.20 (m, 5H), 6.78 (d, J = 8.0 Hz, 1H), 5.45 (bs, 1H), 3.61 (s, 2H), 3.47 (dt, J = 3.8, 5.4 Hz, 2H), 2.81 (t, J = 6.1 Hz, 2H), 2.13-2.03 (m, 2H); ¹³C NMR (75 MHz, CDCl₃): δ 198.1, 146.9, 142.9, 128.5, 128.1, 125.5, 109.3, 47.1, 43.5, 37.2, 23.2.

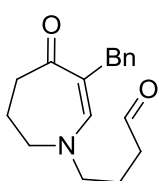


3-phenyl-6,7-dihydro-1H-azepin-4(5H)-one (43). Prepared according to the procedure for **40**. 30% yield; R_f = 0.16 (15:85 Hexanes:EtOAc); ¹H NMR (300 MHz, CDCl₃): δ 7.25-7.06 (m, 5H), 6.75 (d, J = 7.9 Hz, 1H), 6.60 (bs, 1H), 3.23-3.16 (m, 2H) 2.76-2.70 (m, 2H), 2.03-1.93 (m, 2H); ¹³C NMR (75 MHz, CDCl₃): δ 197.9, 149.4, 141.0, 129.9, 127.7, 125.4, 111.7, 46.6, 43.7, 24.3.



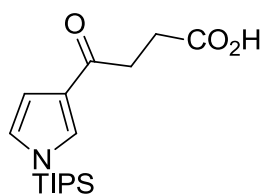
3-benzyl-1-(4,4-dimethoxybutyl)-6,7-dihydro-1H-azepin-4(5H)-one (44s). Amine **42** (745 mg 3.7 mmol, 1 eq) was dissolved in 15mL of DMF and cooled to 0 °C. Sodium hydride (180 mg, 4.1 mmol, 1.1 eq) was added in portions and the mixture was stirred for 30 minutes. Then alkyl bromide **33** (4.4 mmol,

1.2 eq) was added dropwise to the reaction. The reaction mixture was allowed to stir for 2 hours and then it was diluted with water and extracted with ethyl acetate. The combined extracts were washed with 25% LiCl to remove DMF. The extracts were concentrated *in vacuo* and purified using column chromatography on SiO₂. 77% yield; $R_f = 0.10$ (25:75 Hexanes:EtOAc); ¹H NMR (300 MHz, CDCl₃): see spectrum; ¹³C NMR (75 MHz, CDCl₃): see spectrum.



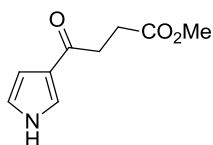
4-(6-benzyl-5-oxo-2,3,4,5-tetrahydro-1H-azepin-1-yl)butanal (44).

Dimethylacetal **44s** (900mg 2.83 mmol) was dissolved in 75mL of a 1:1:4 ratio of TFA:H₂O:CHCl₃. The reaction mixture was allowed to stir for 2 hours and then it was quenched with saturated bicarbonate. The reaction was extracted with CH₂Cl₂ and dried over MgSO₄. The residue was purified by chromatography and isolated as an oil in 77% yield; $R_f = 0.21$ (15:85 Hexanes:EtOAc); ¹H NMR (300 MHz, CDCl₃): see spectrum; ¹³C NMR (75 MHz, CDCl₃): see spectrum.



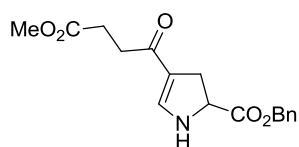
4-oxo-4-(1-(triisopropylsilyl)-1H-pyrrol-3-yl)butanoic acid A solution of succinic anhydride (36 mmol) in DCM was added slowly to a flame dried round bottom flask containing a suspension of AlCl₃ (37 mmol) in

DCM at 0 °C and allowed to stir for 30 min. A DCM solution of TIPS protected pyrrole (33.5 mmol) was added dropwise to the reaction mixture at 0 °C The reaction was stirred at 0 °C for one hour and then for 1 hour at room temperature. The reaction was quenched with ice water and the product was extracted with EtOAc. The product was purified by column chromatography using 1:1 hexanes:EtOAc. 65% yield.



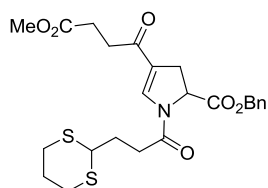
methyl 4-oxo-4-(1H-pyrrol-3-yl)butanoate Carboxylic acid **X** was refluxed for 1 h in a solution of methanol with 10 mol % TsOH. The reaction was

quenched with H₂O and the product extracted with EtOAc and isolated in 90% yield. The crude product was dissolved in THF and stirred with TBAF for 2 h. The solvent was removed and the product was purified using column chromatography.



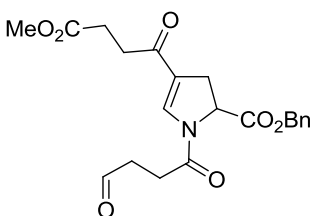
benzyl 4-(4-methoxy-4-oxobutanoyl)-2,3-dihydro-1H-pyrrole-2-carboxylate For a general procedure for the formal [3+2]

cycloaddition. Enone (1.1-1.5eq) was added dropwise to a solution of AgOAc in MeCN. Then a solution of benzylisocyanoacetate in MeCN was added over 2 hours to the reaction mixture in the dark. The solution was allowed to stir for 6-12 h. When silver metal is observed the reaction is usually complete. The reaction mixture was concentrated *in vacuo* and purified using column chromatography on SiO₂ (hexanes:ethyl acetate) to afford analytically pure product as an off white solid.



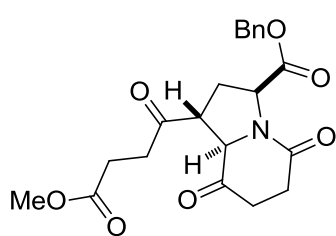
benzyl 1-(3-(1,3-dithian-2-yl)propanoyl)-4-(4-methoxy-4-oxobutanoyl)-2,3-dihydro-1H-pyrrole-2-carboxylate For a general

procedure for amid formation. A solution of acid chloride (1.1eq) in DCM was added to solution of pyrroline (1eq) was added dropwise to a solution of AgOAc in MeCN. Then a solution of benzylisocyanoacetate in MeCN was added over 2 hours to the reaction mixture in the dark. The solution was allowed to stir for 6-12 h. When silver metal is observed the reaction is usually complete. The reaction mixture was concentrated *in vacuo* and purified using column chromatography on SiO₂ (hexanes:ethyl acetate) to afford analytically pure product as an off white solid.



benzyl 4-(4-methoxy-4-oxobutanoyl)-1-(4-oxobutanoyl)-2,3-dihydro-1H-pyrrole-2-carboxylate (106) For a general procedure

for dithiane deprotection. Methyl iodide (15 eq) was added to a MeCN/H₂O solution of dithiane (1 eq) and NaHCO₃. The reaction was allowed to stir at room temperature for 8-24. When the reaction was complete by TLC, the mixture was diluted with DCM and washed with H₂O. The aqueous layer was extracted with DCM and the combined extracts were dried over MgSO₄. The reaction mixture was concentrated *in vacuo* and purified using column chromatography on SiO₂ (hexanes:ethyl acetate) to afford analytically pure product as yellow oil.

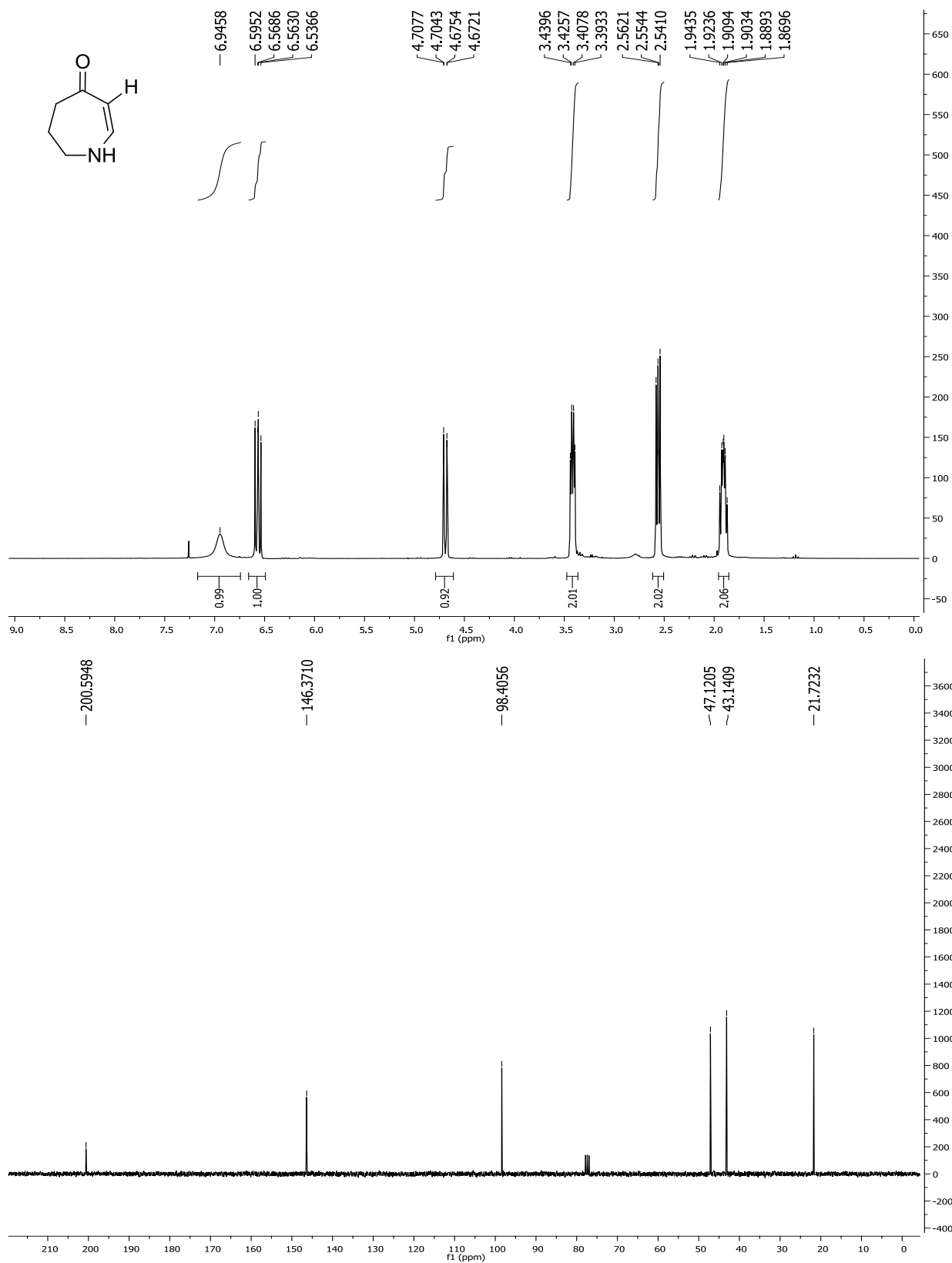


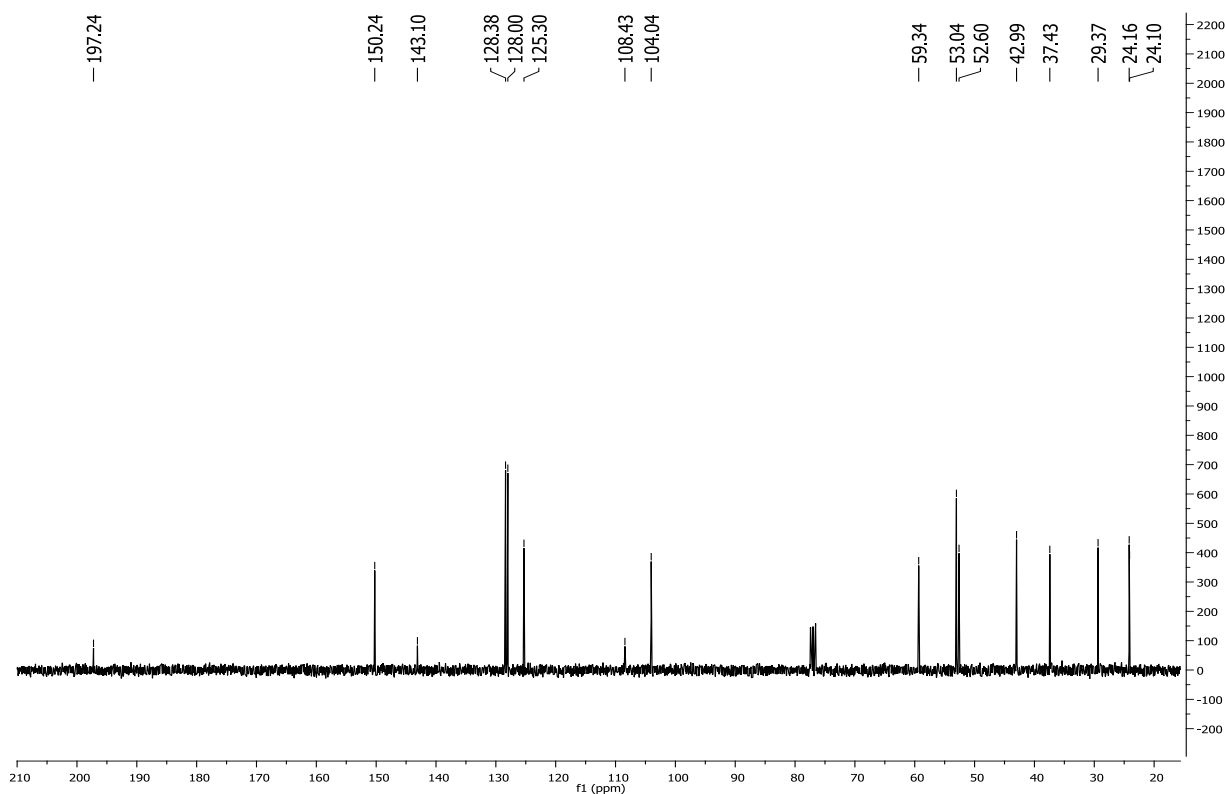
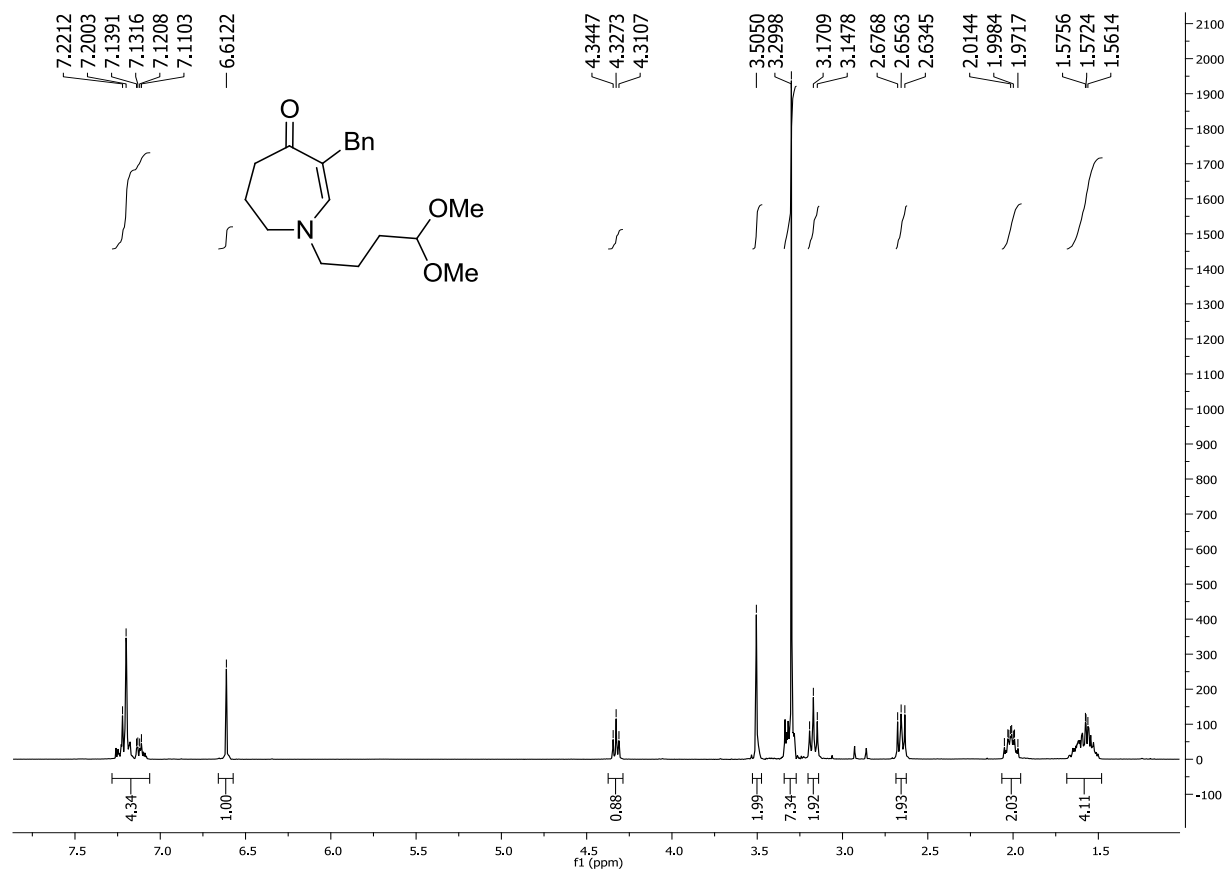
(1R,3S,8aR)-benzyl 1-(4-methoxy-4-oxobutanoyl)-5,8-

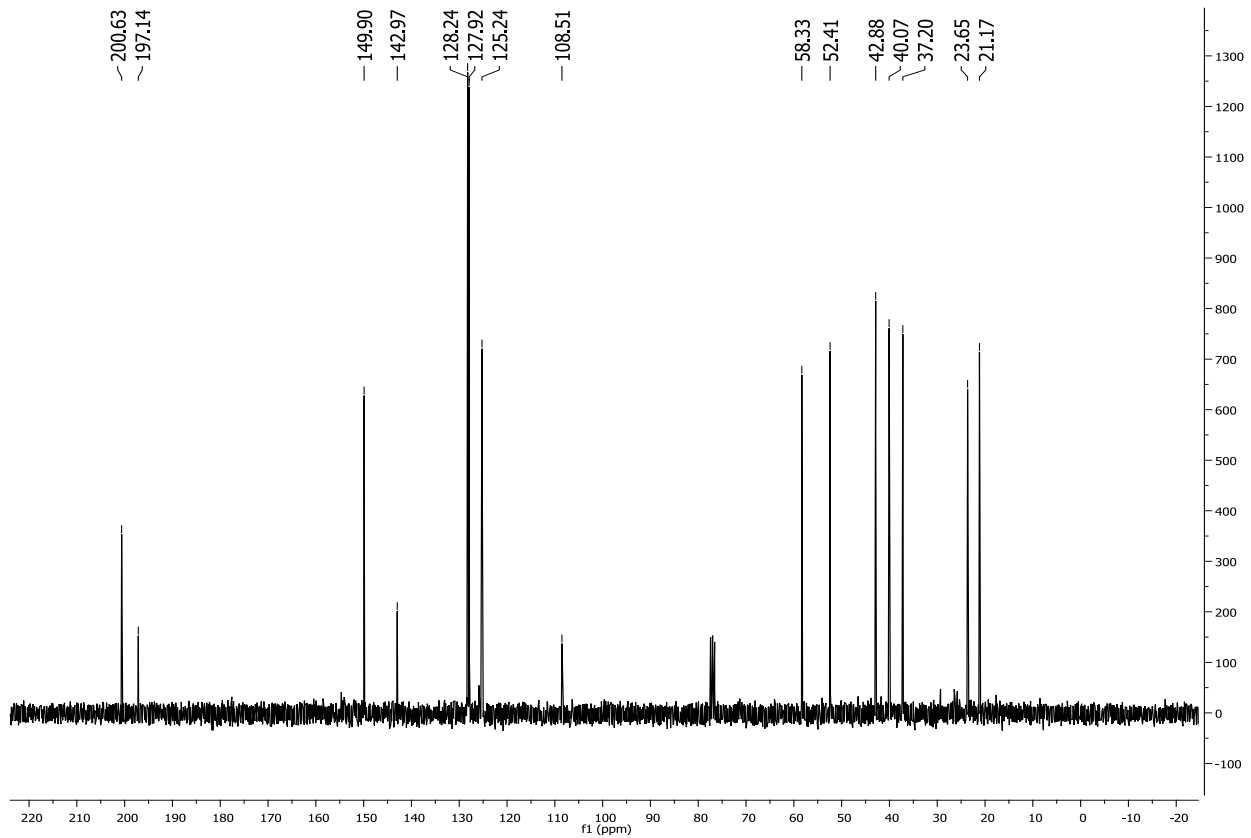
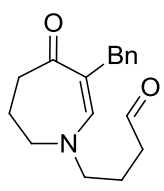
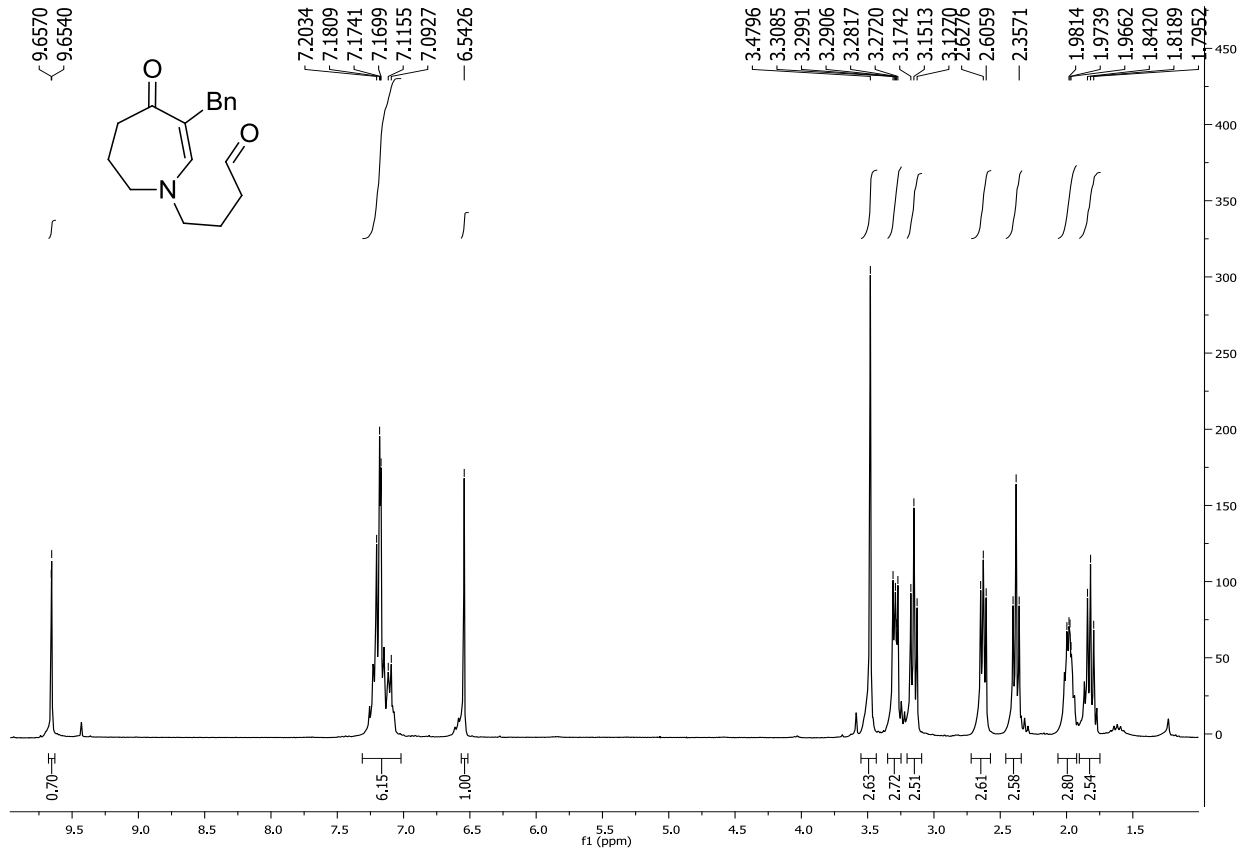
dioxooctahydroindolizine-3-carboxylate (108) For a general procedure for the Stetter reaction. To a solution of triazolium salt (0.2 eq) in PhMe was added a solution of KHMDS (0.18eq). The

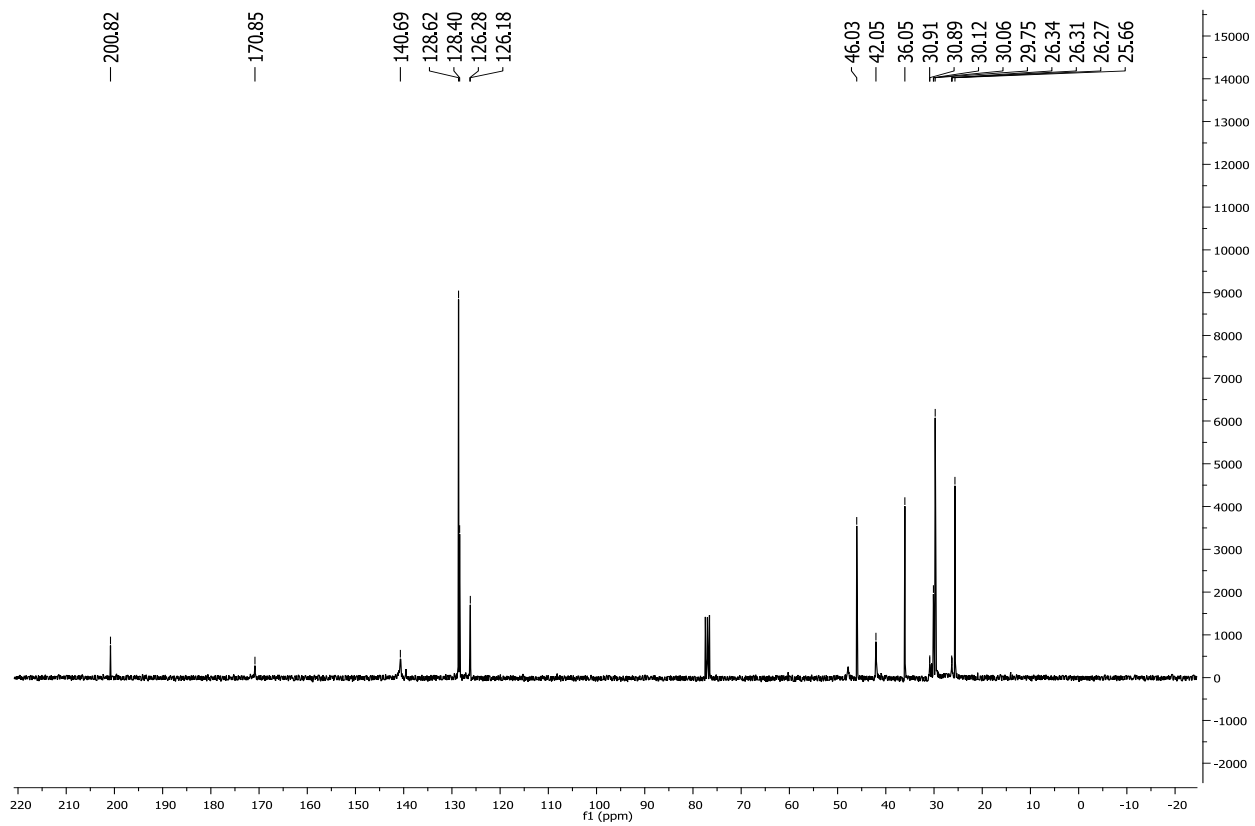
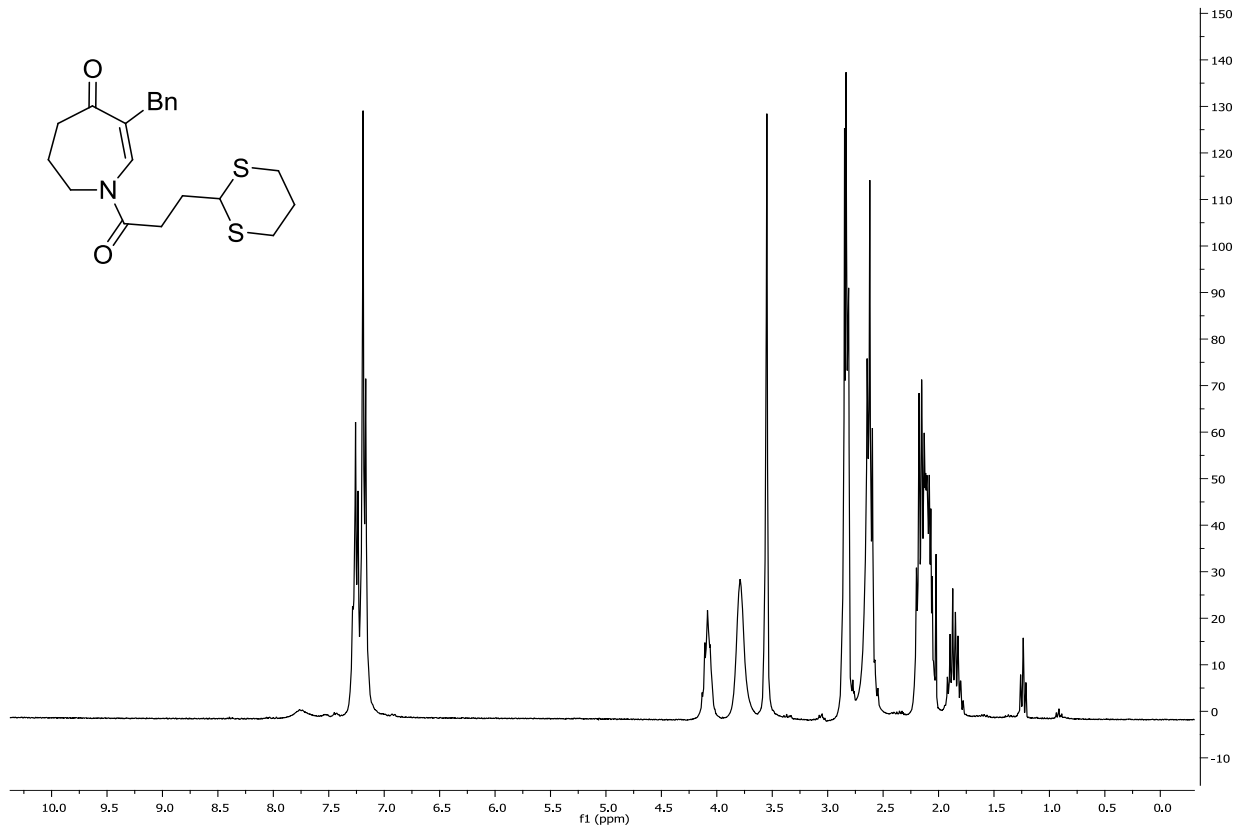
reaction mixture was allowed to stir for 30 minutes. Then a dilute solution of aldehyde (1eq) in PhMe was added dropwise of 3 hours. The reaction was then heated to 60 °C for 12 hours. The reaction mixture was concentrated *in vacuo* and purified using column chromatography on SiO₂ (hexanes:ethyl acetate) to afford analytically pure product as an off white solid.

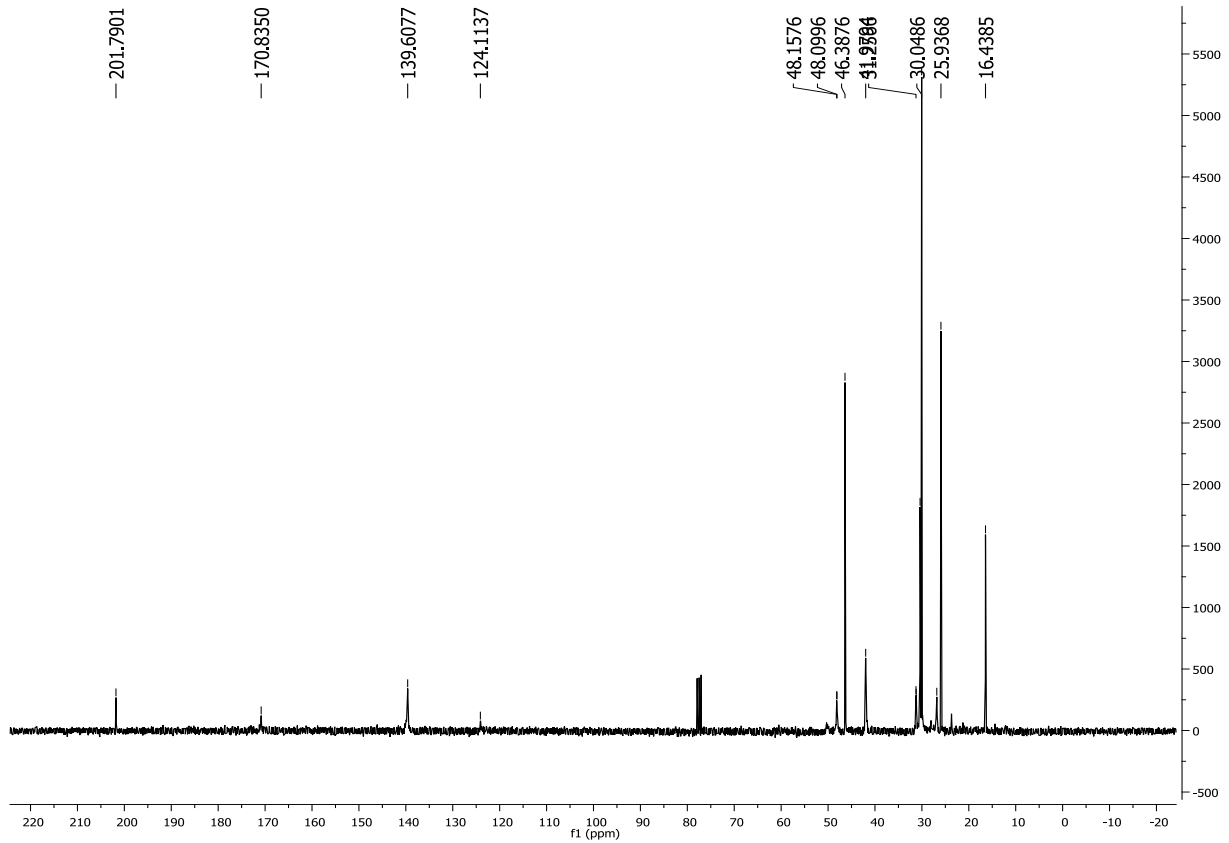
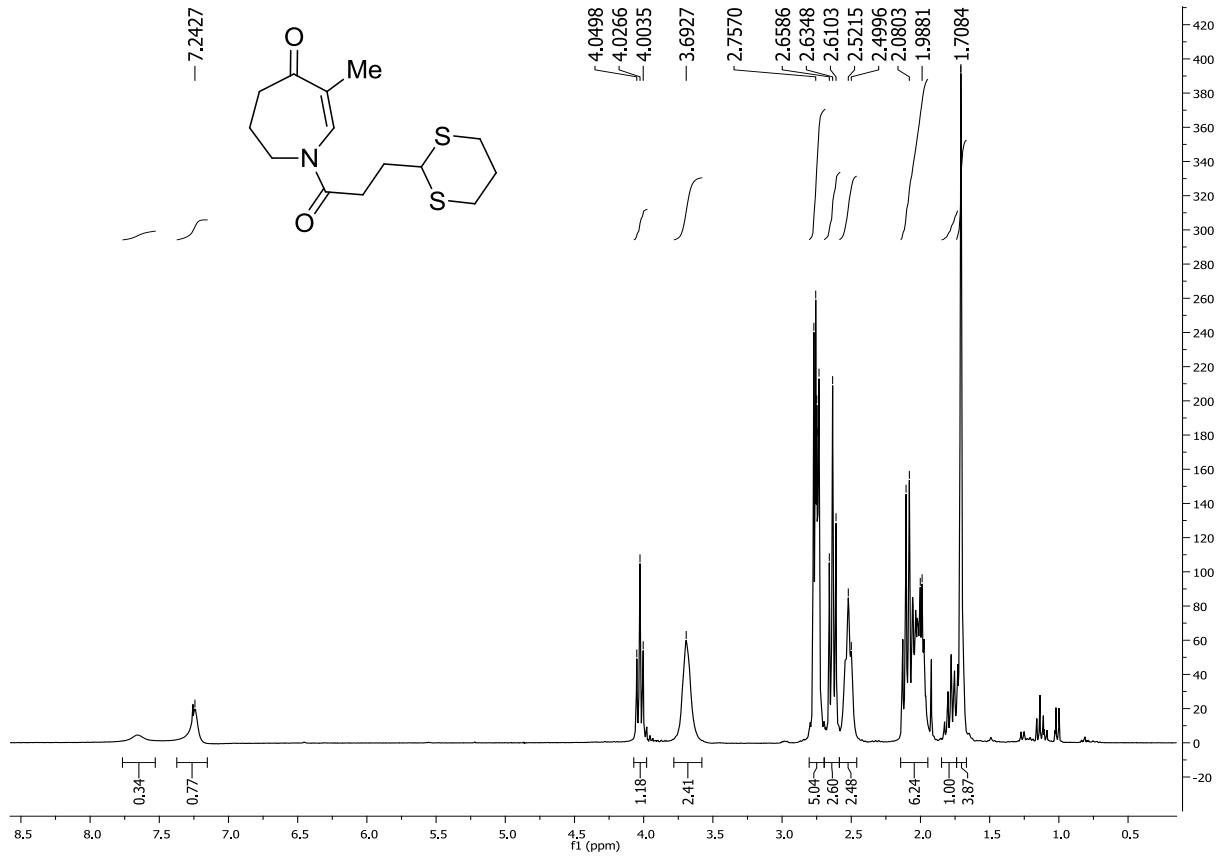
¹H NMR and ¹³C NMR Spectra of New Compounds

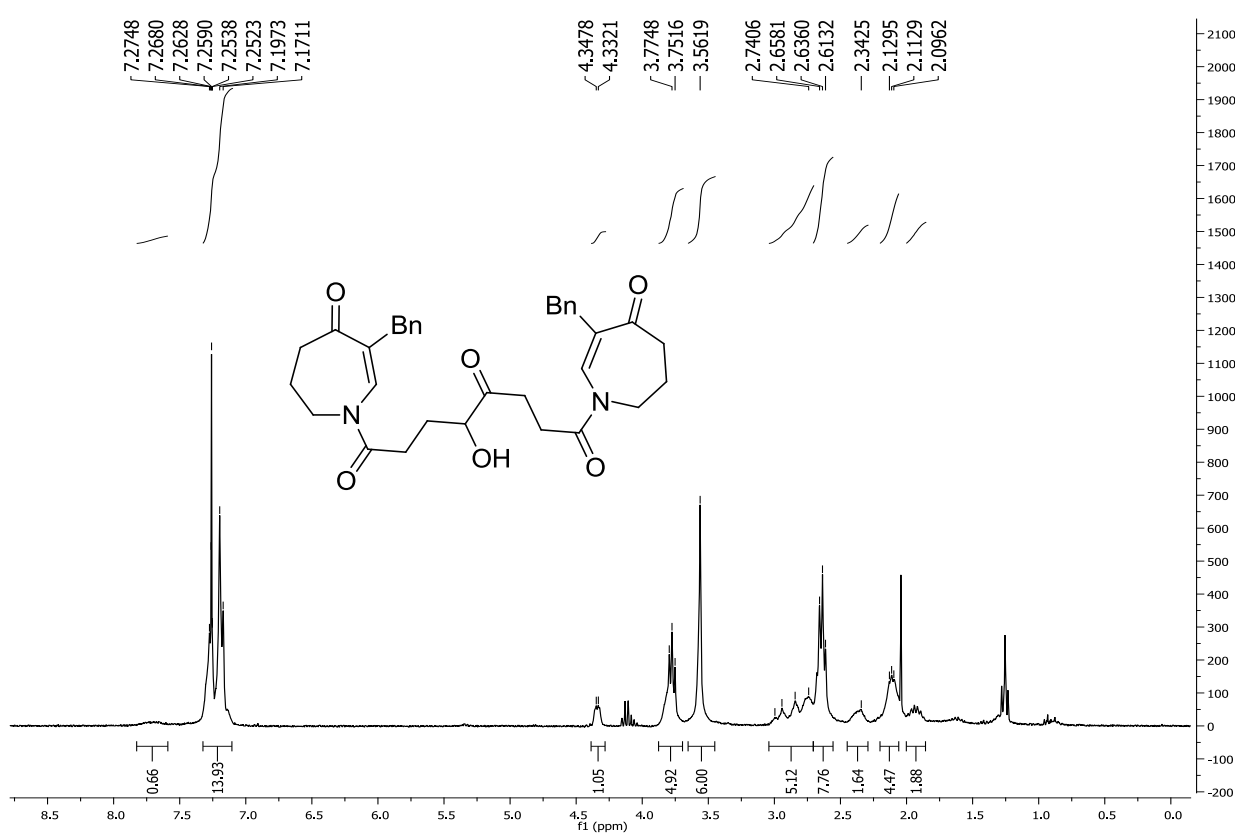
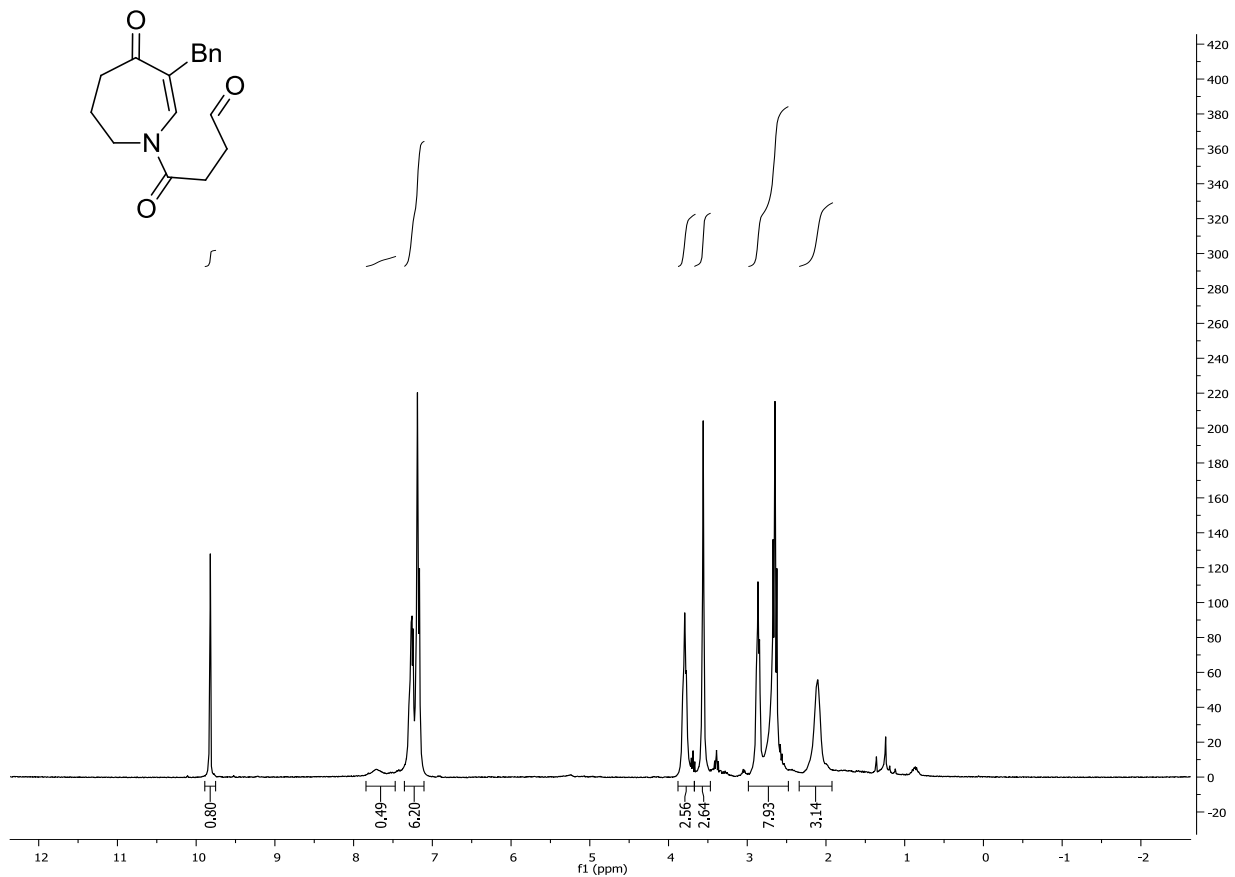


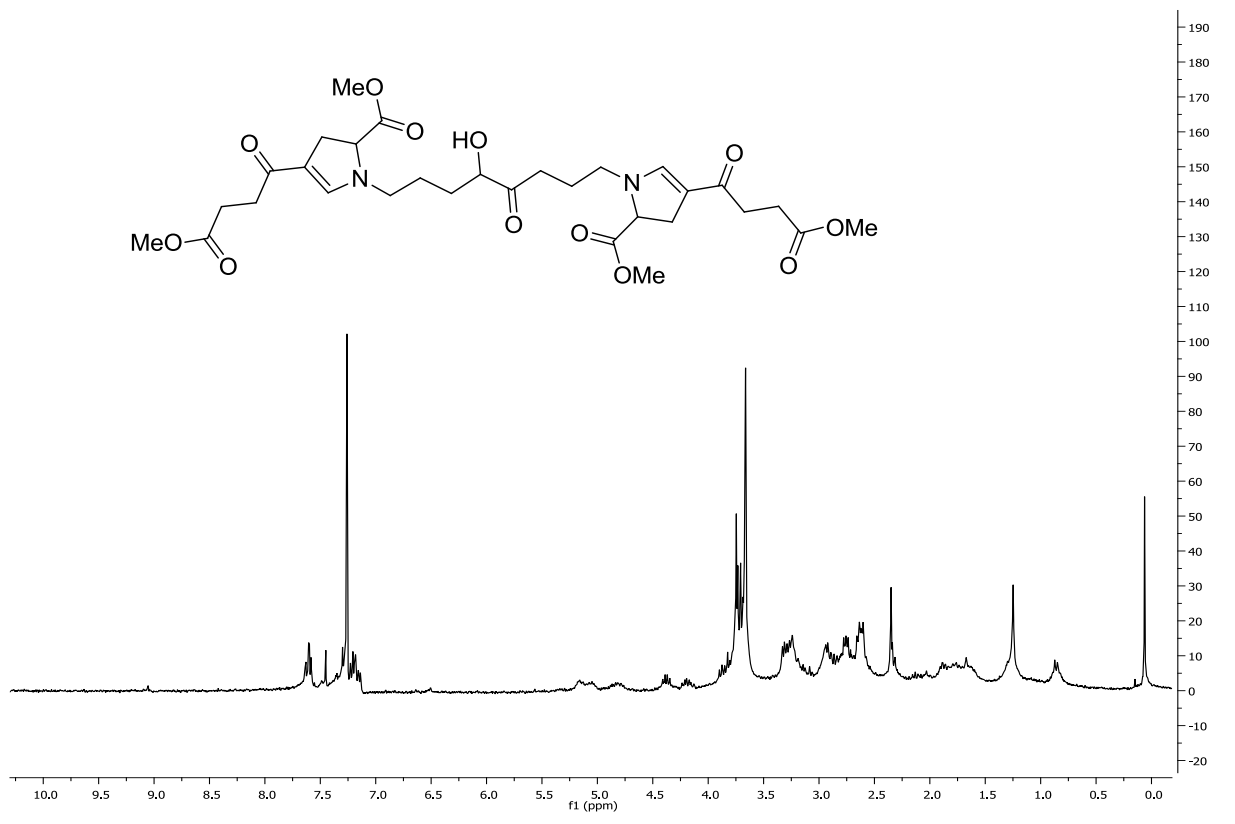
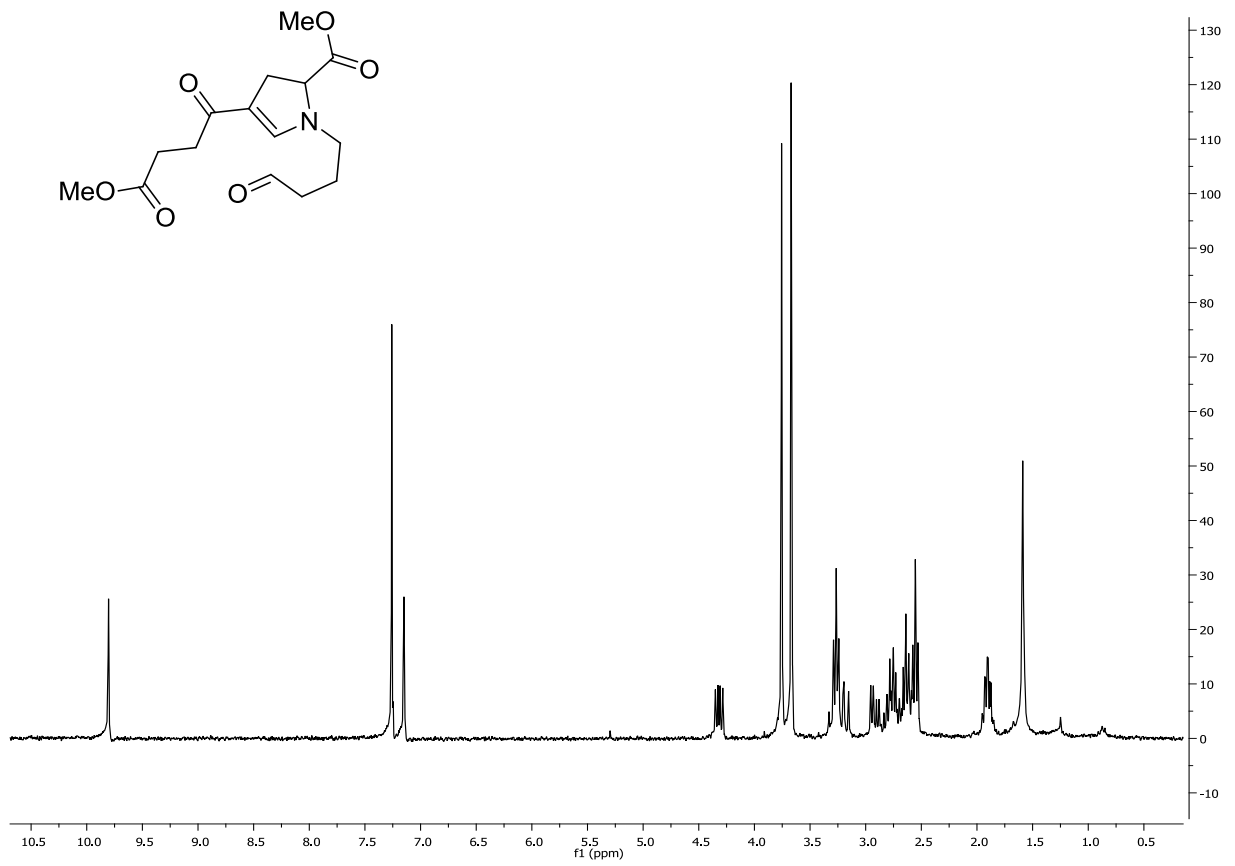


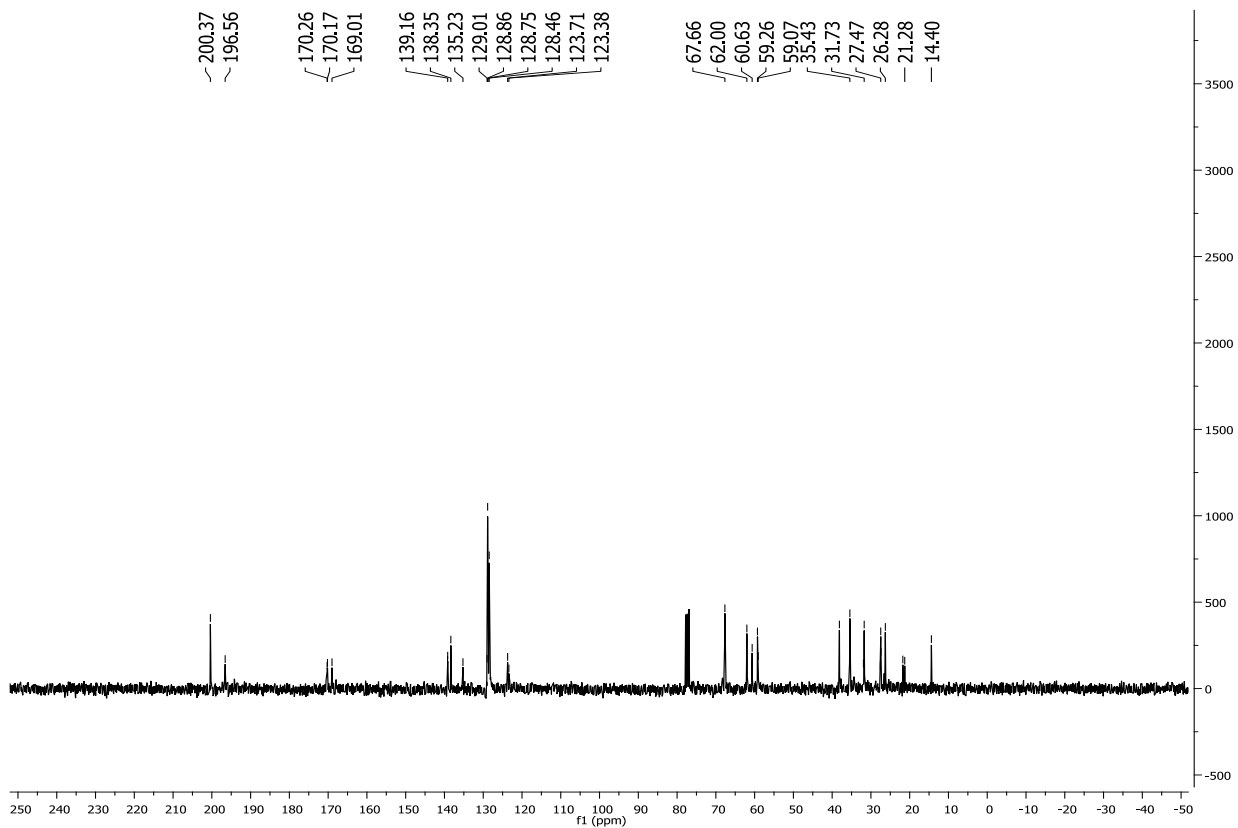
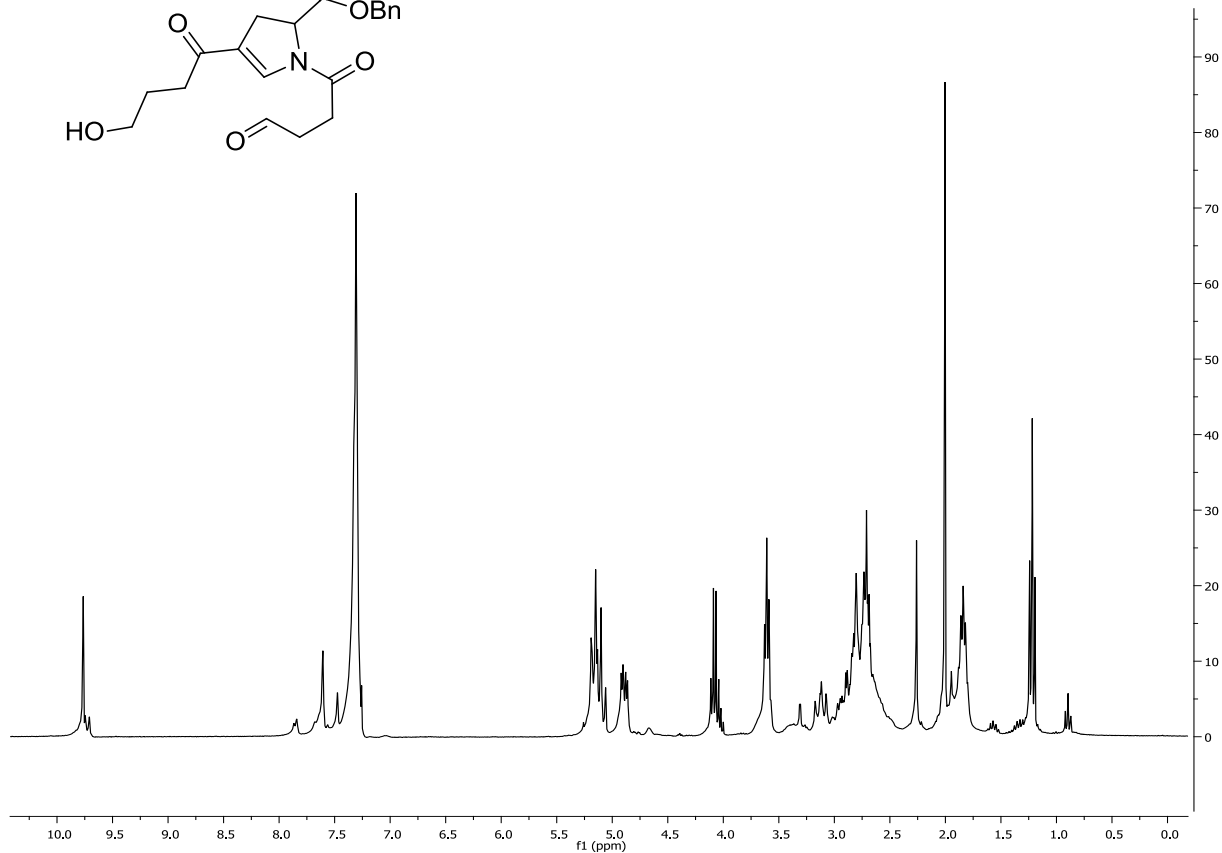
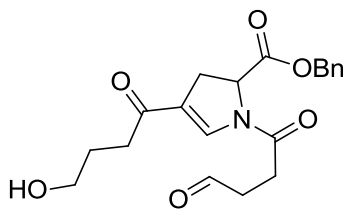


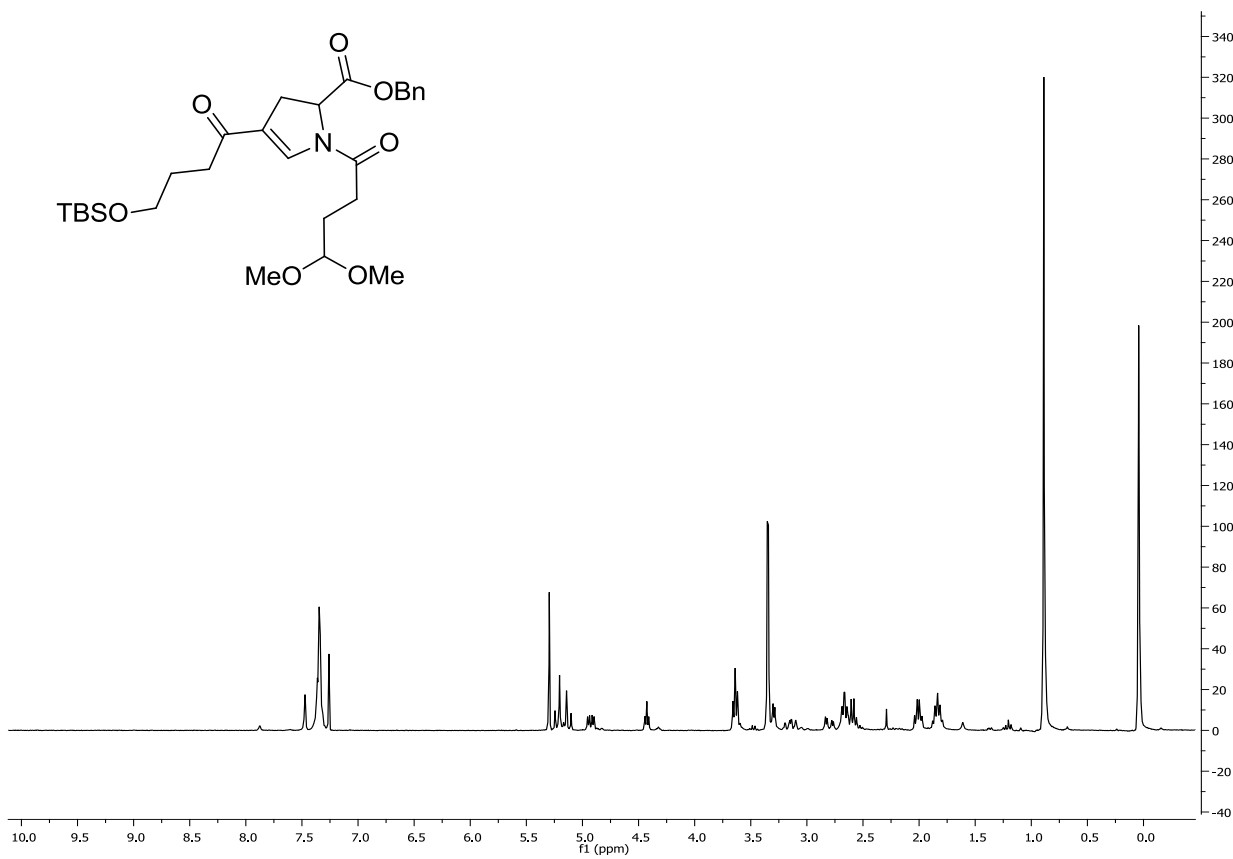
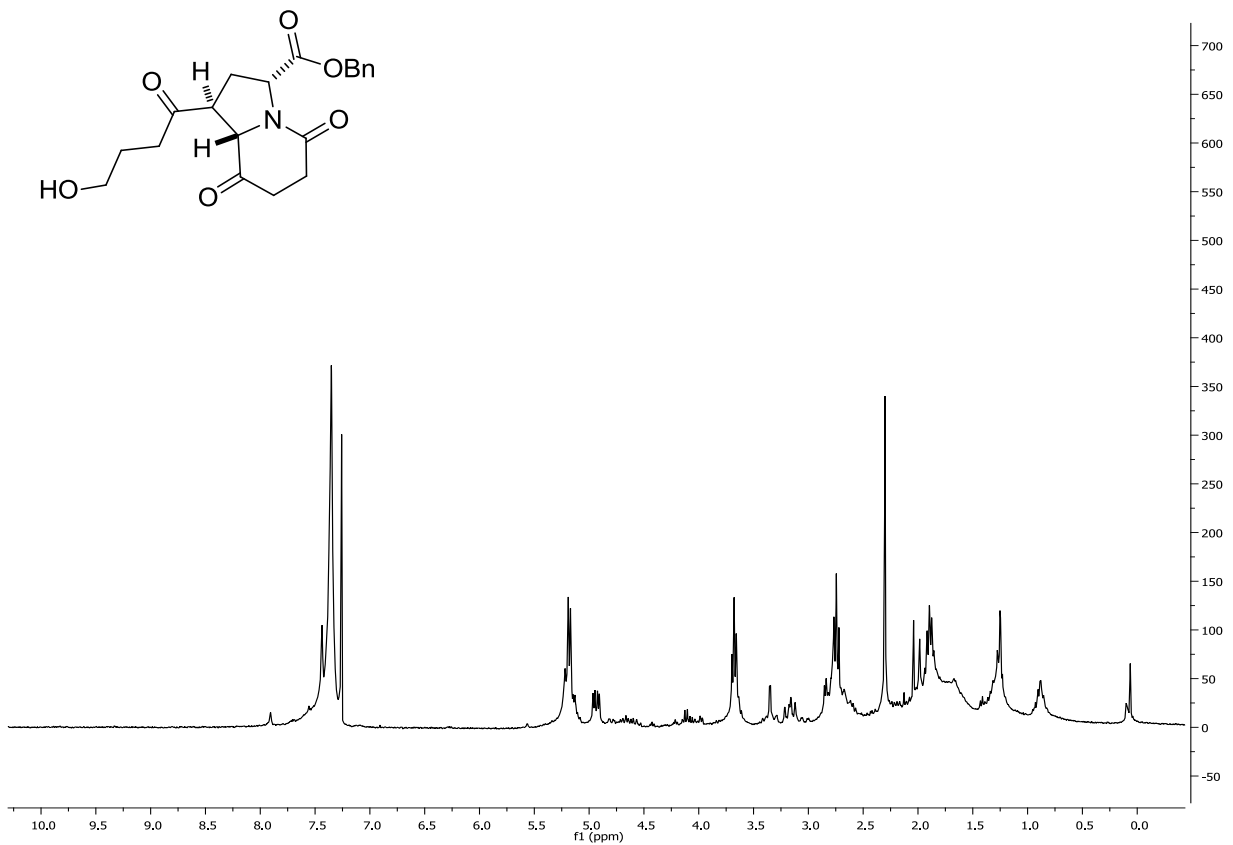


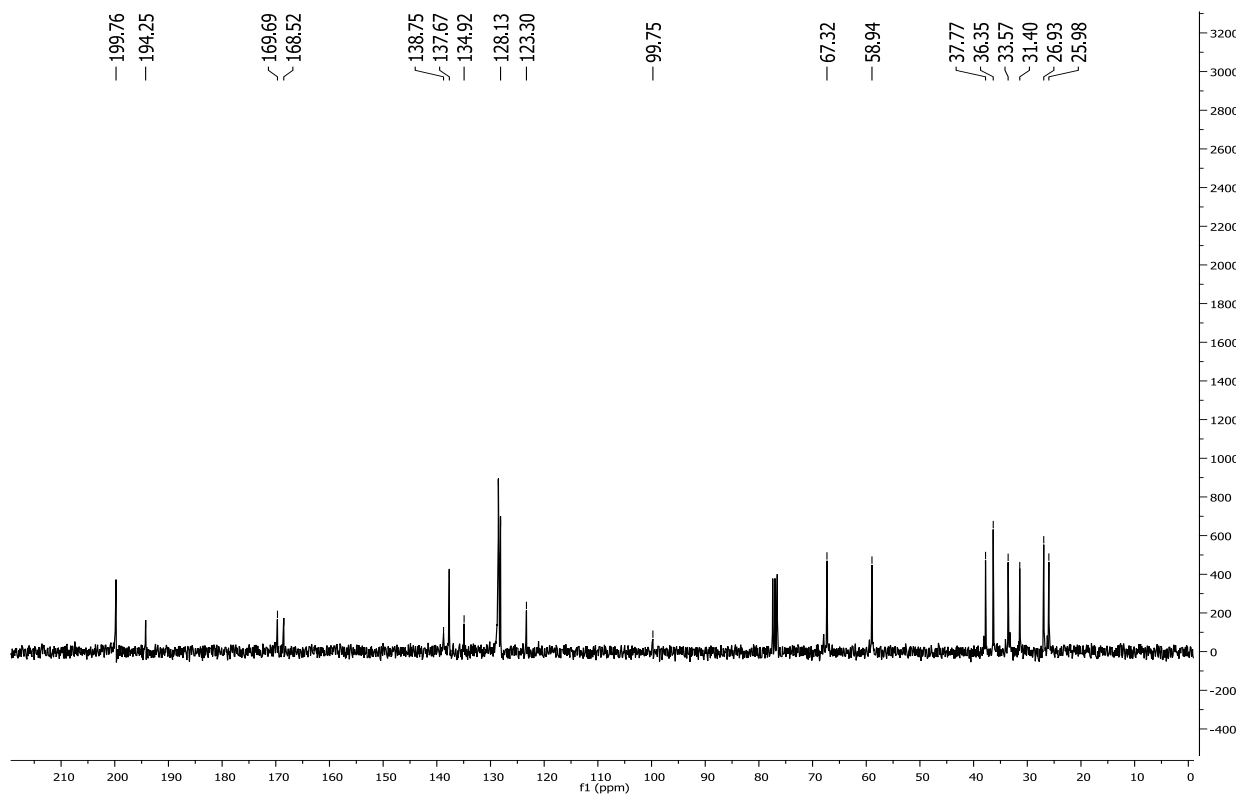
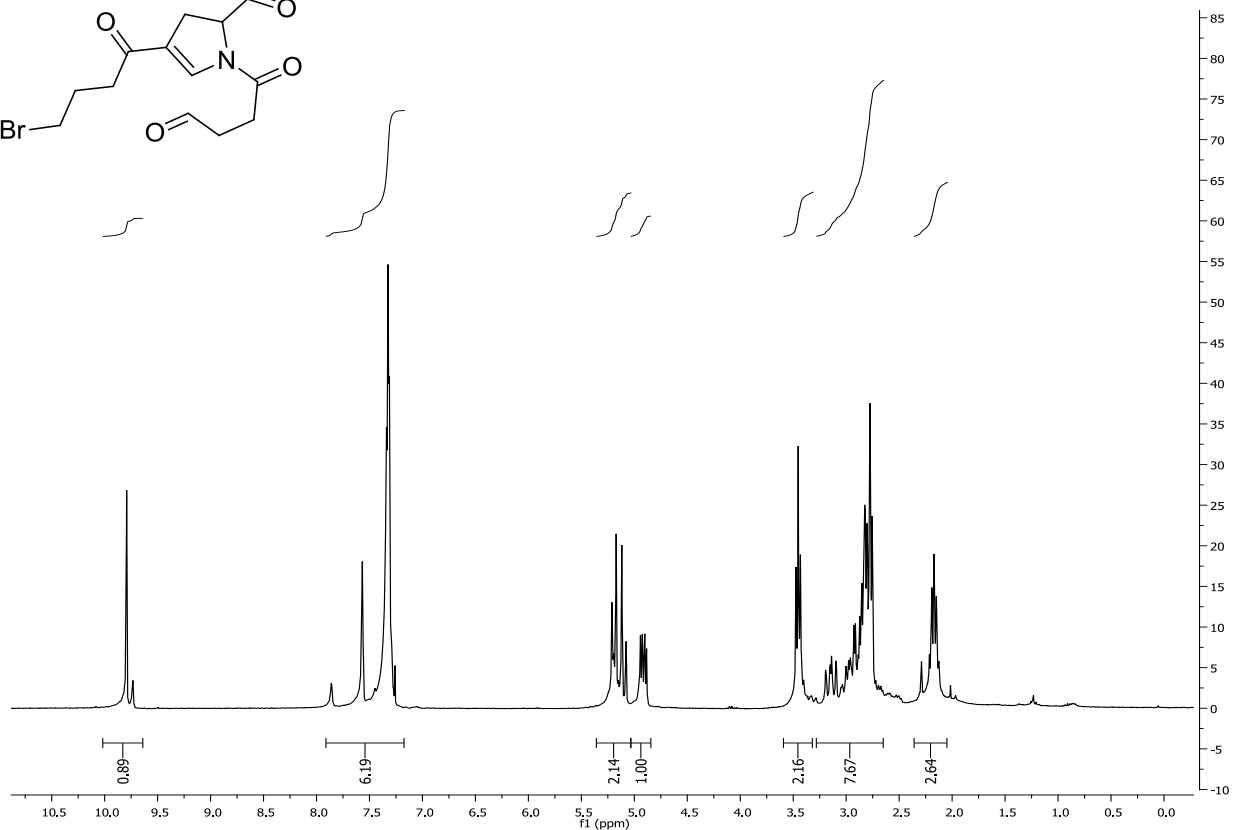
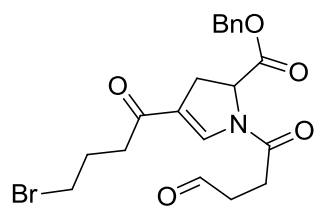


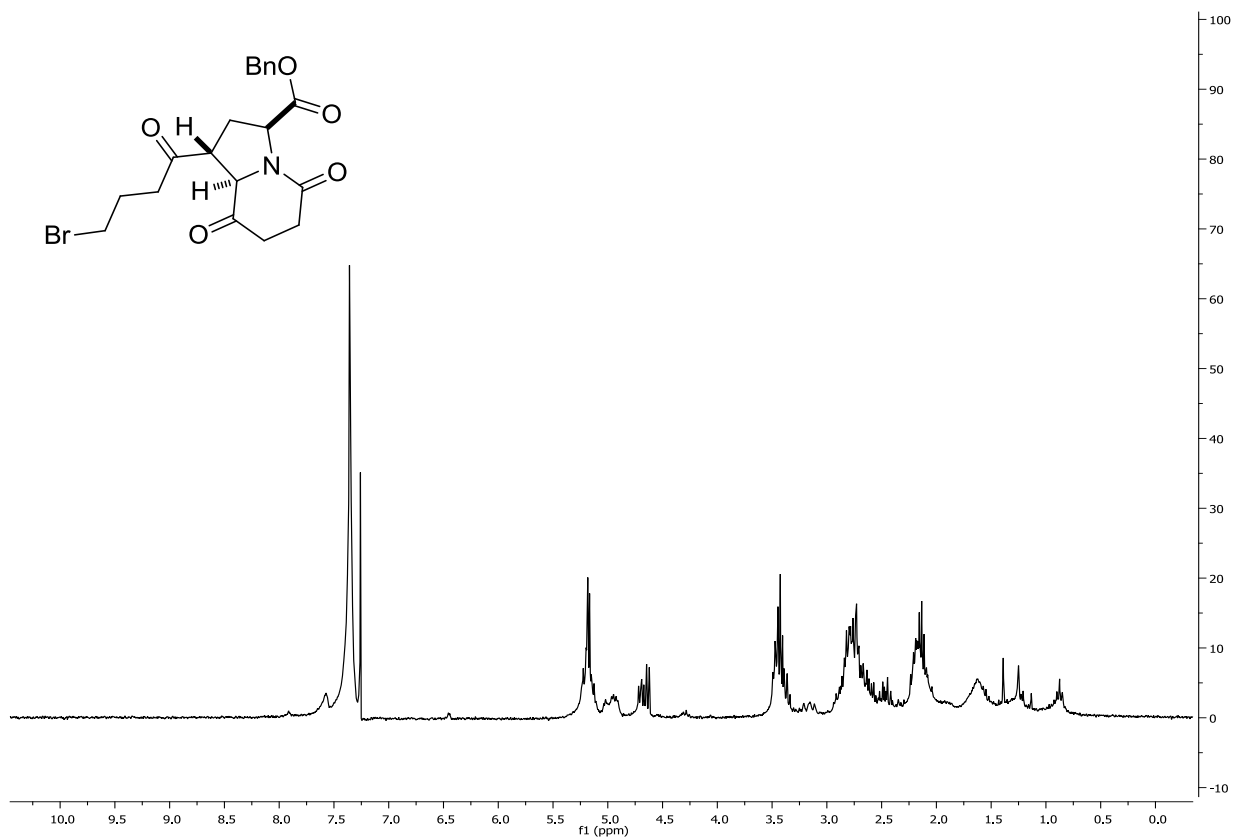
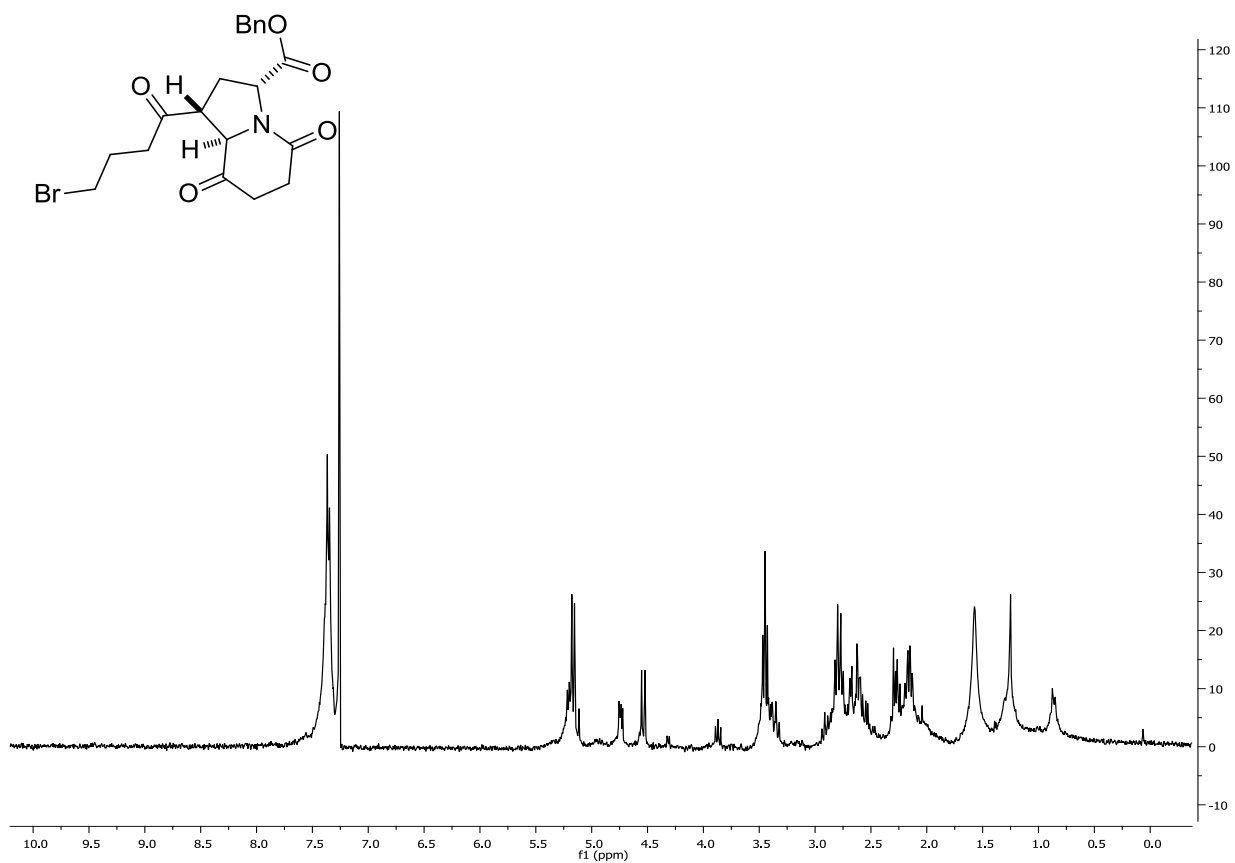


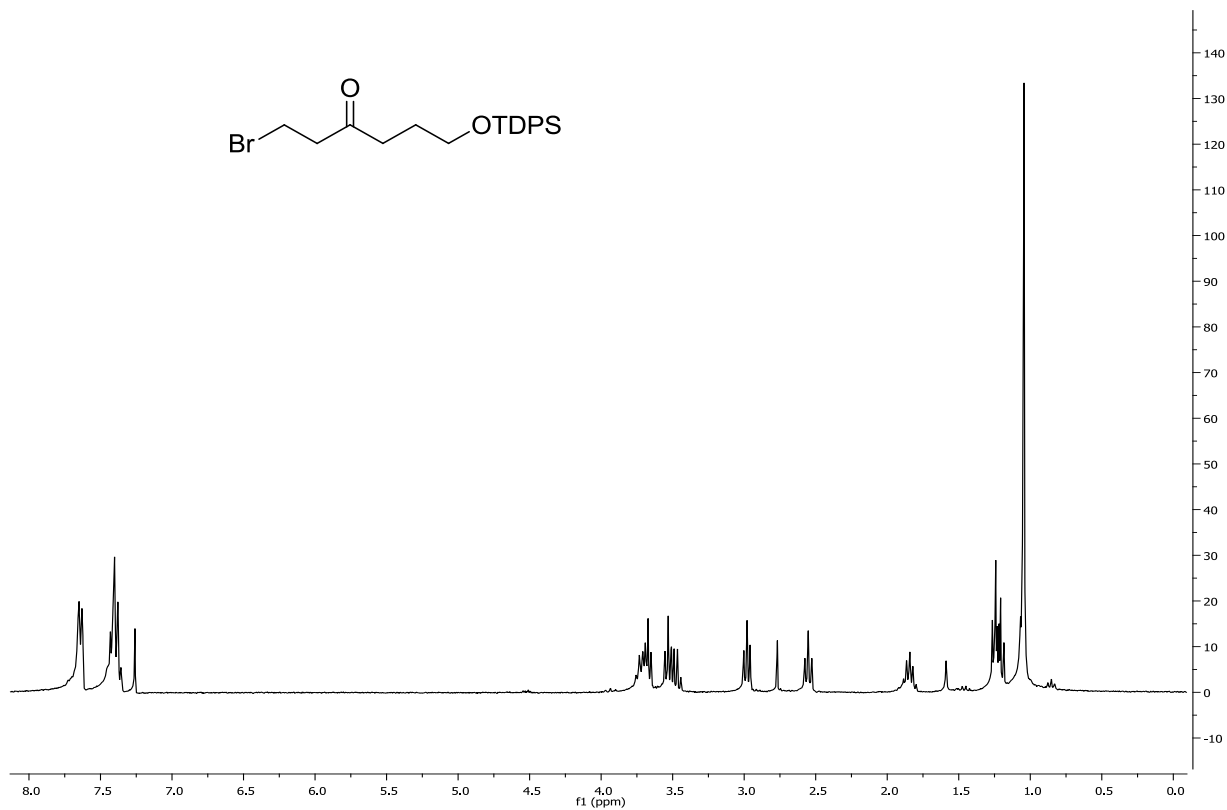
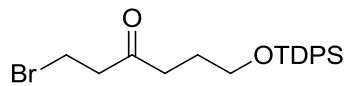
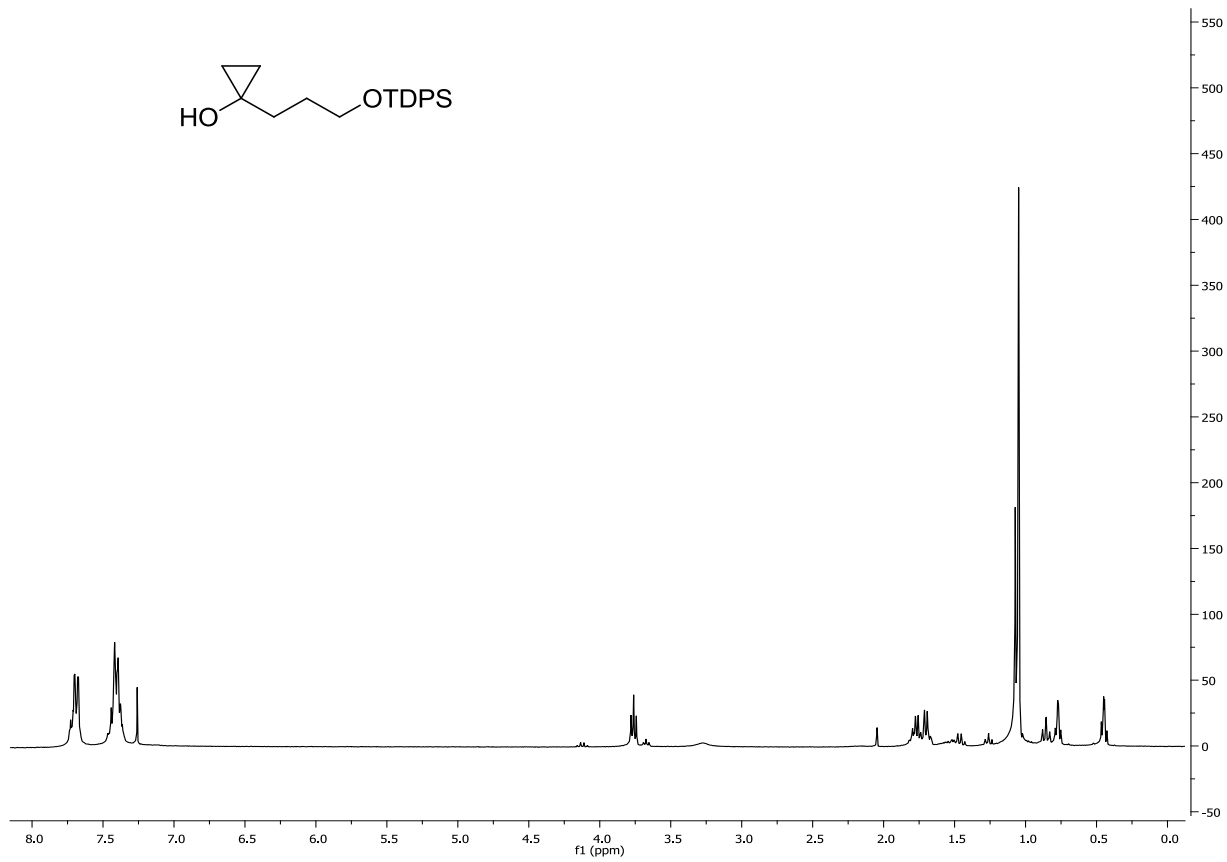
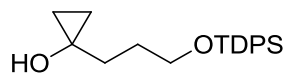


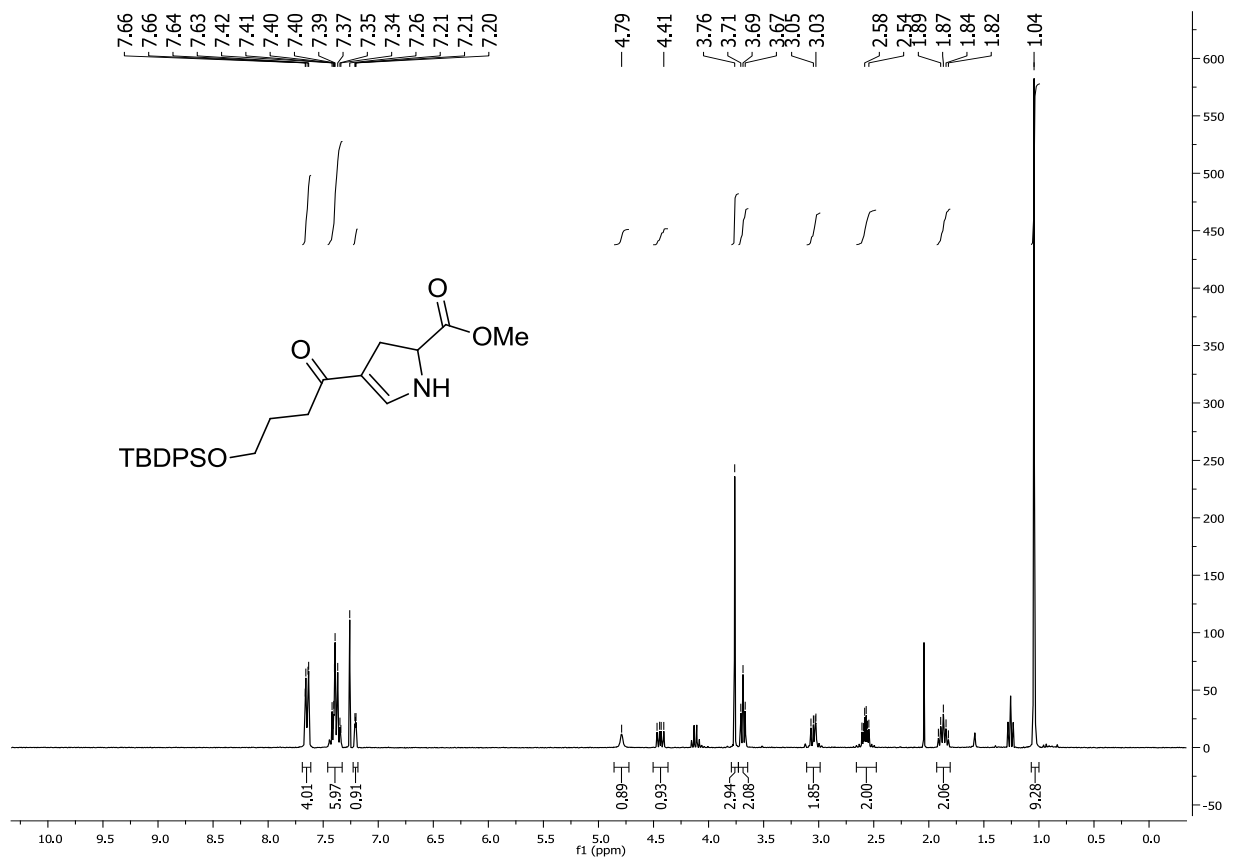
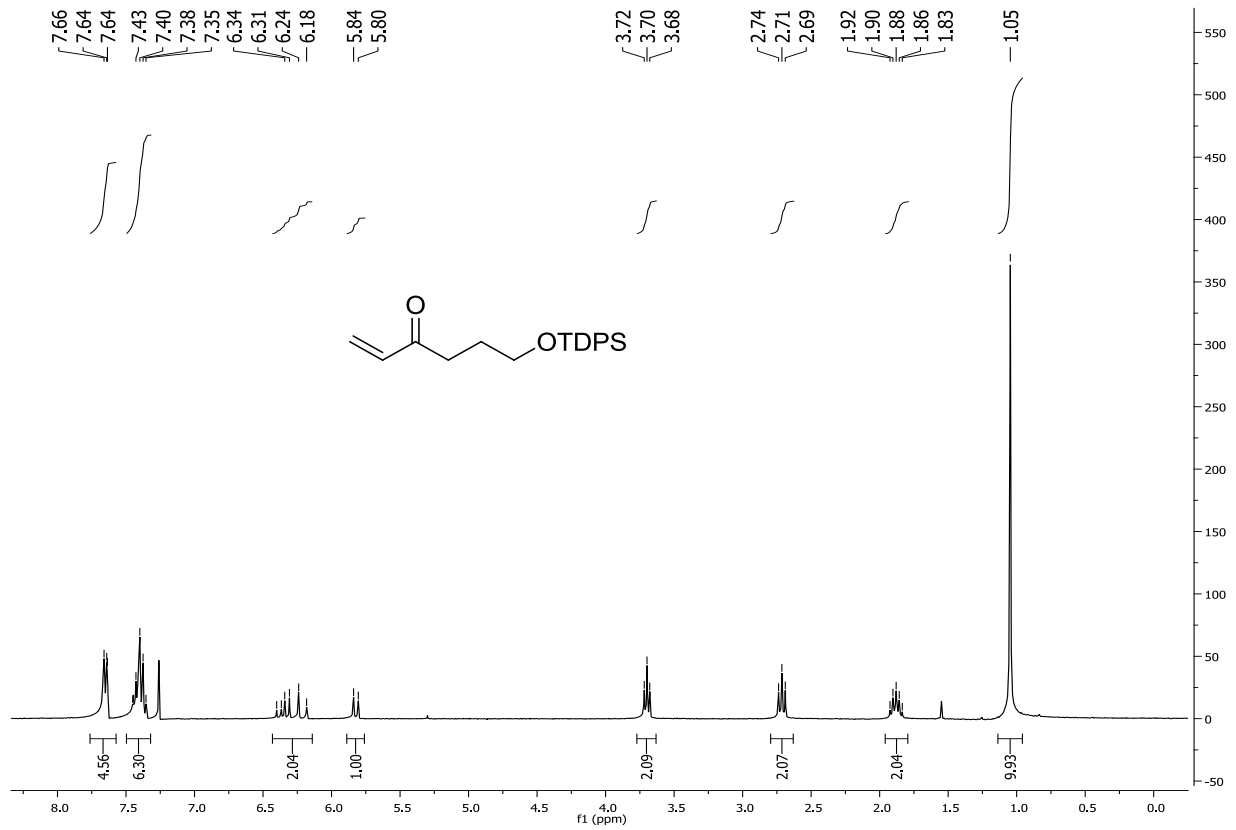


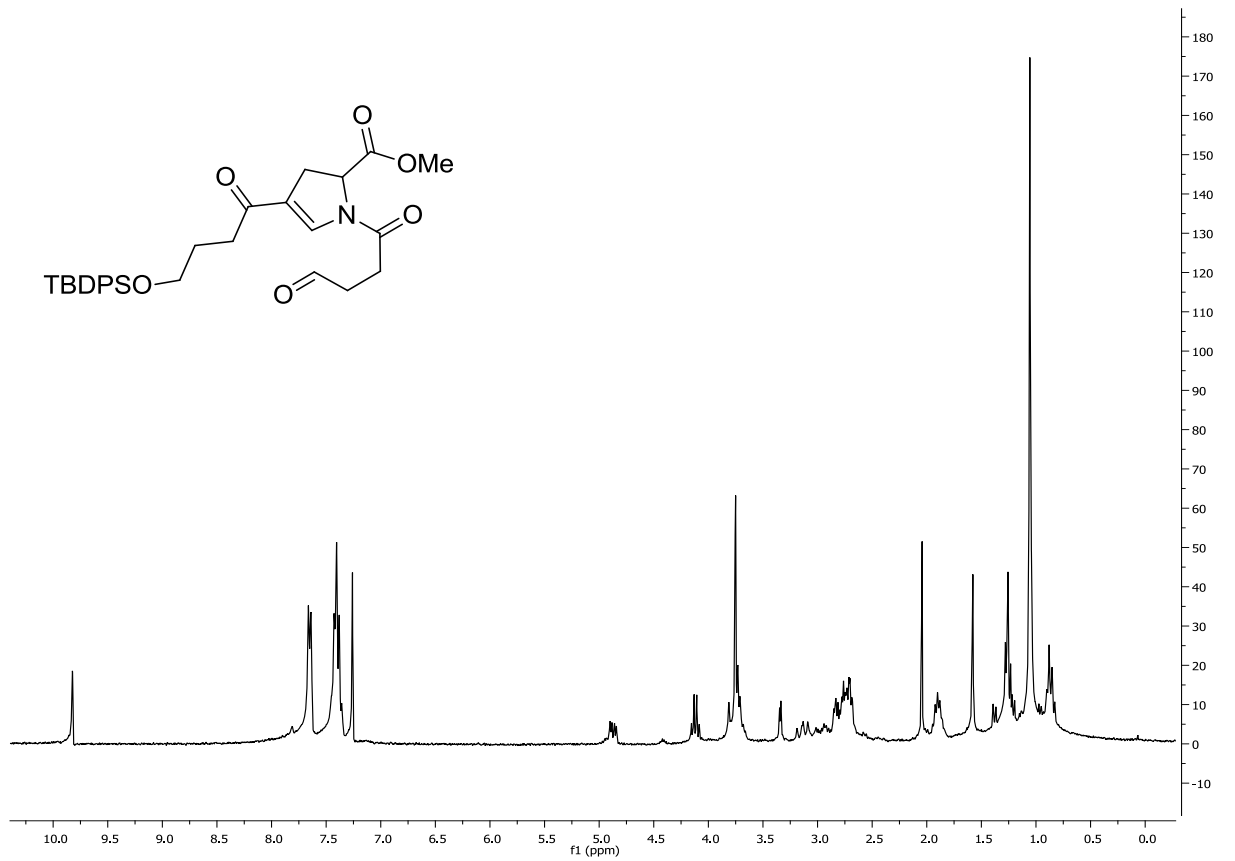
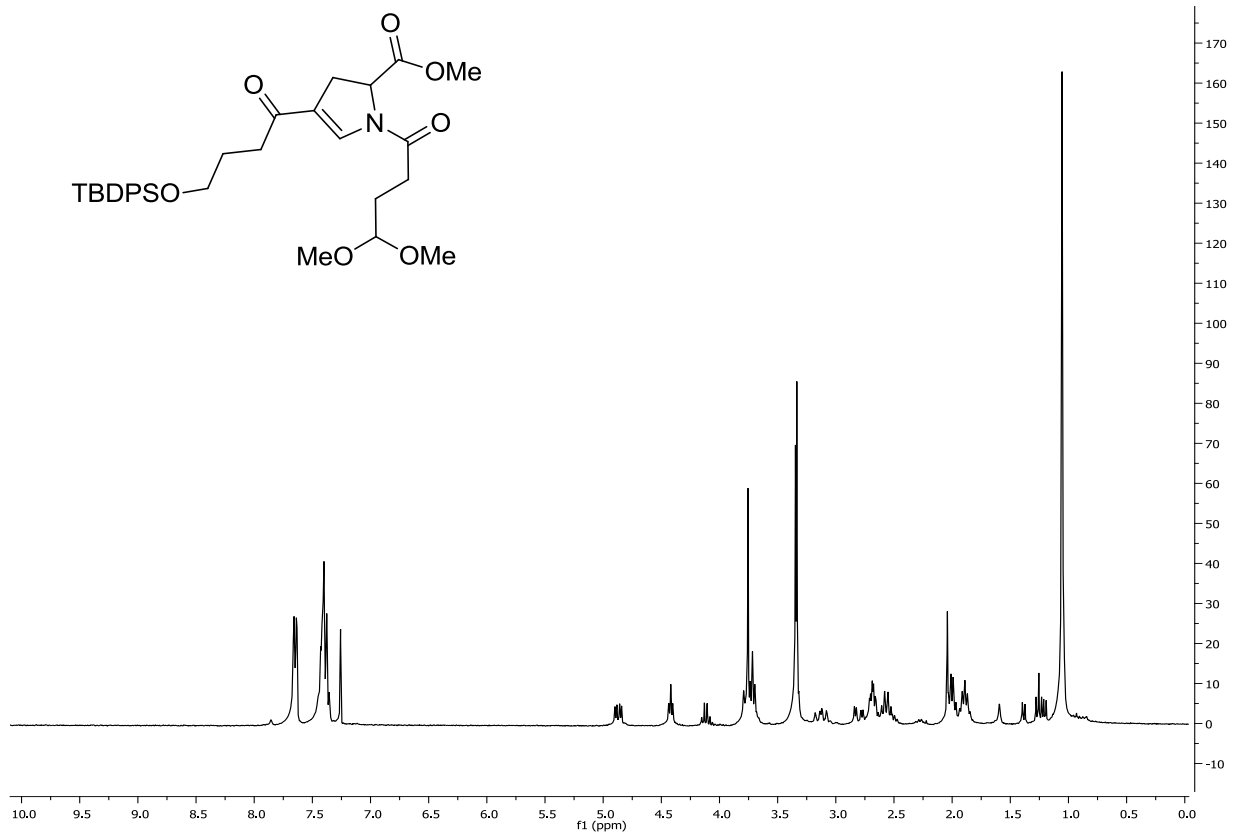


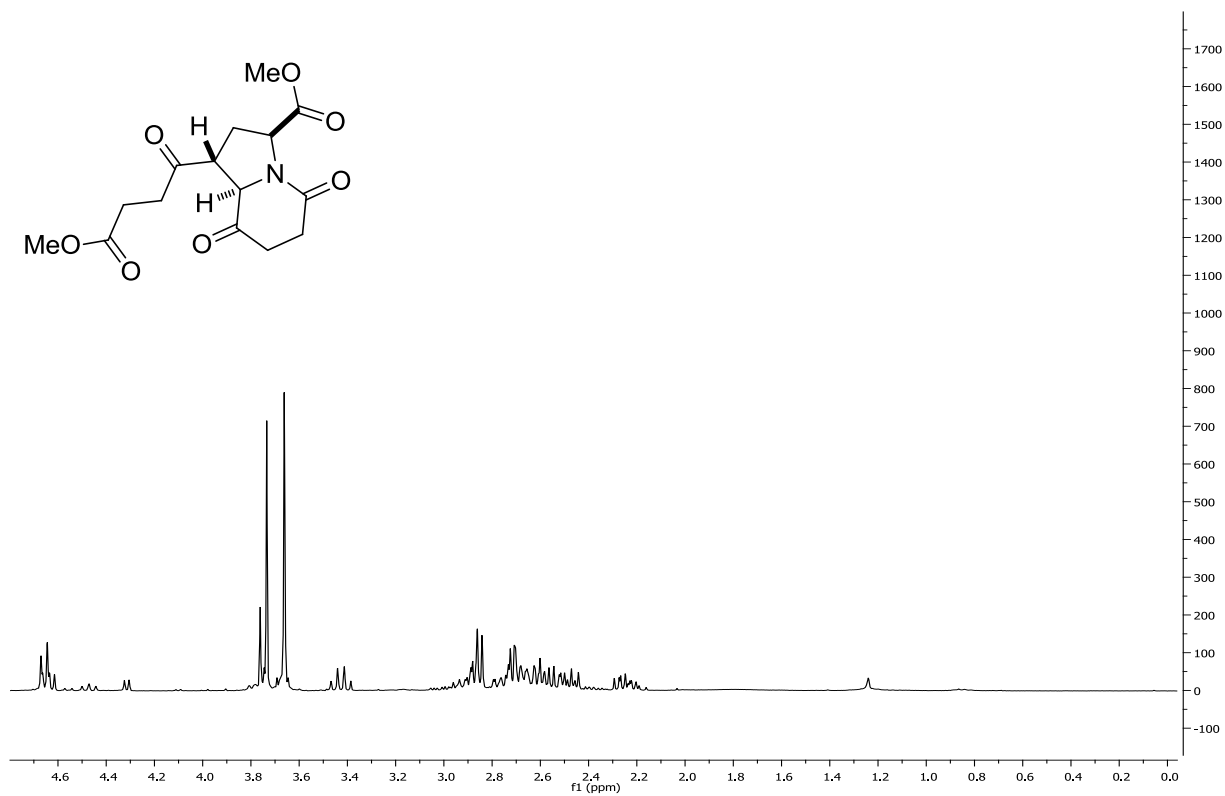
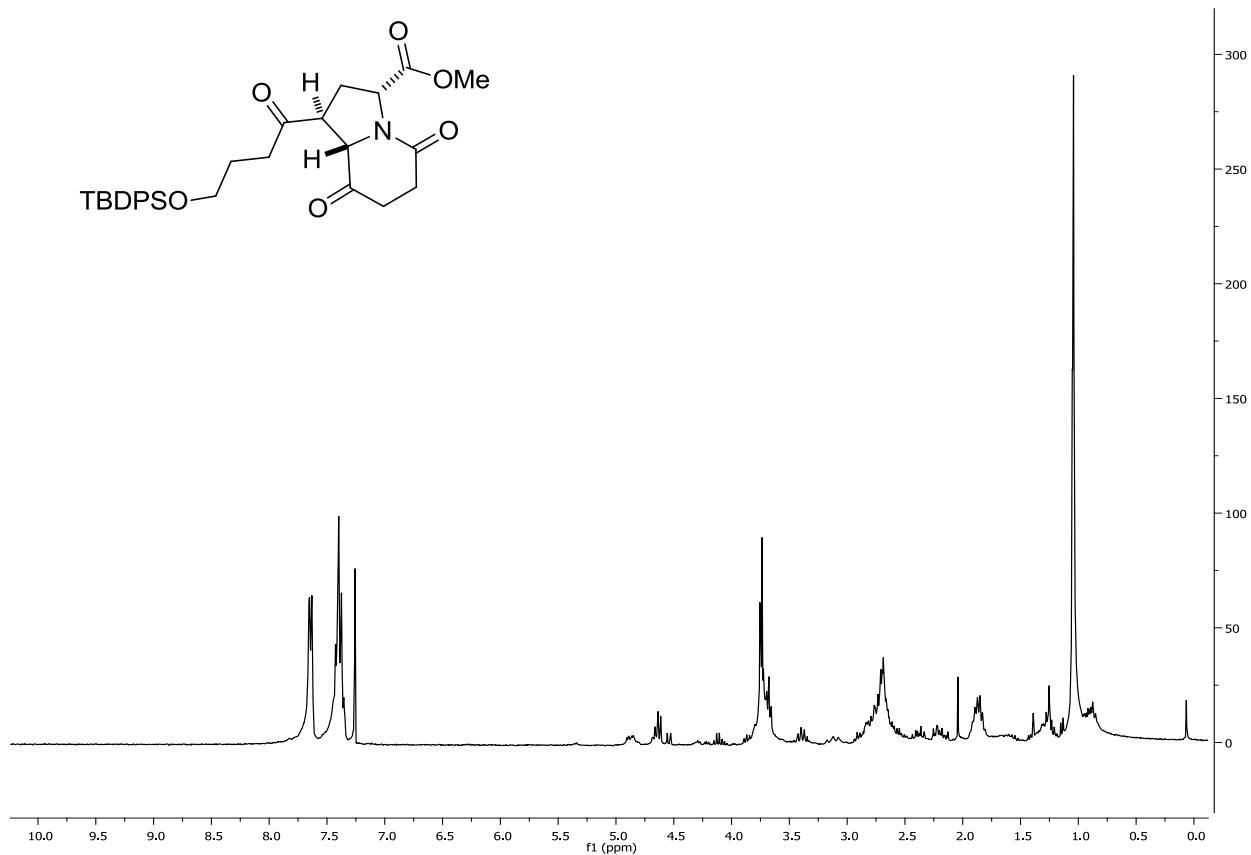












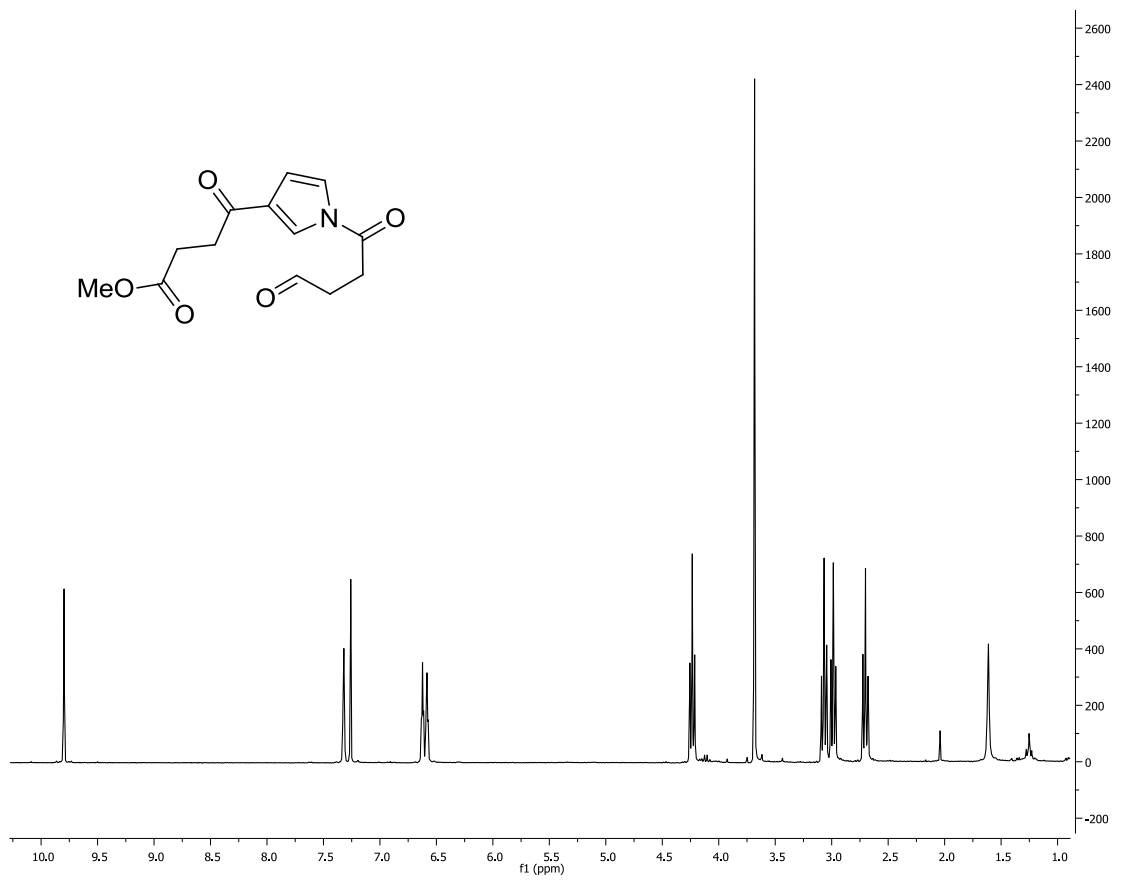
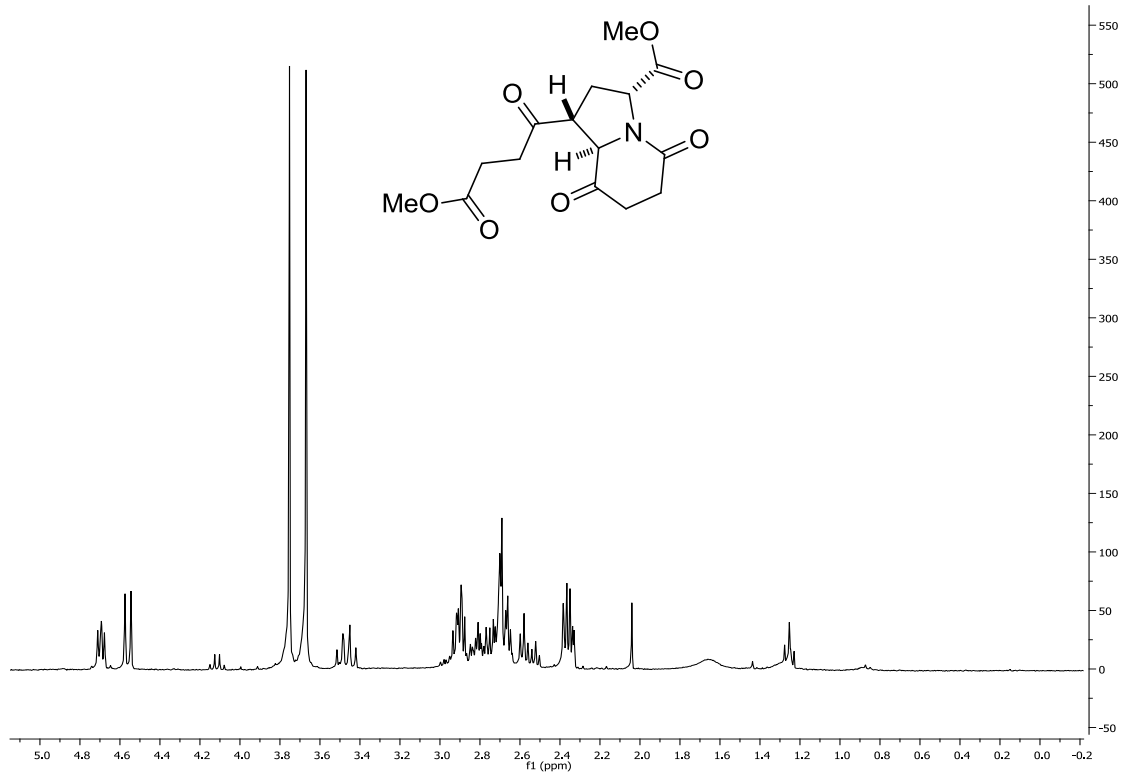


Table A1.1 Crystal data and structure refinement for **108**.

Identification code	rovis86_0m	
Empirical formula	C ₂₁ H ₂₃ N O ₇	
Formula weight	401.40	
Temperature	120 K	
Wavelength	0.71073 Å	
Crystal system	Triclinic	
Space group	<i>P</i> -1	
Unit cell dimensions	<i>a</i> = 8.7837(7) Å	α = 100.664(5)°.
	<i>b</i> = 10.7033(8) Å	β = 105.630(5)°.
	<i>c</i> = 11.2740(9) Å	γ = 102.370(5)°.
Volume	963.25(13) Å ³	
<i>Z</i>	2	
Density (calculated)	1.384 Mg/m ³	
Absorption coefficient	0.104 mm ⁻¹	
<i>F</i> ₀₀₀	424	
Crystal size	0.24 x 0.19 x 0.07 mm ³	
Theta range for data collection	1.94 to 27.10°.	
Index ranges	-11 ≤ <i>h</i> ≤ 11, -13 ≤ <i>k</i> ≤ 13, -14 ≤ <i>l</i> ≤ 14	
Reflections collected	13803	
Independent reflections	4246 [<i>R</i> _{int} = 0.0682]	
Completeness to theta = 27.10°	99.9 %	
Absorption correction	Multi-scan	

Max. and min. transmission	0.9928 and 0.9754
Refinement method	Full-matrix least-squares on F ²
Data / restraints / parameters	4246 / 0 / 263
Goodness-of-fit on F ²	1.032
Final R indices [I>2sigma(I)]	R1 = 0.0548, wR2 = 0.1028
R indices (all data)	R1 = 0.1506, wR2 = 0.1287
Largest diff. peak and hole	0.341 and -0.272 e.Å ⁻³

Table A1.2

Atomic coordinates ($\times 10^4$) and equivalent isotropic displacement parameters ($\text{\AA}^2 \times 10^3$)

for **108**. $U(\text{eq})$ is defined as one third of the trace of the orthogonalized U_{ij} tensor.

x	y	z	U(eq)	
C(1)	4442(3)	7257(3)	7548(3)	21(1)
C(2)	5002(3)	8616(3)	7311(3)	21(1)
C(3)	6196(3)	9456(3)	8620(3)	19(1)
C(4)	7037(3)	8491(2)	9201(3)	19(1)
C(5)	7263(3)	8626(3)	10604(3)	20(1)
C(6)	7478(3)	7419(3)	11058(3)	23(1)
C(7)	7488(3)	6284(3)	10012(3)	23(1)
C(8)	6045(3)	6054(3)	8827(3)	22(1)
C(9)	3086(3)	7225(3)	8161(3)	22(1)
C(10)	315(3)	7294(3)	7779(3)	26(1)
C(11)	-1008(3)	7445(3)	6698(3)	22(1)
C(12)	-2363(3)	6385(3)	5977(3)	24(1)
C(13)	-3525(4)	6497(3)	4928(3)	31(1)
C(14)	-3354(4)	7684(3)	4598(3)	34(1)
C(15)	-2029(4)	8767(3)	5322(3)	34(1)
C(16)	-862(4)	8649(3)	6372(3)	28(1)
C(17)	7337(4)	10707(3)	8563(3)	21(1)

C(18)	6463(3)	11597(3)	7938(3)	24(1)
C(19)	7570(3)	12921(3)	8013(3)	24(1)
C(20)	8335(4)	12841(3)	6975(3)	26(1)
C(21)	10482(4)	13888(3)	6298(3)	45(1)
N(1)	5930(3)	7175(2)	8458(2)	19(1)
O(1)	5048(2)	4975(2)	8254(2)	28(1)
O(2)	7248(2)	9636(2)	11301(2)	25(1)
O(3)	3265(2)	7274(2)	9262(2)	29(1)
O(4)	1678(2)	7182(2)	7291(2)	23(1)
O(5)	8831(2)	10959(2)	8972(2)	27(1)
O(6)	7822(3)	11997(2)	5991(2)	54(1)
O(7)	9656(2)	13874(2)	7255(2)	32(1)

Table A1.3 Bond lengths [\AA] and angles [$^\circ$] for **108**.

C(1)-N(1)	1.460(3)
C(1)-C(9)	1.527(4)
C(1)-C(2)	1.529(4)
C(2)-C(3)	1.536(4)
C(3)-C(17)	1.514(4)
C(3)-C(4)	1.535(3)
C(4)-N(1)	1.473(3)
C(4)-C(5)	1.516(4)
C(5)-O(2)	1.218(3)
C(5)-C(6)	1.504(4)
C(6)-C(7)	1.532(4)
C(7)-C(8)	1.511(4)
C(8)-O(1)	1.226(3)
C(8)-N(1)	1.355(3)
C(9)-O(3)	1.198(3)
C(9)-O(4)	1.340(3)
C(10)-O(4)	1.464(3)
C(10)-C(11)	1.500(4)
C(11)-C(12)	1.387(4)
C(11)-C(16)	1.394(4)
C(12)-C(13)	1.383(4)

C(13)-C(14)	1.377(4)
C(14)-C(15)	1.388(4)
C(15)-C(16)	1.388(4)
C(17)-O(5)	1.218(3)
C(17)-C(18)	1.505(4)
C(18)-C(19)	1.511(4)
C(19)-C(20)	1.496(4)
C(20)-O(6)	1.198(3)
C(20)-O(7)	1.339(3)
C(21)-O(7)	1.453(3)
N(1)-C(1)-C(9)	109.8(2)
N(1)-C(1)-C(2)	102.4(2)
C(9)-C(1)-C(2)	110.3(2)
C(1)-C(2)-C(3)	103.1(2)
C(17)-C(3)-C(4)	115.8(2)
C(17)-C(3)-C(2)	113.6(2)
C(4)-C(3)-C(2)	104.7(2)
N(1)-C(4)-C(5)	109.3(2)
N(1)-C(4)-C(3)	104.0(2)
C(5)-C(4)-C(3)	115.2(2)
O(2)-C(5)-C(6)	123.0(3)
O(2)-C(5)-C(4)	122.0(2)
C(6)-C(5)-C(4)	115.1(2)

C(5)-C(6)-C(7)	113.3(2)
C(8)-C(7)-C(6)	109.8(2)
O(1)-C(8)-N(1)	122.4(3)
O(1)-C(8)-C(7)	124.4(3)
N(1)-C(8)-C(7)	113.2(2)
O(3)-C(9)-O(4)	125.1(3)
O(3)-C(9)-C(1)	125.1(3)
O(4)-C(9)-C(1)	109.7(2)
O(4)-C(10)-C(11)	105.9(2)
C(12)-C(11)-C(16)	118.7(3)
C(12)-C(11)-C(10)	121.0(3)
C(16)-C(11)-C(10)	120.2(3)
C(13)-C(12)-C(11)	121.1(3)
C(14)-C(13)-C(12)	119.8(3)
C(13)-C(14)-C(15)	120.2(3)
C(14)-C(15)-C(16)	119.8(3)
C(15)-C(16)-C(11)	120.3(3)
O(5)-C(17)-C(18)	123.0(2)
O(5)-C(17)-C(3)	122.9(2)
C(18)-C(17)-C(3)	114.1(2)
C(17)-C(18)-C(19)	114.7(2)
C(20)-C(19)-C(18)	112.0(2)
O(6)-C(20)-O(7)	123.0(3)

O(6)-C(20)-C(19)	125.5(3)
O(7)-C(20)-C(19)	111.4(3)
C(8)-N(1)-C(1)	122.5(2)
C(8)-N(1)-C(4)	122.8(2)
C(1)-N(1)-C(4)	112.2(2)
C(9)-O(4)-C(10)	115.6(2)
C(20)-O(7)-C(21)	115.5(2)

Symmetry transformations used to generate equivalent atoms:

Table A1.4

Anisotropic displacement parameters ($\text{\AA}^2 \times 10^3$) for **108**. The anisotropic

displacement factor exponent takes the form: $-2p^2 [h^2 a^{*2} U^{11} + \dots + 2 h k a^* b^* U^{12}]$

U11	U22	U33	U23	U13	U12	
C(1)	19(2)	24(2)	23(2)	6(1)	6(1)	11(1)
C(2)	19(2)	26(2)	24(2)	10(1)	8(1)	10(1)
C(3)	18(2)	18(2)	24(2)	7(1)	7(1)	10(1)
C(4)	15(2)	19(2)	25(2)	8(1)	7(1)	10(1)
C(5)	9(1)	24(2)	25(2)	6(1)	4(1)	4(1)
C(6)	22(2)	25(2)	26(2)	12(1)	7(1)	13(1)
C(7)	20(2)	21(2)	31(2)	10(1)	9(1)	10(1)
C(8)	22(2)	21(2)	28(2)	8(1)	13(1)	11(1)
C(9)	21(2)	18(2)	27(2)	10(1)	4(1)	8(1)
C(10)	20(2)	35(2)	30(2)	9(2)	13(1)	12(1)
C(11)	19(2)	28(2)	24(2)	6(1)	11(1)	10(1)
C(12)	16(2)	29(2)	32(2)	7(2)	11(1)	8(1)
C(13)	18(2)	36(2)	37(2)	4(2)	10(2)	6(1)
C(14)	29(2)	50(2)	31(2)	14(2)	9(2)	22(2)
C(15)	39(2)	33(2)	40(2)	16(2)	14(2)	22(2)
C(16)	24(2)	24(2)	34(2)	4(2)	8(1)	8(1)
C(17)	20(2)	24(2)	23(2)	7(1)	10(1)	10(1)

C(18)	25(2)	27(2)	28(2)	12(1)	12(1)	14(1)
C(19)	26(2)	22(2)	30(2)	13(1)	9(1)	13(1)
C(20)	28(2)	23(2)	30(2)	10(2)	12(2)	10(1)
C(21)	53(2)	42(2)	66(3)	25(2)	47(2)	20(2)
N(1)	16(1)	17(1)	23(1)	3(1)	3(1)	5(1)
O(1)	28(1)	19(1)	37(1)	6(1)	9(1)	7(1)
O(2)	24(1)	24(1)	26(1)	4(1)	7(1)	11(1)
O(3)	24(1)	42(1)	28(1)	15(1)	9(1)	16(1)
O(4)	18(1)	30(1)	25(1)	8(1)	9(1)	10(1)
O(5)	17(1)	29(1)	38(1)	14(1)	9(1)	9(1)
O(6)	61(2)	48(2)	42(2)	-9(1)	30(1)	-8(1)
O(7)	34(1)	26(1)	42(1)	8(1)	25(1)	7(1)

Table A1.5Hydrogen coordinates ($\times 10^4$) and isotropic displacement parameters ($\text{\AA}^2 \times 10^3$)

for Rovis86_0m.

x	y	z	U(eq)	
H(1)	4084	6549	6760	26
H(2A)	4077	8972	7037	26
H(2B)	5554	8570	6672	26
H(3)	5533	9722	9142	22
H(4)	8108	8589	9065	22
H(6A)	6592	7112	11386	27
H(6B)	8506	7663	11754	27
H(7A)	8508	6503	9817	27
H(7B)	7417	5484	10306	27
H(10A)	665	8059	8504	31
H(10B)	-81	6508	8043	31
H(12)	-2491	5585	6203	29
H(13)	-4420	5774	4446	37
H(14)	-4130	7759	3888	41
H(15)	-1922	9570	5103	40
H(16)	22	9377	6861	33
H(18A)	5643	11749	8334	29

H(18B)	5886	11142	7048	29
H(19A)	6934	13557	7952	29
H(19B)	8433	13233	8833	29
H(21A)	10579	13018	5997	68
H(21B)	11558	14504	6667	68
H(21C)	9852	14151	5597	68

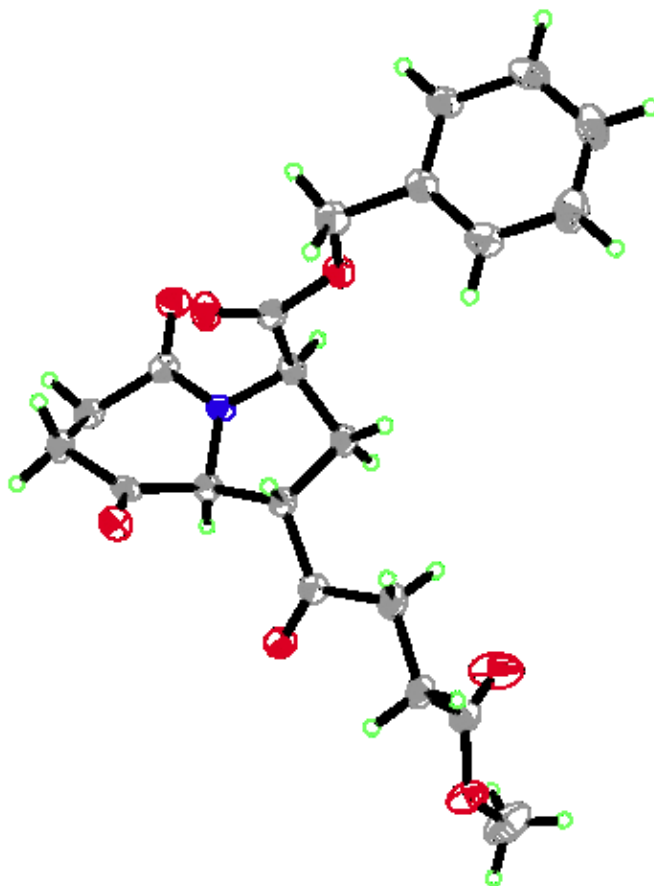


Figure A1.1

Thermal Ellipsoid Plot of **108** at 50% Probability.

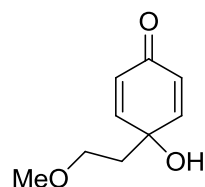
Appendix 2

Chapter 3 Supporting Information

Materials and Methods

All reactions were carried out in oven-dried glassware with magnetic stirring. Dichloroethane (DCE) was distilled from CaH₂. Dichloromethane was degassed with argon and passed through two columns of neutral alumina. Column chromatography was performed on Silicycle Inc. silica gel 60 (230-400 mesh). Thin layer chromatography was performed on Silicycle Inc. 0.25 mm silica gel 60-F plates. Visualization was accomplished with UV light (254 nm) and KMnO₄ followed by heating. ¹H NMR and ¹³C NMR spectra were obtained on Varian 300 or 400 MHz spectrometers in CDCl₃ at ambient temperature and chemical shifts are expressed in parts per million (δ, ppm). Proton chemical shifts are referenced to 7.26 ppm (CHCl₃) and carbon chemical shifts are referenced to 77.0 ppm (CDCl₃). NMR data reporting uses the following abbreviations: s, singlet; bs, broad singlet; d, doublet; t, triplet; q, quartet; m, multiplet; and *J*, coupling constant in Hz. Aldehydes and imines were either purchased from Aldrich or synthesized according to literature procedures. 4-quinols **49** and **57-62** were synthesized according to the literature procedure.¹³⁴ Chiral thiourea **54** and TRIP phosphoric acid **17** were purchased from Aldrich. Catalyst **18** was synthesized as previously reported by List.¹³⁵

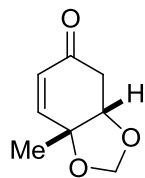
Synthesis of new *p*-Quinols



4-hydroxy-4-(2-methoxyethyl)cyclohexa-2,5-dienone (62). Prepared according to the literature procedure for **2a**¹: 75% yield; white solid; **¹H NMR** (400 MHz, CDCl₃): δ 6.94 (d, *J* = 10.2, 2H), 6.15 (d, *J* = 10.2, 2H), 3.76 (bs, 1H), 3.64 (t, *J* = 5.7 Hz 2H), 3.37 (s, 3H), 2.00 (t, *J* = 5.9 Hz, 2H); **¹³C NMR** (100 MHz, CDCl₃): δ 185.7, 148.5, 130.1, 79.6, 67.3, 58.7, 36.1; cm⁻¹; **HRMS** (ESI-APCI) *m/z* calcd [C₉H₁₂O₃]⁻ ([M - H]): 167.0714; found: 167.0710.

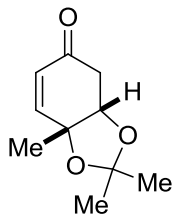
General Procedure for Quinol Desymmetrization:

To a 1 mL vial, with a magnetic stir bar, was added 4-methyl-4-hydroxycyclohexa-2,5-dienone **49** (0.1 mmol, 1.0 equiv), diphenylphosphinic acid (3.6 mg, 0.005 mmol, 0.05 equiv), aldehyde/imine (0.15 mmol, 1.25 equiv), and 1,2-dichloroethane or dichloromethane (0.4 mL). The vial was then sealed, heated to 45 °C and stirred until the starting material disappeared by TLC (12-48h). The reaction was concentrated *in vacuo*. Flash column chromatography 10-20% (hexanes:ethyl acetate) of the resulting clear or yellow residue gave the analytically pure dioxolane in high diastereoselectivity as a white solid or clear oil. Some products decompose slowly upon treatment with SiO₂ so a faster column is best.



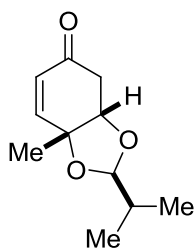
7a-methyl-3a,4-dihydrobenzo[d][1,3]dioxol-5(7aH)-one (71a). Prepared according to the general procedure using paraformaldehyde: 87% yield; >20:1 dr; white solid; *R_f* = 0.16 (80:20 Hexanes:EtOAc); **¹H NMR** (400 MHz, CDCl₃): δ 6.47 (dd, *J* = 10.3, 2.3 Hz, 1H), 6.01 (dd, *J* = 10.3, 1.1 Hz, 1H), 5.04 (d, *J* = 0.7 Hz, 1H), 4.90 (d,

$J = 0.8$ Hz, 1H), 4.09 (dt, $J = 3.3, 2.5$ Hz, 1H), 2.94 (ddd, $J = 17.5, 2.7, 1.1$ Hz, 1H), 2.61 (dd, $J = 17.5, 3.3$ Hz, 1H), 1.51, (s, 3H). ^{13}C NMR (100 MHz, CDCl_3): δ 195.0, 147.7, 129.0, 94.1, 78.9, 76.3, 38.3, 21.1; **HRMS** (ESI-APCI) m/z $[\text{C}_8\text{H}_{11}\text{O}_3]^+$ ($[\text{M} + \text{H}]^+$): calcd 155.0703, found 155.0704.



2,2,7a-trimethyl-3a,4-dihydrobenzo[d][1,3]dioxol-5(7aH)-one (74a). Prepared

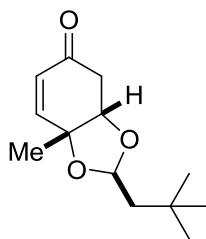
according to the general procedure using acetone: 18% yield; >20:1 dr; white solid; $R_f = 0.17$ (80:20 Hexanes:EtOAc); ^1H NMR (400 MHz, CDCl_3): δ 6.53 (dd, $J = 10.3, 2.4$ Hz, 1H), 5.93 (dd, $J = 10.3, 1.1$ Hz, 1H), 4.31 (dt, $J = 3.4, 2.5$ Hz, 1H), 2.89 (ddd, $J = 17.6, 2.5, 1.1$ Hz, 1H), 2.61 (dd, $J = 17.6, 3.5$ Hz, 1H), 1.46, (s, 3H), 1.39 (d, $J = 0.6$ Hz, 3H), 1.35 (d, $J = 0.6$ Hz, 3H). ^{13}C NMR (100 MHz, CDCl_3): δ 195.2, 150.5, 127.6, 108.8, 78.9, 38.1, 27.4, 27.3, 22.2; **HRMS** (ESI-APCI) m/z $[\text{C}_{10}\text{H}_{15}\text{O}_3]^+$ ($[\text{M} + \text{H}]^+$): calcd 183.1016, found 183.1010.



2-isopropyl-7a-methyl-3a,4-dihydrobenzo[d][1,3]dioxol-5(7aH)-one (70).

Prepared according to the general procedure: 92% yield; >20:1 dr; 42% ee, white solid; $R_f = 0.30$ (80:20 Hexanes:EtOAc); $[\alpha]_D^{20} = -30.6$, $c = 0.0106$ g/ml CH_2Cl_2 ; HPLC analysis: Chiralcel IA column, 99:1 Hexanes:*iso*-propanol, 1.0 ml/min, $\text{RT}_{\text{minor}} = 15.60$ min, $\text{RT}_{\text{major}} = 18.03$ min, 210 nm. ^1H NMR (400 MHz, CDCl_3): δ 6.49 (dd, $J = 10.3$ Hz, 2.2 Hz, 1H) 6.04 (dd, $J = 10.3, 1.1$ Hz, 1H), 4.68 (d, $J = 4.1$ Hz, 1H), 4.08-4.05 (m, 1H), 2.90 (ddd, $J = 17.5, 2.7, 1.1$ Hz, 1H), (dd, $J = 17.5, 3.2$ Hz, 1H), 1.84-1.71 (m, 1H), 1.49, (s, 3H), 0.90 (dd, $J = 6.9, 1.8$ Hz, 6H); ^{13}C NMR (100 MHz, CDCl_3): δ 195.7, 147.8, 129.7,

107.1, 78.8, 77.0, 38.8, 32.6, 21.0, 16.4, 16.2; **HRMS** (ESI-APCI) m/z calcd $[C_{11}H_{17}O_3]^+$ ($[M + H]^+$): 197.1172; found: 197.1180.

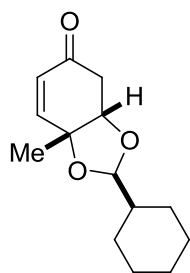


7a-methyl-2-neopentyl-3a,4-dihydrobenzo[d][1,3]dioxol-5(7aH)-one (71b).

Prepared according to the general procedure: 78% yield; >20:1 dr; white solid;

$R_f = 0.34$ (80:20 Hexanes:EtOAc); 1H NMR (400 MHz, $CDCl_3$): δ 6.48 (dd, $J = 10.3, 2.1$ Hz, 1H), 6.07 (dd, $J = 10.3, 1.1$ Hz, 1H), 4.98 (t, $J = 5.0$ Hz, 1H),

4.12-4.08 (m, 1H), 2.89, (ddd, $J = 17.5, 2.7, 1.1$ Hz, 1H), 2.56, (dd, $J = 17.5, 3.3$ Hz, 1H), 1.54 (d, $J = 5.0$ Hz, 2H), 1.49 (s, 3H), 0.93 (s, 9H); ^{13}C NMR (100 MHz, $CDCl_3$): δ 196.0, 147.9, 129.8, 102.4, 78.0, 76.8, 48.2, 38.8, 30.0 (3C), 29.2, 21.4; **HRMS** (ESI-APCI) m/z calcd $[C_{13}H_{21}O_3]^+$ ($[M + H]^+$): 225.1485, found 225.1488.

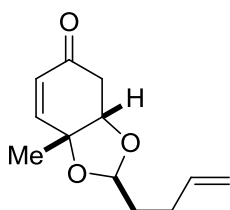


2-cyclohexyl-7a-methyl-3a,4-dihydrobenzo[d][1,3]dioxol-5(7aH)-one (71c).

Prepared according to the general procedure: 91% yield; >20:1 dr; white solid; R_f

$= 0.34$ (80:20 Hexanes:EtOAc); 1H NMR (400 MHz, $CDCl_3$): δ 6.48 (dd, $J = 10.3, 2.2$ Hz, 1H), 6.04 (dd, $J = 10.3, 1.1$ Hz, 1H), 4.66 (d, $J = 4.3$ Hz, 1H), 4.05-

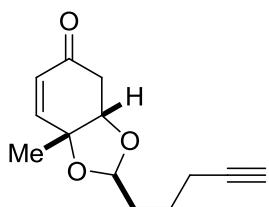
4.02 (m, 1H), 2.89, (ddd, $J = 17.5, 2.7, 1.1$ Hz, 1H), 2.54 (dd, $J = 17.5, 3.2$ Hz, 1H), 1.72-1.42 (m, 6H), 1.48 (s, 3H), 1.20-0.97 (m, 5H); ^{13}C NMR (100 MHz, $CDCl_3$): δ 195.8, 147.9, 129.6, 106.5, 78.6, 76.9, 42.4, 38.7, 26.84, 26.68, 26.3, 25.70, 25.65, 21.0; **HRMS** (ESI-APCI) m/z calcd $[C_{14}H_{21}O_3]^+$ ($[M + H]^+$): 237.1485, found 237.1484.



2-(but-3-en-1-yl)-7a-methyl-3a,4-dihydrobenzo[d][1,3]dioxol-5(7aH)-one (71d).

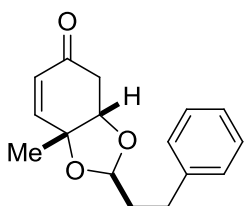
Prepared according to the general procedure: 81% yield; >20:1 dr;

clear oil; $R_f = 0.27$ (80:20 Hexanes:EtOAc); $^1\text{H NMR}$ (400 MHz, CDCl_3): δ 6.47 (dd, $J = 10.3$, 2.1 Hz, 1H), 6.05 (dd, $J = 10.3$, 1.1 Hz, 1H), 5.81 (dddd, $J = 16.8$, 10.2, 6.5, 6.5 Hz, 1H), 5.02 (dq, $J = 17.1$, 1.7 Hz, 1H), 4.97-4.92 (m, 2H), 4.13-4.10 (m, 1H), 2.89 (ddd, $J = 17.5$, 2.7, 1.1 Hz, 1H), 2.56 (dd, $J = 17.5$, 3.2 Hz, 1H), 1.74-1.67, (m, 2H), 1.50, (s, 3H); $^{13}\text{C NMR}$ (100 MHz, CDCl_3): δ 195.6, 147.5, 137.7, 129.8, 114.8, 103.1, 78.5, 77.2, 38.8, 34.0, 27.6, 21.2; **HRMS** (ESI-APCI) m/z calcd $[\text{C}_{12}\text{H}_{19}\text{O}_3]^+$ ($[\text{M} + \text{H}]^+$): 209.1172, found 209.1180.



7a-methyl-2-(pent-4-yn-1-yl)-3a,4-dihydrobenzo[d][1,3]dioxol-5(7aH)-one (71e). Prepared according to the general procedure: 71% yield; >20:1 dr; clear oil; $R_f = 0.23$ (80:20 Hexanes:EtOAc); $^1\text{H NMR}$ (400 MHz,

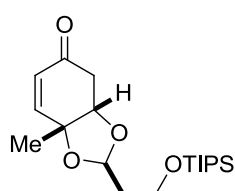
CDCl_3): δ 6.48 (dd, $J = 10.3$, 2.1 Hz, 1H), 6.06 (d, $J = 10.3$, 1.1 Hz, 1H), 4.97 (t, $J = 4.4$ Hz, 1H), 4.13-4.10 (m, 1H), 2.89 (ddd, $J = 17.5$, 2.7, 1.1 Hz, 1H), 2.56 (dd, $J = 17.5$, 3.2 Hz, 1H), 2.22 (ddd, $J = 7.1$, 7.1, 2.6 Hz, 2H), 1.94 (t, $J = 2.6$ Hz, 1H), 1.77-1.57 (m, 4H), 1.50 (s, 3H); $^{13}\text{C NMR}$ (100 MHz, CDCl_3): δ 195.6, 147.5, 129.8, 103.1, 83.9, 78.6, 77.2, 68.7, 38.8, 33.7, 22.4, 21.2, 18.2; **HRMS** (ESI-APCI) m/z calcd $[\text{C}_{13}\text{H}_{17}\text{O}_3]^+$ ($[\text{M} + \text{H}]^+$): 221.1172, found 221.1159.



7a-methyl-2-phenethyl-3a,4-dihydrobenzo[d][1,3]dioxol-5(7aH)-one (71f). Prepared according to the general procedure: 82% yield; white solid; $R_f = 0.21$ (80:20 hexanes:EtOAc); $^1\text{H NMR}$ (400 MHz, CDCl_3): δ 7.29-7.14 (m, 5 H), 6.47 (dd, $J = 10.3$, 2.1 Hz, 1H), 6.04 (dd, $J = 10.3$, 1.1

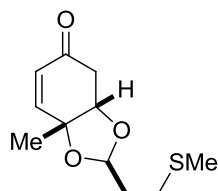
Hz, 1H), 4.96 (t, $J = 4.5$ Hz, 1H), 4.13 (q, $J = 2.7$ Hz, 1H), 2.90 (ddd, $J = 17.5$, 2.7, 1.1 Hz, 1H), 2.73-2.66 (m, 2H), 2.56 (dd, $J = 17.5$, 3.2 Hz, 1H), 1.96-1.89 (m, 2H), 1.50 (s, 3H); $^{13}\text{C NMR}$ (100 MHz, CDCl_3): δ 195.5, 147.5, 141.3, 129.8, 128.4, 128.3, 125.9, 102.9, 78.6, 77.2, 38.8,

36.4, 29.6, 21.2; **HRMS** (ESI-APCI) m/z calcd $[C_{16}H_{19}O_3]^+$ ($[M + H]^+$): calcd 259.1329, found 259.1347.



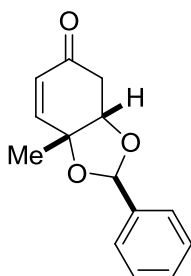
7a-methyl-2-(2-((triisopropylsilyl)oxy)ethyl)-3a,4-dihydrobenzo[d][1,3]dioxol-5(7aH)-one (71g). Prepared according to the general procedure: 77%

yield; 14:1 dr; clear oil; $R_f = 0.20$ (80:20 Hexanes:EtOAc); 1H NMR (400 MHz, $CDCl_3$): δ 6.47 (dd, $J = 10.3, 2.2$ Hz, 1H), 6.05 (dd, $J = 10.3, 1.1$ Hz, 1H), 5.09 (t, $J = 5.1$ Hz, 1H), 4.16 (q, $J = 2.7$ Hz, 1H), 3.80 (t, $J = 6.4$ Hz 2H), 2.89 (ddd, $J = 17.5, 2.7, 1.1$ Hz, 1H), 2.55 (dd, $J = 17.5, 3.2$ Hz, 1H), 1.92-1.78 (m, 2H), 1.50 (s, 3H), 1.06-1.00 (m, 19H); ^{13}C NMR (100 MHz, $CDCl_3$): δ 195.6, 147.6, 129.8, 101.4, 78.3, 77.1, 58.9, 38.8, 38.4, 21.3, 17.9 (6C), 11.9 (3C); **HRMS** (ESI-APCI) m/z calcd $[C_{19}H_{35}O_4Si]^+$ ($[M + H]^+$): 355.2299, found 355.2296.



7a-methyl-2-(2-(methylthio)ethyl)-3a,4-dihydrobenzo[d][1,3]dioxol-5(7aH)-one (71h). Prepared according to the general procedure: 90% yield;

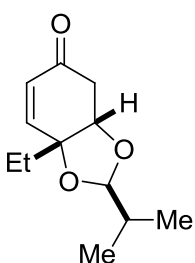
>20:1 dr; clear oil; $R_f = 0.18$ (80:20 Hexanes:EtOAc); 1H NMR (400 MHz, $CDCl_3$): δ 6.47 (dd, $J = 10.3, 2.2$ Hz, 1H), 6.05 (dd, $J = 10.3, 1.1$ Hz, 1H), 5.01 (t, $J = 4.5$ Hz, 1H), 4.12 (q, $J = 2.7$ Hz, 1H), 2.89 (ddd, $J = 17.5, 2.7, 1.1$ Hz, 1H), 2.60- 2.50 (m, 2H), 2.55 (dd, $J = 17.5, 3.2$ Hz, 1H), 2.08 (s, 3H), 1.94-1.87 (m, 2H), 1.50 (s, 3H); ^{13}C NMR (100 MHz, $CDCl_3$): δ 195.4, 147.3, 129.9, 102.2, 78.6, 77.3, 38.7, 34.6, 28.0, 21.1, 15.6; **HRMS** (ESI-APCI) m/z calcd $[C_{11}H_{17}O_3S]^+$ ($[M + H]^+$): 229.0893, found 229.0902.



7a-methyl-2-phenyl-3a,4-dihydrobenzo[d][1,3]dioxol-5(7aH)-one (73b).

Prepared according to the general procedure: 27% yield; white solid; $R_f = 0.1$

(80:20 hexanes:EtOAc); $^1\text{H NMR}$ (400 MHz, CDCl_3): δ 7.52-7.35 (m, 5H), 6.63 (dd, $J = 10.3$, 2.2 Hz, 1H), 6.17 (dd, $J = 10.3$, 1.1 Hz, 1H), 5.84 (s, 1H), 4.36-4.33 (m, 1H), 3.00 (ddd, $J = 17.5$, 2.7, 1.1 Hz, 1H), 2.64 (dd, $J = 17.5$, 3.3 Hz, 1H), 1.62 (s, 3H); $^{13}\text{C NMR}$ (100 MHz, CDCl_3): δ 195.4, 147.3, 138.1, 130.0, 129.4, 129.2, 128.4, 102.8, 79.0, 78.0, 38.6, 21.2; **HRMS** (ESI-APCI) m/z calcd $[\text{C}_{14}\text{H}_{15}\text{O}_3]^+$ ($[\text{M} + \text{H}]^+$): calcd 231.1016, found 231.0923.

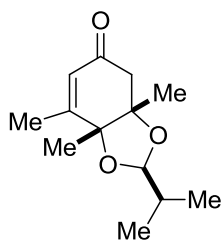


7a-ethyl-2-isopropyl-3a,4-dihydrobenzo[d][1,3]dioxol-5(7aH)-one (72a).

Prepared according to the general procedure: 79% yield; >20:1 dr; clear oil;

$R_f = 0.41$ (80:20 Hexanes:EtOAc); $^1\text{H NMR}$ (400 MHz, CDCl_3): δ 6.50 (dd, $J = 10.4$, 2.1 Hz, 1H), 6.10 (dd, $J = 10.4$, 1.1 Hz, 1H), 4.69 (d, $J = 4.1$ Hz,

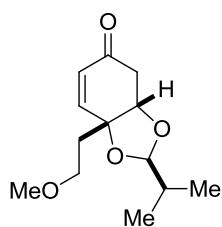
1H), 4.15-4.12 (m, 1H), 2.91 (ddd, $J = 17.6$, 2.6, 1.1 Hz, 1H), 2.53 (dd, $J = 17.6$, 3.4 Hz, 1H), 1.90-1.72 (m, 3H), 1.04 (t, $J = 7.6$ Hz, 3H), 0.90 (dd, $J = 6.9$, 1.9 Hz, 6H); $^{13}\text{C NMR}$ (100 MHz, CDCl_3): δ 196.1, 147.1, 130.6, 106.9, 79.3, 77.1, 39.5, 32.6, 28.3, 16.5, 16.3 7.9; **HRMS** (ESI-APCI) m/z calcd $[\text{C}_{12}\text{H}_{19}\text{O}_3]^+$ ($[\text{M} + \text{H}]^+$): 211.1329, found 211.1219.



2-isopropyl-3a,7,7a-trimethyl-3a,4-dihydrobenzo[d][1,3]dioxol-5(7aH)-one (72e). Prepared according to the general procedure: 63% yield; white solid; $R_f = 0.50$ (67:33 Hexanes:EtOAc); $^1\text{H NMR}$ (400 MHz, CDCl_3): δ

6.0-5.98 (m, 1H), 4.35 (d, $J = 5.6$ Hz, 1H), 2.82 (dd, $J = 17.3$, 1.1 Hz, 1H),

2.42 (d, $J = 17.3$ Hz, 1H), 1.97 (d, $J = 1.4$ Hz, 3H), 1.75-1.65 (m, 1H), 1.41 (s, 3H), 1.25 (s, 3H) 0.90 (dd, $J = 6.7$, 0.3 Hz, 6H); $^{13}\text{C NMR}$ (100 MHz, CDCl_3): δ 195.9, 158.9, 128.8, 106.2, 81.31, 81.25, 45.1, 32.8, 25.4, 18.7, 17.8, 17.1, 17.0; **HRMS** (ESI-APCI) m/z calcd $[\text{C}_{13}\text{H}_{21}\text{O}_3]^+$ ($[\text{M} + \text{H}]^+$): 225.1386, found 225.1387.



2-isopropyl-7a-(2-methoxyethyl)-3a,4-dihydrobenzo[d][1,3]dioxol-

5(7aH)-one (72d). Prepared according to the general procedure: 66% yield;

>20:1 dr; clear oil; $R_f = 0.21$ (67:33 Hexanes:EtOAc); $^1\text{H NMR}$ (400 MHz,

CDCl_3): δ 6.47 (dd, $J = 10.4, 2.1$ Hz, 1H), 6.10 (dd, $J = 10.4$ Hz, 1.0 Hz 1H),

4.68 (d, $J = 4.1$ Hz, 1H), 4.23 (q, $J = 2.8$ Hz, 1H), 3.57 (ddd, $J = 9.9, 5.9, 5.0$ Hz, 1H), 3.49 (ddd,

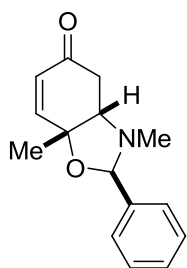
$J = 9.9, 8.1, 4.6$ Hz, 1H), 3.29 (s, 3H), 2.86 (ddd, $J = 17.6, 2.7, 1.1$ Hz, 1H), 2.69 (dd, $J = 17.6,$

3.3 Hz, 1H), 2.12 (ddd, $J = 14.7, 8.1, 5.0$ Hz, 1H) 2.03 (ddd, $J = 14.7, 5.9, 4.6$ Hz, 1H), 1.84-

1.71 (m, 1H), 0.90 (dd, $J = 6.9, 2.0$ Hz, 6H); $^{13}\text{C NMR}$ (100 MHz, CDCl_3): δ 196.4, 146.7,

130.5, 106.7, 78.5, 77.7, 67.6, 58.5, 38.9, 35.5, 32.6, 16.4, 16.3; **HRMS** (ESI-APCI) m/z calcd

$[\text{C}_{13}\text{H}_{21}\text{O}_4]^+$ ($[\text{M} + \text{H}]^+$): 241.1434, found 241.1435.



3,7a-dimethyl-2-phenyl-2,3,3a,4-tetrahydrobenzo[d]oxazol-5(7aH)-one

(75a). Prepared according to the general procedure: ??% yield; >20:1 dr; white

solid; $^1\text{H NMR}$ (400 MHz, CDCl_3): δ 7.41-7.30 (m, 5H), 6.61 (dd, $J = 10.2$ Hz,

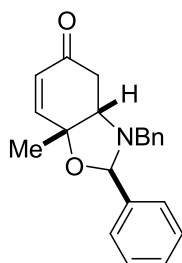
2.1 Hz, 1H) 5.94 (dd, $J = 10.2, 1.1$ Hz, 1H), 4.77 (s, 1H), 2.99 (dt, $J = 3.9, 2.3$

Hz, 1H), 3.73 (s, 3H), 2.80 (ddd, $J = 17.2, 2.4, 1.1$ Hz, 1H), 2.66 (dd, $J = 17.2, 3.9$ Hz, 1H),

2.13, (s, 3H), 1.53 (s, 3H); $^{13}\text{C NMR}$ (100 MHz, CDCl_3): δ 196.2, 151.6, 138.5, 128.4, 128.3,

125.5, 98.6, 78.4, 69.5, 37.0, 35.0, 23.4; **HRMS** (ESI-APCI) m/z calcd $[\text{C}_{15}\text{H}_{18}\text{NO}_2]^+$ ($[\text{M} +$

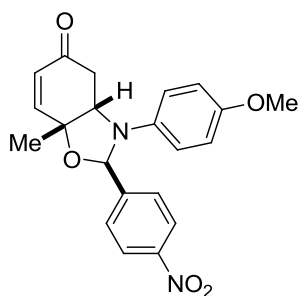
$\text{H}]^+$): 244.1332, found 244.1338.



3,7a-dimethyl-2-phenyl-2,3,3a,4-tetrahydrobenzo[d]oxazol-5(7aH)-one

(75b). $^1\text{H NMR}$ (400 MHz, CDCl_3): δ 7.45-7.40 (m, 2H), 7.32-7.27 (m, 3H),

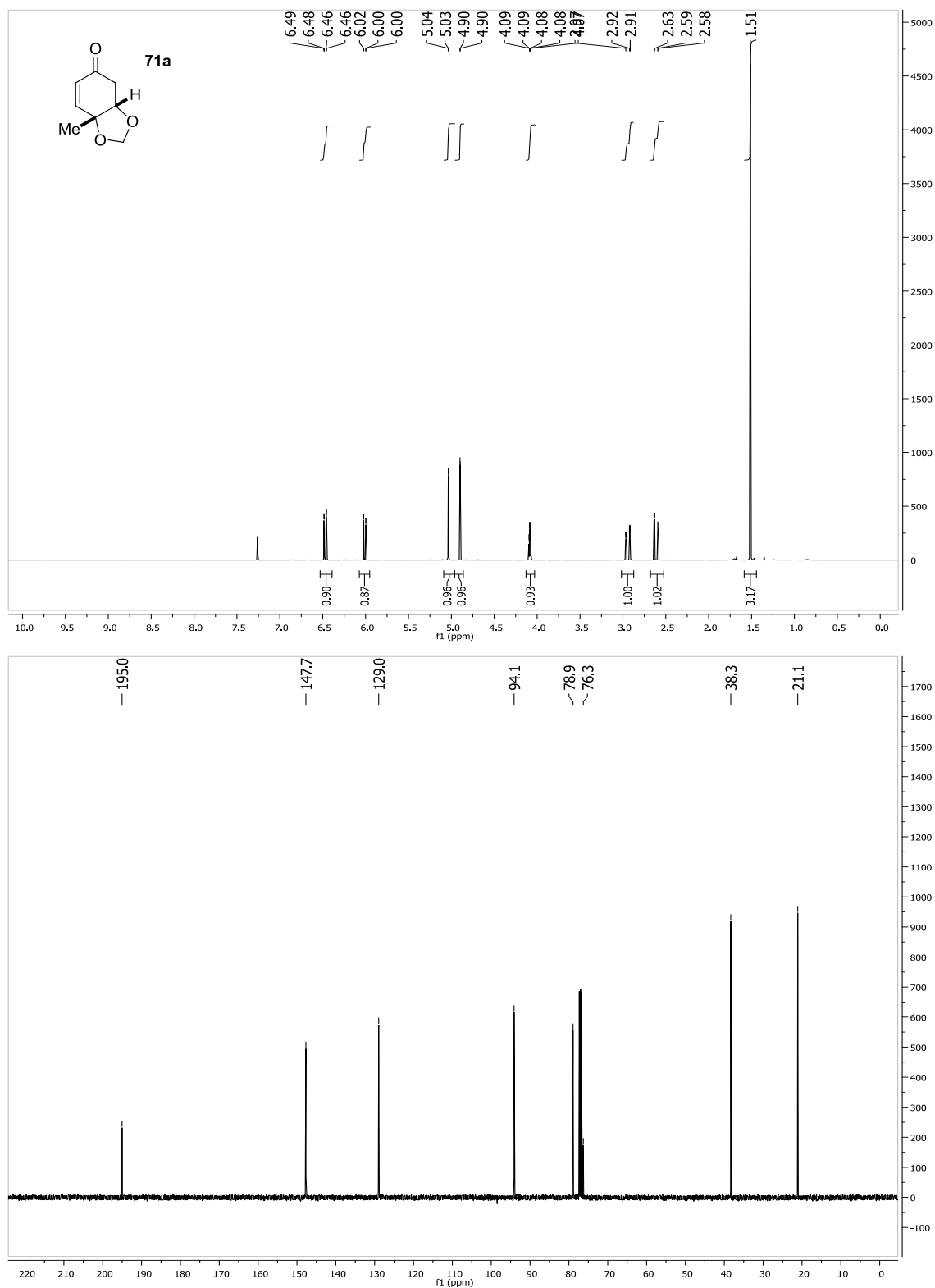
7.24-7.19 (m, 3H), 7.07-7.03 (m, 2H), 6.60 (dd, $J = 10.2$ Hz, 2.0 Hz, 1H) 5.95 (dd, $J = 10.2$, 1.1 Hz, 1H), 5.08 (s, 1H), 3.77 (d, $J = 14.5$ Hz, 1H), 3.53 (d, $J = 14.5$ Hz, 1H), 2.89 (dt, $J = 3.8$, 2.3 Hz, 1H), 2.69 (ddd, $J = 17.1$, 2.5, 1.1 Hz, 1H), 2.55 (dd, $J = 17.1$, 3.8 Hz, 1H), 1.48 (s, 3H); ^{13}C NMR (100 MHz, CDCl_3): δ 196.1, 151.9, 138.7, 136.1, 129.2, 129.0, 128.7, 128.4, 128.2, 127.4, 125.6, 96.2, 78.4, 67.4, 52.8, 37.5, 23.2; HRMS (ESI-APCI) m/z calcd $[\text{C}_{21}\text{H}_{22}\text{NO}_2]^+$ ($[\text{M} + \text{H}]^+$): 320.1645, found 320.1649.

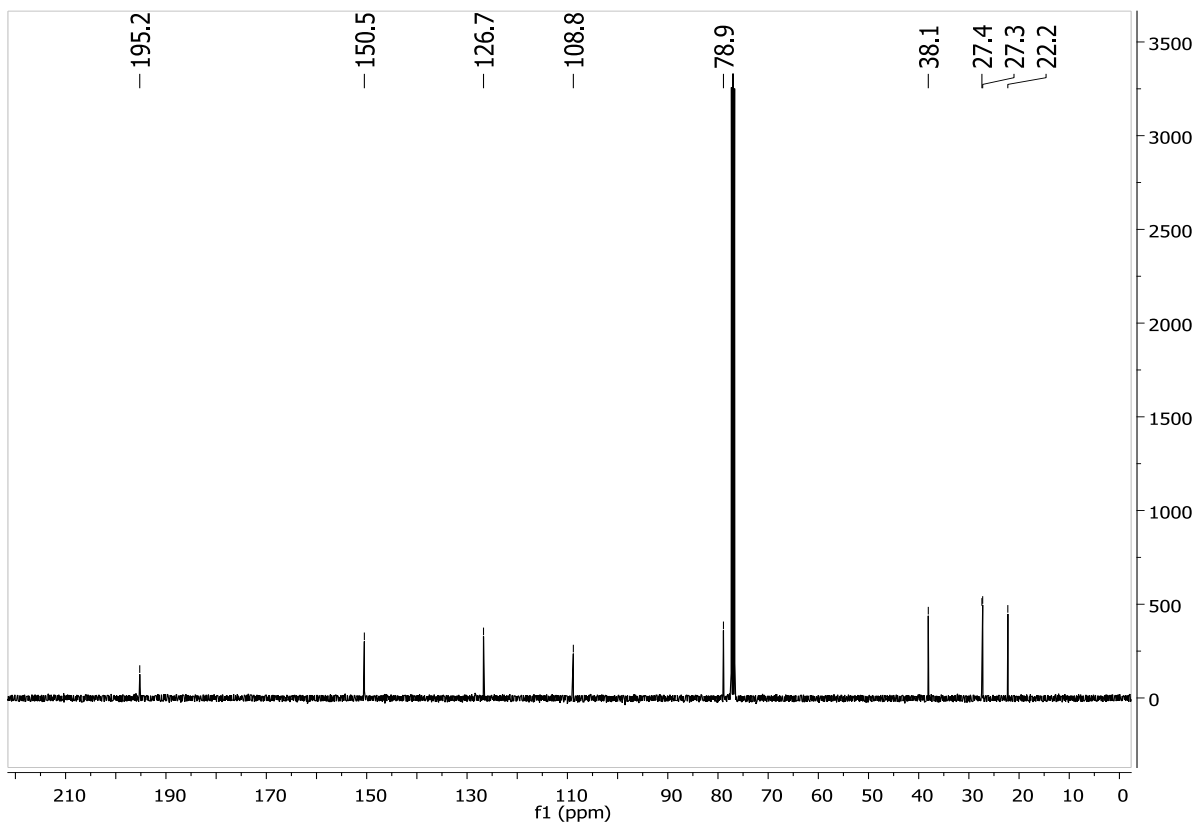
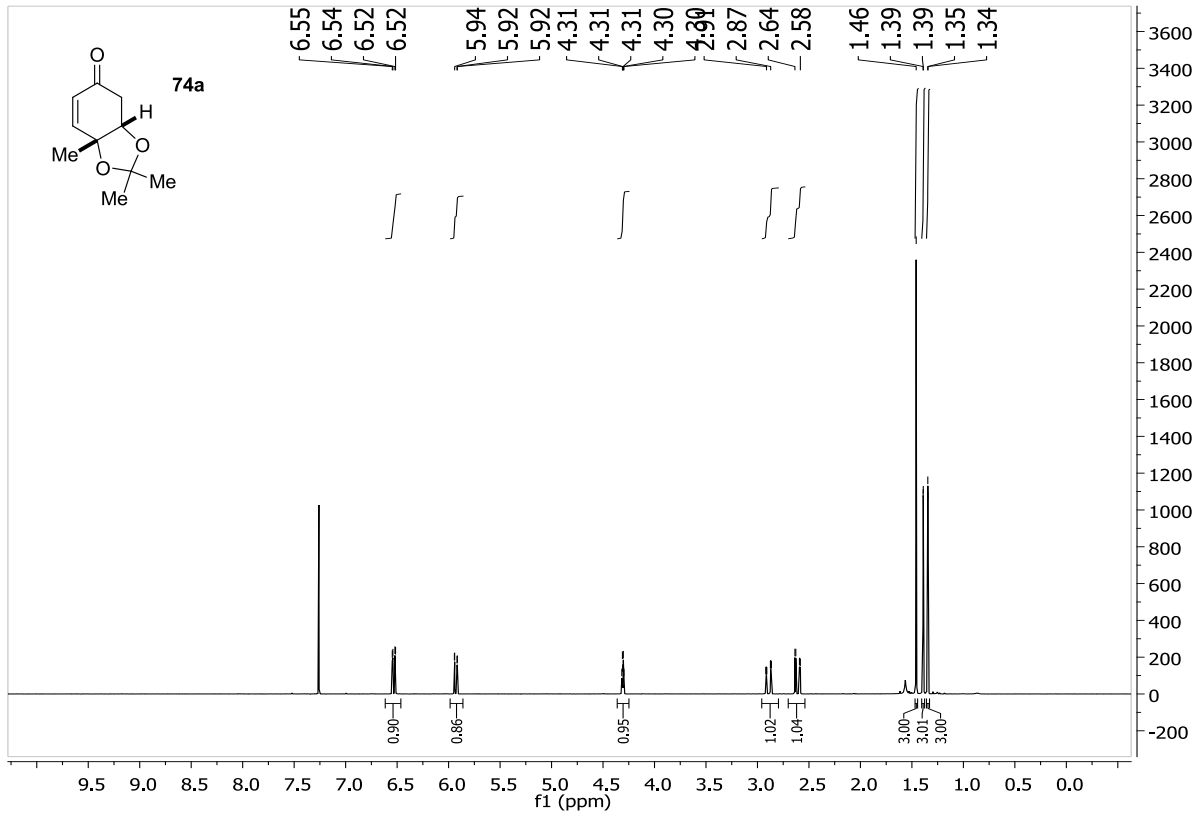


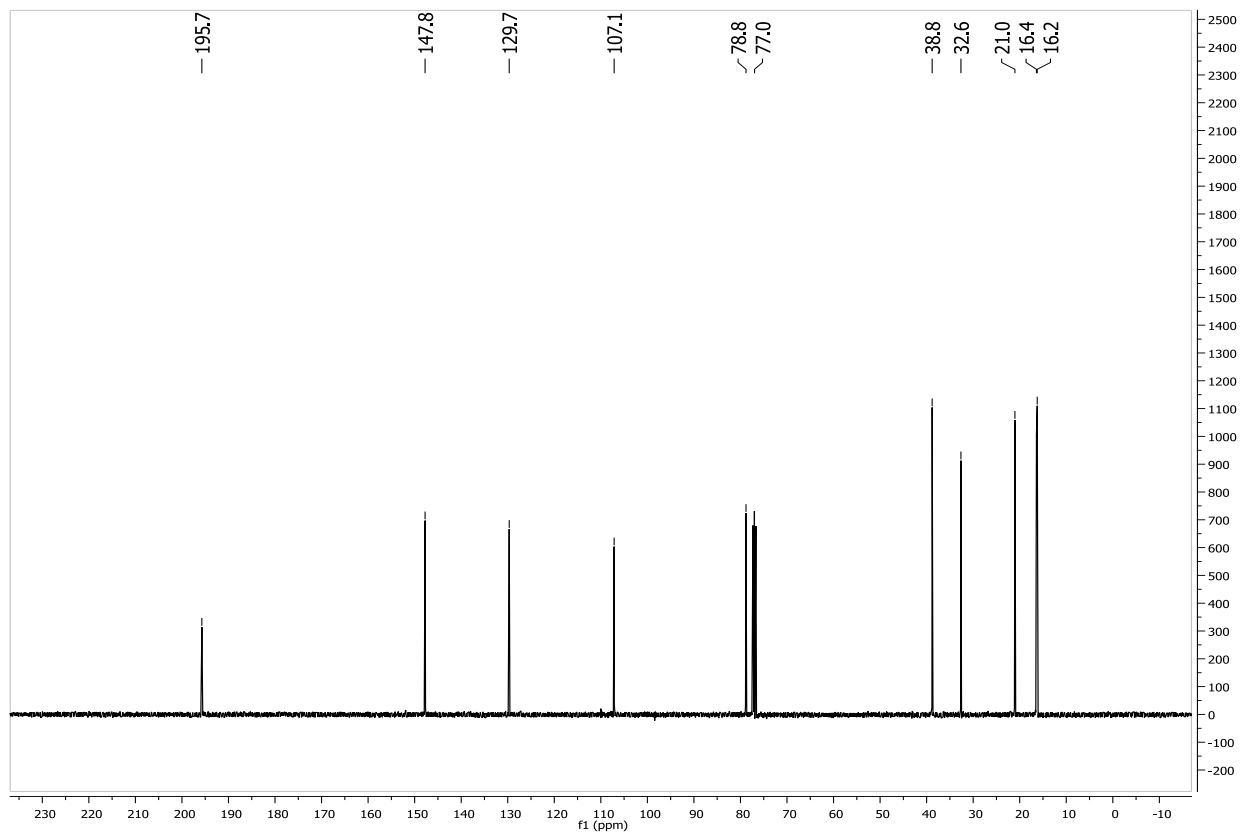
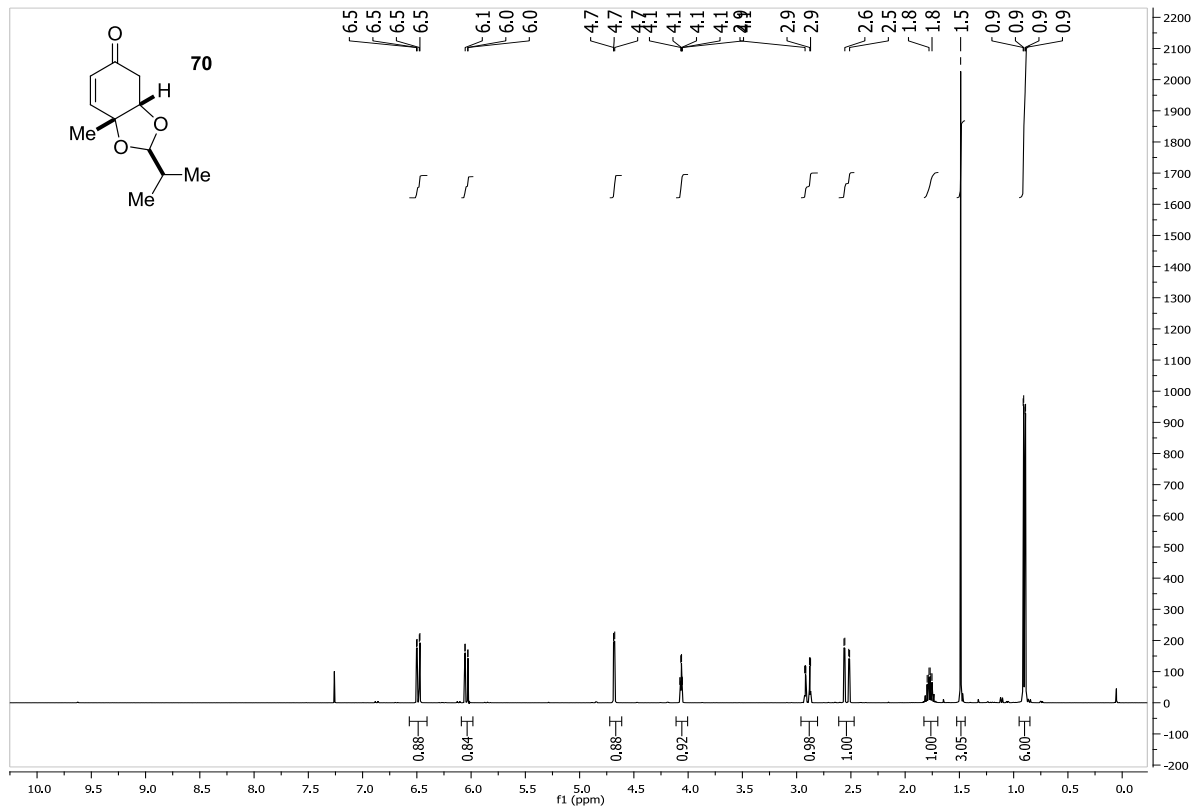
3-(4-methoxyphenyl)-7a-methyl-24-nitrophenyl)-2,3,3a,4-tetrahydro benzo[d]oxazol-5(7aH)-one (75c). Prepared according to the general procedure: 92% yield; >20:1 dr; ??% ee, yellow solid; $R_f = 0.23$ (67:33 Hexanes:EtOAc); $[\alpha]_D^{20} = -??$, $c = 0.0106$ g/ml CH_2Cl_2 ; HPLC analysis: Chiralcel IC column, 80:20 Hexanes:*iso*-propanol, 1.0

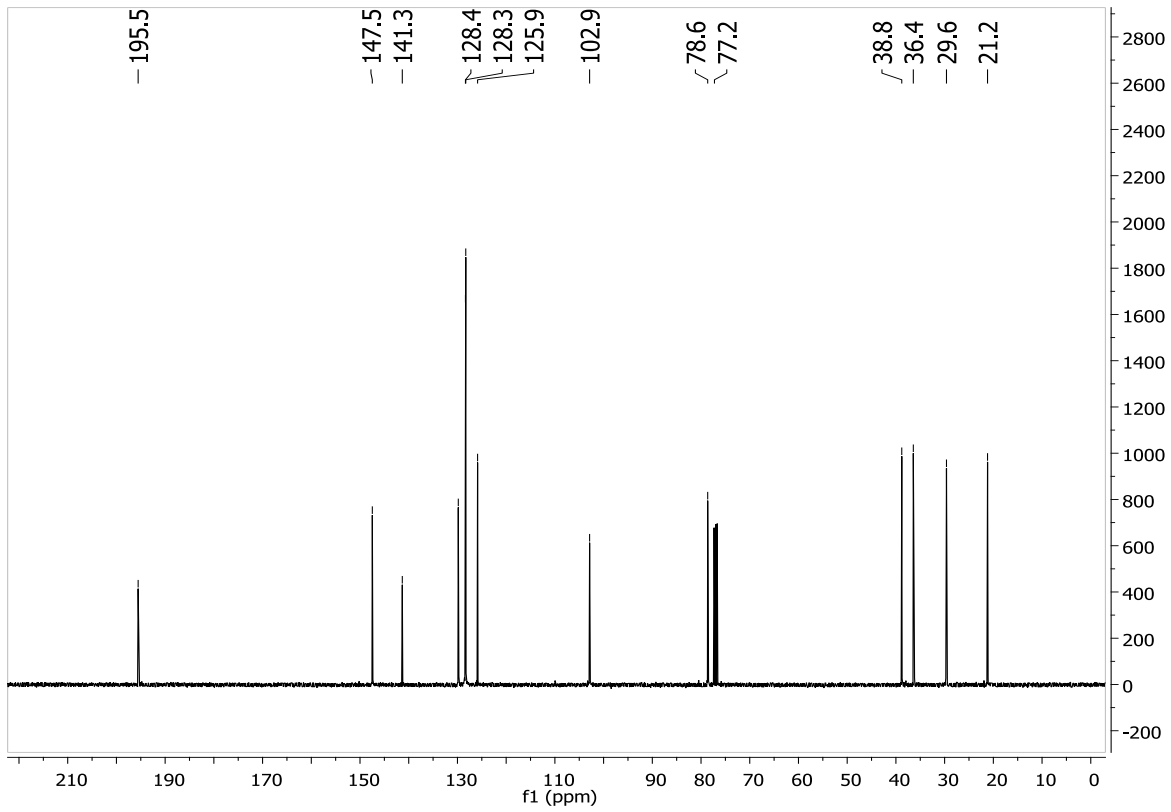
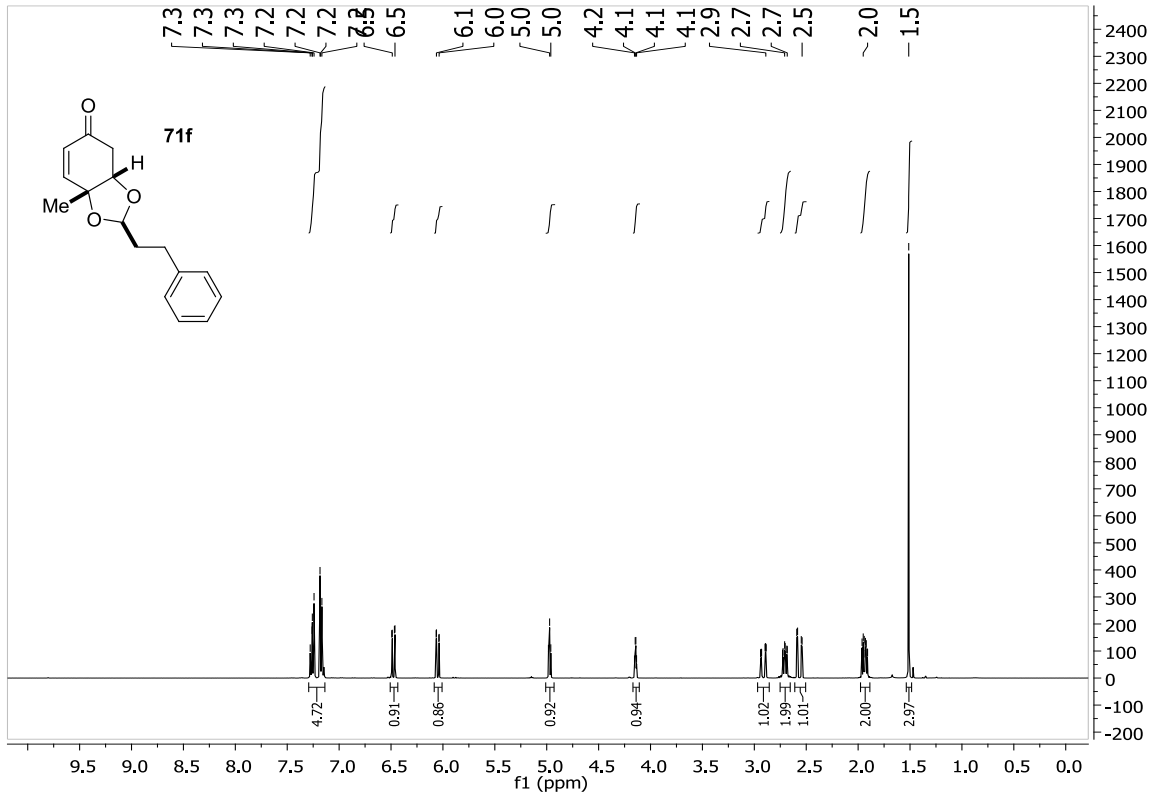
ml/min, $\text{RT}_{\text{minor}} = 35.29$ min, $\text{RT}_{\text{major}} = 54.97$ min, 210 nm. ^1H NMR (400 MHz, CDCl_3): δ 8.14 (d, $J = 8.8$ Hz, 2H), 7.52, (d, $J = 8.6$ Hz, 2H), 6.82-6.89 (m, 4H), 6.46 (dd, $J = 10.3$ Hz, 1.8 Hz, 1H) 5.86 (dd, $J = 10.3$, 0.9 Hz, 1H), 5.74 (s, 3H), 4.02-3.98 (m, 1H), 3.73 (s, 3H), 2.84 (ddd, $J = 17.0$, 2.7, 0.9 Hz, 1H), 2.65 (dd, $J = 17.0$, 3.9 Hz, 1H), 1.84-1.71 (m, 1H), 1.63 (s, 3H); ^{13}C NMR (100 MHz, CDCl_3): δ 195.8, 156.2, 150.4, 148.1, 147.0, 137.3, 128.9, 127.3, 123.4, 122.0, 114.8, 94.8, 79.1, 66.3, 55.5, 37.7, 23.4; HRMS (ESI-APCI) m/z calcd $[\text{C}_{21}\text{H}_{21}\text{N}_2\text{O}_5]^+$ ($[\text{M} + \text{H}]^+$): 381.1445; found: 381.1443.

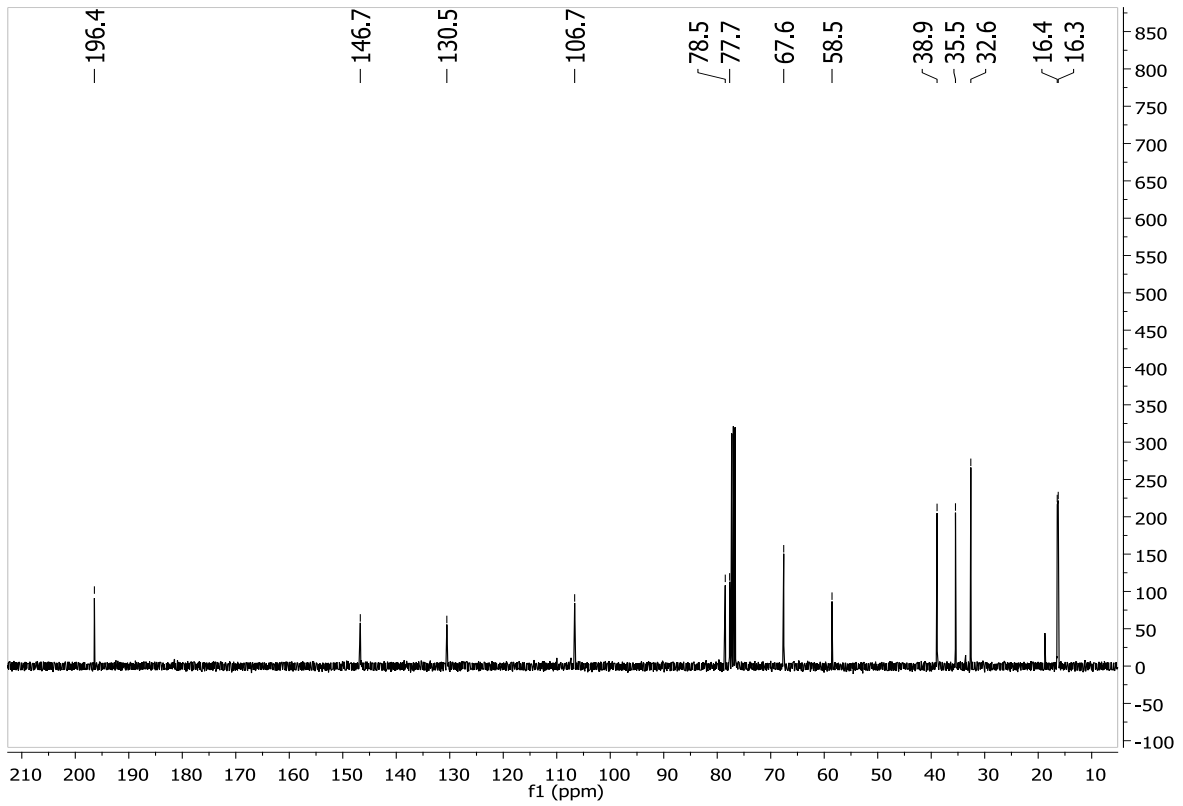
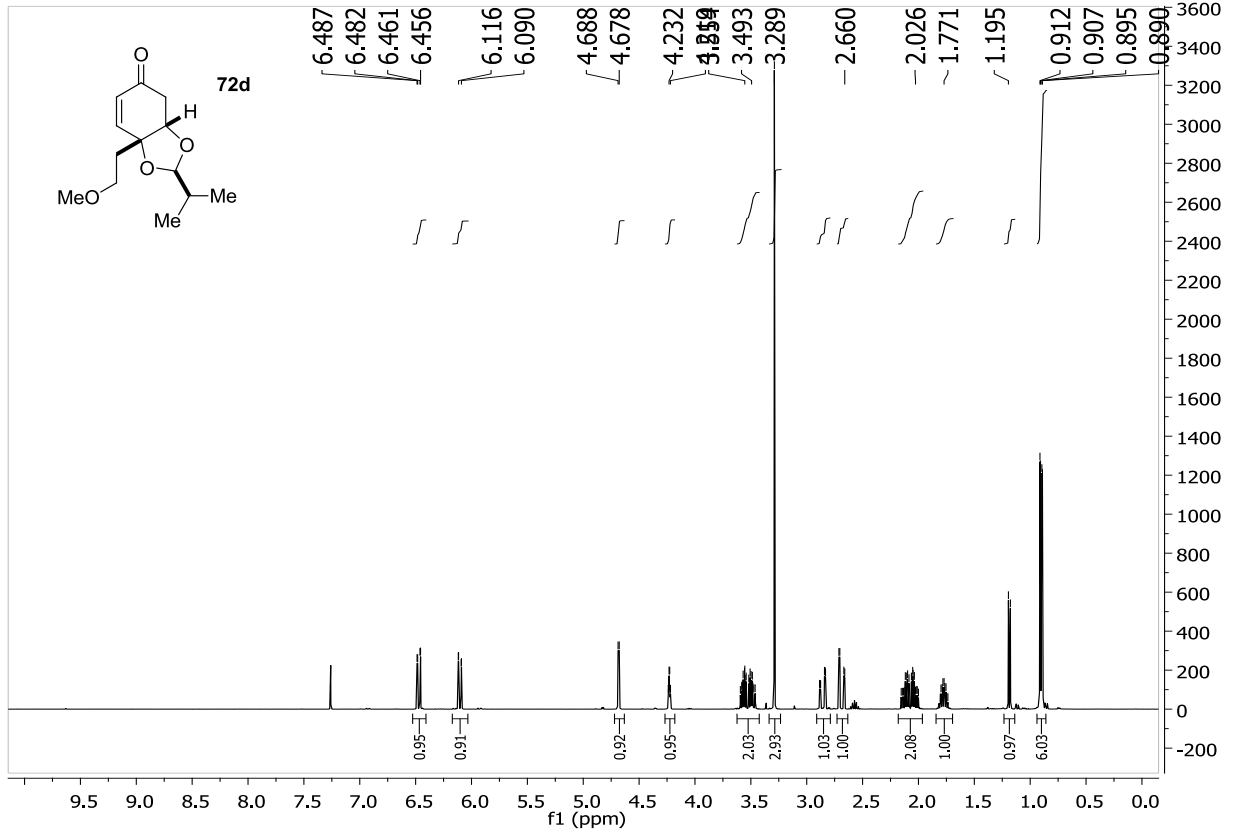
^1H NMR and ^{13}C NMR Spectra of New Compounds

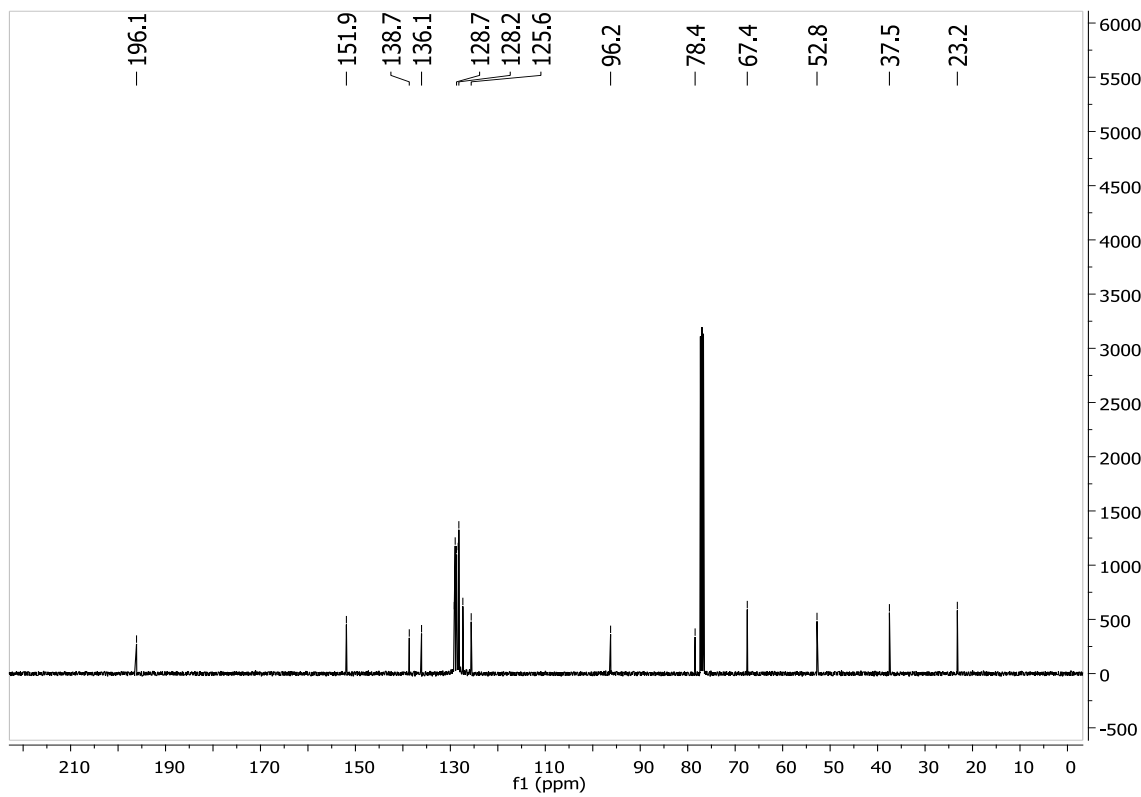
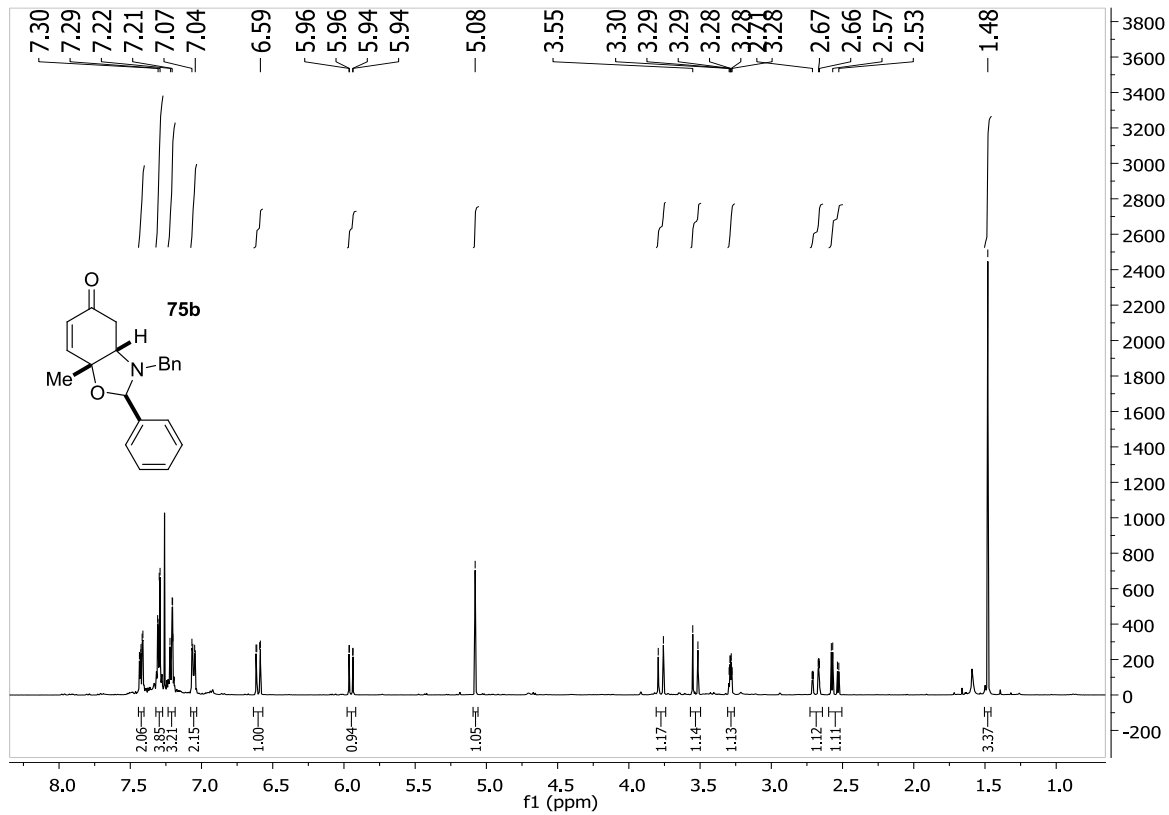












References

- ¹³⁴ Carreno, M. C.; Gonzalez-Lopez, M.; Urbano, A.; *Angew. Chem. Int. Ed.* **2006**, *45*, 2737.
- ¹³⁵ Čorić, I.; Vellalath, S.; List, B. *J. Am. Chem. Soc.* **2010**, *132*, 8536.

Appendix 3

Chapter 4 Supporting Information

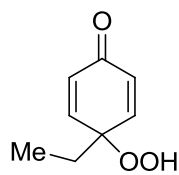
General Methods

All reactions were carried out in oven-dried glassware with magnetic stirring. Dichloroethane (DCE) was degassed with argon and distilled from CaH₂. Dichloromethane was degassed with argon and passed through two columns of neutral alumina. Toluene was degassed with argon and passed through one column of neutral alumina and one column of Q5 reactant. Column chromatography was performed on Silicycle Inc. silica gel 60 (230-400 mesh). Thin layer chromatography was performed on Silicycle Inc. 0.25 mm silica gel 60-F plates. Visualization was accomplished with UV light (254 nm) and KMnO₄ followed by heating.

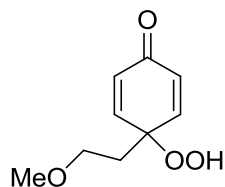
¹H NMR and ¹³C NMR spectra were obtained on Varian 300 or 400 MHz spectrometers in CDCl₃ at ambient temperature and chemical shifts are expressed in parts per million (δ , ppm). Proton chemical shifts are referenced to 7.26 ppm (CHCl₃) and carbon chemical shifts are referenced to 77.0 ppm (CDCl₃). NMR data reporting uses the following abbreviations: s, singlet; bs, broad singlet; d, doublet; t, triplet; q, quartet; m, multiplet; and *J*, coupling constant in Hz.

Aldehydes were either purchased from Aldrich or synthesized according to literature procedures. 4-Peroxyquinols **15** and **42a-42d** were synthesized based off of a literature procedure.¹³⁶ Thiourea was purchased from Aldrich. Catalysts **17-20** and **40** were synthesized as previously reported. Catalysts **37-39** were purchased from Strem and Aldrich. Catalyst **21** and **22** were synthesized using a similar procedure to catalyst **19**.¹³⁷

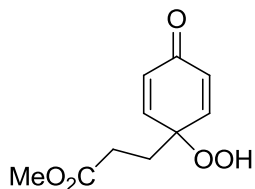
Synthesis of Starting Materials:



4-ethyl-4-hydroperoxycyclohexa-2,5-dienone (42a). Prepared according to the literature procedure for **15** 68% yield; white solid; recrystallized from EtOAc (mp: 75-77); $R_f = 0.11$ (85:15 Hexanes:EtOAc); $^1\text{H NMR}$ (400 MHz, CDCl_3): δ 8.77, (s, 1H), 6.86 (d, $J = 10.2$ Hz, 2H), 6.35, (d, $J = 10.2$ Hz, 2H), 1.74 (q, $J = 7.6$ 2H), 0.85 (t, $J = 7.6$, 3H); $^{13}\text{C NMR}$ (100 MHz, CDCl_3): δ 186.0, 149.3, 131.3, 82.3, 28.9, 7.7; **IR** (NaCl, neat): 3284, 3057, 2981, 2942, 2883, 1671, 1623, 1402, 1182, 1059, 993, 864 cm^{-1} ; **HRMS** (ESI-APCI) m/z calcd [$\text{C}_8\text{H}_9\text{O}_3$] ($[\text{M} - \text{H}]^-$): 153.0557; found: 153.0056.



4-hydroperoxy-4-(2-methoxyethyl)cyclohexa-2,5-dienone (42c). Prepared according to the literature procedure for **15**: 55% yield; yellow oil; $R_f = 0.19$ (50:50 Hexanes:EtOAc); $^1\text{H NMR}$ (400 MHz, CDCl_3): δ 9.65, (s, 1H), 6.95 (d, $J = 10.2$, 2H), 6.28, (d, $J = 10.2$, 2H), 3.44 (t, $J = 5.7$ Hz 2H), 3.29 (s, 3H), 2.01 (t, $J = 5.9$ Hz, 2H); $^{13}\text{C NMR}$ (100 MHz, CDCl_3): δ 185.7, 148.5, 130.1, 79.6, 67.3, 58.7, 36.1; **IR** (NaCl, neat): 3284, 2929, 2878, 2834, 1671, 1626, 1397, 1264, 1178, 1114, 862 cm^{-1} ; **HRMS** (ESI-APCI) m/z calcd [$\text{C}_9\text{H}_{12}\text{O}_4$] ($[\text{M} - \text{H}]^-$): 183.0657; found: 183.0657

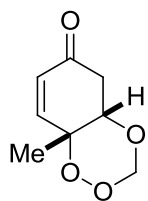


methyl 3-(1-hydroperoxy-4-oxocyclohexa-2,5-dien-1-yl)propanoate (42d). Prepared according to the literature procedure for **15**: 72% yield; white solid; recrystallized from EtOAc (mp: 85-86); $R_f = 0.14$ (67:33 Hexanes:EtOAc); $^1\text{H NMR}$ (400 MHz, CDCl_3): δ 9.25 (s, 1H), 6.89 (d, $J = 10.2$ Hz, 2H), 6.32 (d, $J = 10.2$ Hz, 2H), 3.66 (s, 3H), 2.33 (t, $J = 7.5$ Hz, 2H), 2.08 (t, $J = 7.5$ Hz, 2H); $^{13}\text{C NMR}$ (100 MHz, CDCl_3): δ 185.4, 173.2, 147.9, 131.2, 80.4, 52.1, 30.5, 28.2; **IR** (NaCl, neat): 3320,

3053, 3006, 2958, 2851, 1736, 1672, 1627, 1439, 1205, 1082, 865 cm^{-1} ; **HRMS** (ESI-APCI) m/z calcd $[\text{C}_{10}\text{H}_{11}\text{O}_5]^-$ ($[\text{M} - \text{H}]^-$): 213.0606; found: 211.0612.

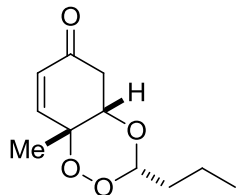
General Procedure for Peroxyquinol Desymmetrization:

To an oven dried 1 mL vial, with a magnetic stir bar, was added 4-methyl-4-hydroperoxycyclohexa-2,5-dienone **15** (0.1 mmol, 1.0 equiv), phosphoric acid **19** (3.6 mg, 0.005 mmol, 0.05 equiv), thiourea **34** (1.8 mg, 0.005 mmol, 0.05 equiv), aldehyde (0.15 mmol, 1.25 equiv), activated 4Å molecular sieves (25 mg) and 1,2-dichloroethane (0.4 mL). The vial was then sealed, heated to 45 °C and stirred until the starting material disappeared by TLC (12-48h). The reaction was concentrated *in vacuo*. Column chromatography 10-20%(hexanes:ethyl acetate) of the resulting yellow residue gave the analytically pure 1,2,4-trioxane as a white solid or clear oil.



(4aS,8aR)-8a-methyl-4a,5-dihydrobenzo[e][1,2,4]trioxin-6(8aH)-one (41a).

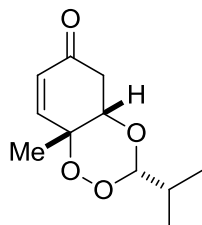
Prepared according to the general procedure: 89% yield; >20:1 dr; 94% ee; white solid; $R_f = 0.16$ (80:20 Hexanes:EtOAc); $[\alpha]_D^{20} = -108.5$, $c = 0.0024$ g/ml CH_2Cl_2 ; HPLC analysis: Chiralcel IA column, 95:5 Hexanes:iso-propanol, 1.0 ml/min, $\text{RT}_{\text{minor}} = 11.59$ min, $\text{RT}_{\text{major}} = 12.69$ min, 210 nm. $^1\text{H NMR}$ (400 MHz, CDCl_3): δ 6.88 (dd, $J = 10.4, 2.7$ Hz, 1H), 6.11 (d, $J = 10.4$ Hz, 1H), 5.42 (d, $J = 8.5$ Hz, 1H), 5.16 (d, $J = 8.5$ Hz, 1H), 4.15 (q, $J = 2.9$ Hz, 1H), 2.71 (d, $J = 3.0$ Hz, 2H), 1.34, (s, 3H). $^{13}\text{C NMR}$ (100 MHz, CDCl_3): δ 194.5, 150.6, 129.8, 95.8, 79.1, 75.8, 40.8, 20.9; **IR** (NaCl, neat): 3043, 2987, 2921, 2865, 1674, 1625, 1388, 1149, 817 cm^{-1} ; **HRMS** (ESI-APCI) m/z $[\text{C}_8\text{H}_{11}\text{O}_4]^+$ ($[\text{M} + \text{H}]^+$): calcd 170.0652, found 170.0653.



(3S,4aS,8aR)-8a-methyl-3-propyl-4a,5-dihydrobenzo[e][1,2,4]trioxin-

6(8aH)-one (41b). Prepared according to the general procedure: 90% yield;

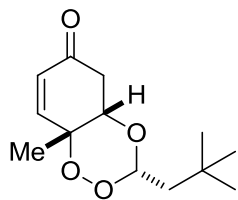
>20:1 dr; 95% ee; clear oil; $R_f = 0.27$ (80:20 Hexanes:EtOAc); $[\alpha]_D^{20} = -67.0$, $c = 0.0031$ g/ml CH_2Cl_2 ; HPLC analysis: Chiralcel IA column, 99:1 Hexanes:*iso*-propanol, 1.0 ml/min, $\text{RT}_{\text{minor}} = 17.57$ min, $\text{RT}_{\text{major}} = 23.80$ min, 210 nm. $^1\text{H NMR}$ (400 MHz, CDCl_3): δ 6.84 (dd, $J = 10.4, 3.0$ Hz, 1H), 6.07 (d, $J = 10.4$ Hz, 1H), 5.25 (t, $J = 5.2$ Hz, 1H), 4.15 (q, $J = 2.9$ Hz, 1H), 2.69 (d, $J = 3.0$ Hz, 2H), 1.53-1.45 (m, 2H), 1.44-1.33 (m, 2H), 1.33 (s, 3H), 0.88 (t, $J = 7.4$ Hz, 3H); $^{13}\text{C NMR}$ (100 MHz, CDCl_3): δ 194.9, 151.0, 129.6, 104.0, 77.7, 76.3, 41.0, 33.7, 20.6, 16.8, 13.8; **IR** (NaCl, neat): 3055, 2936, 2878, 1683, 1460, 1385, 1231, 1094, 835, 783 cm^{-1} ; **HRMS** (ESI-APCI) m/z calcd $[\text{C}_{11}\text{H}_{17}\text{O}_4]^+$ ($[\text{M} + \text{H}]^+$): 213.1121, found 213.1120.



(3S,4aS,8aR)-3-isopropyl-8a-methyl-4a,5-dihydrobenzo[e][1,2,4]trioxin-

6(8aH)-one (16). Prepared according to the general procedure: 92% yield;

>20:1 dr; 96% ee; white solid; $R_f = 0.29$ (80:20 Hexanes:EtOAc); $[\alpha]_D^{20} = -49.5$, $c = 0.0123$ g/ml CH_2Cl_2 ; HPLC analysis: Chiralcel IC column, 97:3 Hexanes:*iso*-propanol, 1.0 ml/min, $\text{RT}_{\text{minor}} = 7.92$ min, $\text{RT}_{\text{major}} = 9.60$ min, 210 nm. $^1\text{H NMR}$ (400 MHz, CDCl_3): δ 6.84 (dd, $J = 10.4$ Hz, 2.7 Hz, 1H) 6.06 (d, $J = 10.4$ Hz, 1H), 5.01 (d, $J = 5.1$ Hz, 1H), 4.14 (q, $J = 2.9$ Hz, 1H), 2.72-2.69 (m, 2H), 1.84-1.71 (m, 1H), 1.33 (s, 3H), 0.88 (d, $J = 3.9$ Hz, 6H); $^{13}\text{C NMR}$ (100 MHz, CDCl_3): δ 195.1, 151.1, 129.5, 101.1, 77.7, 76.3, 41.0, 30.9, 20.5, 16.7, 16.6; **IR** (NaCl, neat): 3041, 2971, 2935, 2880, 1684, 1473, 1388, 1289, 1081, 843 cm^{-1} ; **HRMS** (ESI-APCI) m/z calcd $[\text{C}_{11}\text{H}_{17}\text{O}_4]^+$ ($[\text{M} + \text{H}]^+$): 213.1121; found: 213.1119.

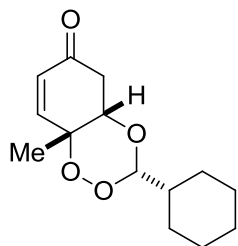


(3S,4aS,8aR)-8a-methyl-3-neopentyl-4a,5-dihydrobenzo[e][1,2,4]trioxin-

6(8aH)-one (41c). Prepared according to the general procedure: 84% yield;

>20:1 dr; 96% ee; white solid; $R_f = 0.30$ (80:20 Hexanes:EtOAc); $[\alpha]_D^{20} = -$

120.0, $c = 0.0047$ g/ml CH_2Cl_2 ; HPLC analysis: Chiralcel IC column, 97:3 Hexanes:*iso*-propanol, 1.0 ml/min, $\text{RT}_{\text{minor}} = 12.32$ min, $\text{RT}_{\text{major}} = 18.11$ min, 210 nm. $^1\text{H NMR}$ (400 MHz, CDCl_3): δ 6.84 (dd, $J = 10.4, 2.8$ Hz, 1H), 6.06 (d, $J = 10.4$ Hz, 1H), 5.25 (t, $J = 4.9$ Hz, 1H), 4.16 (q, $J = 2.9$ Hz, 1H), 2.68, (d, $J = 3.0$ Hz, 2H), 1.46-1.36 (m, 2H), 1.33 (s, 3H), 0.92 (s, 9H); $^{13}\text{C NMR}$ (100 MHz, CDCl_3): δ 194.9, 151.1, 129.6, 103.2, 77.5, 76.3, 45.4, 41.0, 29.8 (3C), 29.2, 20.6; **IR** (NaCl, neat): 3057, 2959, 2902, 2877, 1683, 1452, 1367, 1235, 1108, 1070, 792, 740 cm^{-1} ; **HRMS** (ESI-APCI) m/z calcd $[\text{C}_{13}\text{H}_{21}\text{O}_4]^+$ ($[\text{M} + \text{H}]^+$): 241.1434, found 241.1423.



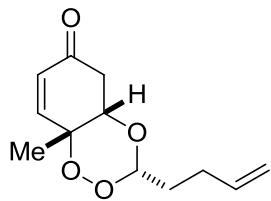
(3S,4aS,8aR)-3-cyclohexyl-8a-methyl-4a,5-dihydrobenzo[e][1,2,4]trioxin-

-6(8aH)-one (41d). Prepared according to the general procedure: 77% yield;

>20:1 dr; 98% ee; white solid; $R_f = 0.32$ (80:20 Hexanes:EtOAc); $[\alpha]_D^{20} = -$

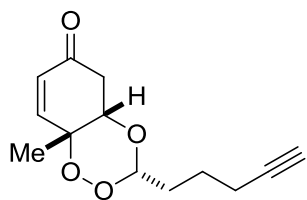
91.8, $c = 0.0073$ g/ml CH_2Cl_2 ; HPLC analysis: Chiralcel IA column, 97:3

Hexanes:*iso*-propanol, 1.0 ml/min, $\text{RT}_{\text{minor}} = 8.30$ min, $\text{RT}_{\text{major}} = 8.97$ min, 210 nm. $^1\text{H NMR}$ (400 MHz, CDCl_3): δ 6.83 (dd, $J = 10.4, 2.7$ Hz, 1H), 6.06 (d, $J = 10.4$ Hz, 1H), 5.01 d, $J = 5.4$ Hz, 1H), 4.13 (q, $J = 2.9$ Hz, 1H), 2.60-2.68, (m, 2H), 1.72-1.42 (m, 6H), 1.32 (s, 3H), 1.20-0.97 (m, 5H); $^{13}\text{C NMR}$ (100 MHz, CDCl_3): δ 195.2, 151.1, 129.5, 106.5, 77.8, 76.3, 41.0, 40.3, 26.83, 26.75, 26.1, 25.48, 25.47, 20.5; **IR** (NaCl, neat): 2932, 2855, 1684, 1450, 1230, 1115, 1065, 780 cm^{-1} ; **HRMS** (ESI-APCI) m/z calcd $[\text{C}_{14}\text{H}_{21}\text{O}_4]^+$ ($[\text{M} + \text{H}]^+$): 253.1434, found 253.1440.



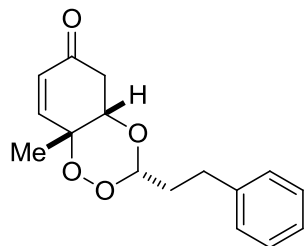
(3S,4aS,8aR)-3-(but-3-en-1-yl)-8a-methyltetrahydrobenzo[e][1,2,4]trioxin-6(7H)-one (41e). Prepared according to the general procedure:

95% yield; >20:1 dr; 97% ee; clear oil; $R_f = 0.40$ (67:33 Hexanes:EtOAc); $[\alpha]_D^{20} = -44.5$, $c = 0.0046$ g/ml CH_2Cl_2 ; HPLC analysis: Chiralcel IC column, 97:3 Hexanes:*iso*-propanol, 1.0 ml/min, $RT_{\text{minor}} = 15.27$ min, $RT_{\text{major}} = 20.12$ min, 210 nm. $^1\text{H NMR}$ (400 MHz, CDCl_3): δ 6.85 (dd, $J = 10.4, 2.8$ Hz, 1H), 6.08 (d, $J = 10.9$ Hz, 1H), 5.75 (dddd, $J = 16.9, 10.2, 6.6, 6.6$ Hz, 1H), 5.28, (t, $J = 5.3$ Hz, 1H), 5.05-4.95 (m, 2H), 4.17 (q, $J = 2.9$ Hz, 1H), 2.73-2.69 (m, 2H), 2.15-2.08 (m, 2H), 1.66-1.59, (m, 2H), 1.34, (s, 3H); $^{13}\text{C NMR}$ (100 MHz, CDCl_3): δ 194.9, 151.0, 137.1, 129.7, 115.4, 103.5, 77.8, 76.4, 41.0, 30.9, 27.5, 20.6; **IR** (NaCl, neat): 3077, 2980, 2934, 2886, 1684, 1642, 1387, 1112, 1063, 915, 782 cm^{-1} ; **HRMS** (ESI-APCI) m/z calcd $[\text{C}_{12}\text{H}_{19}\text{O}_4]^+$ ($[\text{M} + \text{H}]^+$): 225.1121, found 225.1124.



(3S,4aS,8aR)-8a-methyl-3-(pent-4-yn-1-yl)-4a,5-dihydrobenzo[e][1,2,4]trioxin-6(8aH)-one (41f). Prepared according to the general

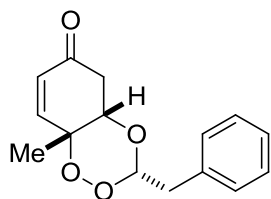
procedure: 83% yield; >20:1 dr; 97% ee; clear oil; $R_f = 0.38$ (67:33 Hexanes:EtOAc); $[\alpha]_D^{20} = -54.3$, $c = 0.0124$ g/ml CH_2Cl_2 ; HPLC analysis: Chiralcel IA column, 95:5 Hexanes:*iso*-propanol, 1.0 ml/min, $RT_{\text{minor}} = 17.52$ min, $RT_{\text{major}} = 25.04$ min, 210 nm. $^1\text{H NMR}$ (400 MHz, CDCl_3): δ 6.85 (dd, $J = 10.4, 2.8$ Hz, 1H), 6.08 (d, $J = 10.4$ Hz, 1H), 5.30 (dd, $J = 4.8, 4.8$ Hz, 1H), 4.17 (dd, $J = 5.9, 3.0$ Hz, 1H), 2.76-2.65 (m, 2H), 2.18 (ddd, $J = 7.0, 7.0, 2.7$ Hz, 2H), 1.94 (t, $J = 2.6$ Hz, 1H), 1.71-1.55 (m, 4H), 1.34 (s, 3H); $^{13}\text{C NMR}$ (100 MHz, CDCl_3): δ 194.8, 150.9, 129.7, 103.5, 83.5, 77.8, 76.4, 68.9, 40.9, 30.7, 22.3, 20.6, 18.1; **IR** (NaCl, neat): 3291, 2963, 2935, 2884, 2116, 1683, 1387, 1231, 1115, 783 cm^{-1} ; **HRMS** (ESI-APCI) m/z calcd $[\text{C}_{13}\text{H}_{17}\text{O}_4]^+$ ($[\text{M} + \text{H}]^+$): 237.1121, found 237.1110.



(3S,4aS,8aR)-8a-methyl-3-phenethyl-4a,5-dihydrobenzo[e][1,2,4]

trioxin-6 (8aH)-one (41g). Prepared according to the general procedure: % yield; 93% ee; white solid; $R_f = 0.21$ (80:20 hexanes:EtOAc); $[\alpha]_D^{20} = -92.4$, $c = 0.0093$ g/ml CH_2Cl_2 ; HPLC

analysis: Chiralcel IC column, 97:3 Hexanes:*iso*-propanol, 1.0 ml/min, $RT_{\text{minor}} = 21.64$ min, $RT_{\text{major}} = 32.11$ min, 210 nm. $^1\text{H NMR}$ (400 MHz, CDCl_3): δ 7.28-7.10 (m, 5 H), 6.84 (dd, $J = 2.7, 10.4$ Hz, 1H), 6.07 (d, $J = 10.4$ Hz, 1H), 5.22 (t, $J = 5.3$ Hz, 1H), 4.12 (q, $J = 2.9$ Hz, 1H), 2.71-2.62 (m, 4H), 1.86-1.78 (m, 2H), 1.30 (s, 3H); $^{13}\text{C NMR}$ (100 MHz, CDCl_3): δ 194.9, 151.0, 140.7, 129.6, 128.4, 128.3, 126.1, 103.1, 77.8, 76.3, 40.9, 33.1, 29.5, 20.5; **IR** (NaCl, neat): 3062, 3028, 2963, 2934, 2887, 1683, 1604, 1497, 1455, 1387, 1202, 1113, 898, 701 cm^{-1} ; **HRMS** (ESI-APCI) m/z calcd $[\text{C}_{16}\text{H}_{19}\text{O}_4]^+$ ($[\text{M} + \text{H}]^+$): calcd 275.1287, found 275.1275.

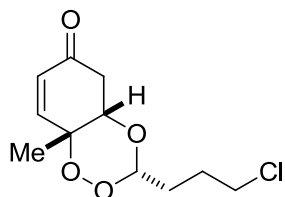


(3S,4aS,8aR)-3-benzyl-8a-methyl-4a,5-dihydrobenzo[e][1,2,4]trioxin-

6(8aH)-one (41h). Prepared according to the general procedure: 83% yield; >20:1 dr; 90% ee; white solid; $R_f = 0.20$ (80:20 Hexanes:EtOAc);

$[\alpha]_D^{20} = -125.0$, $c = 0.0075$ g/ml CH_2Cl_2 ; HPLC analysis: Chiralcel OC column, 80:20 Hexanes:*iso*-propanol, 1.0 ml/min, $RT_{\text{minor}} = 8.14$ min, $RT_{\text{major}} = 9.53$ min, 210 nm. $^1\text{H NMR}$ (400 MHz, CDCl_3): δ 7.29-7.14, (m, 5H), 6.84 (dd, $J = 10.4, 2.7$ Hz, 1H), 6.07 (d, $J = 10.4$ Hz, 1H), 5.41 (d, $J = 5.4$ Hz, 1H), 4.14 (d, $J = 2.9$ Hz, 1H), 2.81 (d, $J = 5.4$ Hz, 2H), 2.68, (dd, $J = 5.4, 3.0$ Hz, 2H), 1.31, (s, 3H); $^{13}\text{C NMR}$ (100 MHz, CDCl_3): δ 194.9, 150.8, 134.6, 129.68, 129.58 (2C), 128.3 (2C), 126.8, 104.3, 77.8, 76.5, 40.9, 38.5, 20.5; **IR** (NaCl, neat): 3063, 3032,

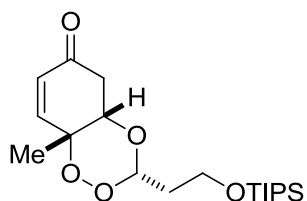
2982, 2888, 1684, 1497, 1455, 1385, 1350, 1281, 1173, 1110, 897, 700 cm^{-1} ; **HRMS** (ESI-APCI) m/z calcd $[\text{C}_{15}\text{H}_{17}\text{O}_4]^+$ ($[\text{M} + \text{H}]^+$): 261.1121, found 261.1119.



(3S,4aS,8aR)-3-(3-chloropropyl)-8a-methyl-4a,5-dihydrobenzo[e]

[1,2,4] trioxin-6(8aH)-one (41i). Prepared according to the general

procedure: 97% yield; >20:1 dr; 97% ee; clear oil; $R_f = 0.36$ (67:33 Hexanes:EtOAc); $[\alpha]_D^{20} = -91.0$, $c = 0.0208$ g/ml CH_2Cl_2 ; HPLC analysis: Chiralcel IA column, 97:3 Hexanes:iso-propanol, 1.0 ml/min, $\text{RT}_{\text{minor}} = 18.97$ min, $\text{RT}_{\text{major}} = 20.00$ min, 210 nm. **^1H NMR** (400 MHz, CDCl_3): δ 6.85 (dd, $J = 10.4, 2.8$ Hz, 1H), 6.08 (d, $J = 10.4$ Hz, 1H), 5.31 (t, $J = 5.1$ Hz, 1H), 4.18 (q, $J = 2.9$ Hz, 1H), 3.50 (t, $J = 6.4$ Hz, 2H), 2.70 (d, $J = 3.0$ Hz, 2H), 1.88-1.80 (m, 2H), 1.74-1.68 (m, 2H), 1.34 (s, 3H); **^{13}C NMR** (100 MHz, CDCl_3): δ 194.8, 150.8, 129.7, 103.1, 77.8, 76.4, 44.4, 40.9, 29.1, 26.3, 20.5; **IR** (NaCl, neat): 3040, 2966, 2935, 2886, 1683, 1445, 1386, 1231, 1150, 1083, 783 cm^{-1} ; **HRMS** (ESI-APCI) m/z calcd $[\text{C}_{11}\text{H}_{17}\text{O}_4\text{Cl}]^+$ ($[\text{M} + \text{H}]^+$): 247.0732, found 247.0734.

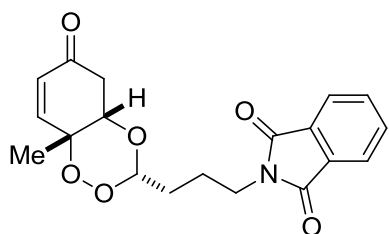


(3S,4aS,8aR)-8a-methyl-3-(2-((triisopropylsilyl)oxy)ethyl)-4a,5-

dihydro benzo[e][1,2,4]trioxin-6(8aH)-one (41j). Prepared according

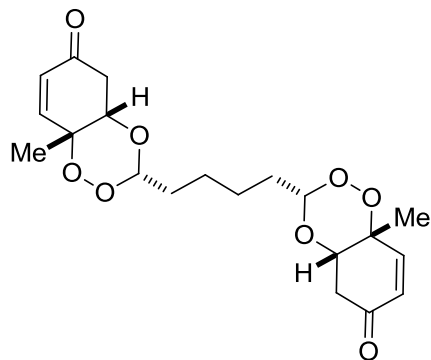
to the general procedure: 71% yield; >20:1 dr; 94% ee; clear oil; $R_f = 0.25$ (80:20 Hexanes:EtOAc); $[\alpha]_D^{20} = -92.4$, $c = 0.0091$ g/ml CH_2Cl_2 ; HPLC analysis: Chiralcel IA column, 97:3 Hexanes:iso-propanol, 1.0 ml/min, $\text{RT}_{\text{minor}} = 10.01$ min, $\text{RT}_{\text{major}} = 14.93$ min, 210 nm. **^1H NMR** (400 MHz, CDCl_3): δ 6.86 (dd, $J = 10.4, 2.7$ Hz, 1H), 6.08 (d, $J = 10.4$ Hz, 1H), 5.48 (t, $J = 5.4$ Hz, 1H), 4.16 (q, $J = 2.9$ Hz, 1H), 3.83-3.69 (m, 2H), 2.71 (d, $J = 2.9$ Hz, 2H), 1.83-1.74 (m, 1H), 1.73-1.64 (m, 1H), 1.35 (s, 3H), 1.13-1.01 (m, 19H); **^{13}C NMR** (100

MHz, CDCl₃): δ 195.0, 151.1, 129.7, 101.9, 77.9, 76.4, 58.0, 41.0, 35.0, 20.6, 17.95 (3C), 17.93 (3C), 11.9 (3C); **IR** (NaCl, neat): 2943, 2867, 1686, 1463, 1385, 1230, 1108, 1071, 883, 681 cm⁻¹; **HRMS** (ESI-APCI) m/z calcd [C₁₉H₃₅O₅Si]⁺ ([M + H]⁺): 371.2248, found 371.2250.



2-(3-((3S,4aS,8aR)-8a-methyl-6-oxo-4a,5,6,8a-tetrahydrobenzo[e][1,2,4]trioxin-3-yl)propyl)isoindoline-1,3-dione (41k). Prepared according to the general procedure: 81% yield; >20:1 dr, 98% ee; white solid; R_f = 0.16 (67:33

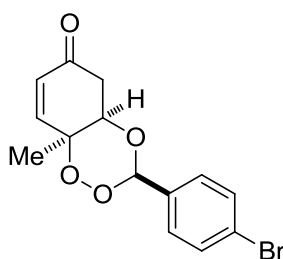
Hexanes:EtOAc); $[\alpha]_D^{20}$ = -103.0, c = 0.0026 g/ml CH₂Cl₂; HPLC analysis: Chiralcel IC column, 70:30 Hexanes:*iso*-propanol, 1.0 ml/min, RT_{minor} = 27.10 min, RT_{major} = 28.20 min, 210 nm. **¹H NMR** (400 MHz, CDCl₃): δ 7.83-7.78 (m, 2H), 7.72-7.66 (m, 2H), 6.83 (dd, J = 10.4, 2.8 Hz, 1H), 6.06 (d, J = 10.4 Hz, 1H), 5.30 (t, J = 5.1 Hz, 1H), 4.16 (q, J = 2.9 Hz, 1H), 3.64 (t, J = 7.2 Hz, 2H), 2.67 (d, J = 2.8 Hz, 2H), 1.79-1.70, (m, 2H), 1.62-1.55 (m, 2H), 1.32 (s 3H); **¹³C NMR** (100 MHz, CDCl₃): δ 194.7, 168.2 (2C), 150.8, 133.9 (2C), 132.0 (2C), 129.7, 123.2 (2C), 103.2, 77.8, 76.3, 40.8, 37.4, 29.1, 22.6, 20.5; **IR** (NaCl, neat): 3061, 2937, 2884, 1772, 1716, 1615, 1398, 1049, 721 cm⁻¹; **HRMS** (ESI-APCI) m/z calcd [C₁₉H₁₉NO₆Na]⁺ ([M + Na]⁺): 380.1105, found 380.1102.



(3S,3'S,4aS,4a'S,8aR,8a'R)-3,3'-(butane-1,4-diyl)bis(8a-methyl-4a,5-dihydrobenzo[e][1,2,4]trioxin-6(8aH)-one (41l). Prepared according to the general procedure: 79% yield; 96% ee; clear oil; R_f = 0.15 (60:40 hexanes:ethyl acetate); $[\alpha]_D^{20}$ = -117.8, c = 0.0026 g/ml CH₂Cl₂; HPLC

analysis: Chiralcel IA column, 60:40 Hexanes:*iso*-propanol, 1.0 ml/min, RT_{minor} = 8.26 min,

RT_{major} = 9.95 min, 210 nm. ¹H NMR (400 MHz, CDCl₃): δ 6.84 (dd, *J* = 2.7, 10.4 Hz, 2H), 6.07 (d, *J* = 10.4 Hz, 2H), 5.23 (t, *J* = 5.2 Hz, 2H), 4.15 (q, *J* = 2.9 Hz, 2H), 2.69 (d, *J* = 3.1 Hz, 4H), 1.53-1.45 (m, 4H), 1.37-1.30 (m, 4H), 1.33 (s, 6H); ¹³C NMR (100 MHz, CDCl₃): δ 194.9, 151.0, 129.6, 103.9, 77.8, 76.3, 41.0, 31.5, 23.1, 20.6; IR (NaCl, neat): 3056, 2949, 2877, 1683, 1463, 1387, 1232, 1144, 1036, 780, 733 cm⁻¹; HRMS (ESI-APCI) *m/z* calcd [C₂₀H₂₇O₈]⁺ ([M + H]⁺): calcd 395.1700, found 395.1697.



(3R,4aR,8aS)-3-(4-bromophenyl)-8a-methyl-4a,5-dihydrobenzo

[e][1,2,4] trioxin-6(8aH)-one (41m). Prepared according to the general

procedure: 66% yield; 91% ee; white solid; R_f = 0.1 (80:20

hexanes:EtOAc); [α]_D²⁰ = +113.7, c = 0.0097 g/ml CH₂Cl₂; HPLC

analysis: Chiralcel IA column, 97:3 Hexanes:*iso*-propanol, 1.0 ml/min, RT_{minor} = 26.89 min,

RT_{major} = 31.31 min, 210 nm. ¹H NMR (400 MHz, CDCl₃): δ 7.41 (d, *J* = Hz, 2H), 7.20 (dd, *J* =

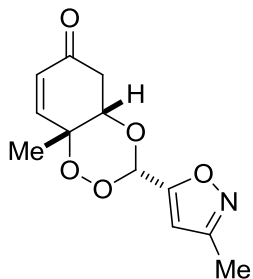
Hz, 2H), 6.85 (dd, *J* = 2.8, 10.4 Hz, 1H), 6.11 (s, 1H), 6.08 (dd, *J* = 0.9, 10.4 Hz, 1H), 4.32 (q, *J*

= 3.0 Hz, 1H), 2.77 (ddd, *J* = 0.9, 3.0, 17.5 Hz, 1H), 2.71 (dd, *J* = 3.1, 17.5 Hz, 1H), 1.36 (s, 3H);

¹³C NMR (100 MHz, CDCl₃): δ 194.6, 150.7, 132.4, 131.7, 129.8, 128.7, 124.5, 102.8, 78.0,

77.0, 40.9, 20.6; IR (NaCl, neat): cm⁻¹; HRMS (ESI-APCI) *m/z* calcd [C₁₄H₁₄O₄Br]⁺ ([M + H]⁺):

calcd 325.0070, found 325.0084.



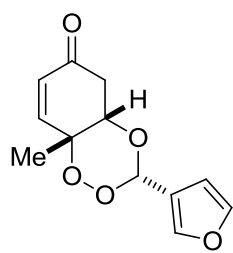
(3S,4aS,8aR)-8a-methyl-3-(3-methylisoxazol-5-yl)-4a,5-dihydrobenzo

[e][1,2,4]trioxin-6(8aH)-one (41n). Prepared according to the general

procedure: 53% yield; 91% ee; white solid; R_f = 0.21 (67:33

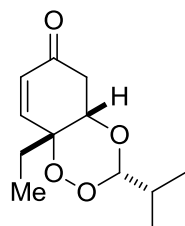
hexanes:EtOAc); [α]_D²⁰ = -84.0, c = 0.0054 g/ml CH₂Cl₂; HPLC analysis:

Chiralcel IA column, 90:10 Hexanes:*iso*-propanol, 1.0 ml/min, $RT_{\text{minor}} = 14.23$ min, $RT_{\text{major}} = 15.84$ min, 210 nm. $^1\text{H NMR}$ (400 MHz, CDCl_3): δ 6.91 (dd, $J = 2.8, 10.4$ Hz, 1H), 6.37 (s, 1H), 6.13 (d, $J = 10.4$ Hz, 1H), 5.98 (s, 1H) 4.39 (q, $J = 2.9$ Hz, 1H), 2.79-2.76 (m, 2H), 2.39 (s, 3H), 1.42 (s, 3H); $^{13}\text{C NMR}$ (100 MHz, CDCl_3): δ 194.2, 170.4, 158.1, 129.8, 99.8, 97.6, 40.7, 20.6, 12.2; **IR** (NaCl, neat): 3142, 2983, 2903, 1682, 1604, 1496, 1347, 1232, 1173, 1087, 1041, 900, cm^{-1} ; **HRMS** (ESI-APCI) m/z calcd $[\text{C}_{12}\text{H}_{14}\text{NO}_5]^+$ ($[\text{M} + \text{H}]^+$): calcd 252.0866, found 252.0866.



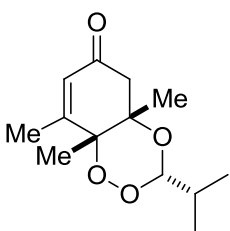
(3S,4aS,8aR)-3-(furan-3-yl)-8a-methyl-4a,5-dihydrobenzo[e][1,2,4]trioxin-6(8aH)-one (41o). Prepared according to the general procedure: 45% yield; 91% ee; clear oil; $R_f = 0.36$ (60:40 hexanes:EtOAc); $[\alpha]_{\text{D}}^{20} = -102.3$, $c = 0.0046$ g/ml CH_2Cl_2 ; HPLC analysis: Chiralcel IA column, 90:10

Hexanes:*iso*-propanol, 1.0 ml/min, $RT_{\text{minor}} = 12.2$ min, $RT_{\text{major}} = 14.1$ min, 210 nm. $^1\text{H NMR}$ (400 MHz, CDCl_3): δ 7.53-7.51 (m, 1H), 7.37 (t, $J = 1.7$ Hz, 1H), 6.91 (dd, $J = 2.8, 10.4$ Hz, 1H), 6.40-6.38 (m, 1H), 6.23 (s, 1H), 6.14 (dd, $J = 0.8, 10.4$ Hz, 1H), 4.35 (q, $J = 3.0$ Hz, 1H), 2.82 (ddd, $J = 0.8, 3.0, 17.5$ Hz, 1H), 2.76 (dd, $J = 3.0, 17.5$ Hz, 1H), 1.41 (s, 3H); $^{13}\text{C NMR}$ (100 MHz, CDCl_3): δ 194.6, 150.8, 141.9, 129.8, 119.7, 108.4, 99.83, 78.0, 76.8, 40.9, 20.6; **IR** (NaCl, neat): 3148, 2892, 1681, 1604, 1504, 1344, 1160, 1064, 986, 876, 811 cm^{-1} ; **HRMS** (ESI-APCI) m/z calcd $[\text{C}_x\text{H}_x\text{O}_x]^+$ ($[\text{M} + \text{H}]^+$): calcd 237.0757, found 237.0753.



(3S,4aS,8aR)-8a-ethyl-3-isopropyl-4a,5-dihydrobenzo[e][1,2,4]trioxin-6(8aH)-one (43a). Prepared according to the general procedure: 79% yield; >20:1 dr; 96% ee; clear oil; $R_f = 0.36$ (80:20 Hexanes:EtOAc); $[\alpha]_{\text{D}}^{20} = -57.7$, $c = 0.0034$ g/ml CH_2Cl_2 ; HPLC analysis: Chiralcel IA column, 99:1 Hexanes:*iso*-

propanol, 1.0 ml/min, $RT_{\text{minor}} = 13.10$ min, $RT_{\text{major}} = 15.71$ min, 210 nm. $^1\text{H NMR}$ (400 MHz, CDCl_3): δ 6.90 (dd, $J = 10.5, 2.7$ Hz, 1H), 6.10 (d, $J = 10.5$ Hz, 1H), 4.98 (d, $J = 5.4$ Hz, 1H), 4.20 (q, $J = 3$ Hz, 1H), 2.69 (d, $J = 3$ Hz, 2H), 1.63-1.88 (m, 3H), 1.00 (t, $J = 7.5$ Hz, 3H), 0.88 (d, $J = 6.9$ Hz, 6H); $^{13}\text{C NMR}$ (100 MHz, CDCl_3): δ 195.2, 150.7, 129.9, 107.0, 79.8, 75.2, 40.8, 30.9, 28.6, 16.64, 16.62, 7.1; **IR** (NaCl, neat): 2972, 2941, 2881, 1689, 1463, 1389, 1194, 1159, 957, 665 cm^{-1} ; **HRMS** (ESI-APCI) m/z calcd $[\text{C}_{12}\text{H}_{19}\text{O}_4]^+$ ($[\text{M} + \text{H}]^+$): 227.1278, found 227.1275.



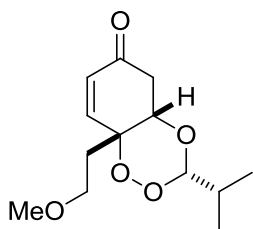
(3S,4aS,8aR)-3-isopropyl-4a,8,8a-trimethyl-4a,5-dihydrobenzo[e]

[1,2,4] trioxin-6(8aH)-one (43b). Prepared according to the general

procedure: 63% yield; 90% ee; white solid; $R_f = 0.50$ (67:33

Hexanes:EtOAc); $[\alpha]_D^{20} = -67.6$, $c = 0.0011$ g/ml CH_2Cl_2 ; HPLC analysis:

Chiralcel IC column, 97:3 Hexanes:*iso*-propanol, 1.0 ml/min, $RT_{\text{minor}} = 17.59$ min, $RT_{\text{major}} = 21.30$ min, 210 nm. $^1\text{H NMR}$ (400 MHz, CDCl_3): δ 5.94-5.92 (m, 1H), 5.21 (d, $J = 4.5$ Hz, 1H), 2.61 (d, $J = 17.1$ Hz, 1H), 2.50 (d, $J = 17.0$ Hz, 1H), 2.04 (s, 3H), 1.77-1.60 (m, 1H), 1.44, (s, 3H), 1.20, (s, 3H) 0.81 (dd, $J = 1.1, 6.9$ Hz, 6H); $^{13}\text{C NMR}$ (100 MHz, CDCl_3): δ 195.1, 161.7, 127.8, 101.4, 82.3, 75.6, 48.0, 30.9, 19.0, 18.29, 18.27, 16.39, 16.28; **IR** (NaCl, neat): 2968, 2933, 2880, 1677, 1460, 1393, 1282, 1081, 957 cm^{-1} ; **HRMS** (ESI-APCI) m/z calcd $[\text{C}_{13}\text{H}_{21}\text{O}_4]^+$ ($[\text{M} + \text{H}]^+$): 241.1434, found 241.1434.

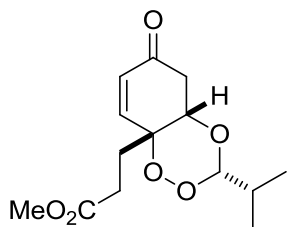


(3S,4aS,8aR)-3-isopropyl-8a-(2-methoxyethyl)-4a,5-dihydrobenzo[e]

[1,2,4] trioxin-6(8aH)-one (43c). Prepared according to the general

procedure: 66% yield; >20:1 dr; 96% ee; clear oil; $R_f = 0.21$ (67:33

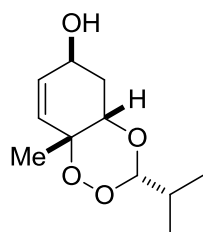
Hexanes:EtOAc); $[\alpha]_D^{20} = -86.2$, $c = 0.0021$ g/ml CH_2Cl_2 ; HPLC analysis: Chiralcel IA column, 95:5 Hexanes:*iso*-propanol, 1.0 ml/min, $\text{RT}_{\text{minor}} = 7.78$ min, $\text{RT}_{\text{major}} = 12.69$ min, 210 nm. **^1H NMR** (400 MHz, CDCl_3): δ 6.85 (dd, $J = 10.4, 2.8$ Hz, 1H), 6.05 (dd, $J = 10.4$ Hz, 0.9 Hz 1H), 4.97 (d, $J = 5.1$ Hz, 1H), 4.27 (q, $J = 2.9$ Hz, 1H), 3.50 (ddd, $J = 5.6, 6.9, 9.8$ Hz, 1H), 3.43 (ddd, $J = 5.6, 6.6, 9.8$ Hz, 1H), 3.28 (s, 3H), 2.75 (dd, $J = 3.0, 17.6$ Hz, 1H), 2.65 (ddd, $J = 1.0, 3.0, 17.6$ Hz, 2H), 1.99 (ddd, $J = 5.6, 6.6, 15.0$ Hz, 1H) 1.88 (ddd, $J = 5.6, 6.8, 15.0$ Hz, 1H), 1.80-1.76 (m, 1H), 0.86 (d, $J = 7.0$ Hz, 6H); **^{13}C NMR** (100 MHz, CDCl_3): δ ; **IR** (NaCl, neat): 2968, 2929, 2879, 1687, 1473, 1392, 1191, 1116, 1082, 1015, 772 cm^{-1} ; **HRMS** (ESI-APCI) m/z calcd $[\text{C}_{13}\text{H}_{21}\text{O}_5]^+$ ($[\text{M} + \text{H}]^+$): 257.1384, found 257.1357.



methyl-3-((3S,4aS,8aR)-3-isopropyl-6-oxo-4a,5,6,8a-tetrahydrobenzo[e][1,2,4]trioxin-8a-yl)propanoate (43d). Prepared according to the general procedure: 67% yield; 95% ee; clear oil; $R_f = 0.40$ (67:33 Hexanes:EtOAc); $[\alpha]_D^{20} = -104.0$, $c = 0.0037$ g/ml CH_2Cl_2 ;

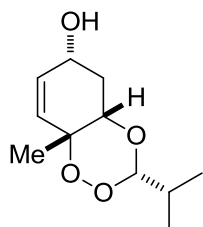
HPLC analysis: Chiralcel IA column, 80:20 Hexanes:*iso*-propanol, 1.0 ml/min, $\text{RT}_{\text{minor}} = 7.38$ min, $\text{RT}_{\text{major}} = 13.80$ min, 210 nm. **^1H NMR** (400 MHz, CDCl_3): δ 6.83 (dd, $J = 10.5, 2.8$ Hz, 1H), 6.09 (d, $J = 10.5$ Hz, 1H), 4.97 (d, $J = 5.1$ Hz, 1H), 4.16 (d, $J = 2.9$ Hz, 1H), 3.66 (s, 3H), 2.75 (dd, $J = 17.7, 3.1$ Hz, 1H), 2.68 (dd, $J = 17.7, 3.0$ Hz, 1H), 2.52 (ddd, $J = 6.2, 9.9, 16.4$ Hz, 1H), 2.40 (ddd, $J = 6.1, 9.9, 16.1$ Hz, 1H), 2.10 (ddd, $J = 6.0, 9.9, 14.8$ Hz, 1H), 2.00 (ddd, $J = 6.2, 9.9, 14.8$ Hz, 1H), 1.80-1.67 (m, 1H), 0.86 (d, $J = 6.9$ Hz, 6H); **^{13}C NMR** (100 MHz, CDCl_3): δ 194.7, 172.7, 149.1, 130.5, 107.0, 78.8, 75.1, 51.9, 40.7, 30.8, 27.1, 16.59, 16.51; **IR** (NaCl, neat): 2969, 2880, 1738, 1688, 1439, 1260, 1175, 1083, 1016, 794 cm^{-1} ; **HRMS** (ESI-APCI) m/z calcd $[\text{C}_{14}\text{H}_{21}\text{O}_6]^+$ ($[\text{M} + \text{H}]^+$): 285.1333, found 285.1318.

Trioxane Derivatives.



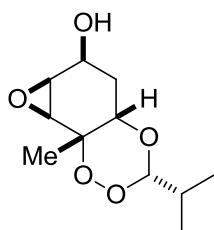
3-isopropyl-8a-methyl-4a,5,6,8a-tetrahydrobenzo[e][1,2,4]trioxin-6-ol (**48**).

Trioxane **16** (233 mg, 1.1 mmol, 1 eq) was added to a solution of $\text{CeCl}_3 \cdot (\text{H}_2\text{O})_7$ (450 mg, 1.2 mmol 1.1 eq) in 3.5 mL of methanol (0.3M). After the mixture was cooled to 0 °C, NaBH_4 was added portionwise. The reaction was stirred at 0 °C for 1 h and then for an 1 h at room temperature. The reaction was quenched with sat. NH_4Cl and the aqueous layer was extracted using EtOAc. The organic extracts were dried with MgSO_4 and concentrated *in vacuo*. Column chromatography on SiO_2 with 25% (hexanes:ethyl acetate) of the residue gave analytically pure **9s** as a clear oil. 96% yield; 4:1 dr; clear oil; R_f (major) = 0.29 (67:33 Hexanes:EtOAc); $^1\text{H NMR}$ (400 MHz, CDCl_3): δ 5.87 (dt, $J = 1.9, 10.4$ Hz, 1H), 5.70 (dt $J = 2.2, 10.4$ Hz, 1H), 4.94 (d, $J = 4.9$ Hz, 1H), 4.53 (ddt, $J = 2.1, 5.9, 8.1$ Hz, 1H), 3.9 (dt, $J = 1.9, 4.2$ Hz, 1H), 2.43 (dddd, $J = 1.7, 4.4, 6.0, 13.5$ Hz, 1H), 1.81-1.70 (m, 2H), 1.63 (bs, 1H), 1.19 (s, 3H), 0.90 (dd, $J = 1.9, 6.9$ Hz, 6H); $^{13}\text{C NMR}$ (100 MHz, CDCl_3): δ 133.0, 131.1, 106.4, 77.2 75.8, 64.7, 36.1, 31.0, 22.5, 16.70, 16.68; **IR** (NaCl, neat): 3364, 3030, 2968, 2936, 2877, 1471, 1395, 1171, 1079, 896 cm^{-1} ; **HRMS** (ESI-APCI) m/z calcd $[\text{C}_{12}\text{H}_{21}\text{O}_4]^+$ 229.1434 ($[\text{M} - \text{OH} + \text{HOCH}_3]^+$): 229.1434, found 229.1428.

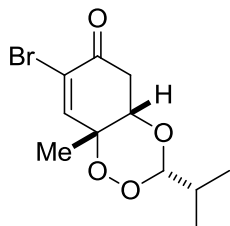


R_f (minor) = 0.51 (67:33 Hexanes:EtOAc); $^1\text{H NMR}$ (400 MHz, CDCl_3): δ 6.03 (ddd, $J = 1.7, 4.7, 10.2$ Hz, 1H), 5.75 (dd, $J = 1.7, 10.2$ Hz, 1H), 4.93 (d, $J = 5.2$ Hz, 1H), 4.04-3.97 (bm, 1H), 3.99 (dt, $J = 2.0, 4.0$ Hz, 1H), 2.96 (bd, $J = 10.2$ Hz, 1H), 2.28 (ddt, $J = 1.6, 3.9, 15.3$ Hz, 1H), 2.06 (ddd, $J = 1.9, 5.2, 15.3$ Hz, 1H), 1.86-1.73 (m, 1H), 1.10 (s, 3H), 0.92 (d, $J = 6.9$ Hz, 6H); $^{13}\text{C NMR}$ (100 MHz,

CDCl₃): δ 131.5, 130.8, 107.3, 77.8, 75.2, 62.4, 32.9, 30.9, 21.4, 17.00, 16.92; **IR** (NaCl, neat): 3557, 3033, 2970, 2935, 2879, 1472, 1409, 1369, 1171, 1073, 895, 809 cm⁻¹; **HRMS** (ESI-APCI) *m/z* calcd [C₁₂H₂₁O₄]⁺ 229.1434 ([M – OH + HOCH₃]⁺): 229.1434, found 229.1429.

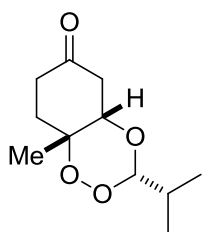


3-isopropyl-7b-methylhexahydrooxireno[2',3':3,4]benzo[1,2-e][1,2,4]trioxin-6-ol (49). To a solution of **48** (43 mg, 0.2 mmol, 1 eq) dissolved in 2 mL of dichloromethane (0.1M) at 0 °C was added *m*-chloroperoxybenzoic (92 mg, (75% pure), 0.4 mmol, 2 eq) The reaction was stirred at 0 °C for 1 hour and then allowed to stir at room temperature for 4 hours. The reaction mixture was concentrated *in vacuo* and purified using column chromatography on SiO₂ with 20% (hexanes:ethyl acetate) to afford analytically pure **9** as a white solid.: 91% yield; white solid; R_f = 0.27 (67:33 Hexanes:EtOAc); **¹H NMR** (400 MHz, CDCl₃): δ 4.92 (d, *J* = 4.7 Hz, 1H), 4.41 (ddd, *J* = 1.2, 5.9, 10.4 Hz, 1H), 3.64 (d, *J* = 5.3 Hz, 1H), 3.49-3.46 (m, 2H), 2.11 (dt, *J* = 5.7, 13.6 Hz, 1H), 1.85-1.74 (m, 1H), 1.71 (s, 1H), 1.39 (ddd, *J* = 1.1, 10.4, 13.6 Hz, 1H), 1.21 (s, 3H), 0.92 (d, *J* = 6.9 Hz, 6H) ; **¹³C NMR** (100 MHz, CDCl₃): δ 106.0, 75.6, 74.8, 65.2, 59.3, 55.9, 31.1, 29.6, 18.3, 16.62, 16.47; **IR** (NaCl, neat): 3407, 2970, 2939, 2878, 1462, 1396, 1268, 1184, 1089, 1001, 939, 874, 820, 672 cm⁻¹; **HRMS** (ESI-APCI) *m/z* calcd [C₁₁H₂₂NO₅]⁺ ([M + NH₄]⁺): calcd 248.1492, found 248.1438.



7-bromo-3-isopropyl-8a-methyl-4a,5-dihydrobenzo[e][1,2,4]trioxin-6-one (51). To a solution of **16** (238 mg, 1.12 mmol, 1 eq) in 8 mL CCl₄ (0.14M) at 0 °C was added Br₂ (75 μL, 1.46 mmol, 1.3 eq). The reaction was allowed to stir for 30 minutes at 0 °C and then 0.5 mL of NEt₃

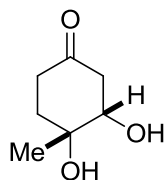
was added and the reaction was warmed to room temperature. The reaction mixture was concentrated *in vacuo* and purified using column chromatography on SiO₂ with 15% (hexanes:ethyl acetate) to afford analytically pure **10** as an off white solid (245 mg, 0.84 mmol). 75% yield; off white solid; Note: The dibromide intermediate can be isolated in 4:1 dr if no NEt₃ is added. R_f = 0.28 (80:20 Hexanes:EtOAc); ¹H NMR (400 MHz, CDCl₃): δ 7.29 (d, *J* = 2.6 Hz, 1H), 5.01 (d, *J* = 5.1 Hz, 1H), 4.17 (q, *J* = 2.9 Hz, 1H), 2.95 (dd, *J* = 3.1, 17.3 Hz, 1H), 2.78 (dd, *J* = 2.9, 17.3 Hz, 1H), 1.84-1.71 (m, 1H), 1.37 (s, 3H), 0.88 (dd, *J* = 1.6, 7.0 Hz, 6H); ¹³C NMR (100 MHz, CDCl₃): δ 187.2, 151.2, 123.7, 107.1, 79.6, 76.0, 40.5, 30.8, 20.2, 16.65, 16.50; IR (NaCl, neat): 3047, 2971, 2935, 2880, 1702, 1612, 1472, 1268, 1082, 1032, 968, 796, 687 cm⁻¹; HRMS (ESI-APCI) *m/z* calcd [C₁₁H₁₉NO₄Br]⁺ ([M + NH₄]⁺): calcd 308.0492, found 310.0484.



3-isopropyl-8a-methyltetrahydrobenzo[e][1,2,4]trioxin-6(7H)-one(45).

Trioxane **16** (51.4 mg, 0.242 mmol, 1 eq), 5% Rh/Al₂O₃ (25 mg, 0.012 mmol, 0.05 eq) and PtO₂ (2.7 mg, 0.012, 0.05 eq) were placed in a round bottom flask and dissolved in 2.5 mL of ethyl acetate (0.1M). A balloon of H₂ was placed on the reaction vessel and it was stirred at room temperature for 1 h. The crude mixture was filtered through a plug of Celite and concentrated *in vacuo*. Column chromatography on SiO₂ with 15% (hexanes:ethyl acetate) of the residue gave analytically pure **11** as a clear oil. Note: If the reaction is left longer the trioxane will reduce to **12**. : 81% yield; clear oil; R_f = 0.50 (67:33 Hexanes:EtOAc); ¹H NMR (400 MHz, CDCl₃): δ 4.93 (d, *J* = 5.0 Hz), 3.96-3.93 (m, 1H), 3.00, (td, *J* = 5.8, 13.6 Hz, 1H), 2.64 (dd, *J* = 3.8, 15.9 Hz, 1H), 2.57-2.36 (m, 3H), 1.88-1.75 (m, 1H), 1.36 (s, 3H), 0.93 (d, *J* = Hz, 6H); ¹³C NMR (100 MHz, CDCl₃): δ 206.8, 107.9, 78.56, 78.24, 43.6, 37.7, 30.9, 28.1, 19.8, 16.72, 16.60; IR (NaCl, neat): 2970,

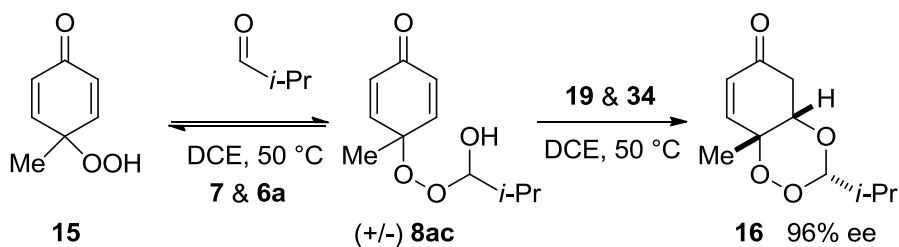
2879, 1717, 1472, 1219, 1144, 1079, 954 cm^{-1} ; **HRMS** (ESI-APCI) m/z calcd $[\text{C}_{11}\text{H}_{19}\text{O}_4]^+$ ($[\text{M} + \text{H}]^+$): 229.1434, found 229.1434.



3,4-dihydroxy-4-methylcyclohexanone (47). To a solution of **45** (12.8 mg, 0.06 mmol, 1 eq) dissolved in 0.3 mL of acetic acid (0.2M), was added zinc dust (19.5 mg, 0.299 mmol, 5 eq). The solution was stirred for 6 h and then filtered through

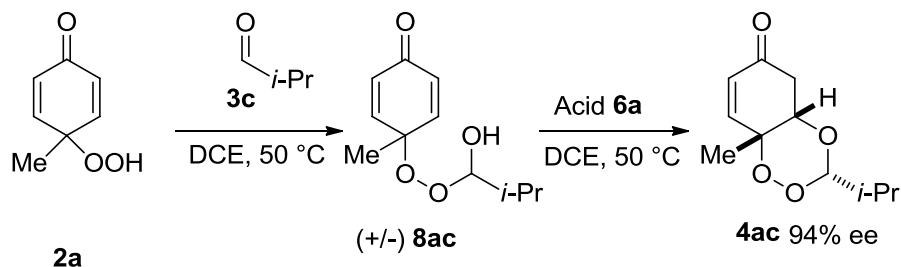
a pad of SiO_2 to afford the product as a clear oil in 75% yield. Notes: The reaction proceeds by reducing **11** to the dioxolane which is cleaved under acidic conditions to afford the diol. If **4ac** is reacted under these conditions then *p*-cresol is the only product. 85% yield; clear oil; $R_f = 0.20$ (50:50 Hexanes:EtOAc); $^1\text{H NMR}$ (400 MHz, CDCl_3): δ 3.74 (dd, $J = 14.7, 3.8$ Hz, 1H), 2.70-2.53 (m, 2H), 2.56, (dd, $J = 1.8, 5.7$ Hz, 1H), 2.30-1.95 (bs, 2H), 2.25 (dddd, $J = 14.7, 4.9, 4.9, 1.8$ Hz, 1H), 2.11 (ddd, $J = 14.0, 4.9, 1.2$ Hz, 1H), 1.66 (dddd, $J = 16.7, 14.0, 11.6, 5.1$ Hz, 1H), 1.40 (s, 3H); $^{13}\text{C NMR}$ (100 MHz, CDCl_3): δ 209.0, 74.5, 70.4, 46.0, 36.9, 33.9, 25.6; **IR** (NaCl, neat): 3414, 2970, 2933, 1709, 1417, 1260, 1129, 1066, 921cm^{-1} ; **HRMS** (ESI-APCI) m/z calcd $[\text{C}_7\text{H}_9\text{O}_2]^-$ ($[\text{M} - \text{H}]^-$): calcd 125.0608, found 125.0607.

Mechanistic Studies



The above reaction was carried out using the general procedure and it was monitored by chiral HPLC by taking aliquots from the reaction at 5 min, 1h, 6h, and 12 h. The ee of **8ac** was always 0% and the ee for **4ac** was 96% throughout the course of the reaction.

HPLC analysis: Chiralcel IC column, 90:10 Hexanes:*iso*-propanol, 1.0 ml/min, 210nm. **4ac** (96% ee) $RT_{\text{minor}} = 8.33$ min, $RT_{\text{major}} = 9.31$ min, **8ac** (0% ee) $RT = 10.11$ min, $RT = 11.69$ min, **2a** $RT = 20.00$ min.

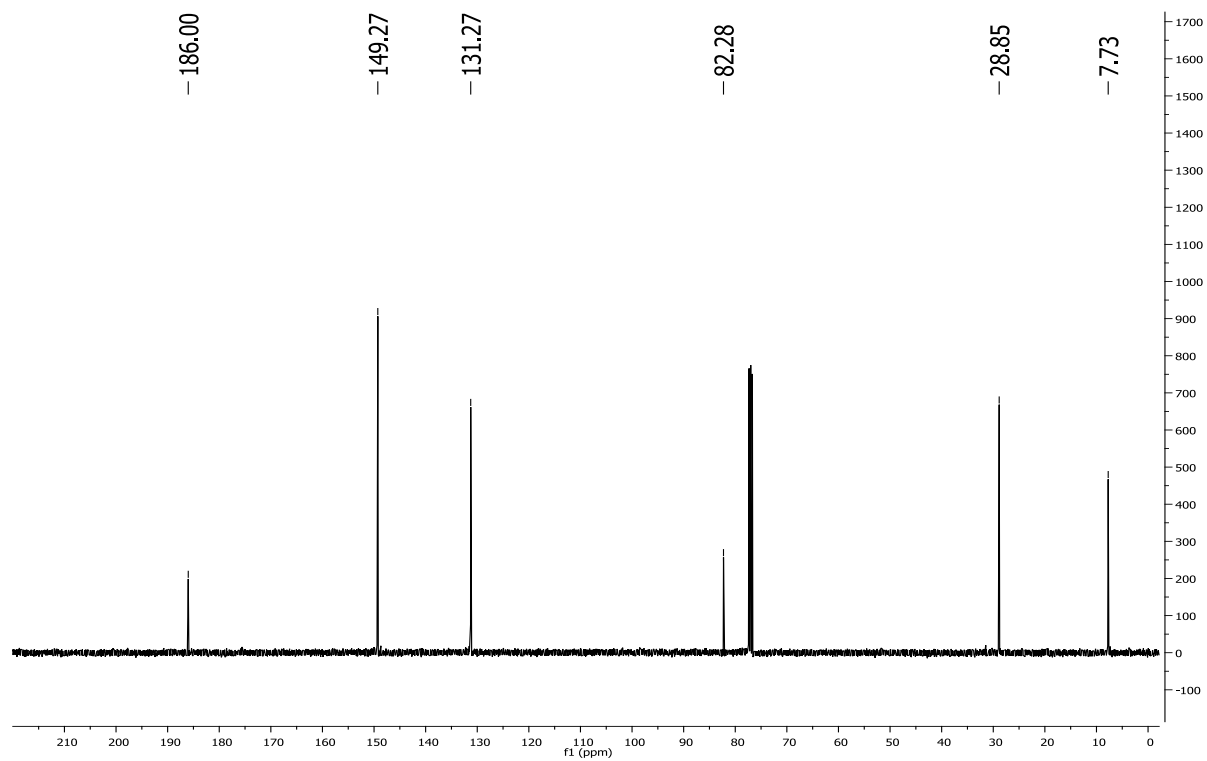
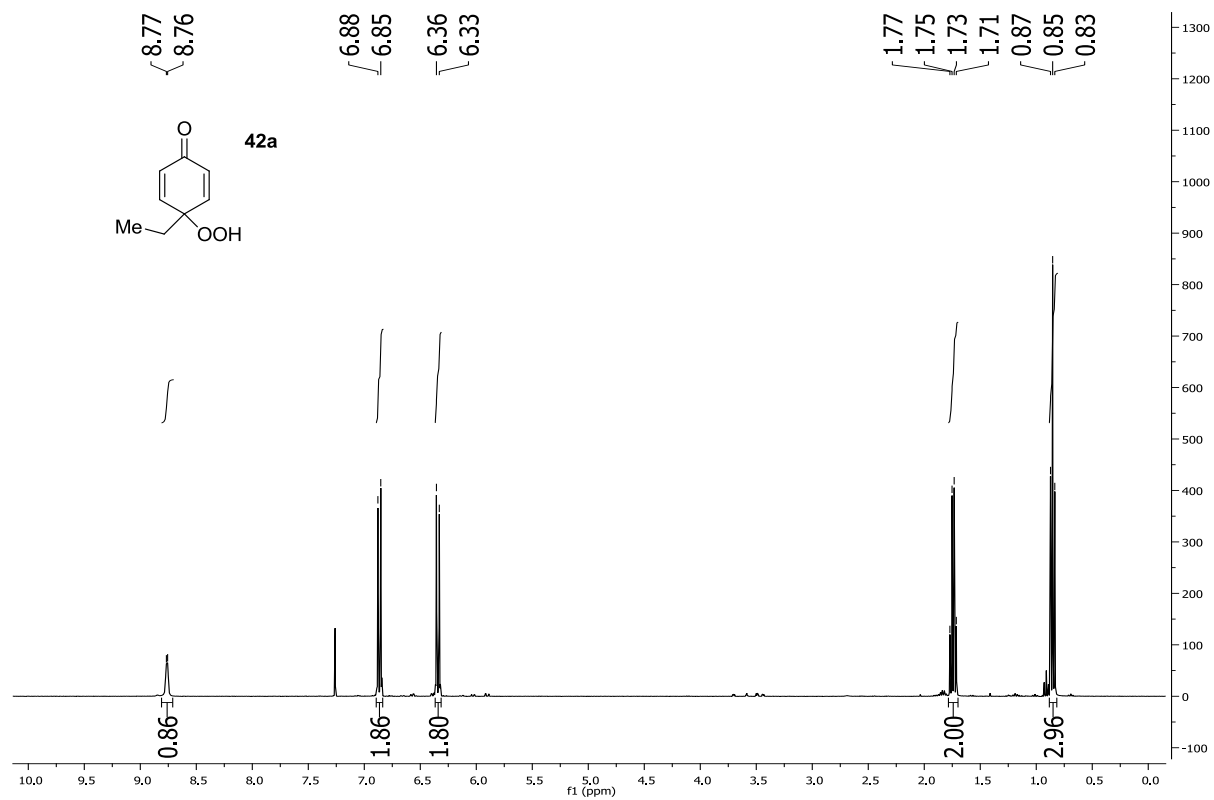


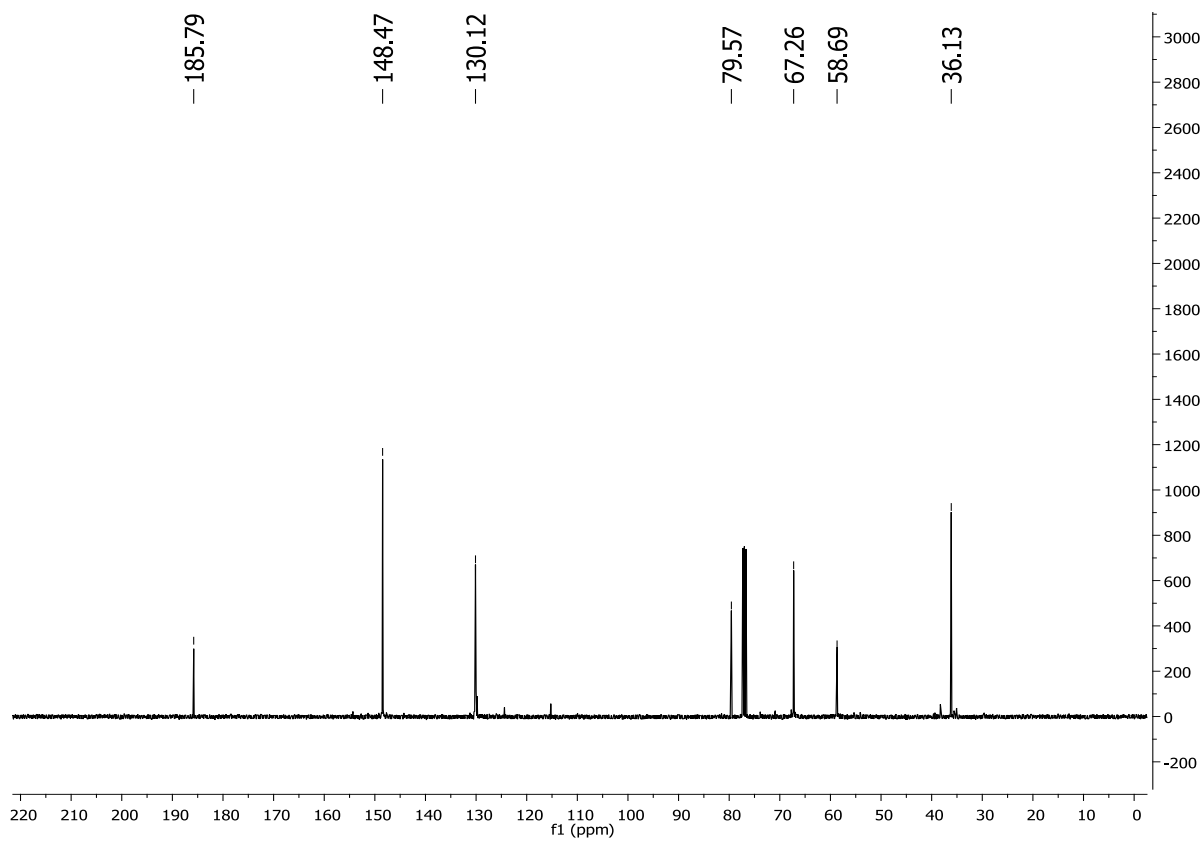
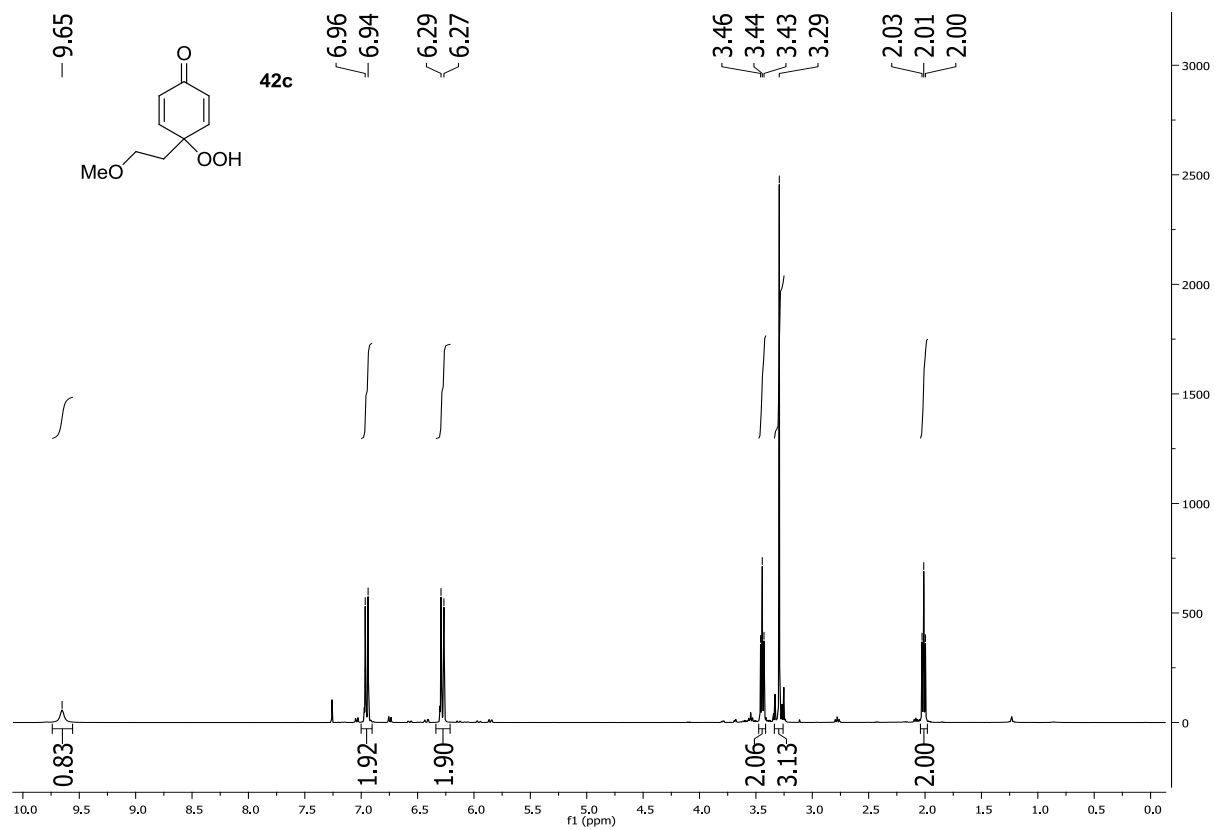
4-((1-hydroxy-2-methylpropyl)peroxy)-4-methylcyclohexa-2,5-dienone (**8ac**)

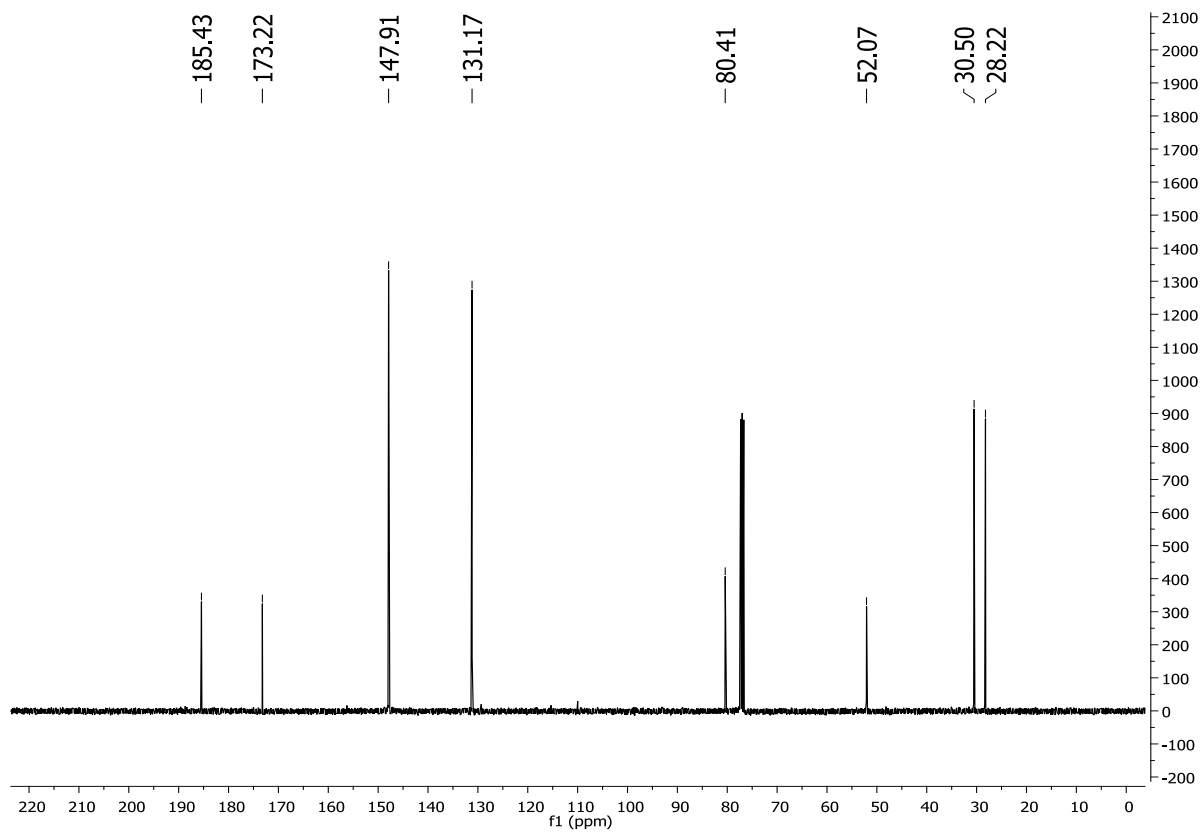
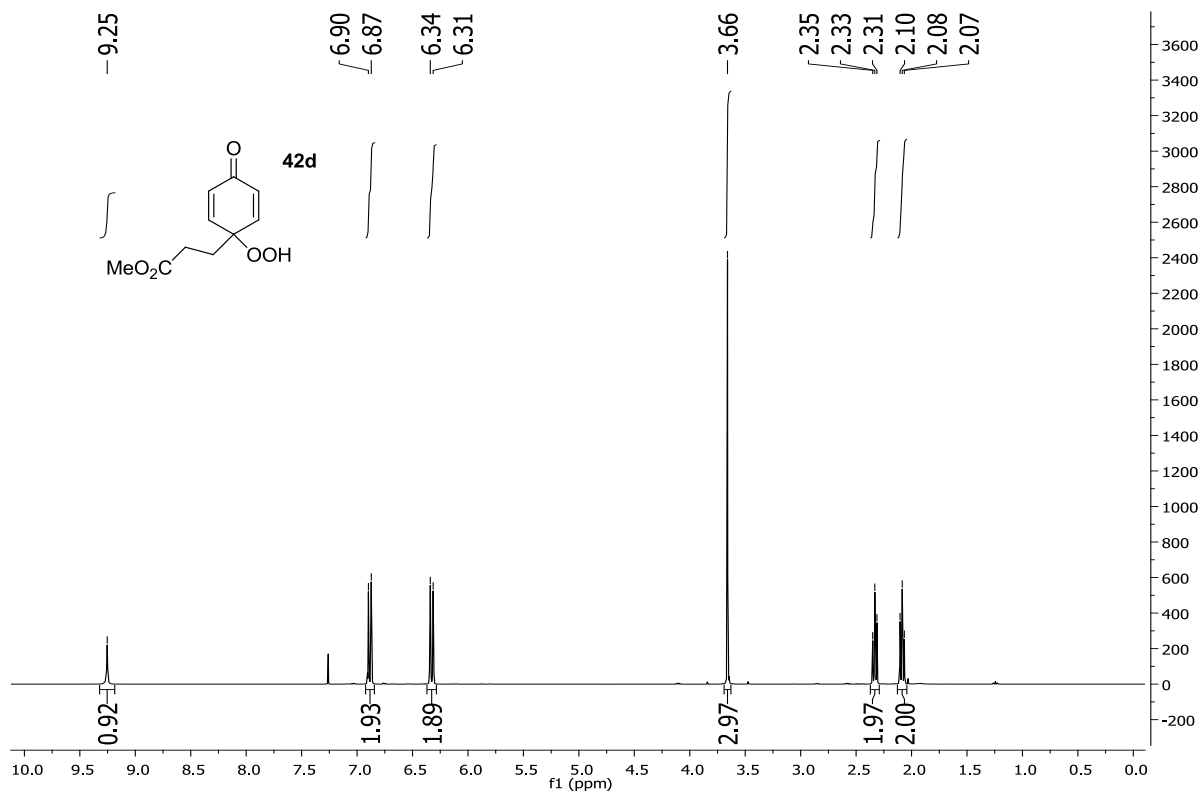
(+/-) **8ac** was synthesized by heating **2a** and **3c** in DCE at 50 °C. The reaction was concentrated *in vacuo* to remove any excess **3c**. **2a** was not removed because it co-elutes with (+/-) **8ac** and (+/-) **8ac** decomposes slowly on SiO₂. (+/-) **8ac** was analyzed by chiral HPLC and found to be racemic. The mixture of (+/-) **8ac** and **2a** were subject to the standard reaction conditions and reaction went to complete conversion in 94% ee.

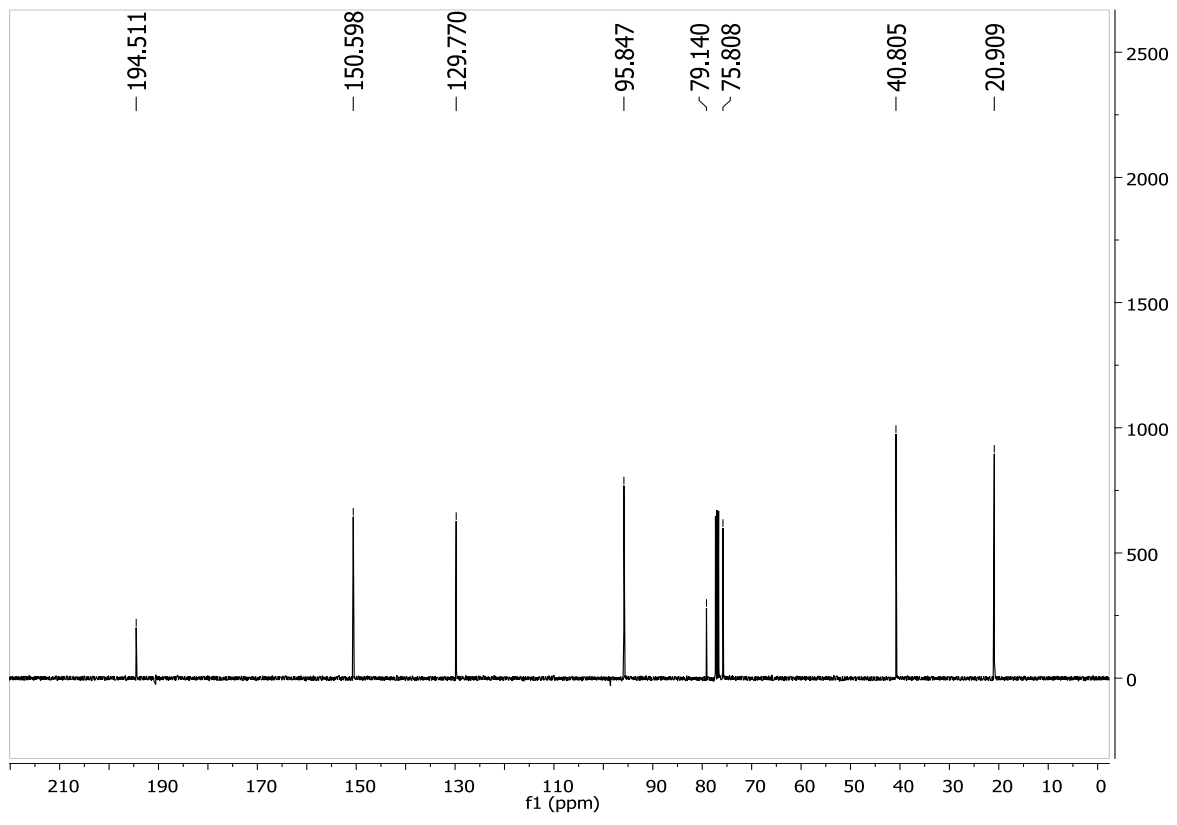
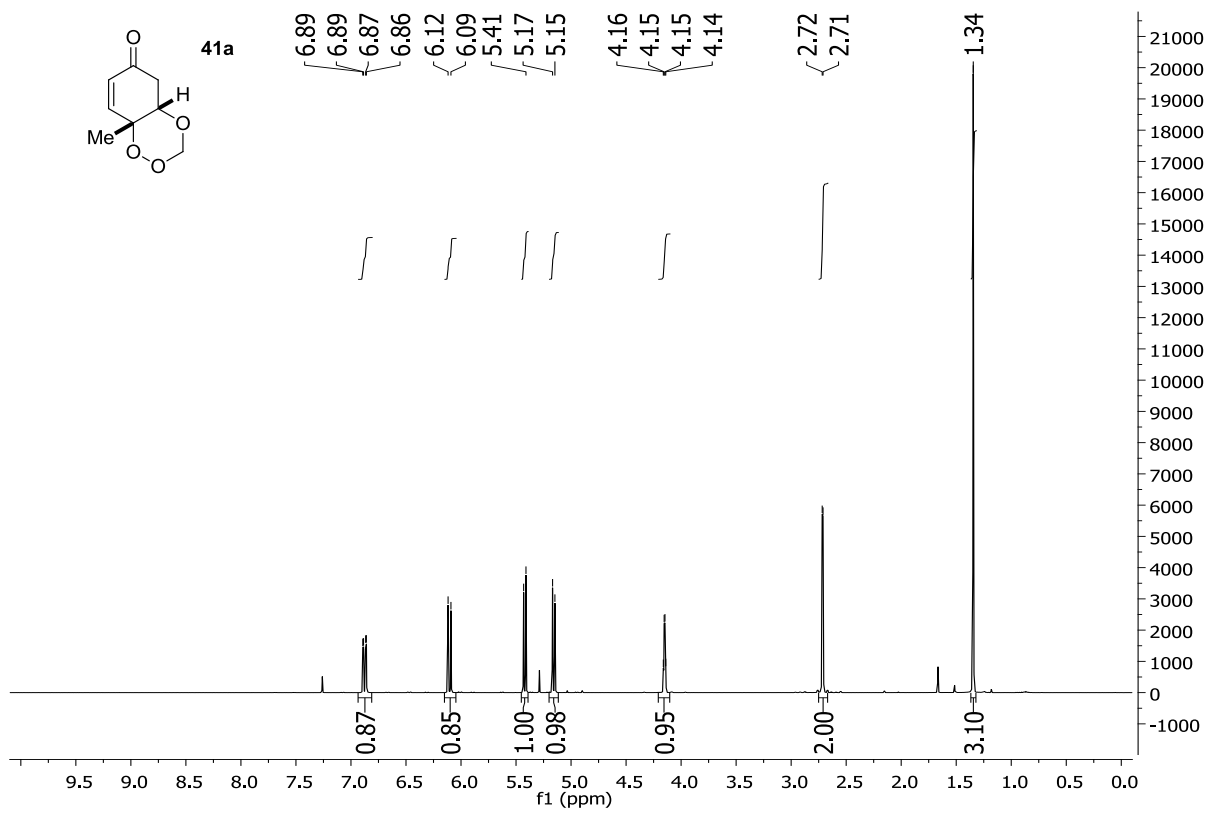
¹H NMR (300 MHz, CDCl₃): δ 6.96-6.84 (m, 2H), 6.11 (m, 2H), 4.88 (d, $J = 5.8$ Hz, 1H), 3.25 (bs, 1H), 1.77-1.68 (m, 1H), 1.37 (s, 3H), 0.89 (d, $J = 6.9$ Hz, 3H), 0.85 (d, $J = 6.8$ Hz, 3H).

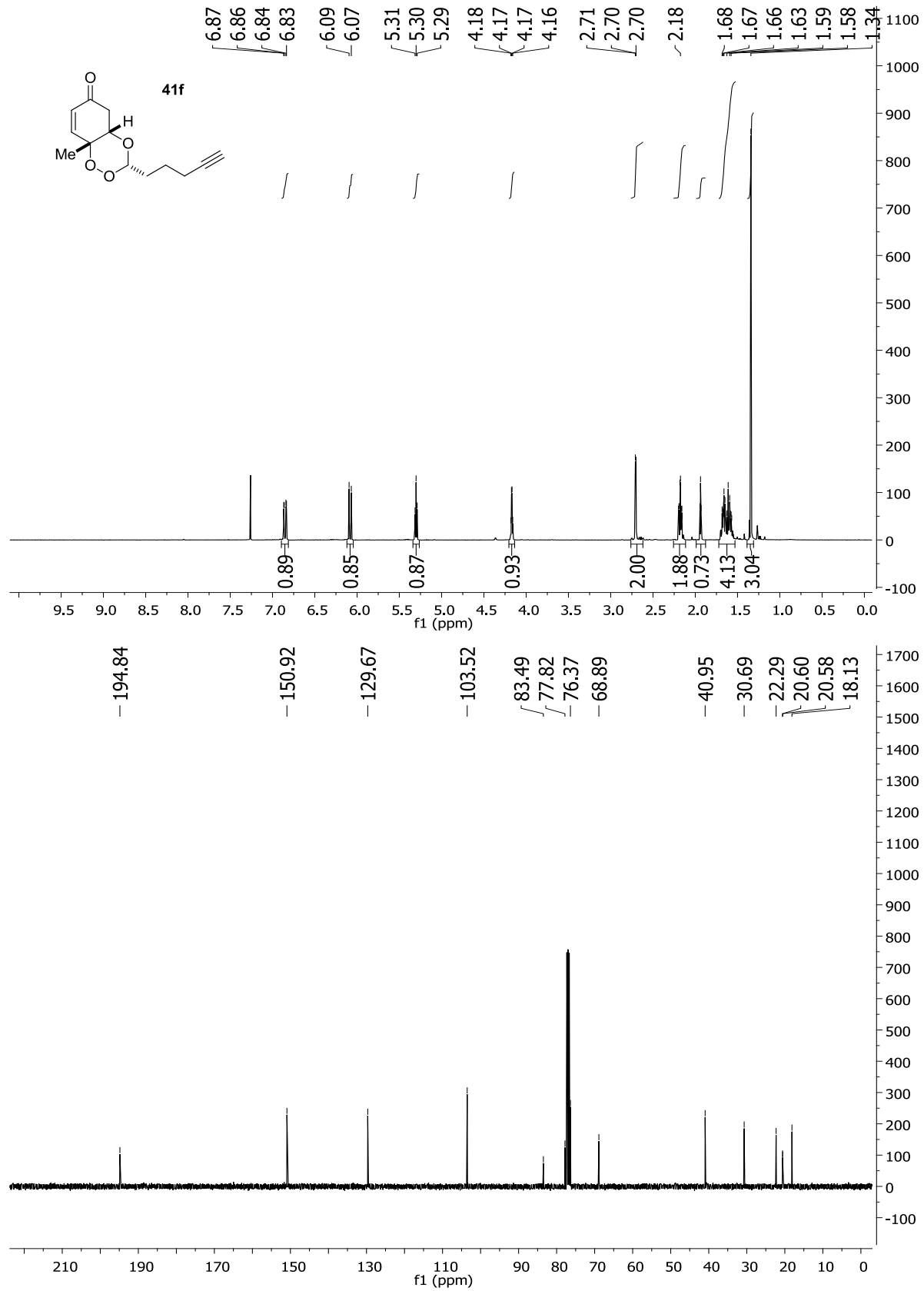
^1H NMR and ^{13}C NMR Spectra of New Compounds

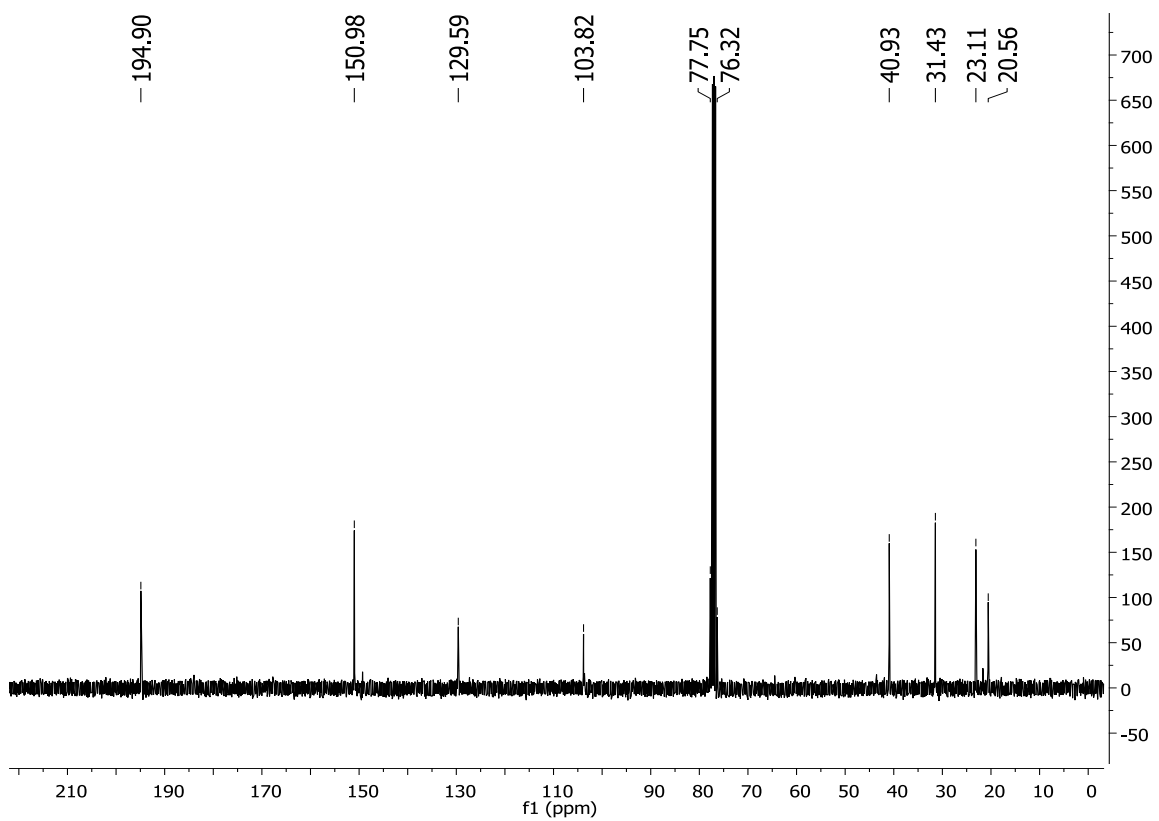
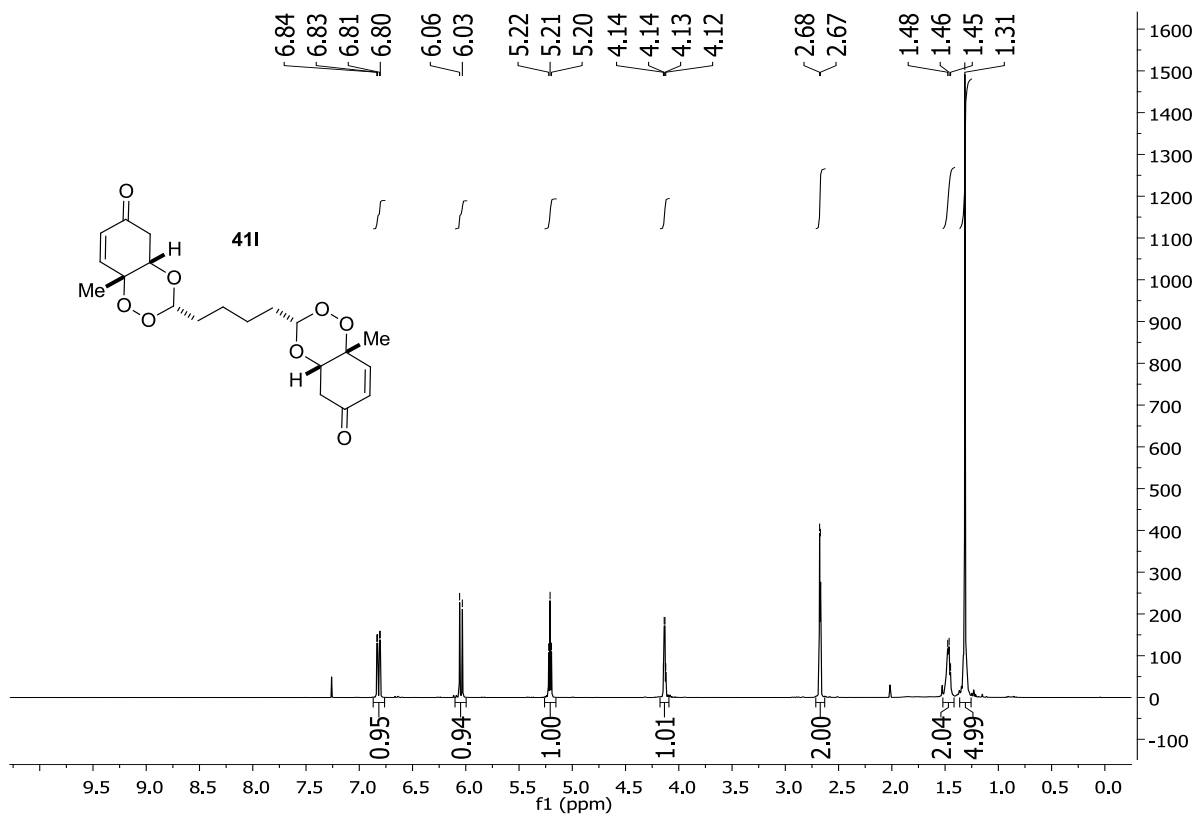


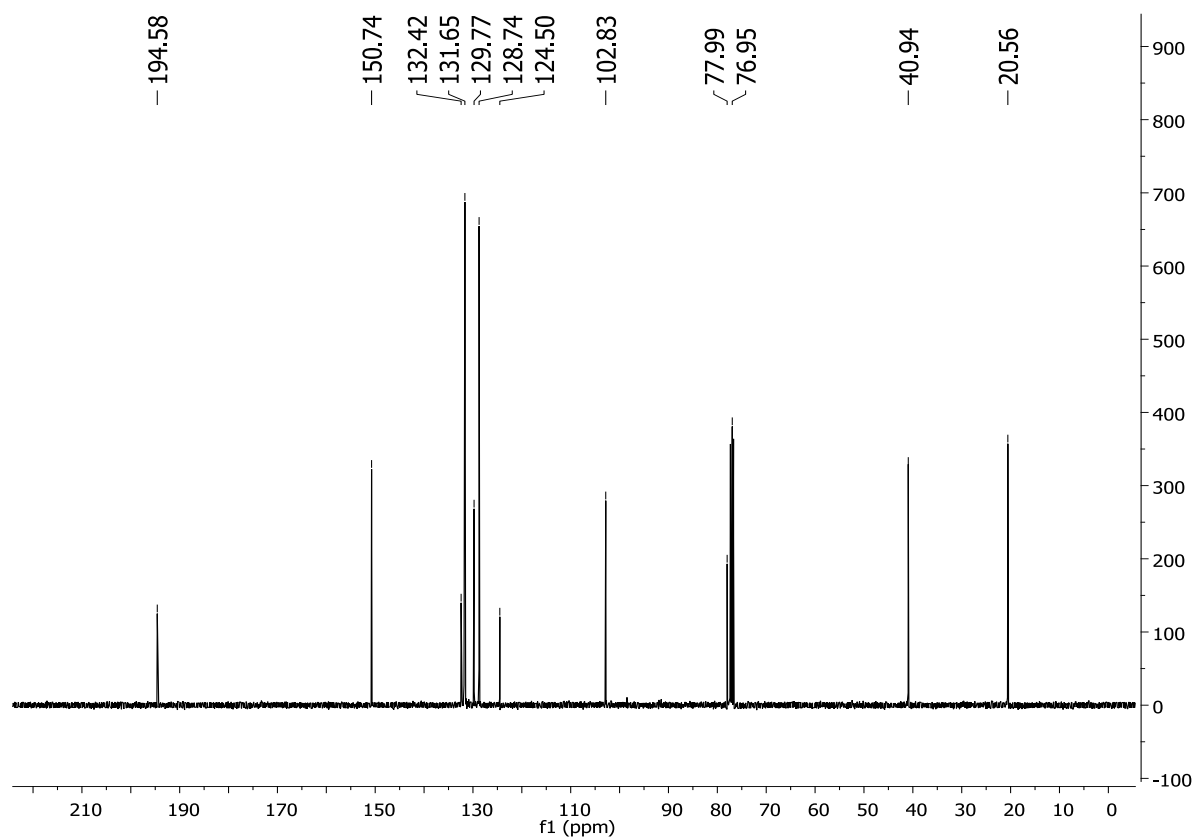
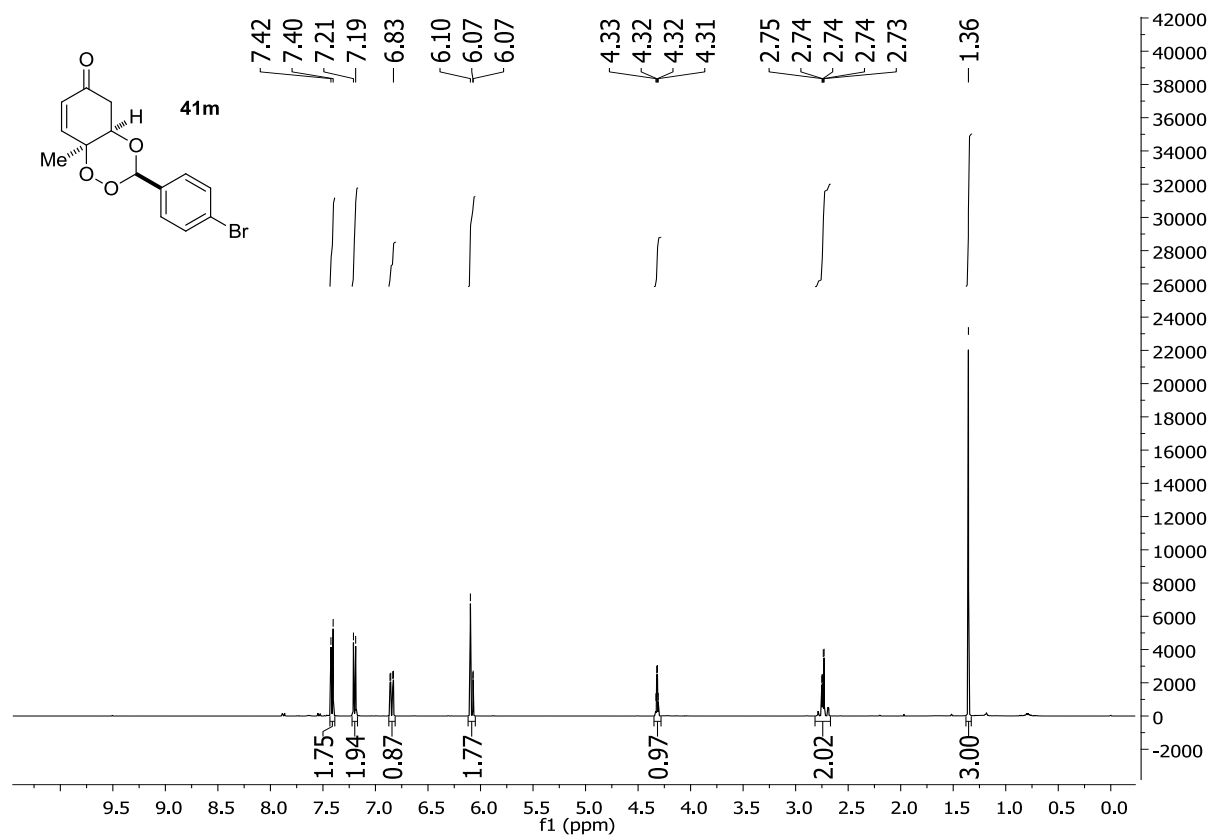


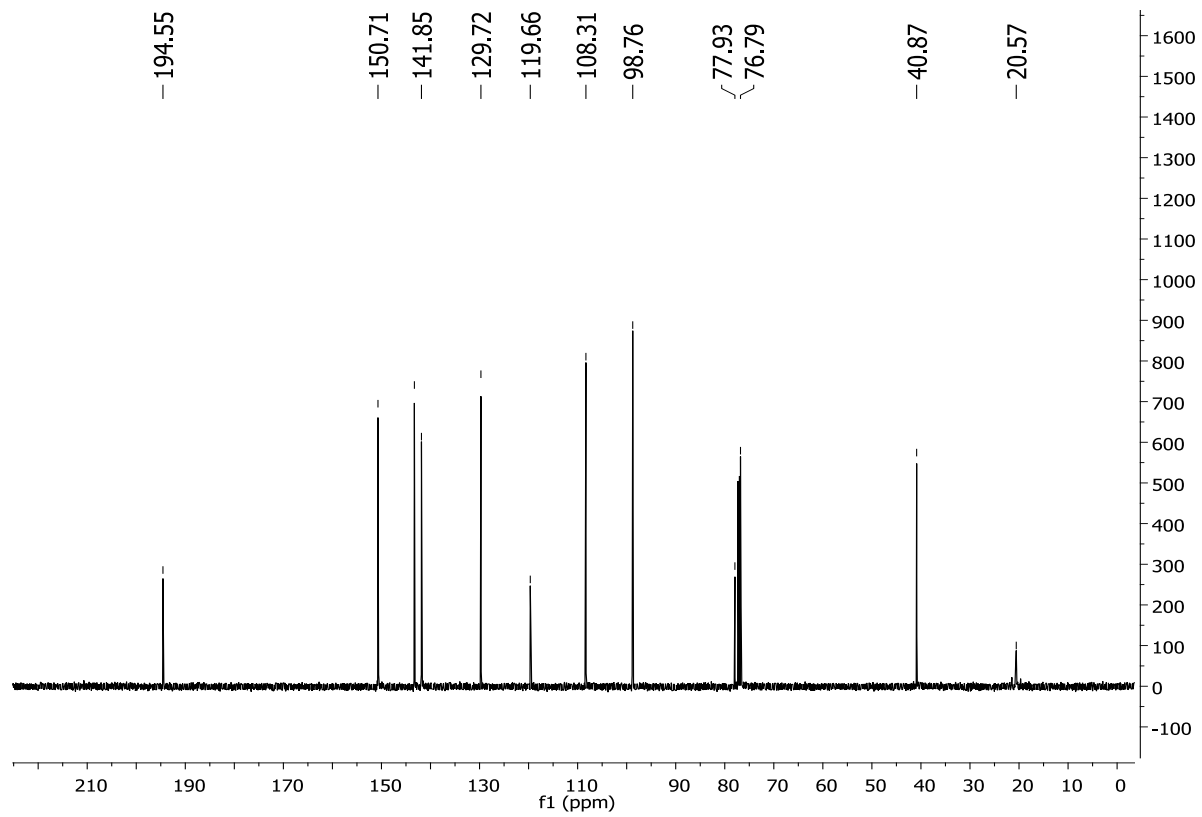
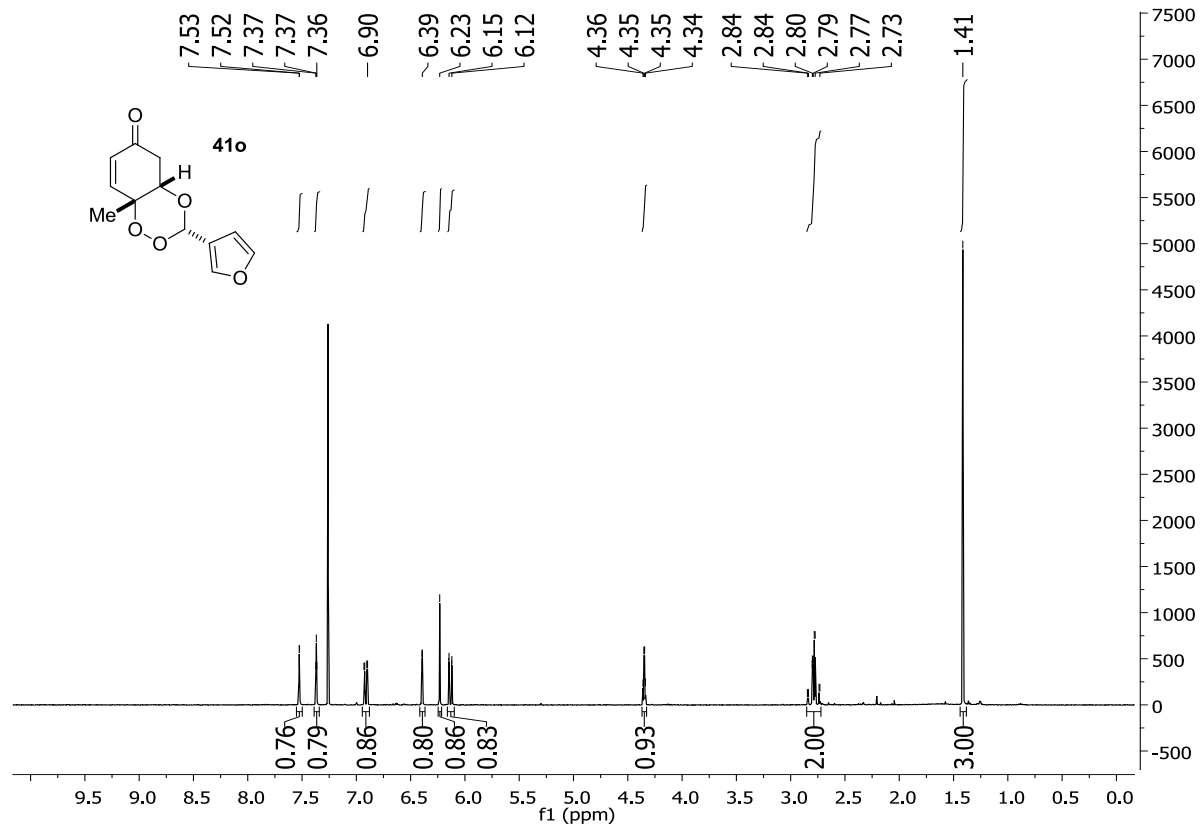


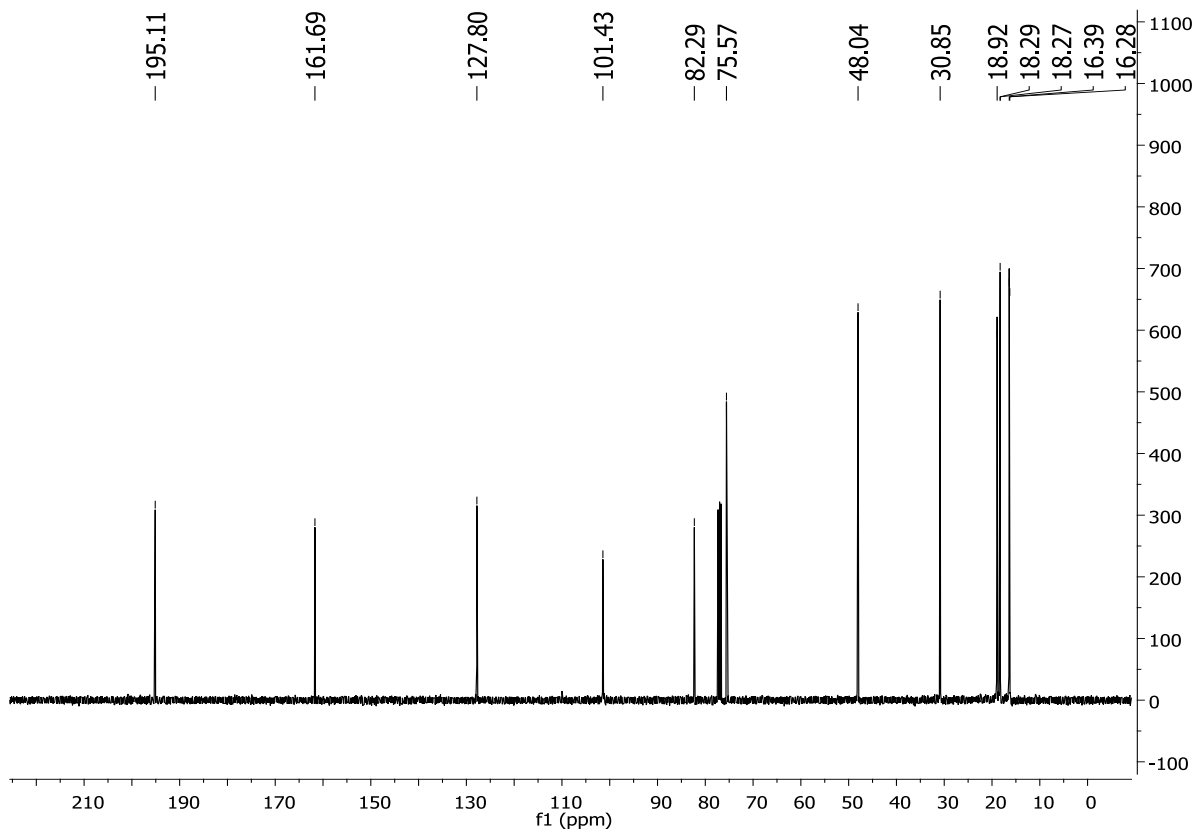
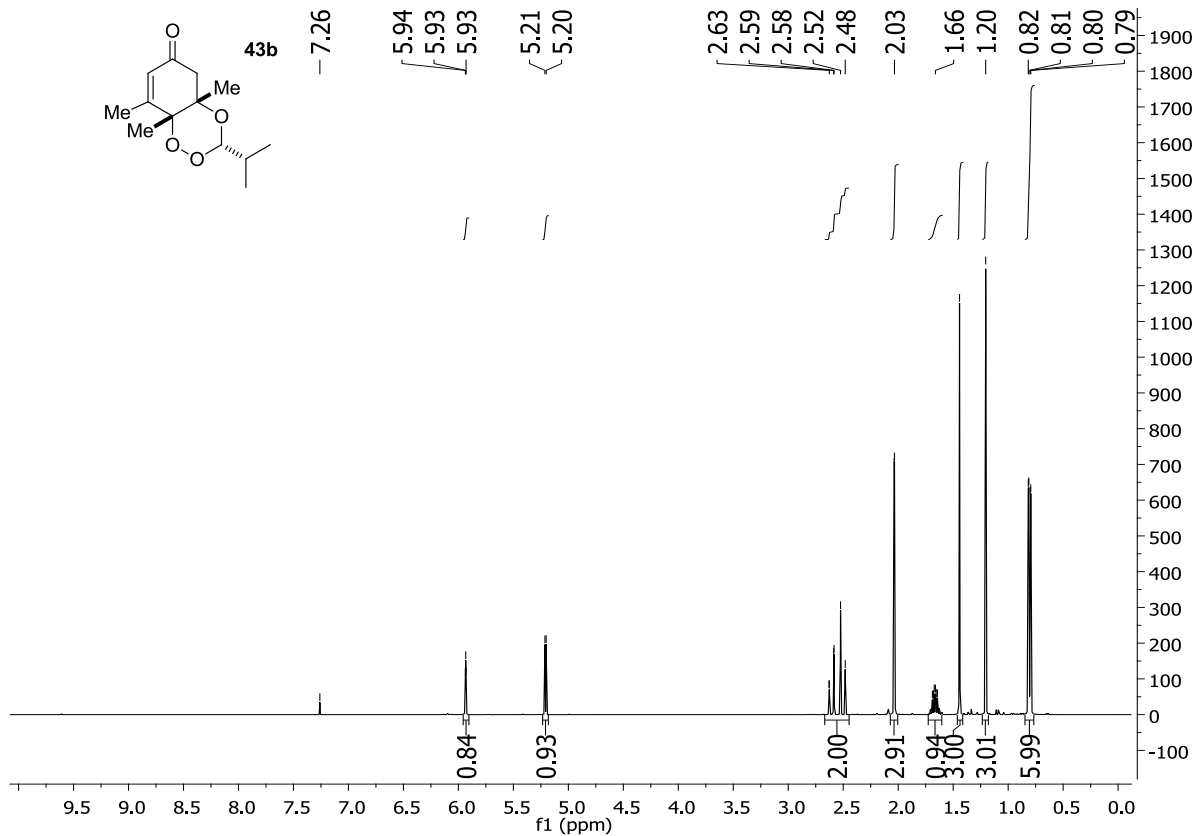


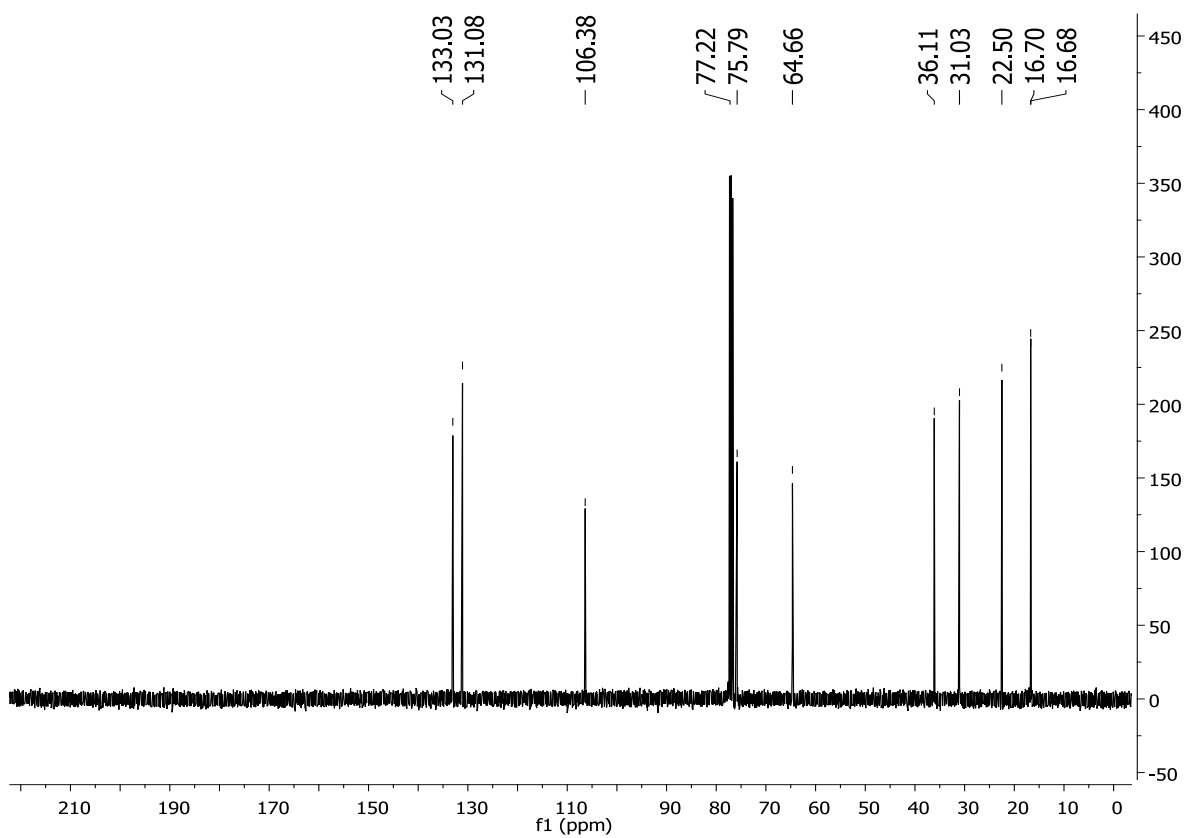
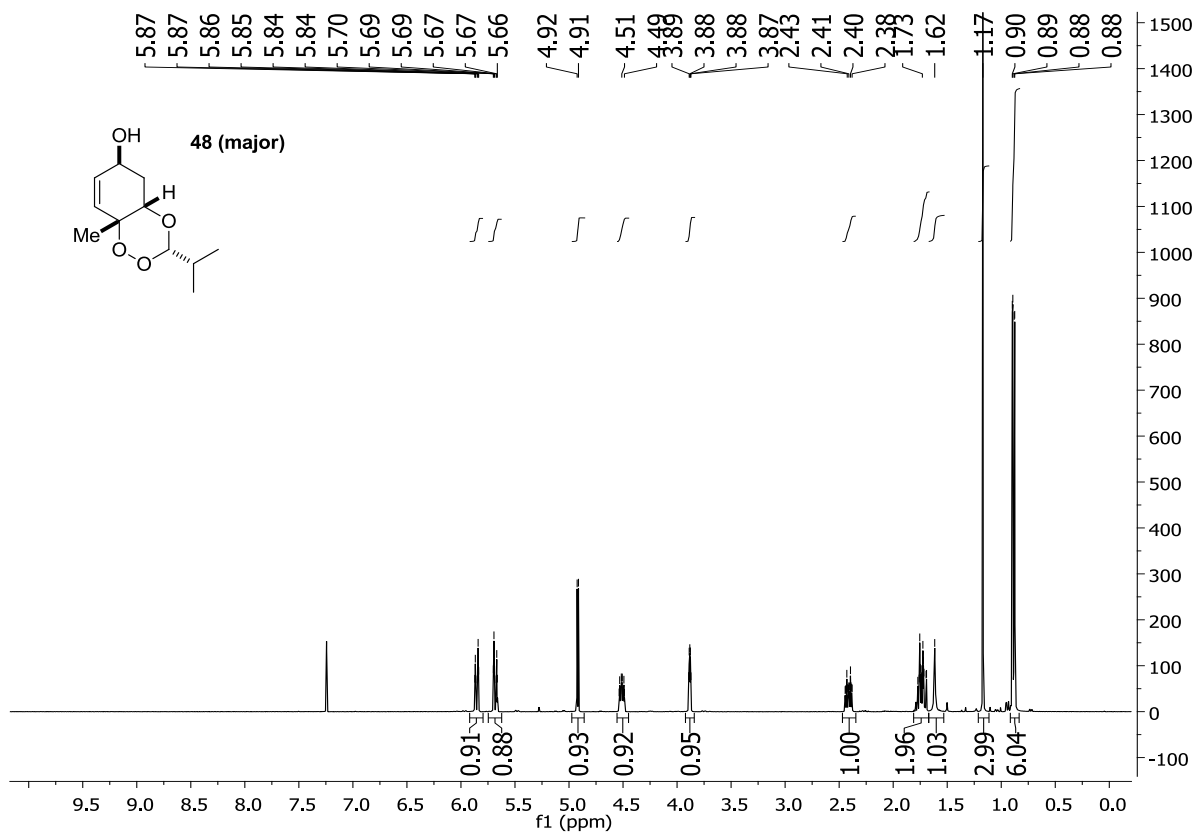


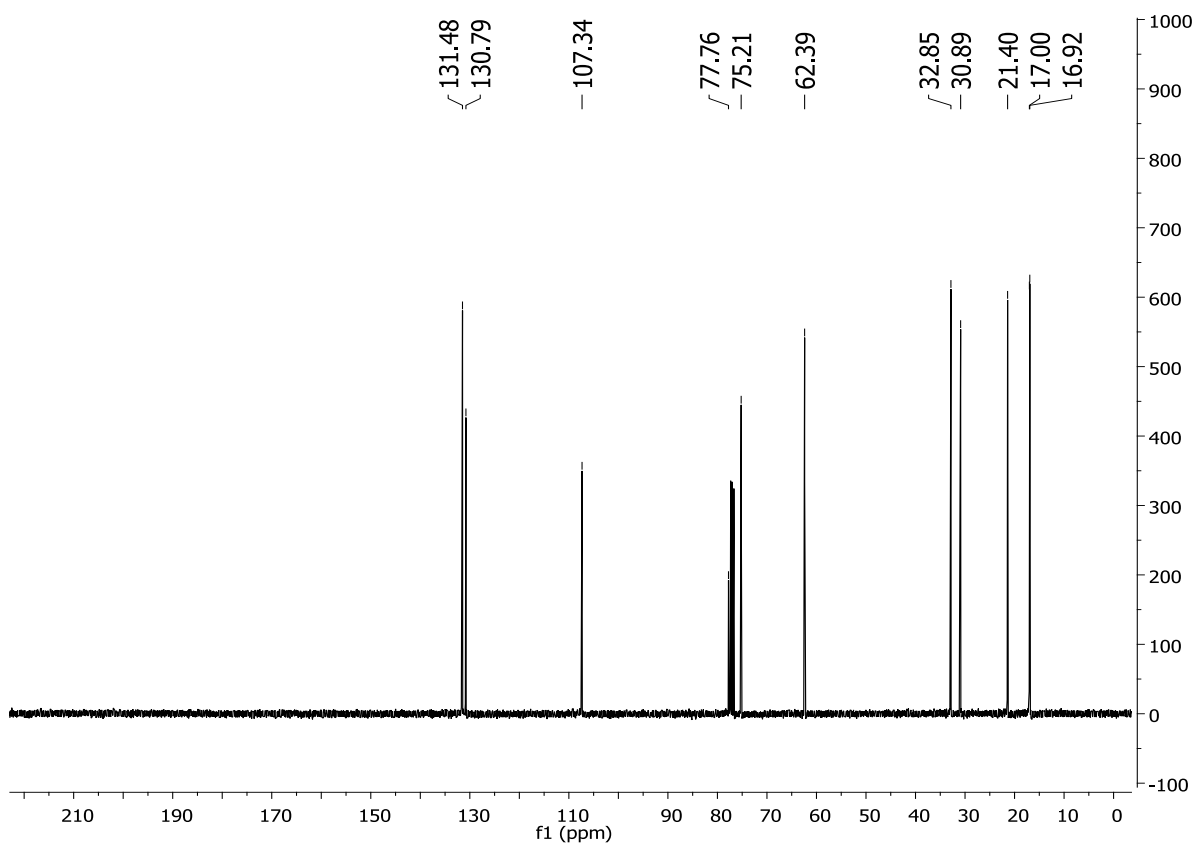
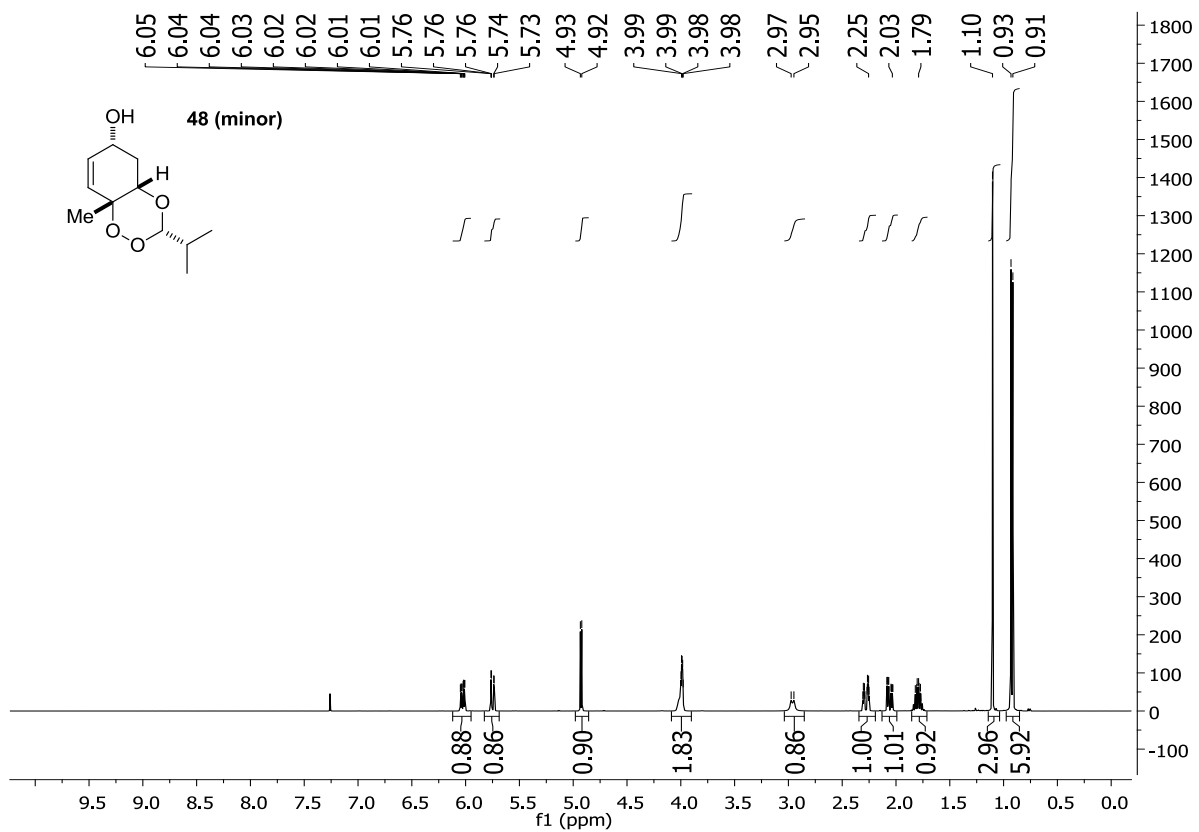


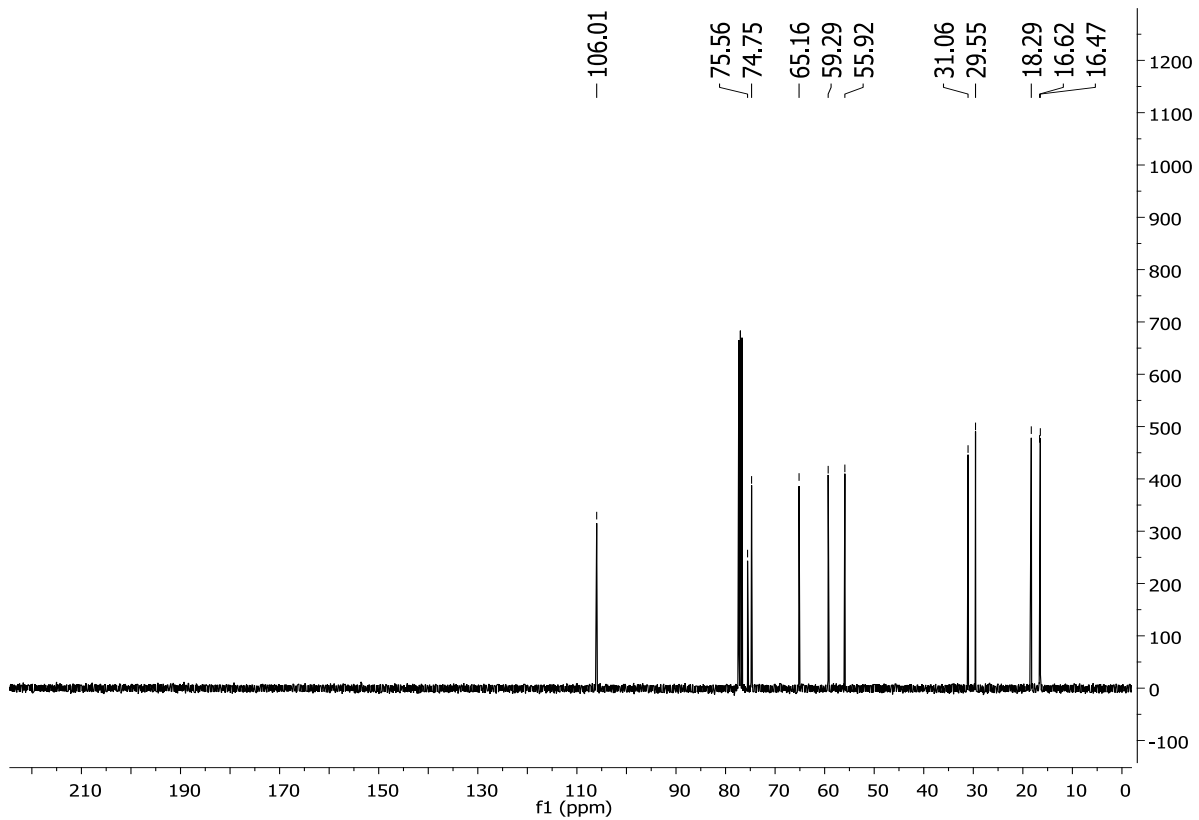
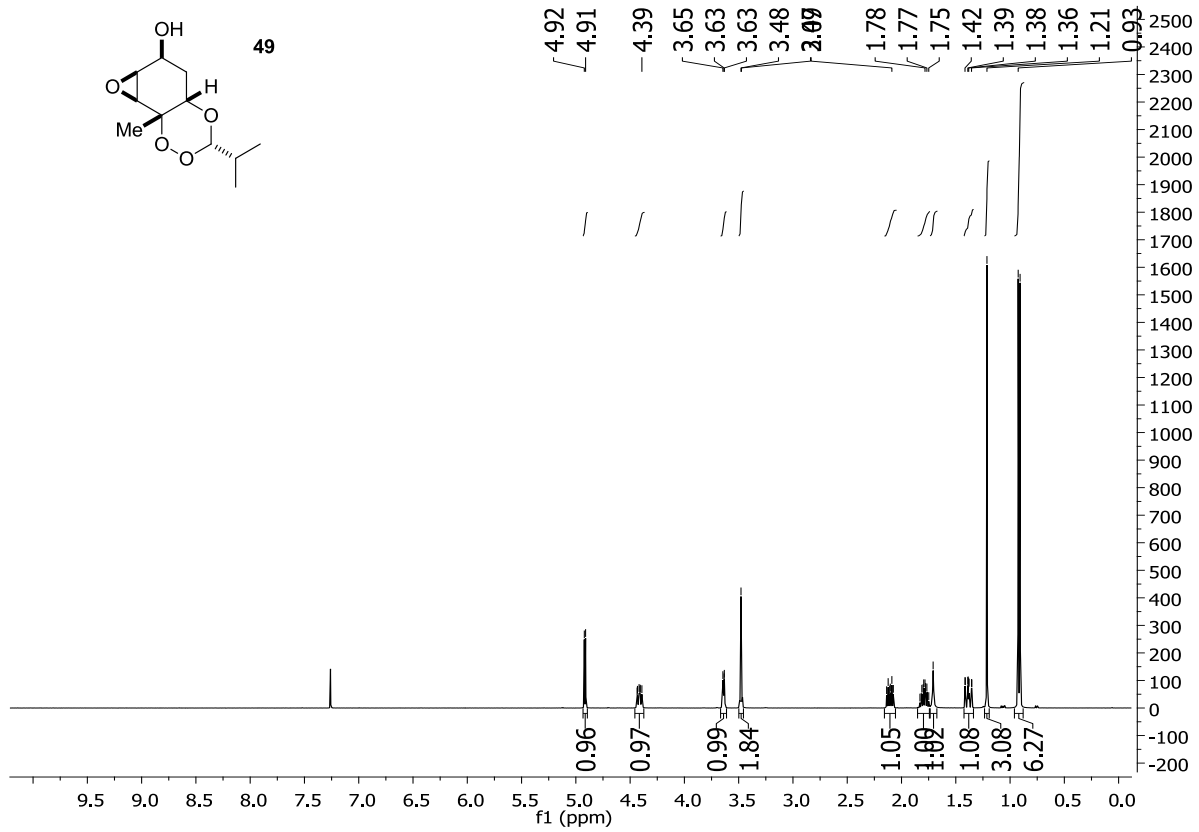
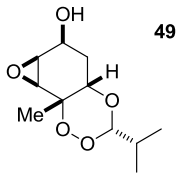


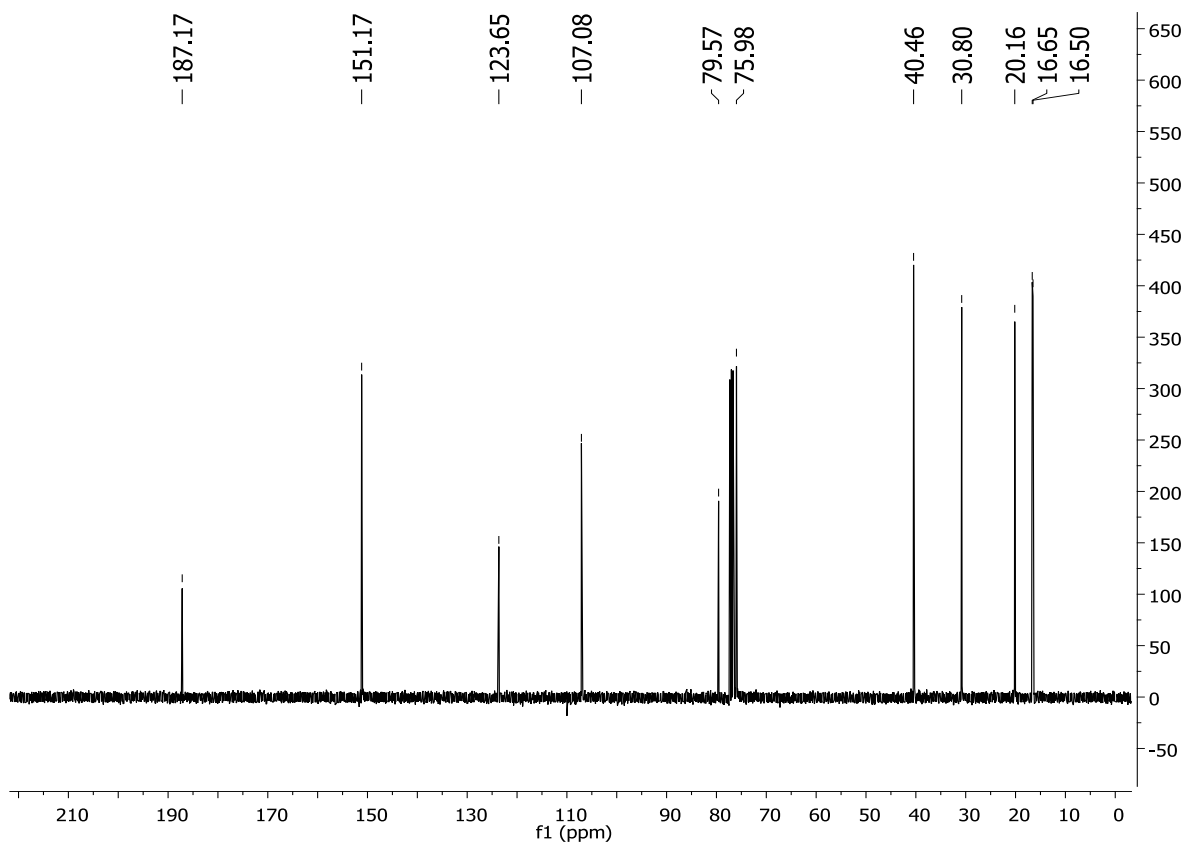
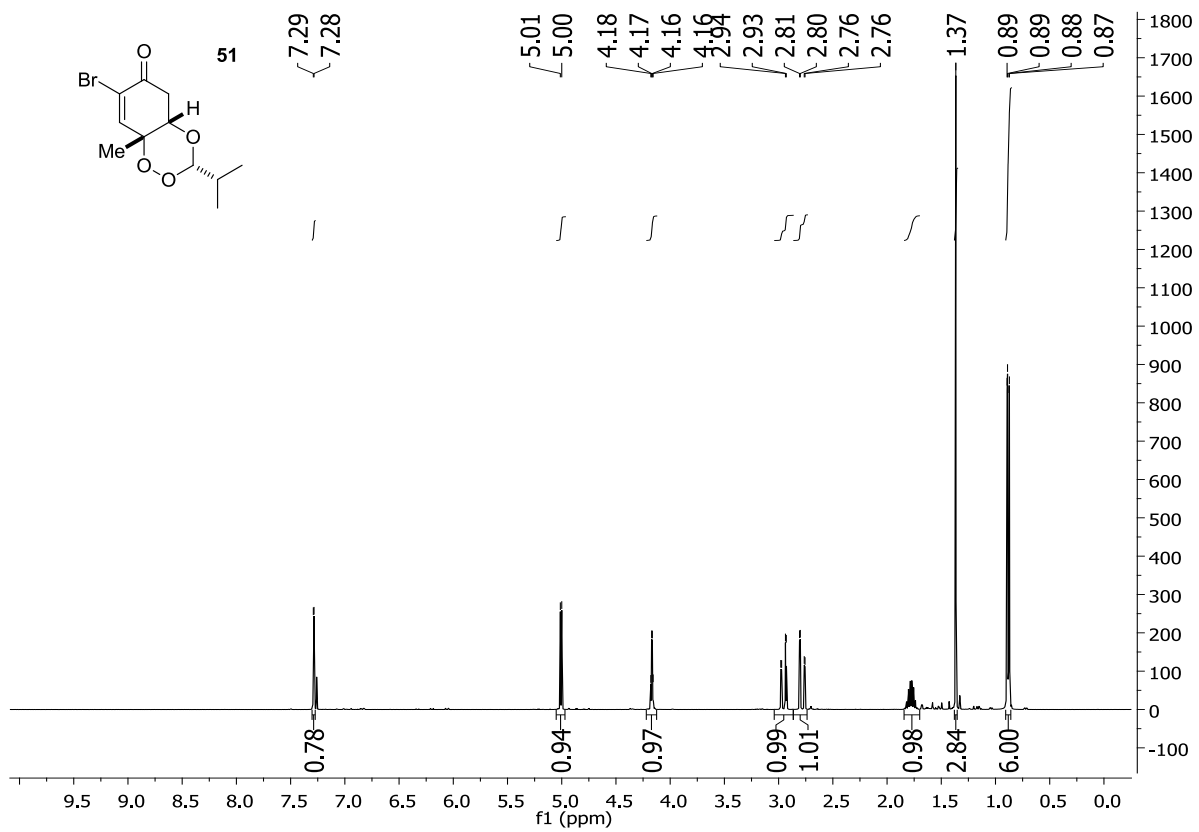


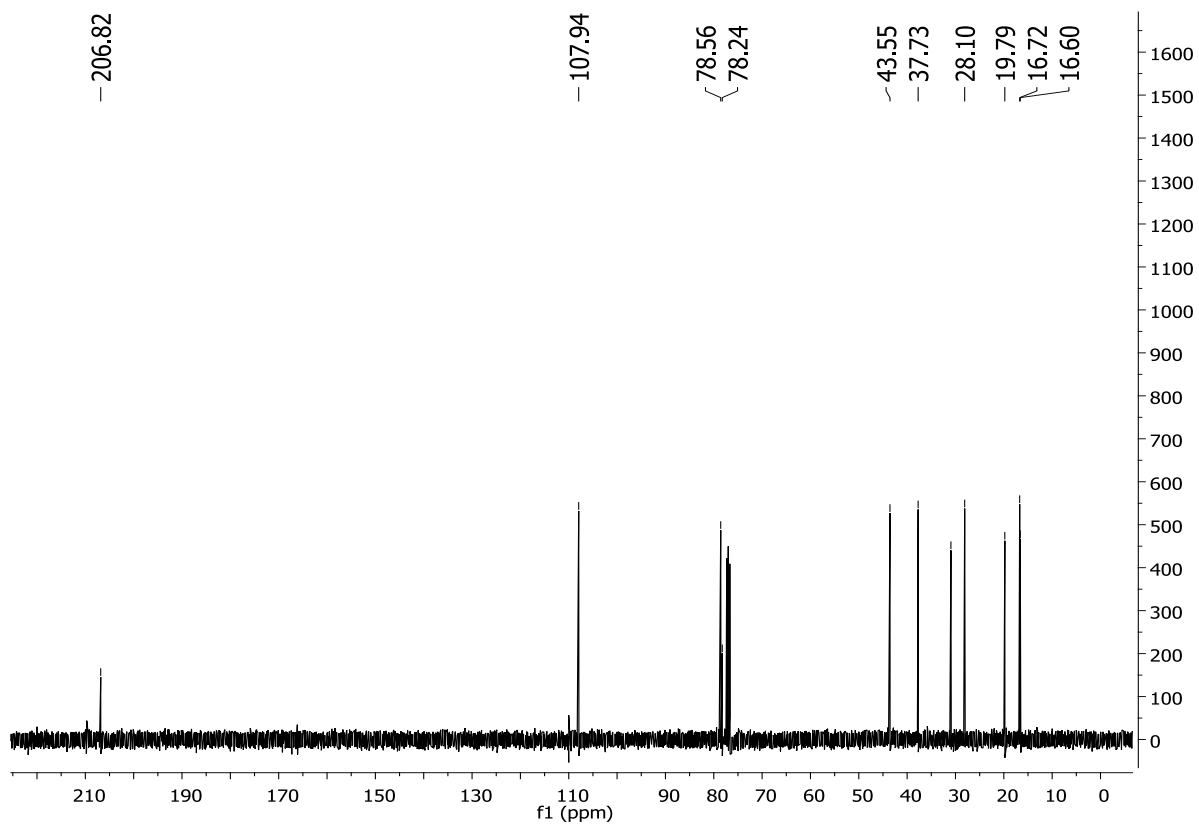
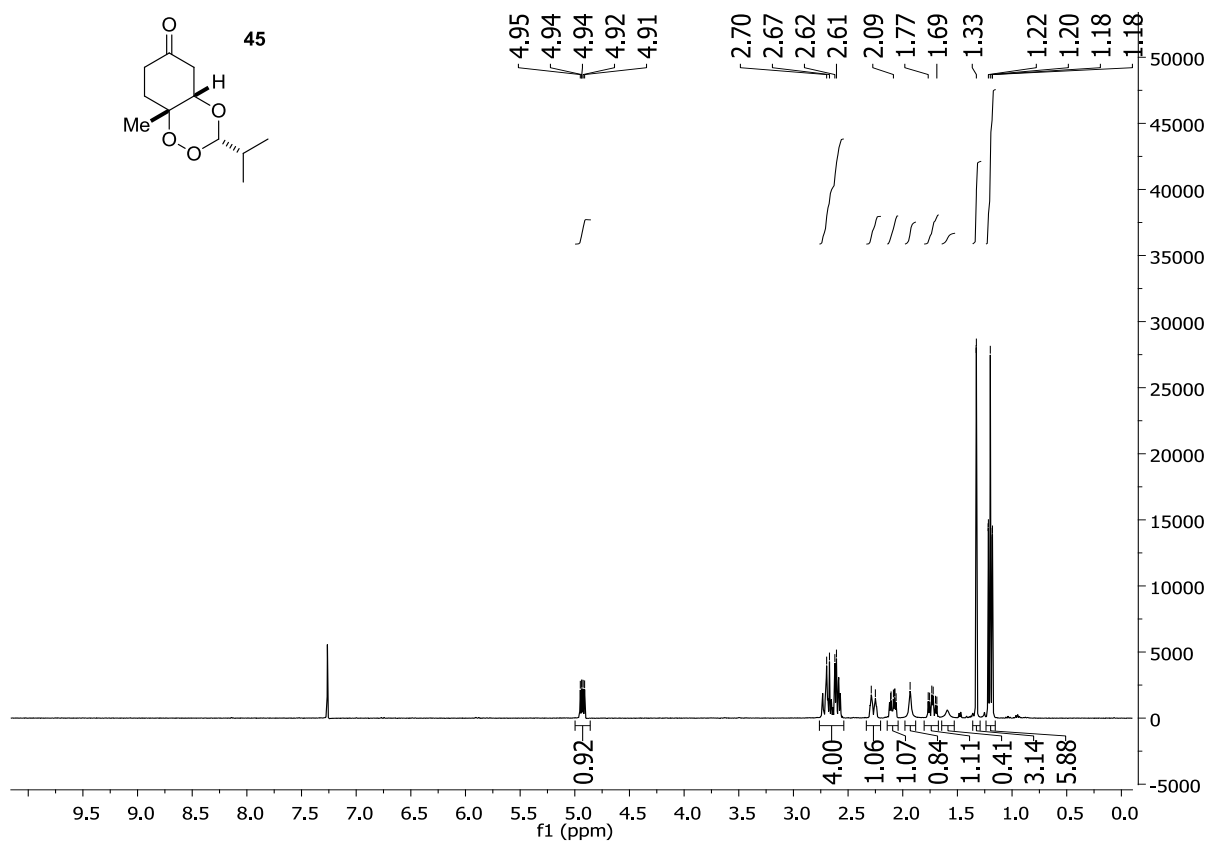
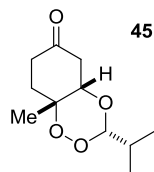


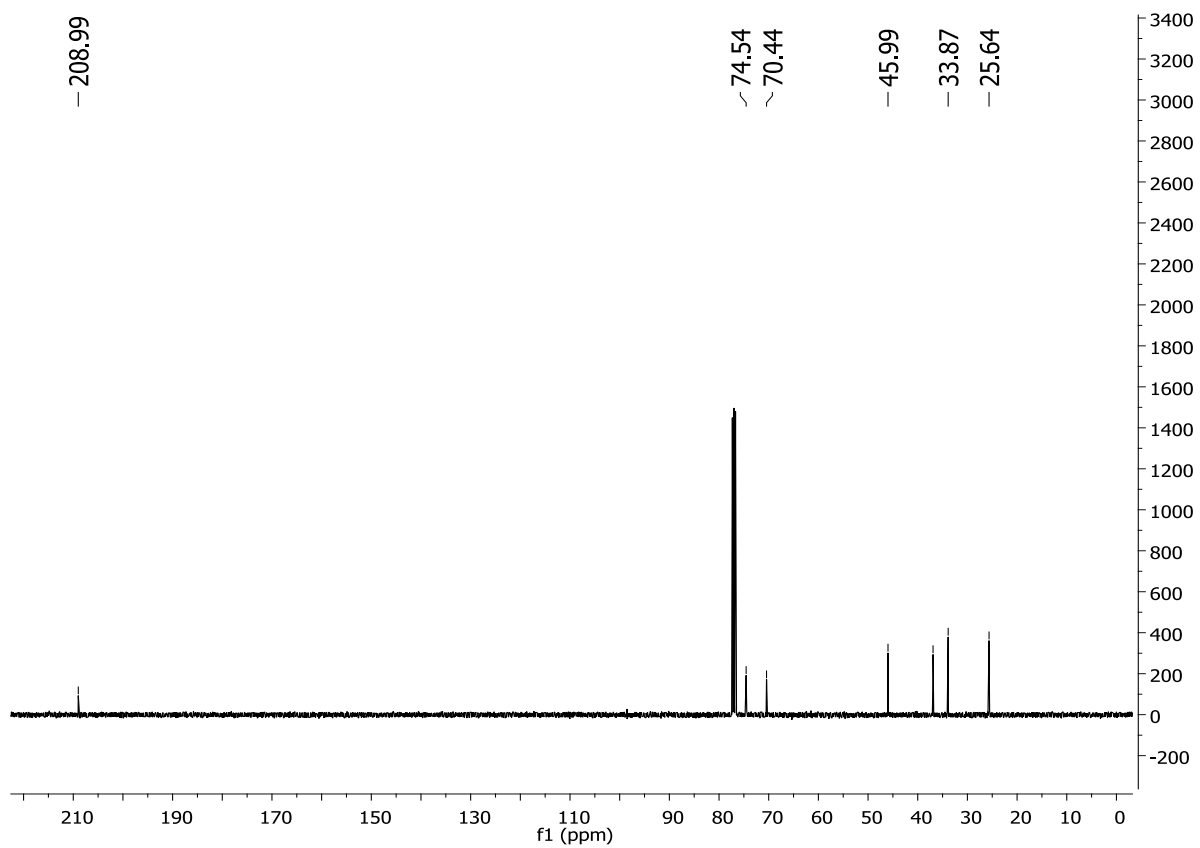
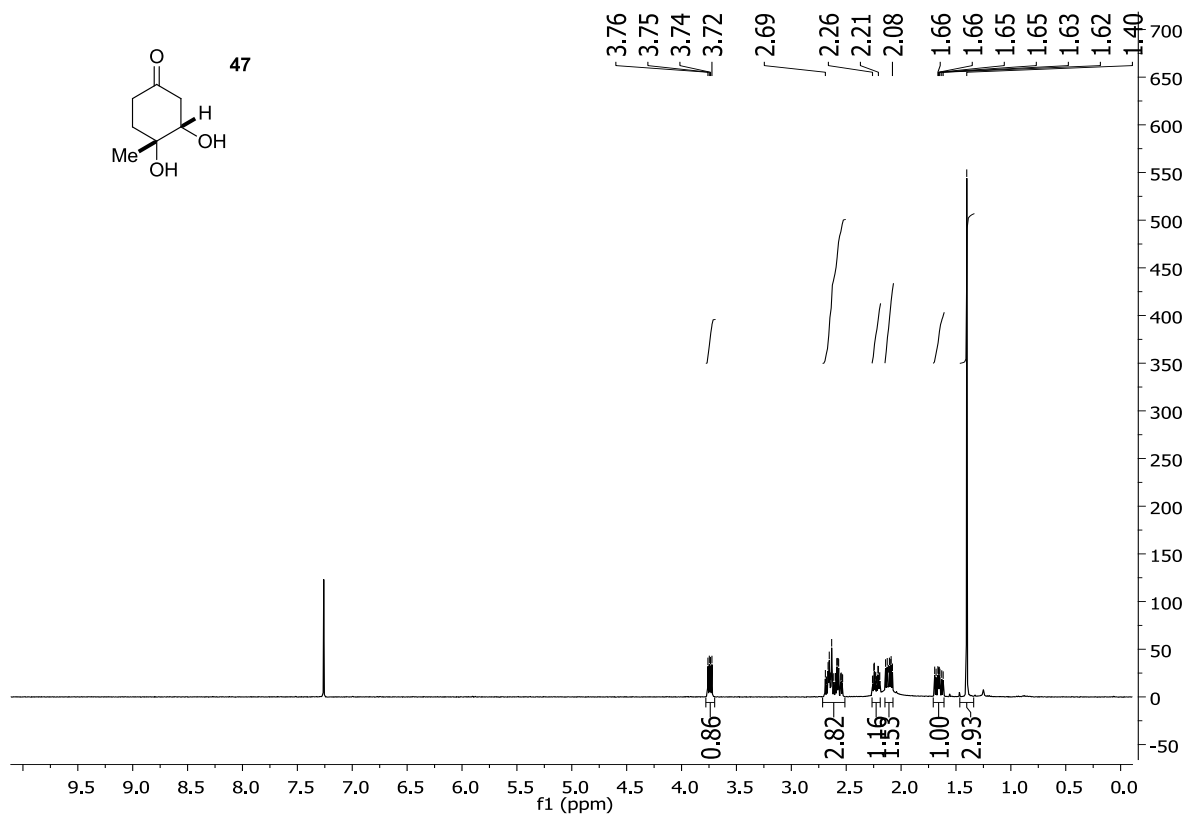
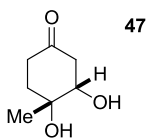












Crystallographic Data for 41m

Table A3.1

Crystal data and structure refinement for (41m).

Identification code	rovis130_0m
Empirical formula	C ₁₄ H ₁₃ BrO ₄
Formula weight	325.15
Temperature	120(2) K
Wavelength	0.71073 Å
Crystal system	Orthorhombic
Space group	<i>P</i> 2 ₁ 2 ₁ 2 ₁
Unit cell dimensions	$a = 7.0393(3) \text{ \AA}$ $\alpha = 90^\circ$. $b = 10.7218(4) \text{ \AA}$ $\beta = 90^\circ$. $c = 17.8586(7) \text{ \AA}$ $\gamma = 90^\circ$.
Volume	1347.86(9) Å ³
Z	4
Density (calculated)	1.602 Mg/m ³
Absorption coefficient	3.056 mm ⁻¹
F(000)	656
Crystal size	0.28 x 0.17 x 0.15 mm ³
Theta range for data collection	2.22 to 29.13°.
Index ranges	-9 ≤ h ≤ 9, -14 ≤ k ≤ 13, -24 ≤ l ≤ 24
Reflections collected	29435

Independent reflections	3638 [R(int) = 0.0420]
Completeness to theta = 29.13°	100.0 %
Absorption correction	Semi-empirical from equivalents
Max. and min. transmission	0.6639 and 0.4784
Refinement method	Full-matrix least-squares on F ²
Data / restraints / parameters	3638 / 0 / 174
Goodness-of-fit on F ²	1.096
Final R indices [I > 2sigma(I)]	R1 = 0.0318, wR2 = 0.0548
R indices (all data)	R1 = 0.0493, wR2 = 0.0709
Absolute structure parameter	0.009(9)
Largest diff. peak and hole	0.698 and -0.443 e.Å ⁻³

Table A3.2

Atomic coordinates ($\times 10^4$) and equivalent isotropic displacement parameters ($\text{\AA}^2 \times 10^3$)

for **41m**. $U(\text{eq})$ is defined as one third of the trace of the orthogonalized U_{ij} tensor.

	x	y	z	$U(\text{eq})$
Br(1)	3192(1)	-2371(1)	8429(1)	43(1)
C(1)	5337(4)	-1314(3)	8579(2)	27(1)
C(2)	6892(5)	-1758(2)	8964(2)	29(1)
C(3)	8435(5)	-976(2)	9058(1)	25(1)
C(4)	8420(4)	232(2)	8773(1)	21(1)
C(5)	6819(4)	658(2)	8391(1)	25(1)
C(6)	5269(4)	-120(3)	8287(1)	27(1)
C(7)	10083(4)	1074(3)	8880(1)	23(1)
C(8)	11035(4)	3001(2)	9403(1)	20(1)
C(9)	10186(4)	4140(2)	9778(1)	22(1)
C(10)	8784(4)	4811(2)	9290(2)	24(1)
C(11)	9187(4)	4808(2)	8484(2)	27(1)
C(12)	10594(5)	4124(3)	8188(2)	28(1)
C(13)	13861(4)	3959(3)	8742(2)	32(1)
C(14)	11926(5)	3341(2)	8648(1)	24(1)

O(1)	9505(3)	2133(2)	9294(1)	20(1)
O(2)	10650(3)	1463(2)	8148(1)	28(1)
O(3)	12404(3)	2201(2)	8256(1)	30(1)
O(4)	7415(3)	5350(2)	9550(1)	33(1)

—

Table A3.3Bond lengths [Å] and angles [°] for **41m**.

Br(1)-C(1)	1.907(3)
C(1)-C(2)	1.377(4)
C(1)-C(6)	1.383(4)
C(2)-C(3)	1.383(4)
C(3)-C(4)	1.391(4)
C(4)-C(5)	1.394(4)
C(4)-C(7)	1.491(4)
C(5)-C(6)	1.386(4)
C(7)-O(1)	1.415(3)
C(7)-O(2)	1.428(3)
C(8)-O(1)	1.437(3)
C(8)-C(9)	1.515(4)
C(8)-C(14)	1.531(3)
C(9)-C(10)	1.500(4)
C(10)-O(4)	1.216(3)
C(10)-C(11)	1.467(4)
C(11)-C(12)	1.341(4)
C(12)-C(14)	1.504(4)
C(13)-C(14)	1.524(4)
C(14)-O(3)	1.448(3)

O(2)-O(3)	1.479(3)
C(2)-C(1)-C(6)	122.4(3)
C(2)-C(1)-Br(1)	119.6(2)
C(6)-C(1)-Br(1)	118.0(2)
C(1)-C(2)-C(3)	118.4(3)
C(2)-C(3)-C(4)	120.9(3)
C(3)-C(4)-C(5)	119.3(3)
C(3)-C(4)-C(7)	120.7(3)
C(5)-C(4)-C(7)	119.9(2)
C(6)-C(5)-C(4)	120.3(2)
C(1)-C(6)-C(5)	118.7(3)
O(1)-C(7)-O(2)	108.9(2)
O(1)-C(7)-C(4)	109.1(2)
O(2)-C(7)-C(4)	106.2(2)
O(1)-C(8)-C(9)	106.7(2)
O(1)-C(8)-C(14)	110.0(2)
C(9)-C(8)-C(14)	111.0(2)
C(10)-C(9)-C(8)	112.8(2)
O(4)-C(10)-C(11)	121.9(3)
O(4)-C(10)-C(9)	121.8(2)
C(11)-C(10)-C(9)	116.2(2)
C(12)-C(11)-C(10)	122.1(3)

C(11)-C(12)-C(14)	123.4(2)
O(3)-C(14)-C(12)	110.6(2)
O(3)-C(14)-C(13)	102.3(2)
C(12)-C(14)-C(13)	112.0(2)
O(3)-C(14)-C(8)	108.7(2)
C(12)-C(14)-C(8)	111.0(2)
C(13)-C(14)-C(8)	111.9(2)
C(7)-O(1)-C(8)	112.0(2)
C(7)-O(2)-O(3)	105.71(19)
C(14)-O(3)-O(2)	108.70(18)

Symmetry transformations used to generate equivalent atoms:

Table A3.4

Anisotropic displacement parameters ($\text{\AA}^2 \times 10^3$) for **41m**. The anisotropic

displacement factor exponent takes the form: $-2\pi^2 [h^2 a^{*2} U^{11} + \dots + 2 h k a^* b^* U^{12}]$

	U11	U22	U33	U23	U13	U12
Br(1)	35(1)	37(1)	57(1)	-18(1)	0(1)	-6(1)
C(1)	25(2)	25(2)	31(2)	-12(1)	3(1)	0(1)
C(2)	34(2)	19(1)	34(2)	-3(1)	6(2)	3(2)
C(3)	27(2)	22(1)	27(1)	-3(1)	1(1)	5(1)
C(4)	24(2)	20(1)	18(1)	-4(1)	8(1)	3(1)
C(5)	34(2)	23(1)	18(1)	-1(1)	3(1)	6(1)
C(6)	27(2)	30(2)	23(1)	-8(1)	-3(1)	9(1)
C(7)	31(2)	20(1)	19(1)	0(1)	3(1)	3(1)
C(8)	22(2)	24(1)	16(1)	2(1)	-4(1)	0(1)
C(9)	25(2)	21(1)	19(1)	0(1)	-2(1)	-4(1)
C(10)	27(2)	16(1)	28(1)	1(1)	-1(1)	-1(1)
C(11)	30(2)	25(1)	26(1)	8(1)	-8(1)	-3(1)
C(12)	35(2)	29(2)	21(1)	6(1)	-3(1)	-9(1)
C(13)	26(2)	36(2)	34(2)	6(1)	4(1)	-5(1)
C(14)	25(2)	25(1)	21(1)	2(1)	2(1)	-1(1)
O(1)	24(1)	17(1)	19(1)	-1(1)	2(1)	-1(1)
O(2)	35(1)	27(1)	22(1)	-4(1)	8(1)	-5(1)

O(3)	28(1)	29(1)	32(1)	-3(1)	10(1)	-3(1)
O(4)	30(1)	27(1)	42(1)	0(1)	2(1)	5(1)

Table A3.5Hydrogen coordinates ($\times 10^4$) and isotropic displacement parameters ($\text{\AA}^2 \times 10^3$) for **41m**.

	x	y	z	U(eq)
H(2)	6903	-2581	9161	35
H(3)	9522	-1267	9320	30
H(5)	6790	1485	8201	30
H(6)	4183	161	8020	32
H(7)	11143	628	9140	28
H(8)	12019	2623	9736	24
H(9A)	9546	3880	10246	26
H(9B)	11223	4722	9914	26
H(11)	8428	5307	8162	32
H(12)	10757	4135	7659	34
H(13A)	14704	3403	9024	48
H(13B)	13712	4746	9015	48
H(13C)	14413	4125	8248	48

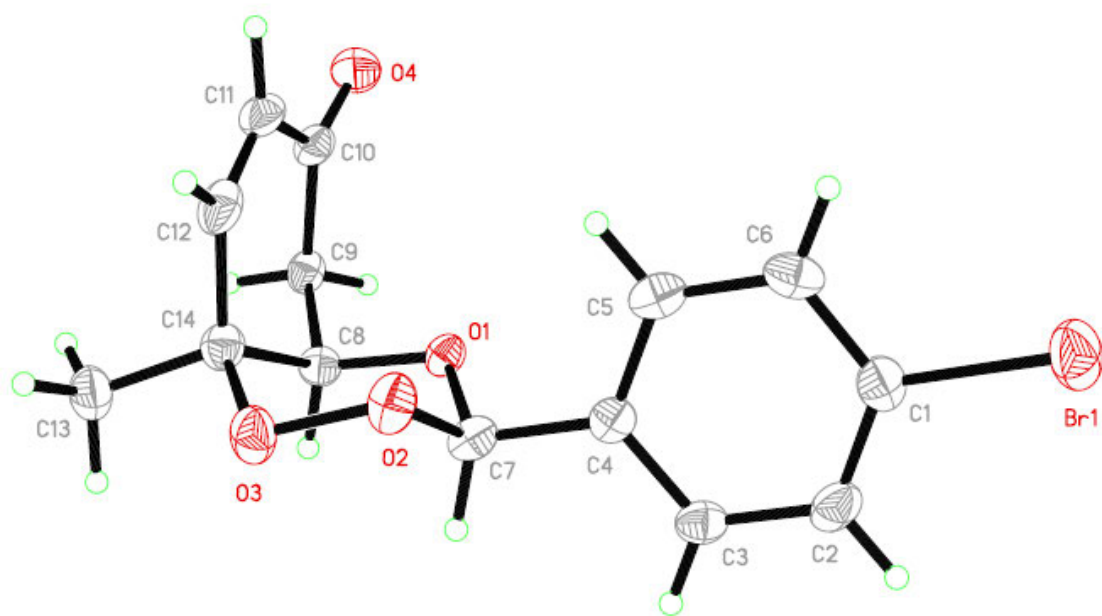


Figure A3.1

Thermal Ellipsoid Plot of **41m** at 50% Probability.

References

- ¹³⁶ Carreno, M. C.; Gonzalez-Lopez, M.; Urbano, A.; *Angew. Chem. Int. Ed.* **2006**, *45*, 2737.
- ¹³⁷ Čorić, I.; Vellalath, S.; List, B. *J. Am. Chem. Soc.* **2010**, *132*, 8536.

Appendix 4

Chapter 5 Supporting Information

General Methods

All reactions were carried out in oven-dried glassware with magnetic stirring. Dichloroethane (DCE) was degassed with argon and distilled from CaH_2 . Dichloromethane was degassed with argon and passed through two columns of neutral alumina. Toluene was degassed with argon and passed through one column of neutral alumina and one column of Q5 reactant. Column chromatography was performed on Silicycle Inc. silica gel 60 (230-400 mesh). Thin layer chromatography was performed on Silicycle Inc. 0.25 mm silica gel 60-F plates. Visualization was accomplished with UV light (254 nm) and KMnO_4 followed by heating.

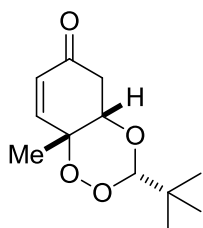
^1H NMR and ^{13}C NMR spectra were obtained on Varian 300 or 400 MHz spectrometers in CDCl_3 at ambient temperature and chemical shifts are expressed in parts per million (δ , ppm). Proton chemical shifts are referenced to 7.26 ppm (CHCl_3) and carbon chemical shifts are referenced to 77.0 ppm (CDCl_3). NMR data reporting uses the following abbreviations: s, singlet; bs, broad singlet; d, doublet; t, triplet; q, quartet; m, multiplet; and J , coupling constant in Hz.

Aldehydes, ketones and imines were either purchased from Aldrich or synthesized according to literature procedures. 4-Peroxyquinols were synthesized based off of a literature procedure.

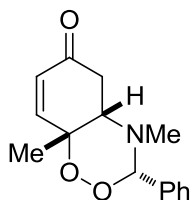
General Procedure for Trioxanes or Dioxazinanes:

To an 1 mL vial, with a magnetic stir bar, was added 4-methyl-4-hydroperoxycyclohexa-2,5-dienone (1 mmol, 1.0 equiv), Amberlyst 15 (~100 mg), aldehyde, ketone or imine (1.25 mmol, 1.25 equiv) and 1,2-dichloroethane (3 mL). The vial was then sealed, heated to 45 °C and stirred

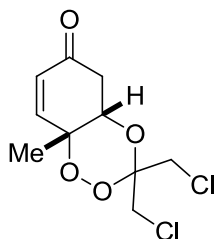
until the starting material disappeared by TLC (4-12h). The reaction was concentrated *in vacuo*. Column chromatography 10-30%(hexanes:ethyl acetate) of the resulting yellow residue gave the analytically pure 1,2,4-trioxane or 1,2,4-dioxazinane as a white solid or clear oil.



(3S,4aS,8aR)-3-(tert-butyl)-8a-methyl-4a,5-dihydrobenzo[e][1,2,4]trioxin-6(8aH)-one (17). Prepared according to the general procedure: 75% yield; >20:1 dr; $^1\text{H NMR}$ (400 MHz, CDCl_3): δ 6.84 (dd, $J = 10.3, 2.8$ Hz, 1H), 6.06 (d, $J = 10.3$ Hz, 1H), 4.89 (s, 1H), 4.15 (q, $J = 2.9$ Hz, 1H), 2.77-2.65 (m, 2H), 1.33 (s, 3H), 0.87 (s, 9H). $^{13}\text{C NMR}$ (100 MHz, CDCl_3): δ 195.2, 151.1, 129.4, 108.6, 77.7, 76.4, 41.0, 34.9, 24.5, 20.5. **HRMS** (ESI-APCI) m/z calcd $[\text{C}_{12}\text{H}_{17}\text{O}_4]^+$ ($[\text{M} + \text{H}]^+$): 227.1278, found 227.1265.

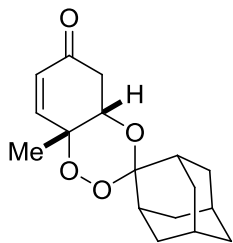


(3S,4aS,8aR)-4,8a-dimethyl-3-phenyl-3,4,4a,5-tetrahydrobenzo[e][1,2,4]dioxazin-6(8aH)-one (15). Prepared according to the general procedure: 57% yield; >20:1 dr; $^1\text{H NMR}$ (400 MHz, CDCl_3): δ 7.43-7.30 (m, 5H), 6.93 (dd, $J = 2.4, 10.3$ Hz, 1H), 6.12 (dd, $J = 1.3, 10.3$ Hz, 1H), 5.18 (s, 1H), 2.98 (q, $J = 2.7$ Hz, 1H), 2.92 (ddd, $J = 1.3, 2.9, 16.9$ Hz, 1H), 2.69 (dd, $J = 2.9, 16.9$ Hz, 1H), 2.0 (s, 3H), 1.45 (s, 3H). $^{13}\text{C NMR}$ (100 MHz, CDCl_3): δ 196.5, 152.4, 135.1, 130.1, 128.9, 128.8, 128.5, 98.7, 79.6, 65.6, 39.3, 36.4, 21.7.



(4aS,8aR)-3,3-bis(chloromethyl)-8a-methyl-4a,5-dihydrobenzo[e][1,2,4]trioxin-6(8aH)-one (36). Prepared according to the general procedure: 46% yield; >20:1 dr; $^1\text{H NMR}$ (400 MHz, CDCl_3): δ 6.83 (dd, $J = 2.7, 10.4$ Hz,

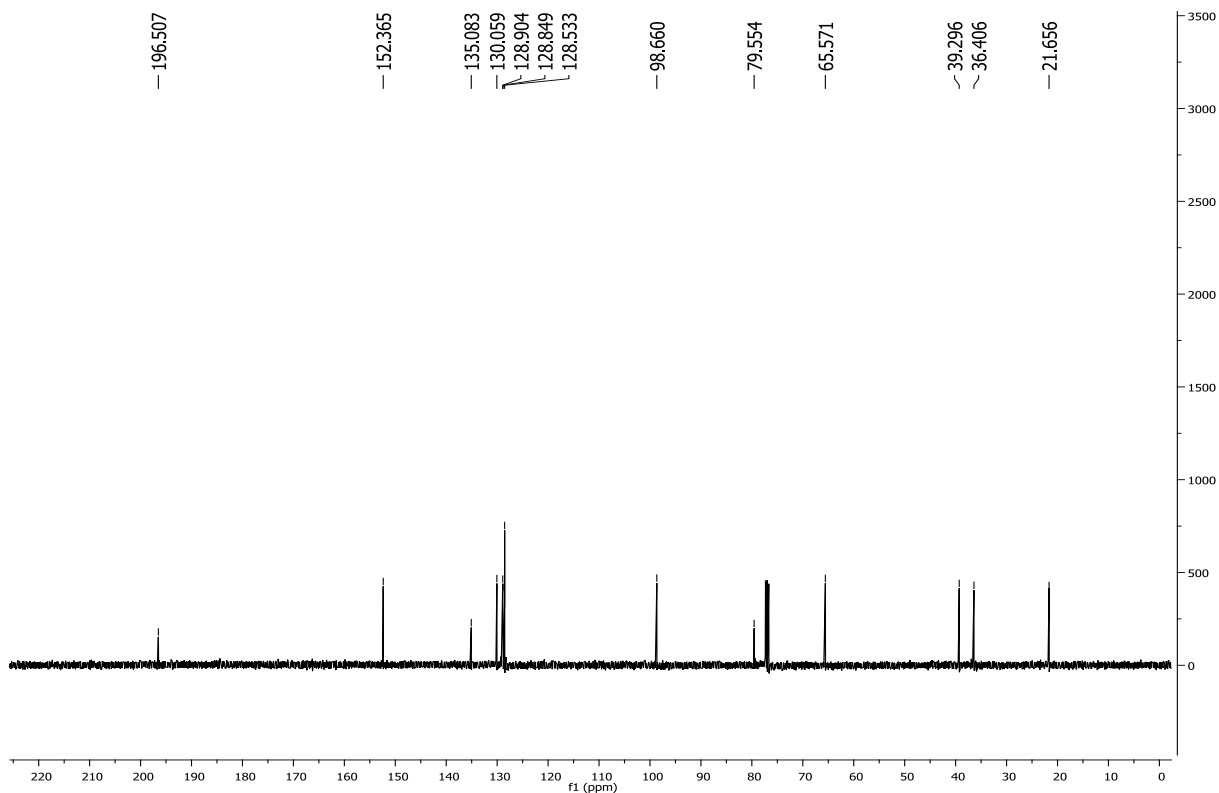
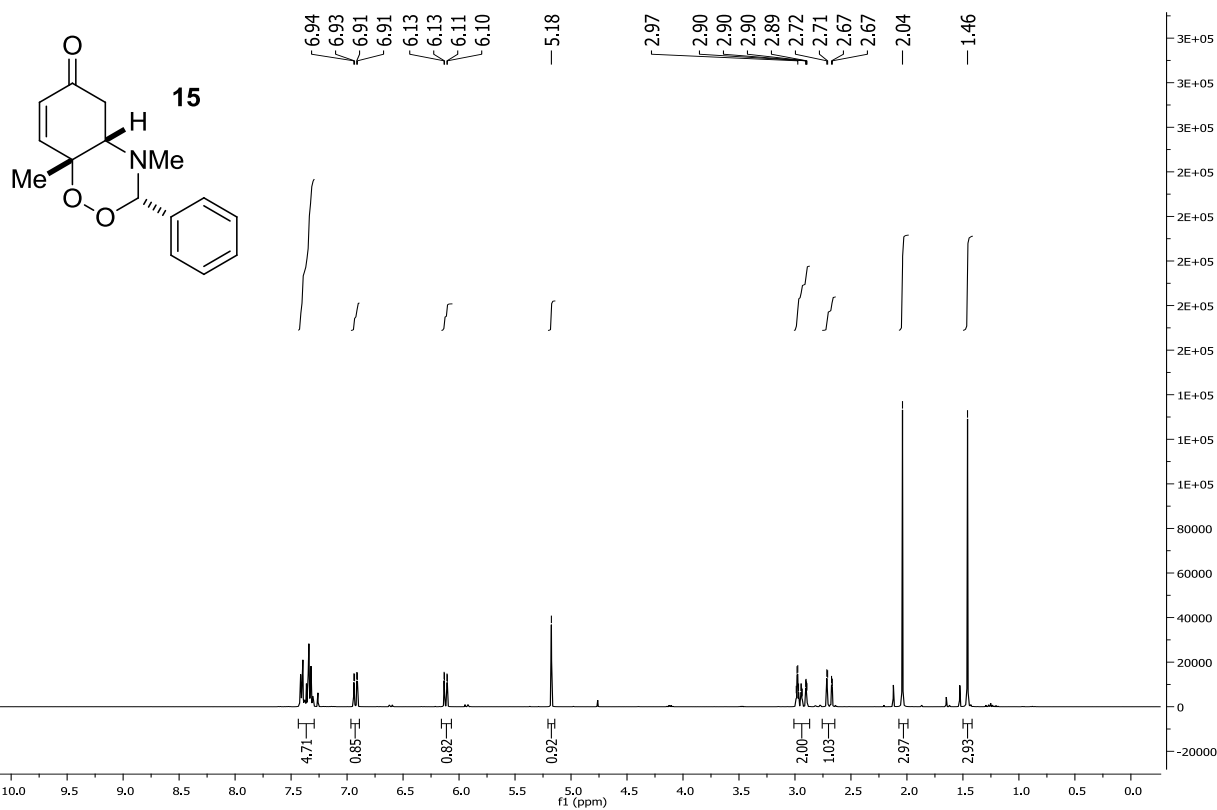
1H), 6.12 (dd, $J = 1.0, 10.4$ Hz, 1H), 4.41 (q, $J = 2.9$ Hz, 1H), 4.23 (d, $J = 12.5$ Hz, 1H), 4.07 (d, $J = 12.5$ Hz, 1H), 3.61 (d, $J = 12.3$ Hz, 1H), 3.48 (d, $J = 12.3$ Hz, 1H), 2.75 (ddd, $J = 1.0, 3.0, 17.6$ Hz, 1H), 2.68 (dd, $J = 3.0, 17.6$ Hz, 1H), 1.40 (s, 3H). ^{13}C NMR (100 MHz, CDCl_3): δ 193.8, 149.1, 130.1, 102.2, 78.0, 71.9, 43.1, 40.3, 38.4, 20.5.

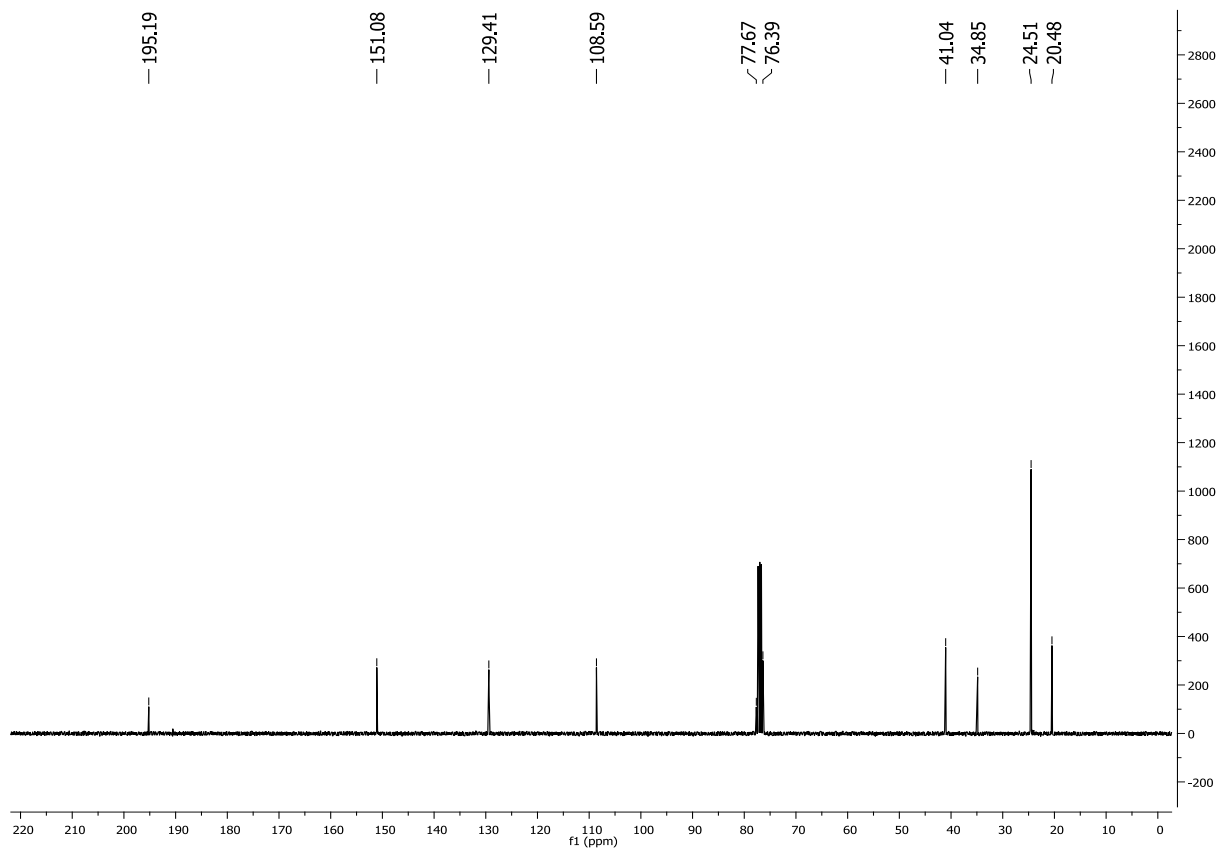
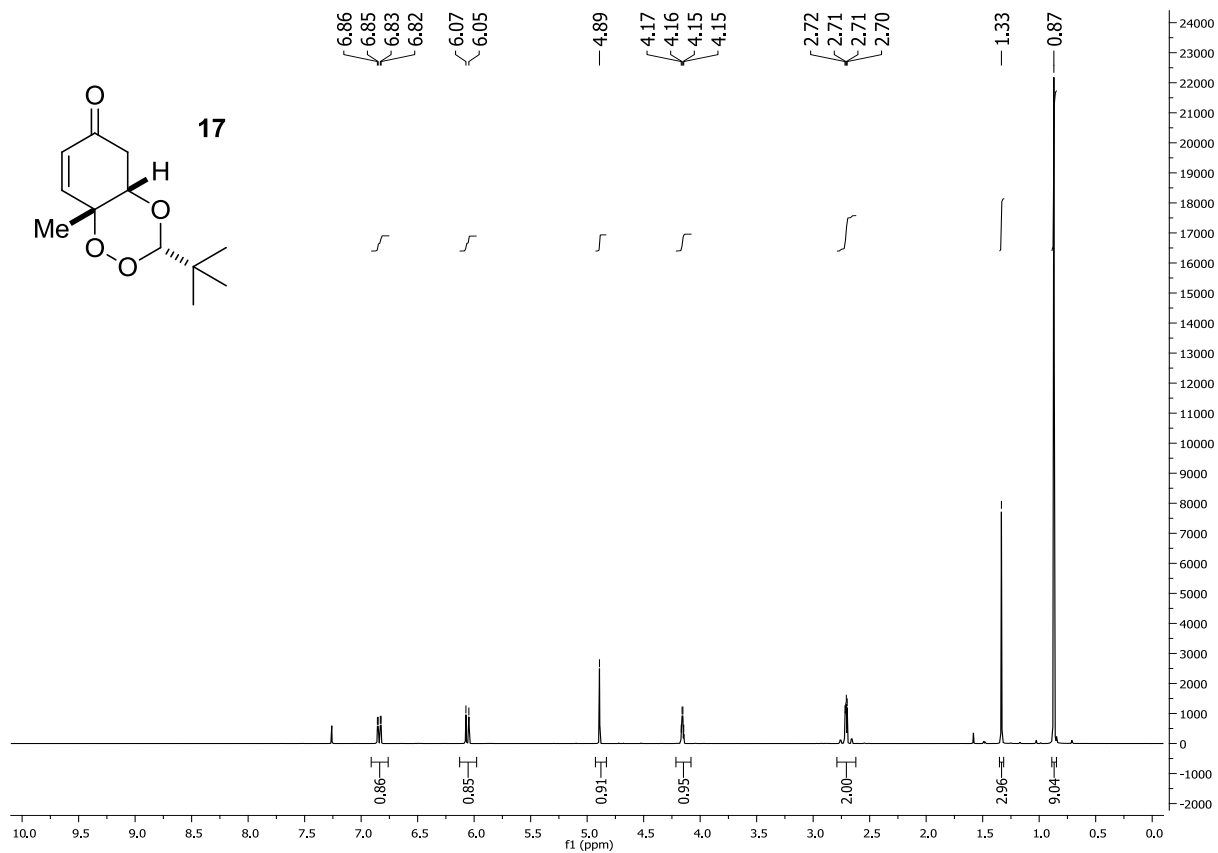
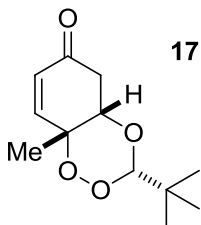


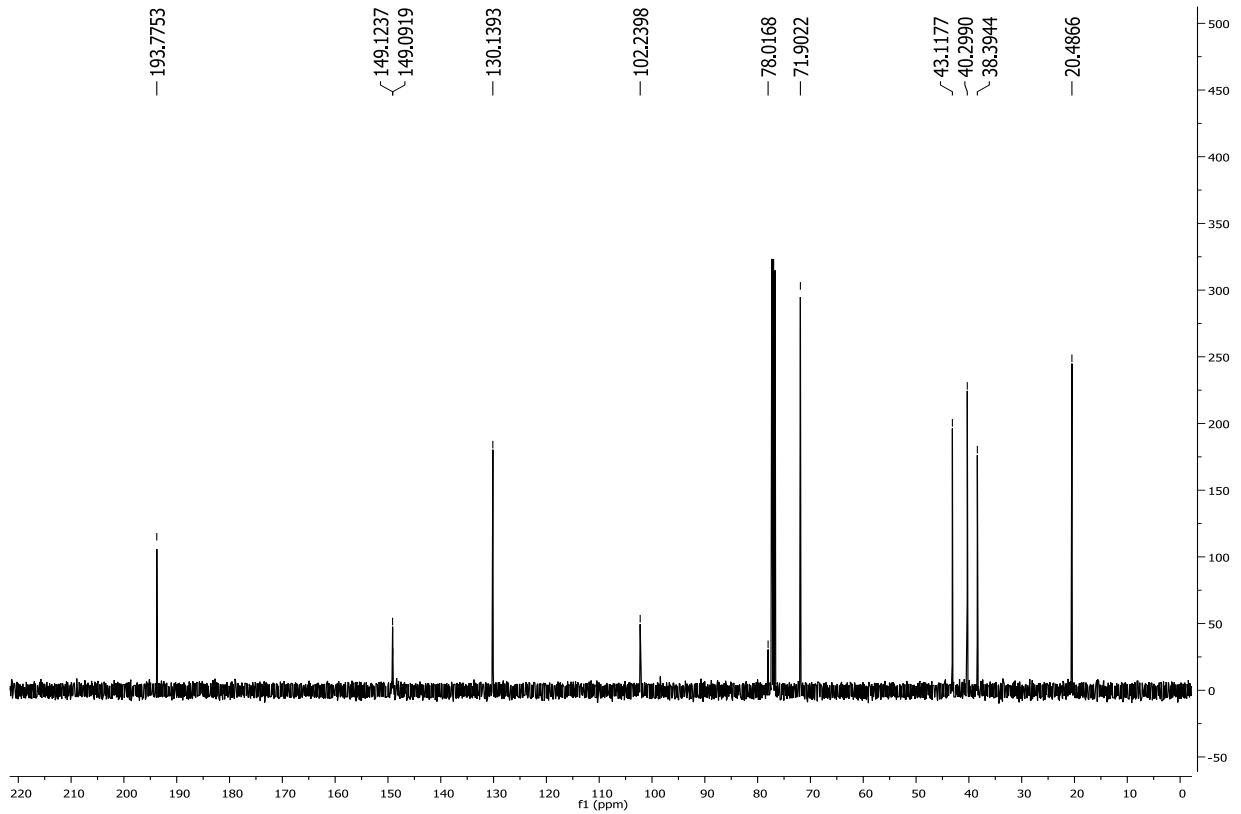
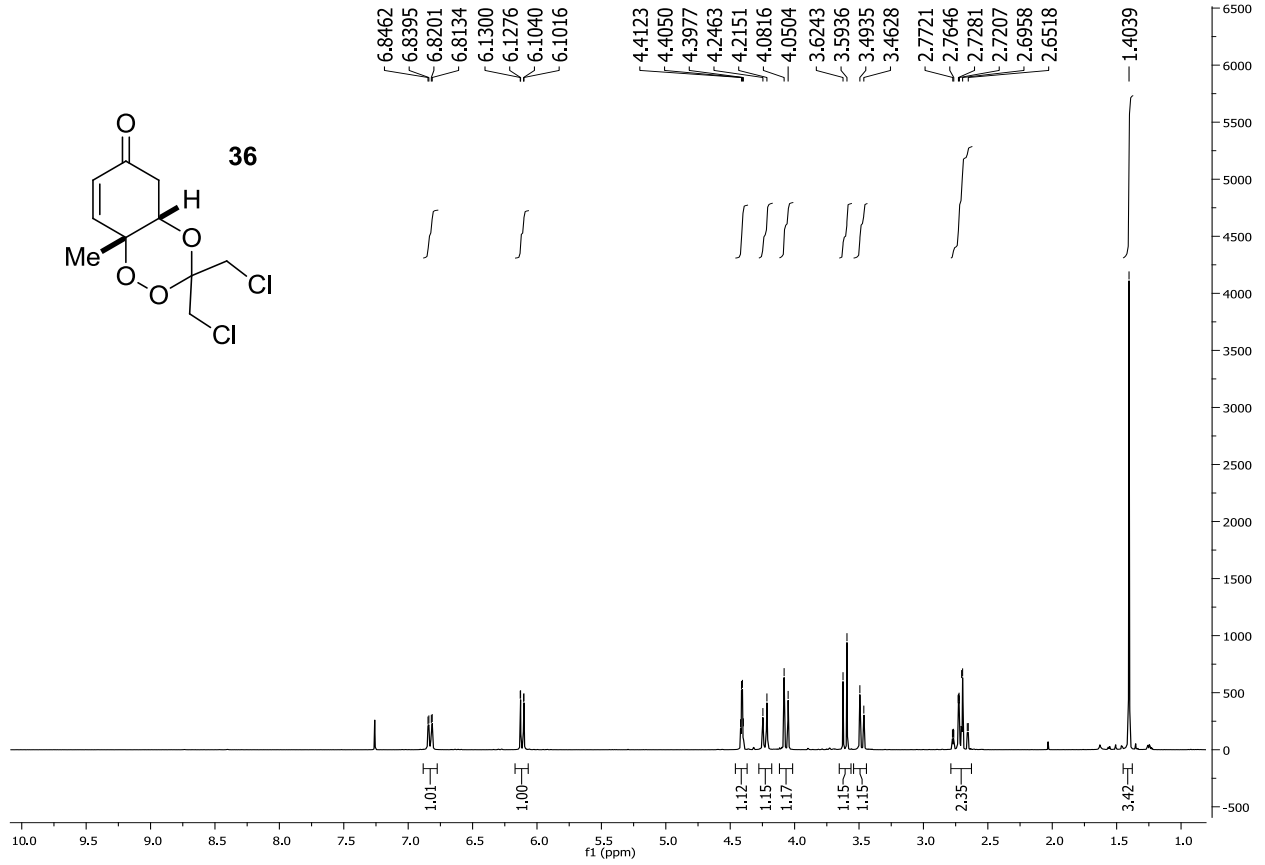
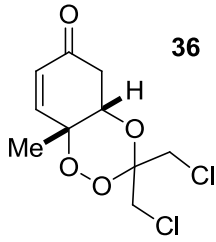
(3S,4aS,8aR)-3-(tert-butyl)-8a-methyl-4a,5-dihydrobenzo[e][1,2,4]trioxin-6(8aH)-one (17). Prepared according to the general procedure: 56% yield; >20:1 dr; ^1H NMR (400 MHz, CDCl_3): δ 6.86 (d, $J = 10.3$ Hz, 1H), 6.08 (d, $J = 10.3$ Hz, 1H), 4.38 (s, 1H), 4.15 (q, $J = 2.9$ Hz, 1H), 2.92 (bs,

1H), 2.72-2.69 (m, 2H) 2.10-1.50 (m, 14H), 1.34 (s, 3H).

¹H NMR and ¹³C NMR Spectra of New Compounds







Cancer Cell Cytotoxicity Methods

The D17 canine osteosarcoma cell line was obtained from American Type Culture Collection, (Manassas, VA). The M21 human melanoma cell line was generously provided by Dr. M. Albertini (University of Wisconsin-Madison). The human MDA-MB231 breast, A549 lung, and PC3 prostate carcinoma cell lines were generously provided by Dr. D. Gustafson (Colorado State University). All cells were grown in minimal essential medium supplemented with 5% heat-inactivated fetal bovine serum (HyClone, Logan, UT), 5% heat-inactivated newborn calf serum (HyClone), 100 units/ml penicillin-streptomycin (Mediatech, Herndon, VA), 2 mM L-glutamine (Mediatech), 1 mM sodium pyruvate (Mediatech), and 1X nonessential amino acid solution (Sigma, St. Louis, MO) at 37°C in a humidified atmosphere containing 5% CO₂. All cell lines were serially passaged by trypsinization.

Stocks of artemisinin derivatives and synthetic trioxanes were stored in DMSO. Cells were plated at 2,000 cells/well in 200 µL medium in 96-well plates and allowed to adhere overnight. The plates were then washed and the medium replaced with medium containing varying concentrations of trioxane in quintuplicate. The final concentration of DMSO never exceeded 1%. After 72 h, the relative viable cell number was assessed using Alamar Blue™ (Promega, Madison, WI) according to the manufacturer's instructions. Relative fluorescence was expressed as a percentage of untreated cells and the IC₅₀ was then calculated for each cell line by nonlinear regression analysis fitting to a sigmoidal dose-response curve, using Prism v4.0b for Macintosh (GraphPad Software, Inc., San Diego, CA). For conditions where a regression curve could not be fit, IC₅₀ was estimated from the plotted growth inhibition curve.

Results

Cyotoxicities of **18** were obtained with various canine cancer cell lines (Table A4.1).

Table A4.1

Cell Line	Cell Type	IC ₅₀ (μM)
STSA1	Soft-tissue sarcoma	18.51
Oswald	T-cell lymphoma	19.07
MH	Histiocytic Sarcoma	19.93
Nike	Histiocytic Sarcoma	22.31
CMIL10C2	Melanoma	24.8
D17	Osteosarcoma	26.63
1771	B-cell lymphoma	29.98
MacKinley	Osteosarcoma	43.47
CML6M	Melanoma	59.15
DEN-HSA	Soft-tissue Sarcoma	60.59
CLBL1	B-cell lymphoma	60.9
K9TCC	Bladder carcinoma	67.47
C2	Mast cell tumor	85.57
DH82	Histiocytic Sarcoma	101.7
Abrams	Osteosarcoma	106.8
Moresco	Osteosarcoma	126.9
Vogel	Osteosarcoma	135.4
OS2.4	Osteosarcoma	135.7
Gracie	Osteosarcoma	168.8
	Mammary	
CMT12	Carcinoma	198.1
CTAC	Thyroid Carcinoma	222.4
Bliley	Bladder carcinoma	262.8
	Mammary	
CMT27	Carcinoma	264.8
17CM98	Melanoma	394.9